

2024-01-11

# Middle Pleistocene paleoenvironmental reconstruction through phytolith analysis at the Manyara Beds, northern Tanzania

Bundala, Mariam Joseph

---

Bundala, M. J. (2024). Middle Pleistocene paleoenvironmental reconstruction through phytolith analysis at the Manyara Beds, northern Tanzania (Doctoral thesis, University of Calgary, Calgary, Canada). Retrieved from <https://prism.ucalgary.ca>.

<https://hdl.handle.net/1880/117952>

*Downloaded from PRISM Repository, University of Calgary*

UNIVERSITY OF CALGARY

Middle Pleistocene paleoenvironmental reconstruction through phytolith analysis at the  
Manyara Beds, northern Tanzania

by

Mariam Joseph Bundala

A THESIS

SUBMITTED TO THE FACULTY OF GRADUATE STUDIES  
IN PARTIAL FULFILMENT OF THE REQUIREMENTS FOR THE  
DEGREE OF DOCTOR OF PHILOSOPHY

GRADUATE PROGRAM IN ARCHAEOLOGY

CALGARY, ALBERTA

JANUARY, 2024

© Mariam Joseph Bundala 2024

## ABSTRACT

This project is aimed at developing a detailed habitat reconstruction for hominins living at the Manyara Beds of Northern Tanzania during the early Middle Pleistocene using phytolith remains. The dissertation comprises three interlinked, but independent studies.

The first study examines the phytolith assemblages from modern surface soils and plants to create a referential baseline for studying phytoliths from the *Acacia-Commiphora* ecosystem surrounding the Manyara Beds, the same plant regions in which our ancestors reside. Phytoliths from 21 species of plants, including 11 unstudied taxa from this ecosystem, were characterized. Twenty-five composite surface soil samples from five sites were also analyzed. Using Stromberg's 2003 classification and interpretive scheme, this study has demonstrated that the dominant phytoliths for *Commiphora* are polyhedral epidermal cells, and *Acacia* is a rare producer of blocky-faceted rectangular plate morphotypes.

The second study examines phytolith assemblages from archaeological and non-archaeological sites within the six-meter zone of the uppermost part of the lower Manyara Beds. In general, phytolith assemblage from archaeological and non-archaeological sites confirms the persistence of C<sub>4</sub> grasslands. However, varied habitats were available for the Acheulean tool-making hominins at archaeological site MK 4, which featured palms, woody dicots, sedge, and grasslands taxa, including high proportions of warm arid and moist loving C<sub>3</sub> and C<sub>4</sub> PACMADs and dry adapted C<sub>4</sub> chloridoids. There is also a small presence of wet-loving panicoids. The palms, sedges, Commelinaceae, and other aquatic monocots indicate that Manyara Beds were well-watered, at least with the occurrence of freshwater springs or rivers near the Lake shores. Therefore, inferences from phytolith assemblages from the Manyara Beds are consistent with the common predictions of many Plio-Pleistocene sites near the lake shores, pointing to hominin's dependence on water and food resources such as plants and game.

The third study presents the analysis of 106 stone tool residue samples from the MK4 site to understand the function of the small flake assemblage found there. Ten tools yielded phytoliths, including two flaked and eight core tools. Phytoliths revealed the exploitation of plant resources, including grasses, palms, sedges, woody dicots, and other unknown taxa.

## ACKNOWLEDGEMENTS

Every major project rests on the shoulders of many people. Therefore, I am happy to thank many people, organisations, and institutions for their help, support, ideas, care, nerves, understanding, hospitality, and love throughout this dissertation project.

First and foremost, I am grateful to my supervisor Dr. Susanne Cote whose consistent support in the entire process of this thesis has proven invaluable. She has been a thoughtful and helpful supervisor and greatly promoted this dissertation through countless discussions and exchanges of ideas about its approach, methods, theoretical background, and interpretation of results. Maybe even more important is her early trust in my scientific abilities and providing the necessary space to think and resources through additional training.

In the early stages of this project, Dr. Rahab Kinyanjui graciously hosted my visit to her National Museums of Kenya laboratory. During this trip, she spent extensive time with me in her lab reviewing phytolith slides, to preliminary assess the phytolith assemblages at the Manyara Beds. Also, I have learned much about column, botanical, and surface soils sampling in the field while working with Dr. Kinyanjui. In the latter stages, I was privileged to visit Dr. Caroline Strömberg's lab at the University of Washington. During this visit I learned a great deal about phytolith analysis techniques. I learned new extraction methods that work perfectly in older sediments, including the samples used in this dissertation. She spent an immense amount of her time reviewing my phytolith slides, morphological classifications, statistical analysis, and discussing counting strategies, classification, and interpretive schemes. I am indebted to both individuals for their generosity and assistance. I hope to continue working with both of you in the future.

Further thanks to my supervisory Drs. Brian Kooyman and Matthew Walls for always being there in case of the additional need to talk and providing thoughtful comments and cautions on the dissertation project. Dr. Brian Kooyman has always guided me into this new venture of my training in phytoliths analysis. Through him I have learned a great deal of phytoliths analytical methods, using a microscope, taking sides, and often talk about what to do next when I encounter problems in my data. I am also grateful to my external and internal examination committee members, Drs. Caroline Strömberg and Andria Dawson.

There is also financial support for every thesis. In addition to support from the Department of Anthropology and Archaeology, I received funding from Queen Elizabeth II Diamond Jubilee Scholarship, the J.B. Hyne Graduate Scholarship, the Leakey's Baldwin Fellowship, and the Martha Biggar Anders Memorial Award. My fieldwork, phytolith analytical laboratory, equipment, and additional supplies were provided by research grants from the East African Regional Council Award,

John C. Carter Endowment for Archaeology Research, the Leakey Foundation, the Wenner-Gren Foundation, the Paleontological Scientific Trust, and the University of Dar es Salaam. These grants allowed me to conduct several research trips starting from 2019, run my independent research, create part-time employment to the local people in Makuyuni Town, and take additional trainings at the NMK and Strömberg labs.

Life as a doctoral candidate and in general would not be worth a thing without the loving and encouraging staff in the Department of Anthropology and Archeology and my fellow graduate students at U of C. Jeremy Leyden had helped to keep my feet on the ground and remain sane since we became friends when we were assigned to teach Arky 201. Thanks for inviting me to the Friday drinks and listening when I need a friend to talk to. I am also grateful for your unconditional help finalizing touches on my English writing. Thank you to my lab members (Primate Paleobiology lab members), and all my colleagues here at U of C who often spared time to chat with me; thank you all for creating space for me to fit in. Throughout this research, Kris Russell Markin assisted my lab work by helping me with lab supplies and equipment.

I am indebted to my colleagues at the University of Dar es Salaam, Department of Archaeology and Heritage Studies, especially Pastory Bushozi, Frank Maselle and Charles Saanane (retired) for supporting this study particularly its logistics loaning of field equipment.

I am also grateful to the University of Dar es Salaam for providing me with research clearance. The Antiquities Department, Ministry of Natural Resources and Tourism, for granting me research permits and permission to borrow artifacts for study at the University of Calgary.

I would also like to thank my field crew: Neemia Simon, Abraham Massawe, Rogers Robert, Venance Bundala, Pazza Hitson, Michael Lugwalu, Albert Samweli, Henry Masawe, Alex John (Rest in Peace dear friend), and our cooks Mama Elia, Mama Richard: without these great people and helpers here, the time spend in the field for this dissertation would have not been fun at all. I would also like to thank my Tanzanian community here in Calgary for making me feel at home, special thanks to my young sister Wazia Paul for dealing with my never-ending complaints about my writing and lab work. Special thanks to Chris Nambari for his technical help in fixing my laptop. Many thanks to my other family in Kenya, especially Husna Mashaka for her help in the lab and Silvia Wemanya.

## **DEDICATION**

I dedicate this dissertation to the memory of my lovely father, Joseph Marien Bundala, whom I wish could be here today to witness this, and to my mother, Amina Amiri, who kept faith in me and for always being there for me, supporting and accepting my decision to study archaeology abroad while taking over the motherly role for my son. My son Lucky for his endless questions on my whereabouts, and to my brothers Amiri, Ally, and Venance. I thank you all for providing me and encouraging my efforts.

Mama, this dissertation is, to a large extent, the outcome of your care and upbringing.

## TABLE OF CONTENTS

<b>ABSTRACT .....</b>	<b>ii</b>
<b>ACKNOWLEDGEMENTS.....</b>	<b>iii</b>
<b>DEDICATION.....</b>	<b>v</b>
<b>TABLE OF CONTENTS .....</b>	<b>vi</b>
<b>LIST OF TABLES.....</b>	<b>viii</b>
<b>LIST OF FIGURES .....</b>	<b>ix</b>
<b>LIST OF ABBREVIATIONS .....</b>	<b>xi</b>
<b>Chapter 1: Introduction .....</b>	<b>1</b>
<b>Previous Geological and Archaeological Research at Manyara .....</b>	<b>2</b>
Research Objectives .....	8
Chapter 2.....	8
Chapter 3.....	10
Chapter 4.....	11
<b>Research Design and Methodology .....</b>	<b>13</b>
<b>Theoretical Framework .....</b>	<b>13</b>
Drivers of Climate and Environmental Change.....	14
The East African Rift System Lakes and Human Evolution.....	16
Environmental Hypotheses of Hominin Evolution.....	17
The Manyara Beds and Environmental Hypotheses.....	20
<b>Significance.....</b>	<b>21</b>
<b>Literature Cited .....</b>	<b>23</b>
<b>Chapter 2: What phytoliths are preserved in the modern soils in the vicinity of the Manyara beds, and how do they help inform those found in ancient assemblages? .....</b>	<b>32</b>
<b>Abstract .....</b>	<b>32</b>
<b>Introduction.....</b>	<b>32</b>
<b>Materials and Methods .....</b>	<b>36</b>
Study Area.....	36
Plant collection and extraction .....	39
Surface soil and extraction.....	42
Statistical methods.....	46
<b>Results.....</b>	<b>48</b>
Modern plant samples .....	51
Phytoliths found in grasses .....	51
Statistical analysis .....	53
Phytoliths found in non-grasses.....	57
Statistical analysis .....	60
Surface soil phytoliths.....	64
Statistical analysis .....	68
<b>Discussion .....</b>	<b>73</b>
<b>Conclusions.....</b>	<b>81</b>

<b>Literature Cited .....</b>	<b>82</b>
Chapter 3: Were there any vegetation cover changes through time and space in the lower Manyara Beds? What kind of microhabitats were hominins using in the Lake Manyara region during the Middle Pleistocene? .....	89
<b>Abstract .....</b>	<b>89</b>
<b>Introduction .....</b>	<b>89</b>
<b>Material and Methods .....</b>	<b>91</b>
Study Sites .....	91
Phytolith extraction and analytical procedures .....	102
Phytolith morphotypes and taxonomic interpretation .....	103
Statistical analysis .....	104
<b>Results .....</b>	<b>107</b>
Phytolith assemblages: site-based results .....	107
Archaeological sites .....	115
Non-Archaeological sites .....	120
Results from Statistical analysis .....	124
<b>Discussion .....</b>	<b>131</b>
<b>Conclusions .....</b>	<b>135</b>
<b>Literature cited .....</b>	<b>136</b>
Chapter 4: What phytoliths are preserved on stone tools? .....	143
<b>Abstract .....</b>	<b>143</b>
<b>Introduction .....</b>	<b>143</b>
<b>The Manyara Beds and their Lithic Assemblages .....</b>	<b>145</b>
<b>Materials and methods .....</b>	<b>147</b>
Study Area .....	147
Phytolith extraction .....	153
Counting and Classification .....	155
<b>Results .....</b>	<b>157</b>
Results from control samples .....	157
Results from stone tools residues .....	158
Testing for the Authenticity of Artifact Residues .....	166
<b>Discussion and Interpretation .....</b>	<b>168</b>
<b>Conclusions .....</b>	<b>172</b>
<b>Literature Cited .....</b>	<b>173</b>
Chapter 5: Conclusions and Future Research .....	180
<b>Conclusions .....</b>	<b>180</b>
<b>Future Research .....</b>	<b>182</b>
<b>Literature Cited .....</b>	<b>183</b>
Appendices .....	185
Appendix A: An Excel spreadsheet contains all the raw data for the thesis .....	185
Appendix B: Phytolith morphotype descriptions .....	186
Appendix C: Figures of representative modern phytoliths. ....	191



## LIST OF TABLES

<b>Table 2-1:</b> Plant species used in this study. ....	41
<b>Table 2-2:</b> Descriptions of the five modern surface soil plots used in this study and the plants found growing on the soil plot. ....	43
<b>Table 2-3:</b> Morphotype code and interpretive scheme used in this study. ....	50
<b>Table 2-4:</b> Normality test for grass species.....	54
<b>Table 2-5:</b> Kruskal-Wallis test for GSSC phytoliths .....	54
<b>Table 2-6:</b> Phytolith production in non-grasses species.....	58
<b>Table 2-7:</b> Normality test for diagnostic non-grass phytoliths .....	61
<b>Table 2-8:</b> Kruskal-Wallis test for diagnostic non-grass phytoliths.....	61
<b>Table 2-9:</b> Dunn’s post hoc values for non-grass phytoliths.....	61
<b>Table 2-10:</b> Normality test for diagnostic phytoliths morphotypes in surface soils.....	69
<b>Table 2-11:</b> Kruskal-Wallis test for diagnostic morphotypes.....	69
<b>Table 2-12:</b> Dunn’s post hoc test results .....	70
<b>Table 3-1:</b> Lithostratigraphic section for MK 4-Geo-section 1.....	96
<b>Table 3-2:</b> Lithostratigraphic sections for MK 4-Geo-section 2 .....	97
<b>Table 3-3:</b> Lithostratigraphic section for MK 2 Site. ....	98
<b>Table 3-4:</b> Lithological section for the MK 17 Site. ....	98
<b>Table 3-5:</b> Lithological section for the MKRV-1 Site. ....	99
<b>Table 3-6:</b> Lithological section for the MKRV-2 Site. ....	99
<b>Table 3-7:</b> Lithological section for the MKRV 3 Site.....	100
<b>Table 3-8:</b> Lists of phytolith types included in this study .....	105
<b>Table 3-9:</b> Phytolith recovery per sample, listed by plant functional type. ....	109
<b>Table 3-10:</b> Ft-ratio t-test values .....	124
<b>Table 3-11:</b> Aridity index t-test values.....	124
<b>Table 3-12:</b> Normality table for plants functional types for all samples (n=50).....	125
<b>Table 3-13:</b> Kruskal-Wallis value for the samples.....	125
<b>Table 3-14:</b> Dunn’s post hoc value for plants functional types .....	126
<b>Table 4-1:</b> Summary of the archaeological assemblage from Layer 3.....	153
<b>Table 4-2:</b> Morphotype classes used in this study.....	156
<b>Table 4-3:</b> Sediments sample beneath artifacts (control samples). ....	157
<b>Table 4-4:</b> List of Manyara Bed artifacts that yielded phytoliths (n = 10) .....	159
<b>Table 4-5:</b> Phytoliths found on ten stone tools. ....	160
<b>Table 4-6:</b> Grass phytoliths found on each artifact. ....	161

## LIST OF FIGURES

<b>Figure 1-1:</b> Map of Tanzania showing the location of the study area Makuyuni town.....	3
<b>Figure 1-2:</b> Stratigraphic section of the Manyara Beds showing the approximately 5.5-meter zone of focus for this study. Adapted and modified from Wolf et al. (2010); Kaiser et al. (2010); and (Schwartz et al., 2012). .....	5
<b>Figure 1-3:</b> Hypothetical gene frequency fluctuation in response to varying environments to assess variability selection. ....	20
<b>Figure 2-1:</b> Map of the study area showing sites for botanical and surface soil collections.....	38
<b>Figure 2-2:</b> Surface soil plan showing the 10 x 10-meter pinch sampling. ....	44
<b>Figure 2-3:</b> Photos of the study area showing the five soil sampling locations. ....	45
<b>Figure 2-4:</b> Percentage of grass silica short cell phytoliths in each grass species. ....	52
<b>Figure 2-5:</b> Percentage of plant functional types in species per diagnostic GSSC phytoliths. ....	53
<b>Figure 2-6:</b> Correspondence analysis of diagnostic phytolith morphotypes in grass. Ordination diagram of axes 1-3.....	56
<b>Figure 2-7:</b> Hierarchical cluster dendrogram showing similarity of plant functional types for diagnostic GSSC phytoliths.....	57
<b>Figure 2-8:</b> Percentage of phytoliths morphotypes per species.....	59
<b>Figure 2-9:</b> Percentage of plant functional types in non-grass plants per species.....	60
<b>Figure 2-10:</b> CA results of phytolith morphotypes in non-grass species. Ordination diagram of axis 1 and 2. ....	63
<b>Figure 2-11:</b> Cluster analysis of non-grass samples similarity of plant function types per diagnostic phytoliths. ....	64
<b>Figure 2-12:</b> Count frequency of plant functional types represented by phytoliths at each site, broken down for the five samples. ....	66
<b>Figure 2-13:</b> Count frequency of GSSC phytoliths per sample at each site. ....	67
<b>Figure 2-14:</b> Count frequency of plant functional types represented by GSSC morphotypes per sample.....	68
<b>Figure 2-15:</b> Cluster analysis of soil samples similarity of plant functional types per diagnostic phytoliths for each site. ....	71
<b>Figure 2-16:</b> CA of sites (n=5) and functional groups (n=7).....	72
<b>Figure 3-1:</b> Map of the study area (Makuyuni town) showing the sampling sites in the Manyara Beds. ....	92
<b>Figure 3-2:</b> Correlation of Manyara Beds stratigraphy and magnetostratigraphy with the geological time scale and geomagnetic polarity time scale.....	93
<b>Figure 3-3:</b> Left photograph shows the “Red Brick Tuff” observed near the Makuyuni River Valley (approximately 500 m from MK 4) during survey the 2021 fieldwork in this study.....	95
<b>Figure 3-4:</b> Geo-section 1 from MK 4 site showing column sampling 2 metres from excavation Unit 1. ....	96
<b>Figure 3-5:</b> Generalized stratigraphic column of the Manyara Beds near Makuyuni town showing the sampling sections in relation to 6-metre section of the uppermost part of the lower member	

and the upper-lower member contact (which is either the Hollywood Tuff or laterally equivalent Red Brick Tuff).....	101
<b>Figure 3-6:</b> Percentage of phytolith morphotypes at each site's sample.....	108
<b>Figure 3-7:</b> Comparison of the FI-t ratio and $I_{ph}$ index for the archaeological and non-archaeological sites at the Manyara Beds.....	112
<b>Figure 3-8:</b> Percentage of GSSC phytolith categories per sample. ....	113
<b>Figure 3-9:</b> Count frequency of plant functional types.....	114
<b>Figure 3-10:</b> Selected distinctive and diagnostic phytoliths recovered from MK4-GS1 site. ....	116
<b>Figure 3-11:</b> Selected distinctive and diagnostic phytoliths recovered from MK4-GS2. ....	118
<b>Figure 3-12:</b> Selected key phytoliths from Site MK 17. ....	119
<b>Figure 3-13:</b> MKRV 1 selected distinctive phytolith morphotypes. ....	120
<b>Figure 3-14:</b> Key phytolith morphotypes from MKRV 2. ....	121
<b>Figure 3-15:</b> Selected distinctive and diagnostic phytoliths recovered from MKRV 3 ....	123
<b>Figure 3-16:</b> Cluster dendrogram showing similarity values of environment using the Single Linkage method based on Euclidean distance from the Manyara Bed Samples (n=50).....	128
<b>Figure 3-17:</b> CA of resulted plants functional types (n=14) from diagnostic phytoliths (n=43) and samples (n=50).....	130
<b>Figure 4-1:</b> Map of Arusha region showing the location of the study area of the Manyara Beds near Makuyuni Town in association to other archaeological sites in Northern Tanzania. ....	146
<b>Figure 4-2:</b> Map of MK4 showing the location of the 2021 excavation unit. ....	147
<b>Figure 4-3:</b> The generalized stratigraphic column of the Manyara Beds.....	148
<b>Figure 4-4:</b> Excavation plan at MK 4. ....	150
<b>Figure 4-5:</b> Wall profile showing the eleven layers identified from the first 2 by 2 unit after excavation (Unit A/B).....	151
<b>Figure 4-6:</b> Phytolith frequencies per artifact.....	161
<b>Figure 4-7:</b> Frequencies of grass phytoliths found on all artifacts that produced phytoliths. ....	162
<b>Figure 4-8:</b> Selected diagnostic phytoliths found in stone tool residues. ....	166
<b>Figure 4-9:</b> Comparison of phytolith assemblages from Geo-section 1 sample #MK4-GS1-L3 and artifacts. ....	167

## LIST OF ABBREVIATIONS

Phytolith-based plant functional groupings:

DICOT-GEN—woody and herbaceous ‘dicotyledonous’ angiosperms (typically produced by many non-monocotyledonous plants)

FI-GEN— general forest indicator

CONI/MONO— conifer/monocotyledon (typically produced by many conifers and monocotyledons)

SEDGE— diagnostic to sedge

GRASS/MONO-ND— nondiagnostic grass/monocotyledon

GSSCP— grass silica short cell (diagnostic to grass)

GRASS-D— diagnostic non-GSSC grass

AQ-MONO-aquatic monocots

OTH— other non-GSSC phytoliths

GRASS/MONO— grass/monocotyledon

PACMAD— grass clade that are members of Panicoideae, Arundinoideae, Chloridoideae, Micrairoideae, Aristidoideae, and Danthonioideae (Grass Phylogeny Working Group II, 2012; Grass Phylogeny Working Group, 2001)

DICOT-WO— Woody dicotyledon

MD material/surface (“MD material/surface (M+S) = morphotypes consisting of MD material are made up of light, transparent, opaque silica with small black (organic?) grains inside and have a verrucate, somewhat diffuse (not well-defined) surface

MD surface— usually irregularly distributed and grooved or furrowed surfaces

Mya— Million years ago

Kya— Thousand years ago

## Chapter 1: Introduction

The main goal of this dissertation is to develop a detailed habitat reconstruction for the Manyara Beds using phytolith remains. The Manyara Beds sample a poorly studied stratigraphic interval in the early Middle Pleistocene of Tanzania between 780,000 to 633,000 years ago. Phytoliths are microscopic plant remains formed when hydrated silicon dioxide is deposited within and between the cells of living plants (Piperno, 2006; Rashid et al., 2019; Shakoor et al., 2014; Strömberg, 2004; Strömberg et al., 2018). They can be deposited in stems, leaves, fruits, bark, and roots. After the plant's death and decay the resulting cell-shaped silica casts are released into the soil forming a highly localized assemblage that can survive in sediments for millions of years (Barboni, 2014; Piperno, 2006; Strömberg et al., 2018).

The Middle Pleistocene is a vital period for human evolution. The Middle Pleistocene starts with the shift from a reversed to a normal magnetic polarity about 780 thousand years ago (kya) and ends at the beginning of the last interglacial around 130 kya (Johnson & McBrearty, 2012; McBrearty, 2001; Smith et al., 2019; Tryon et al., 2006). This period is very complex but important to the understanding of human evolution, particularly as it relates to the taxonomy of the Middle Pleistocene fossil record, a subject of intensive debate (Pearson, 2000; Rightmire, 2008; Stringer, 2012). This debate arose because Middle Pleistocene fossils show a wide range of variation, many are fragmented, and others are derived from a poorly dated set of materials (Buck & Stringer, 2014; Rightmire, 2008; Stringer, 2012).

In Africa, two speciation events have been documented during the Middle Pleistocene period associated with the replacement of *H. erectus* across a broad range by the *H. heidelbergensis* (*sensu lato*), eventually giving rise to anatomically modern humans in Africa around 315 kya (Pearson, 2000; Rightmire, 2001, 2008; Stringer, 2012). This period also saw major technological shifts from the Early Stone Age (Acheulean) to a more diverse stone tool technology in the Middle Stone Age (MSA) around 300 kya, and the emergence of so-called behavioral modernity (McBrearty, 2001; McBrearty & Brooks, 2000; Tryon et al., 2006). Paleoanthropologists and paleolithic archaeologists have attempted to explain the fundamental changes and adaptations associated with the extinction or appearance of hominin species, including our own (Maslin et al., 2015; Potts, 1998a, 1998b; Trauth et al., 2015). Environmental pressures, including cooling, drying, and climatic instability, are often invoked as drivers of hominin evolution in East Africa (Castañeda et al., 2016; Dupont et al., 2011; Grove et al., 2015; Potts, 1998a).

Unlike Eurasia, the Middle Pleistocene paleoanthropological record in Africa is sparse (Benito-Calvo et al., 2014; Maddux et al., 2015; Manzi, 2004; Rightmire, 1996, 2008). This is specifically true for the earliest phase of the Middle Pleistocene (780-600 Kya) where only a few

fragmented hominin fossils have been recovered in Africa (Maddux et al., 2015; Rightmire, 2008). The most critical sites in Eastern Africa include Olorgesailie, Nandung'a (Kenya), Ternifine (Algeria), Bodo (Ethiopia), and Olduvai Gorge (Tanzania) (Maddux et al., 2015; Potts, 2013; Rightmire, 1996, 2008). The Manyara Beds in Northern Tanzania also provide an early Middle Pleistocene record of human evolution (Frost et al., 2012, 2017; Schwartz et al., 2012). Although the archaeological sites in these deposits are less well known compared to other localities in Africa, these deposits could potentially add to existing knowledge concerning human evolution during the early Middle Pleistocene period (Schwartz et al., 2012).

Manyara is an ideal place to examine the role of habitat change and human evolution because the deposits document evidence of numerous periods of environmental variability related to the enlargement and shrinkage of paleo-lake Manyara throughout the Middle Pleistocene (Bachofer et al., 2018; Ring et al., 2005; Schwartz et al., 2012). Such changes to the lake's shorelines created lake flats and a succession of vegetation zones that provided complex mosaic habitats for hominin occupation starting in the early Middle Pleistocene (Bachofer et al., 2014; Frost et al., 2012; Giemsch et al., 2018). Hominin occupation has been documented through the discovery of numerous stone tools assigned to the Early Late Acheulean industry, and the presence of hominin remains at Makuyuni Site 4 (MK 4) and Makuyuni Site 2 (MK 2) (Frost et al., 2012; Kaiser et al., 2010). These hominin remains (a partial parietal and a root from a left upper incisor) are highly fragmentary. However, due to their age (of approximately 780,000-633,000 years ago) the finds have been attributed to *Homo* sp. (Frost et al., 2012).

### **Previous Geological and Archaeological Research at Manyara**

The Manyara Beds are exposed to the south, north, and east of the current Lake Manyara (Kaiser et al., 2010; Ring et al., 2005; Schwartz et al., 2012). Lake Manyara is within the southern termination of the Tanzania rift which is part of the East African Rift System (EARS) (Ring et al., 2005). The fossiliferous sites in this study are located east of the Manyara Beds near the Makuyuni village in the Arusha region, northern Tanzania (Figure 1-1).



**Figure 1-1:** Map of Tanzania showing the location of the study area Makuyuni town.

The Manyara Beds are approximately 30 meters thick and consist of two distinctive subunits: The upper and lower members (figure 1-2) (Ring et al., 2005). The lower member (up to 15 m thick) comprise of lacustrine deposits greyish in color (Frost et al., 2012; Kaiser et al., 2010; Schwartz et al., 2012; Wolf et al., 2010). The base (oldest deposits) of the lower member was deposited between 1.3 and 0.98 million years ago (mya) and reached a maximum thickness of 15 m at about 0.633 mya (Schwartz et al., 2012). The upper member (12-15 m thick) consists of terrestrial and fluvial deposits that are reddish-brown in color (Frost et al., 2012; Kaiser et al., 2010; Schwartz et al., 2012; Wolf et al., 2010). The base of the upper member is assumed to have been deposited at around 0.633 mya, while the top reached its maximum thickness between 0.27 and 0.44 mya (Schwartz et al., 2012).

The approximately 5.5-meter section (Figure 2) of the uppermost part of the lower member and the lower-upper contact yields a variety of artifacts (some of which can be recovered in situ), mammal remains (including hominins), and diverse vertebrate fossils, including fish (Frost et al., 2012; Kaiser et al., 2010; Schwartz et al., 2012). This layer is preliminary calibrated chronostratigraphically by Schwartz et al. (2012). There is a  $^{40}\text{Ar}/\text{Ar}^{39}$  date of 0.633 mya  $\pm 0.039$  from a pumice rich unit at the base of the Upper Member from Makuyuni Site 16. Furthermore, a paleomagnetic reversal of 0.784-0 mya (Bruhnes Chron) was documented from sediment samples 5.5 meters below the lower-upper member contact (Schwartz et al., 2012). This paleomagnetic reversal is associated with stratigraphic layers that include well-researched fossil and lithic tool localities in MK 4 and MK 2 (Frost et al., 2012; Schwartz et al., 2012).

The lower member is well exposed near Makuyuni village, approximately 20 km east of the present eastern shorelines of Lake Manyara, and probably was about 100 meters higher than its current level marking the Pleistocene high-level of the paleo-lake (Bachofer et al., 2014; Kaiser et al., 2010). The entire regional extent of the Manyara Beds is unknown, but the known exposures represent at least 125 km<sup>2</sup> surrounding Makuyuni town (Kaiser et al., 2010). A good portion of these beds is well exposed at UTM coordinates Zone 37M, ranging between 0176800 East and 0177600 North 177814, and 9606300 East and 9606700 North (Giemsch et al., 2018; Schwartz et al., 2012).



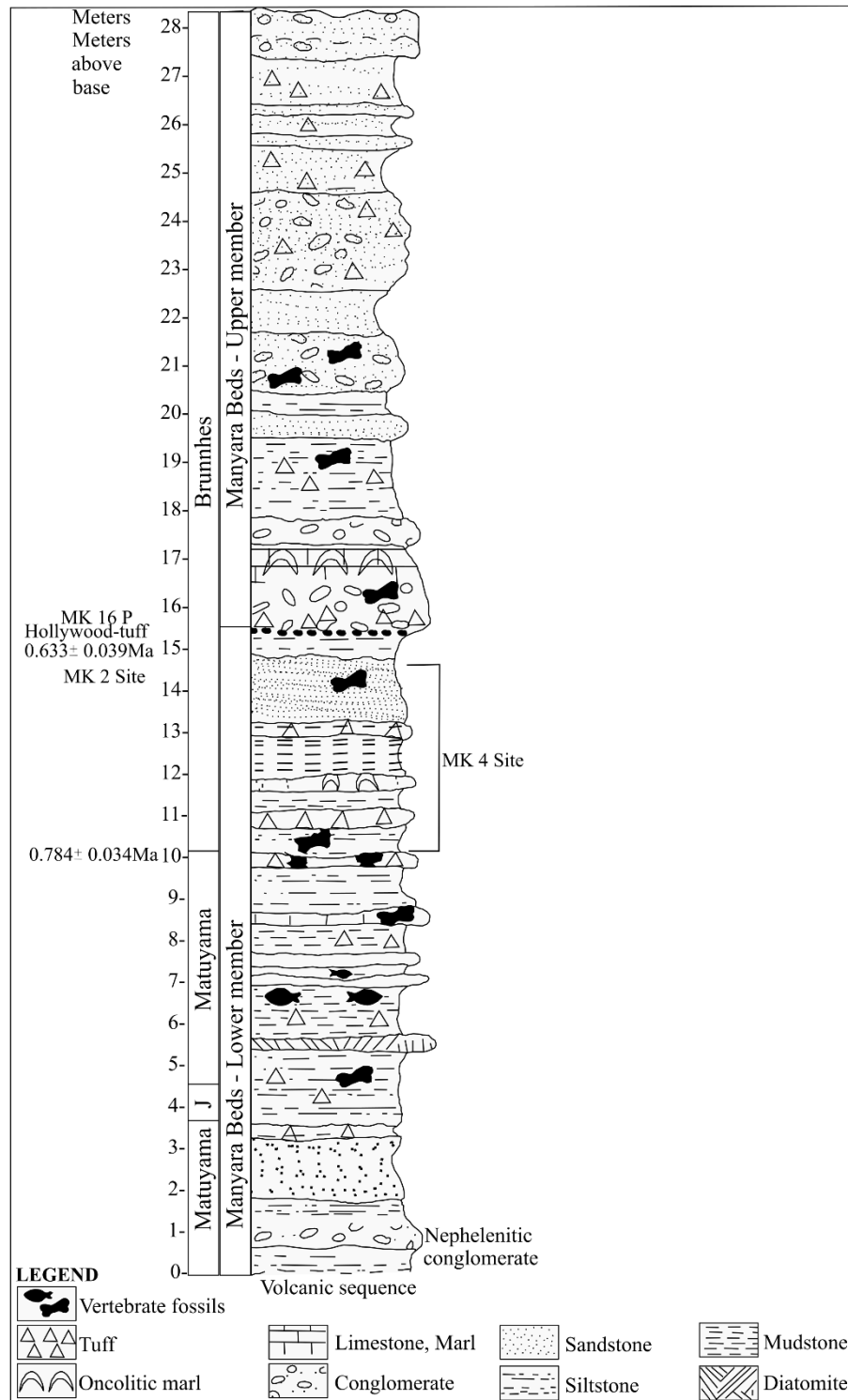


**Figure 1-2:** Stratigraphic section of the Manyara Beds showing the approximately 5.5-meter zone of focus for this study. Adapted and modified from Wolf et al. (2010); Kaiser et al. (2010); and (Schwartz et al., 2012).

Research at the Manyara Beds is limited compared to nearby paleoanthropological sites (e.g., Olduvai Gorge, Peninj, and Laetoli) because of the relative paucity of hominin remains (Kaiser et al., 2010; Schwartz et al., 2012). Jager (1913), Reck (1921), and Reck and Kohl-Larsen (1936), cited

in Kaiser et al. (2010), initially described the exposures surrounding the Lake Manyara basin. The paleoanthropological and paleontological potential was reported first by Mary Leakey and Louis Leakey, who briefly stopped at the Manyara Beds during their excursions to Olduvai Gorge (Kaiser et al., 2010; Kent, 1942). Geological, archaeological, and paleontological investigations were conducted in 1935 by the East African Archaeological Research Expedition (Kent, 1942). Kent (1942) documented grey and greenish, well-laminated ash-clay with sandstone lenticels and thin calcareous lacustrine beds rich in fish and occasional mammal remains. He reported the occurrence of fossil remains attributed to *Hippopotamus*, *Hipparion*, *Equus*, *Elephas*, *Rhinoceros simus*, Giraffidae, and *Phacochorus*. He examined fauna assemblages, conducted lithological comparisons with Olduvai Bed II and III, and documented artifact ages (Chellean tools). As a result, Kent (1942) suggested that the Manyara Beds date to the Lower or Middle Pleistocene.

Keller et al. (1975) re-examined the geology of the Manyara and Engaruka Basin (from 1969- to 1970) to reconstruct the paleoenvironment and understand the archaeology of the Pleistocene Lake Manyara deposits. They reported the occurrence of Early Stone Age tools (Acheulean) near Makuyuni village, but no collections were made. They further reported the occurrence of Late Stone Age tools from two caves near the study area, where microliths have been found in association with pottery. Keller et al. (1975) documented numerous beaches and eight terraces, suggesting that the lake's level frequently fluctuated as it retreated from its maximum expansion. In addition, terrace cliffs showed various areas of erosion, suggesting subsidence and lake advancement, implying that the lake level responsible for the highest shoreline features occurred within a short duration. In addition, Keller et al. (1975) collected microbotanical samples from a core taken from a well (Well 2) near Manjingu Hill. Their initial analysis showed that this sample was rich in pollen, but no specific taxonomic identifications were made.

The Hominid Research Corridor Project re-examined the Manyara Beds near Makuyuni village and conducted the first systematic survey from 1993 to 2000 (Kaiser et al., 1995; Schwartz et al., 2012). As a result, the Makuyuni area was subdivided into numbered 'MK areas' (after the village name 'Makuyuni'), ranging from kilometer to meter-scale areas that were defined by the presence of various vertebrate remains, lithic artifacts, and geological features (Kaiser et al., 2010, 1995; Schwartz et al., 2012). Some MK areas were later subdivided into additional geologic localities to designate significant geological samples (e.g., GT6/7-1) or geological trenches (e.g., MK80-T1) (Schwartz et al., 2012). The 1993-1994 research expeditions led to the discovery of two fragmentary hominin remains tentatively attributed to the genus *Homo* (Frost et al., 2012; Kaiser et al., 2010; Schwartz et al., 2012). Also, more collections were made on vertebrate remains belonging to seven

families: Cercopithecidae, Elephantidae, Equidae, Rhinocerotidae, Suidae, Hippopotamidae, and Bovidae all tentatively assigned to the late Pliocene period <2.5 Mya (Kaiser et al., 2010).

During the 2000s, research activities continued at the Manyara Beds, which consolidated the previously established geology of the area, resulted in the recovery of more vertebrate remains, and documented more archaeological sites. Also, greater efforts were made to understand early hominin behavior and ecology (Bachofer et al., 2014, 2018; Frost et al., 2012; Wolf et al., 2010). As a result of the research conducted in the early 2000s, more fossil remains have been identified, expanding the known fauna assemblage to include significant collections of bovids (Antilopini, Hippotragini, Bovini, Reduncini) equids (*Equus* and *Eurygnathohippus*), and suids (*Nyanzachoerus kanamensis*, *Metridiochoerus andrewsi*, *Metridiochoerus compactus*, and *Phachoecorus* sp). Other fossils include Cichlidae, Osteichthyes, Chelonidae, Crocodilia, Giraffidae, *Hippopotamus*, *Ceratotherium*, *Elephas*, Carnivora (presumably *Panthera*), Thryonomyidae (Rodentia), Cercopithecidae, and Hominidae (Primates) (Frost et al., 2012, 2017; Kaiser et al., 2010; Wolf et al., 2010).

In the Manyara Beds, MK 4 Site emerged as the primary fossil and artifact collection site (Frost et al., 2012, 2017; Giemsch et al., 2018; Kaiser et al., 2010; Schwartz et al., 2012; Wolf et al., 2010). However, the association between fossil fauna remains and stone tools is poorly understood (Giemsch et al., 2018; Kaiser et al., 2010; Schwartz et al., 2012, 2012; Wolf et al., 2010). Nevertheless, substantial research has been done concerning the origin of the fossil fauna and its mode of accumulation. The fauna assemblages showed a high percentage of carnivore tooth marks, and hence carnivores are said to be the primary agent of accumulation (Frost et al., 2012, 2017; Giemsch et al., 2018; Kaiser et al., 2010; Schwartz et al., 2012; Wolf et al., 2010).

In terms of archaeology two lithic inventory exists (i) Series 1, derived from surface collections and dominated by handaxes made of volcanic rocks; and (ii) Series 2, derived from excavation and dominated by small quartz tools corresponding best to the Oldowan inventory from Olduvai Gorge (Kaiser et al., 2010). Giemsch et al. (2018) conducted a detailed analysis of the Series 1 (Acheulean) artifacts obtained from the surface at MK 4, MK 91, MK 101, and MK 123. Handaxes, flakes, flake tools (scrappers), and cores dominate the lithic assemblage (Giemsch et al., 2018). The dominant raw materials are basalt at MK 4 and 91, and quartzite at MK 101 and 123. Both raw materials occur in the immediate vicinity of the sites (Giemsch et al., 2018; Kaiser et al., 2010; Shubi, 2016). The Series 2 lithic assemblage is dominated by a light-duty tool kit comprised of cores, polyhedrons, core scrapers, scrapers, and choppers (Kaiser et al., 2010). In Series 2, the dominant raw material is quartz. Tool sizes are smaller than 7 cm in length, and tools are made from flakes and chips. Kaiser et al. (2010) proposed that the difference between the Acheulean tools from the

surface and those from the excavation is not attributable to the sorting process in the shallow water zone of the paleo-lake but, rather, that a tiny area at the site (where excavated tools occur) represents evidence of special economy.

The geology, sedimentology, and stratigraphy of the paleolake Manyara deposits have received some limited study, but little is known about the ancient environment and its relationship with hominin habitat use at this location. Previous research on the bovid community composition (n=41) suggests that the lower Manyara Beds had a mixture of open and closed woodland habitats (Frost et al., 2012; Giemsch et al., 2018; Kaiser et al., 2010). The upper member was dominated by grass-dependent bovids (Kaiser et al., 2010). Stable carbon isotopes, mesowear, and microwear analyses on equid teeth from the lower member suggested a grazing diet in a C<sub>4</sub>-dominated environment (Wolf et al., 2010). However, these findings are derived from a small sample of equid molars (n=8) for stable isotope analysis (Wolf et al., 2010) and bovid teeth (n=41) for bovid community composition (Kaiser et al., 2010). The imprecise nature of these previous paleohabitat studies necessitates a micro-botanical analysis of the Manyara Beds to generate detailed paleoenvironmental data.

## Research Objectives

The overall goal of this dissertation is to establish a detailed paleoenvironmental reconstruction of the Manyara Beds. There are three main objectives. The first is to examine phytolith production by plants and their preservation in modern soils in the vicinity of the Manyara Beds. The second is to document vegetation change through time and space and to reconstruct hominin microhabitats by examining phytolith assemblages from the upper 5.5 meters of the lower member and the contact zone between the Lower and Upper Members of the Manyara Beds. This zone is where most artifacts and fossils are found (Frost et al., 2012; Schwartz et al., 2012). The third objective is to identify the phytolith types found adhering to stone tool that could potentially assist in determining plants that hominins are using. I approach each of the three objectives of this dissertation as an independent study. These objectives were ultimately achieved by examining the following broad questions, each corresponding to a chapter in the dissertation.

## Chapter 2

*Question 1: What phytoliths are preserved in the modern soils at the vicinity of the Manyara Beds, and how do they differ from those found in ancient assemblages?*

This chapter examines modern phytolith assemblages in the vicinity of the Manyara Beds to establish a reference baseline for interpreting ancient phytoliths in Chapter 3. Phytolith analysis has been successfully employed as a microbotanical technique for vegetation reconstruction at Plio-Pleistocene hominin sites in Africa (Albert et al., 2006; Esteban et al., 2017; Mercader et al., 2009,

2019). The application of phytoliths in paleoenvironmental reconstruction often goes hand in hand with the study of phytolith production in modern plants and soils. Studies of phytolith production in modern plants and soils are conducted to understand how specific vegetation types/plant communities are represented in the soil or sediment record (Cabanès et al., 2011; Cabanès & Shahack-Gross, 2015; Madella & Lancelotti, 2012; Piperno, 2006). Such studies help to develop an understanding of pre-deposition and post-deposition effects on phytoliths after being released into soils (Esteban et al., 2017; Madella and Lancelotti, 2012; Piperno, 2006). Pre-deposition factors such as the plant's genetics and environment influence the forms and sizes of phytoliths produced, subsequently influencing phytolith durability and survival rates. The size and the level of silicification of phytolith forms creates different levels of durability for phytoliths after being released into soils (Cabanès & Shahack-Gross, 2015). Post-deposition processes such as dissolution (chemical attack) and translocation may remove or even sometimes add phytoliths to a sediment record (Madella & Lancelotti, 2012; Piperno, 2006).

One of the fundamental questions investigated in many paleoenvironmental studies is how well soil phytoliths reflect phytoliths produced by modern vegetation. In Africa, several studies have been carried out to address this question using modern plants and soils in the vicinity of various Plio-Pleistocene hominin sites (Albert et al., 2006; Esteban et al., 2017; Kinyanjui, 2013, 2018; Mercader et al., 2009). These studies aimed to establish criteria for examining the accuracy and reliability of phytoliths to interpret ancient phytoliths assemblages.

Modern vegetation and surface soils in the vicinity of the Manyara Beds have not been sampled for phytoliths. Vegetation types in the setting of the Manyara Beds belong to the great Somali-Maasai phytogeographical region (White, 1983). Woodlands and grasslands dominates, specifically *Acacia* and *Commiphora*, which are widespread in the study area (Ruffo et al., 2002; White, 1983). For the current study, modern phytolith assemblages surrounding the Manyara Beds needed to first be characterized. Once established, this will be applied to study the ancient assemblages at the Manyara Beds to address taphonomic issues. Twenty-one plants and twenty-five composite modern surface soils, some obtained directly from underneath the plants, were collected from the surroundings of the Manyara Beds for phytolith analysis.

Predictions:

1. I expect to find high phytolith production in plants, although not all morphotypes will be preserved in the soils beneath. I anticipate that heavily silicified cells, like short cells, will tend to have a higher representation in soils than the less silicified forms such as stomata, hairs, hat-shaped forms in sedge, large sized long cells, and thin epidermal cells, which dissolve quickly after deposition (Albert et al., 2006; Cabanès et al., 2011; Madella &

Lancelotti, 2012; Piperno, 2006; Strömberg, 2004). Previous research from the *Acacia-Commiphora* ecosystem demonstrates that various forms of tabular, blocks, globular facetate, short saddles, rondels, and small bilobates with concave ends are found. However, the short cell phytoliths are not overrepresented in the soils (Mercader et al., 2019). Therefore, it is reasonable to predict that grass short cell phytoliths will be less abundant in the *Acacia-Commiphora* ecosystem of the Manyara Beds and elongate/tabular forms and the morphotypes from woody dicots will be well represented. Therefore, vegetation boundaries can be easily discerned in the *Acacia-Commiphora* ecosystem.

2. As a result of different taphonomic processes that act on modern phytolith assemblages, I expect to find various forms of destruction. Breakage creates fragmented particles in phytolith assemblages, which are often difficult to identify. For instance, larger phytoliths and narrow points of grass phytolith morphotypes such as the mid-shank of bilobates tend to break easily (Madella & Lancelotti, 2012). Regarding grass silica short cells, I expect to see more saddles and/or rondel types than bilobates. Typically, their taxonomic significance in fossil assemblages cannot be easily established; this might bias vegetation interpretation (Alexandre et al., 1997; Madella & Lancelotti, 2012; Piperno, 2006).

### Chapter 3

*Question 2: Were there any vegetation cover changes through time and space in the lower Manyara Beds? What kind of microhabitats were hominins using in the Lake Manyara region during the Middle Pleistocene?*

This chapter reconstructs the plant ecosystems that characterized the transition from the lower member towards the contact of the lower-upper Manyara Beds. My focus will be on the top 5.5 meter of the lower member, dated between 780,000-633,000 years ago represents a 147,000-year paleoenvironmental record. This section is best exposed at two hominin sites, MK 4 and MK 2 (Schwartz et al., 2012). Previous research has shown this to be the most fossil and artifact-rich section of the Manyara Beds (Frost et al., 2012; Giemsch et al., 2018; Kaiser et al., 2010). Sediments for phytolith analysis were collected vertically at archaeological sites MK 4, MK 2, MK 17, and other non-archaeological sites near the Makuyuni river.

Predictions:

1. In completing a paleoenvironmental reconstruction, I anticipate observing a series of vegetation transitions corresponding to the expansion and contraction of the lake through time and space. The lacustrine deposits at MK 4 have been interpreted to represent the maximum lake level (Kaiser et al., 2010). Climate changes in the past are thought to have created seasonal shifts that resulted in the formation of lake flats while fostering a specific

succession of vegetation in the surroundings of the paleo-lake (Bachofer et al., 2018; Kaiser et al., 2010). As a result of the lake's variability, I expect to see periods when the lake margins are closer to sites and other times when the margins are further away. When these sites are closer to the lake edge, I expect to find evidence of plants indicative of the wetland environment. Likewise, I assume to find evidence of terrestrial plants such as gallery forest, woodlands, or grassland when the lake contracts. Previous research on the bovid community composition suggests that the Lower Manyara Beds had a mixture of open and closed woodland habitats in the vicinity of paleo-lake Manyara (Kaiser et al., 2010). In addition, stable carbon and oxygen isotope analysis on equid teeth suggests that Manyara equids fed mainly on C<sub>4</sub> grasses (Wolf et al., 2010).

2. Regarding hominin microhabitat use, it is reasonable to predict that hominins are using environments near lake shores because of their typical dependence on water and food resources such as wild game. Past research has indicated that Plio-Pleistocene hominin sites are concentrated in mosaic environments such as lakesides, often near open grassland or woodland habitats, or along riverside gallery forests (Bunn et al., 1980). At the Manyara Beds, both artifacts and hominin fossils have been found at the 5.5-meter transition layer between the Lower-Upper Member, which is said to indicate hominins' use of the near-shore environment during the early Middle Pleistocene (Bachofer et al., 2018; Giemsch et al., 2018; Kaiser et al., 2010). The most important archaeological site MK 4, has been interpreted to have been deposited in a shallow water lacustrine environment (Kaiser et al., 2010). Therefore, the results of this study will help categorize hominin ecological preferences within the Lower Manyara Beds.

## Chapter 4

### *Question 3: What phytoliths are preserved on stone tools?*

The Manyara Bed sites are rich in fossil fauna remains and stone tools, but their specific associations are not well known (Frost et al., 2012; Giemsch et al., 2018; Kaiser et al., 2010). At MK 4, for instance, it is possible to recover stone tools from their presumably original context through excavation. However, the available taphonomic work suggests that the fossil fauna assemblage at MK 4 represents a "carnivore attrition assemblage" (Kaiser et al., 2010:69). The absence of recognizable evidence of hominin activity in the accumulated fossil assemblage, and the fact that lithic tools occur at the same levels, suggest that MK 4 represents a palimpsest site where hominin lithic tools occur in areas where fossil fauna accumulate naturally (Frost et al., 2012; Kaiser et al., 2010). This study, therefore, attempts to document phytoliths preserved on stone tools to understand plant utilization by hominins at Manyara.

Several researchers have demonstrated the potential for recovering phytoliths from stone tools such as flakes, grinding stones, and pottery at more recent sites dating to the late Pleistocene and Holocene periods (e.g., Barton et al., 1998; Hardy et al., 2008; Hayes et al., 2018; Kealhofer et al., 1999; Piperno, 2009; Sobolik, 1996; Zarrillo et al., 2008). Many of these younger sites possess well-documented phytolith residues recovered from stone tools that represent specific domesticated plants. For instance, (Piperno et al., 2009) reported the presence of phytolith assemblages representing domestic species such as squash (*Cucurbita*) and maize from an assemblage of 21 ground stones and five chipped stone tools from Central Balsas River Valley, Mexico (8700 years ago). In another example, Chandler-Ezell et al. (2006) documented 16 stone artifacts with phytolith from casavas underground storage organs from a household layer dated between 2800-2400 years at Valdivia 3 site at Real Alto in Ecuador.

A total of 106 stone tools retrieved from a single excavation unit (4x2 meters trench) at MK 4 are available for analysis. The stone tools were excavated and collected along with their adhering matrixes. Soil samples from beneath the tools were collected and examined for phytoliths following methods developed by Hart (2011) and Dominguez-Rodrigo et al. (2001). Collecting the underlying sediment is essential to test for artifact contamination. Such data will provide a baseline to identify contaminated artifacts (see Hart, 2011).

Predictions:

1. I will not find phytoliths on all the assessed stone tools. Although archaeologists have documented plant residues on chipped stone artifacts since the mid-1970s (e.g., Briuer, 1976), few studies have demonstrated the potential for interpreting phytoliths at older assemblages (e.g., Barton et al., 1998; Kealhofer et al., 1999b; Sobolik, 1996). I assume that phytoliths on stone tools will be rare because of different phytolith preservation methods in different environments or because hominins did not use tools to exploit plants.
2. We know it is possible to recover phytolith residues on stone tools from ancient archaeological contexts (Dominguez- Rodrigo et al., 2001). For example, (Dominguez-Rodrigo et al., 2001) recovered dicot morphotypes from 1.5 Mya stone tools (two handaxes) from Peninj, Northern Tanzania. It is more likely to find dicot morphotypes and few monocots. It is possible to recover dicots from stone tools because of the activities such as chopping, carving, slicing, incising, scraping, and boring associated with working on woody plants (see Dominguez- Rodrigo et al., 2001; Hardy & Garufi, 1998).



## Research Design and Methodology

This dissertation required two phases of research. In this two-phase design, the first phase informed the second. The first phase involved detailed botanical sampling and modern soil collection while conducting a detailed vegetation surrounding the study sites in conjunction with botanist Mr. Emanuel Mboya (retired from the Natural History Museum of Arusha and who works part-time with the Tropical Pesticides Research Institute, National Herbarium of Tanzania section in Arusha). The first phase of research has two purposes: first, to provide control data for the interpretation of the ancient assemblage and secondly, to document phytolith production from plants that have not previously been documented in the *Acacia-Commiphora* ecoregion.

The second phase involved detailed excavations at archaeological and the establishing geo-sections both at archaeological and non-archaeological sites to sample ancient sediments. Two excavation units were opened at archaeological site MK 4 and MK 2. At MK 4, stone tools were sampled from a 4 x 2-meter excavation unit, and ancient sediments were collected vertically from a wall profile after excavation. At MK 2, ancient sediments were collected vertically after excavation from a 2 x 1meter excavation unit. Additionally, several geo-sections were opened at archaeological sites, MK 4 (n=2), and MK 17 (n=1), with the intent to collect ancient sediments from naturally exposed sediment profiles. With respect to non-archaeological sites, three geo-section were opened at naturally exposed sediment profiles along the Makuyuni river.

## Theoretical Framework

This dissertation aims to develop a detailed habitat reconstruction for hominins living in a small area of northern Tanzania during the early Middle Pleistocene between 780,000 and 633,000 years ago. A habitat is defined as a place where an organism or species lives. The habitat contains resources necessary for a given species to live and includes places unoccupied by the organism and aspects of the surrounding environment (Potts, 1998a, 1998b; Vrba, 1988, 1993). Habitats tend to fluctuate, and certain areas may shift, shrink, disappear, appear, and expand through time (Potts, 1998a, 1998b; Vrba, 1988, 1993). All species (including hominins) are habitat-dependent (Potts, 1998a, 1998b; Vrba, 1988, 1993). Therefore, understanding the typical early hominin habitat is critical to understanding key trends in human evolution such as bipedal walking, tool use, large brain development, language, and complex behaviors. Therefore, it is critical to characterize hominin habitats by examining questions such as, how did regional and local environmental conditions influence hominin food resources? and What climatic conditions did they experience?

Initial attempts to address these questions proposed that early hominin adaptations were shaped by increased aridification and its subsequent effects. This was known as the savanna hypothesis (Cohen et al., 2016; Lupien et al., 2020; Potts, 1998a; Potts et al., 2020; Shultz & Maslin,

2013). The savanna hypothesis suggested that long term aridity led to the development of an open savanna ecosystem, and through time subsequent challenges forced early hominins to adapt to these drying trends (Cohen et al., 2016; Lupien et al., 2020; Potts, 1998a, 2013; Potts et al., 2020; Shultz & Maslin, 2013; Trauth et al., 2015). However, from the 1980s to the present, scientists working in Africa have made significant advances in revealing fine-scale data with better chronological control demonstrating that the period was characterized by rapid, short periods of global climate variability and extreme environmental shifts driven by Earth's movements (Cohen et al., 2016; deMenocal, 2004; Lupien et al., 2020; Potts, 1998a, 2013; Potts et al., 2020; Shultz & Maslin, 2013; Trauth et al., 2015). This new data illustrates multiple incidences of environmental instability that coincide with the first and last appearance of hominins and other animals, new technological innovations, and dispersal events within the fossil record (Cohen et al., 2016; deMenocal, 2004; Grove et al., 2015; Lupien et al., 2020; Potts, 1998a, 2013; Potts et al., 2020; Shultz & Maslin, 2013; Trauth et al., 2005, 2007, 2015). This new paleoenvironmental and paleoclimate data led to the emergence of sophisticated ideas such as the turnover pulse, variability selection, and pulsed variability hypotheses to justify the mechanisms for the evolution of hominins and the ecosystems in which they lived (Cohen et al., 2016; deMenocal, 2004; Grove et al., 2015; Lupien et al., 2020; Potts, 1998a, 2013; Potts et al., 2020; Shultz & Maslin, 2013; Trauth et al., 2005, 2007, 2015; Vrba, 1988, 1993).

### **Drivers of Climate and Environmental Change**

In East Africa, long-term regional and global climate change seems to be controlled by the Earth's orbital movements and tectonic activity, especially in relation to the development of the EARS (Maslin et al., 2015; Potts, 1998a, 1998b; Potts & Faith, 2015; Shultz & Maslin, 2013; Trauth et al., 2007; Vrba, 1988).

**Earth orbit variations** alter the latitudinal and seasonal distribution of solar radiation, which directly affect climate by causing (i) sequential warming and cooling, (ii) reorganization of atmospheric circulation, and (iii) extreme variation in the intensity and geographic scale of seasonal rainfall in the tropics (Bartlein & Prentice, 1989; Bennett, 1990; Buis, 2020). Variation in solar insolation impacts the beginning and end of glacial periods (Bartlein & Prentice, 1989; Bennett, 1990; Buis, 2020). To calculate how much incoming solar radiation reaches the top of Earth, Serbian scientist Milutin Milankovitch examined three types of Earth orbital movement known as Milankovitch cycles; eccentricity, obliquity, and precession cycles which predict the occurrence of Ice Ages (Buis, 2020).

*Eccentricity* measures the departure in the shape of Earth's orbit around the sun from nearly circular (no eccentricity) to elliptical (eccentricity) (Buis, 2020; Campisano, 2012). Eccentricity has two cyclicities, a short one with an average of 100,000 years and a longer cycle with a periodicity of

413,000 years (Bartlein & Prentice, 1989; Campisano, 2012). Eccentricity affects temperature and therefore accounts for the different lengths of seasons in the Northern Hemisphere (Buis, 2020). When eccentricity is low (nearly circular), the length of seasons is equal, and higher eccentricity causes seasons to have slightly different lengths (Buis, 2020). Earth's eccentricity is near its circular shape and gradually decreases in the short phase of about 100,000 years (Buis, 2020). The total variation in global annual insolation due to the eccentricity cycle is minimal because of minor changes in eccentricity (Buis, 2020). Therefore, they cause a slight change in annual seasonal climate variations.

*Obliquity* measures the angle of Earth's axis tilt during rotation as it travels around the sun (Buis, 2020). For the past 1 million years, orbit inclination has varied between 22.1 and 24.5 degrees, at 41,000 year cycles (Bartlein & Prentice, 1989; Buis, 2020; Campisano, 2012). When the tilt angle is high, it creates more extreme seasons. Sustained inclination causes periods of deglaciation, while low tilts cause glaciation in higher latitudes (Buis, 2020). Earth's axis is currently sloped at 23.4 degrees and is slowly decreasing to complete the 41,000 years cycle (Buis, 2020). When obliquity decreases, it slowly moderates Earth's seasons causing progressively warmer winters and cooler summers.

*Precession* defines the movement of the Earth's axis rotation away from a fixed position of stars with a periodicity of 19,000 to 23,000 years (Bennett, 1990; Campisano, 2012; Trauth et al., 2005). The movements correspond to tidal forces caused by the gravitational pull of the Sun and Moon, which causes Earth to protrude at the equator and alter its rotation (Bennett, 1990; Buis, 2020). Seasonal precession effects make seasons severe in one hemisphere and less extreme in another.

Evidence from ocean cores on the West and East coast of Africa, and Lake cores from the EARS lakes has shown that African climate and vegetation covers were highly variable from the early Pliocene to the present (Potts, 1998a, 2013). For instance, lake cores and sediments from hominin sites from Olduvai Gorge, Turkana, and other localities document several short-term and long-term climate changes that affected the adaptive ecology of Plio- Pleistocene hominins (Behrensmeyer et al., 1997; Potts, 2002, 2013). On the other hand, ocean cores in the West and East coasts of Africa document three phases of wet conditions in East Africa at 2.7-2.5 mya, 1.9-1.7 mya, and 1.1-0.1 mya superimposed on a longer-term trends on aridification (deMenocal, 2004; Trauth et al., 2007). This long-term aridification began around 2.8 mya, linked to the precision forcing of 23 to 19 Kya, 1.7 Mya related to the 41 kya Obliquity, and approximately 1.0 mya associated with eccentricity force dominated by the 100 kya cycle (Potts, 1998a; Trauth et al., 2005, 2007).

The available detailed climatic reconstructions in the African Middle Pleistocene climate revealed very few connections between climate variability and orbital forcing. For instance, the rainfall variations between 1.0 Mya and 0.8 Mya are associated with orbital forcing, mainly eccentricity (Castañeda et al., 2016; Potts et al., 2020). Conversely, a detailed analysis of the Middle Pleistocene deposits from Lake cores drills recovered by the Olorgesailie Drilling Project and Koora Basin revealed climatic conditions with very little influence of orbital forcing (Potts et al., 2020). In their multiproxy analysis, Potts et al. (2020) highlighted incidences of increased resource fluctuation as the leading cause of the transition from the Early Stone Age Industry (Acheulean) to the early Middle Stone Age (MSA) technology between 500 and 300 kya. Also, fauna turnover whereby megagrazers of the southern Kenya rift persisted from 1.0 mya to 500 kya then declined around 400 kya because of landscape fragmentation and resource fluctuation (Potts et al., 2020; Potts & Faith, 2015). They suggested that increased volcano-tectonic activities that caused faults in both basins disrupted hydrological systems such as surface runoff, soil moisture, water availability, disrupted woody/grassy vegetation, and created patchiness of resources in the landscape in response to climatic variations (Potts et al., 2020).

#### The East African Rift System Lakes and Human Evolution

The EARS is a critical place for understanding human evolution. Several Plio-Pleistocene sites document hominin utilization of lakeshore habitat (e.g., Olduvai, Natron (Tanzania), Magadi, Olorgesailie, Baringo-Bogoria, Turkana (Kenya), Omo and Afar (Ethiopia), which illustrate the presence of numerous large and deep lakes (Maslin et al., 2015; Potts, 1998a, 2013; Potts et al., 2020; Roach et al., 2016; Shultz & Maslin, 2013; Trauth et al., 2005). Several researchers have acknowledged that near-water habitats, specifically the availability of freshwater near the EARS paleo-lakes and the presence of foraging resources such as plants and animals, created selective pressures altering the behavior and evolution of the genus *Homo* in East Africa (Maslin et al., 2015; Potts, 1998a, 2013; Potts et al., 2020; Roach et al., 2016; Shultz & Maslin, 2013; Trauth et al., 2005).

Recently, lake core drilling projects have shown the importance of the Rift lakes in providing climatic indicators and a landscape analog for evaluating missing environmental records relating to critical evolutionary events (Cohen et al., 2016; Potts et al., 2020; Shultz & Maslin, 2013). Also, a considerable number of researchers agree that the appearance and disappearances of EARS lakes created selective environmental pulses linked to numerous developments in human evolution, including a dispersal to Eurasia, an increase in brain size, the development of new technologies, and the emergence of complex social behaviors (deMenocal, 2004; Maslin et al., 2015; Potts, 2002, 2013; Potts & Faith, 2015; Shultz & Maslin, 2013).

## Environmental Hypotheses of Hominin Evolution

**The turnover pulse hypothesis (TPH):** argues for large-scale climatic change causing progressive habitat transformation as the driving force behind speciation, extinction, and dispersal events (Cohen et al., 2016; Donges et al., 2011). Vrba (1985, 1988, 1993, 1992) observed periods of extreme and rapid change in the African ungulate fossil records caused by environmental changes during the Late Pliocene 2.5 mya. These environmental shifts caused rapid extinction (occurring in pulses) for species with specialized diets and the speciation of new species with a more generalized diet. The TPH asserts that fluctuations in climate impact the distribution of resources in the physical environment and that this can split animal populations into geographically and genetically isolated groups that evolve into new species (Vrba, 1988, 1993). The TPH utilized evidence from the global climatic changes associated with the expansion of the ice sheets at the poles and tectonic changes that influenced the local climate (Vrba, 1988). The period around 2.5 mya saw global cooling events (the shifts from warm, moist conditions to colder ones), which initiated the spread of a more arid and open vegetation environment in East Africa.

The bovid faunal record from the Turkana (Kenya) and Omo (Ethiopia) Basins were analyzed and showed multiple events of faunal turnover and extinction around 2.6-2.4 mya. These events were associated with the change from forested to open grassland habitats in these regions. Vrba (1988) also suggested that the TPH can be applied to hominins; specifically, the emergence and dispersal of genus *Homo* and the extinction of *Paranthropus*, which were associated with the emergence of arid open-grassland environments (Potts, 1998a; Vrba, 1988). The TPH was criticized for its poor application to paleoanthropological records. For instance, fossil faunas in East Africa show a slower rate of turnover events than should be predicted by the turnover hypothesis (e.g., Kingston et al., 1994). A study by Behrensmeyer et al. (1997) established a more refined late Pliocene chronology for the Turkana Basin from 3 to 1 mya. They documented the persistence of some specialized species from 3 to 2 mya. It highlighted a prolonged turnover between 2.5 to 0.7 mya resulting in a gradual change from forested to more open habitats not a 'pulse' as previously suggested.

**The Variability Selection Hypothesis (VSH):** The TPH highlighted multiple periods of environmental fluctuation, creating the basis for the variability selection hypothesis (Potts, 1996b, 1998a, 1998b). The VSH and TPH share one thing in common: each hypothesis predicts how evolutionary events occur in response to an inevitable progression of past environments (Potts, 2002). The TPH assumes cooling and drying as relevant drivers of hominin evolution, while the VSH suggests that increased environmental variability and resource uncertainty is vital in human evolution (Potts, 2002).

The VSH hypothesis predicts the adoption of versatile behaviors and survival strategies in response to increasingly variable environments (Potts, 1998a, 1998b, 2002; Potts & Faith, 2015). Potts (1996b:922) presents a conceptual model (see figure 1-3) that shows how the lake environment fluctuates, creating periods of extreme variability that could drive extinction and speciation events (Potts, 1996b, 1998a, 1998b; Potts & Faith, 2015). The model analyses concern competition between 'specialist' alleles and either 'generalist or versatile' alleles at a given location. Versatile organisms specialize in dealing with habitat fluctuations, while specialist organisms lives in a restricted environment (Grove, 2011; Potts, 1998b; Vrba, 1993). That is, hominin species and populations will experience different degrees of natural selection because of progressive shifts in the environment, and eventually, a group will be isolated. As a result, over multiple periods of environmental oscillations some groups would develop a broad set of alleles (adaptations) influencing various aspects of an organism's diet, cognition, and other function may become dominant because they enrich environmental data processing and novel problem solving (Potts, 1998a, 1998b, 2013). These populations (the versatile) will be flexible and therefore persisting over a long period of environmental instability (Potts, 1998a, 1998b, 2013). This is the potential means by which human evolution occurred.

Furthermore, Potts (1998b:85) suggests that variability selection produces "complex structures or behaviors designed to respond to novel and unpredictable adaptive settings". This flexibility can be seen in the anatomical structures and behavioral changes found in the paleoanthropological and archaeological records, including the locomotor adaptation (bipedalism) of early australopithecines, specific dental structures or foraging strategies that show a shift to newly available food types, large brain and complex cognitive response, and the emergence of distinct social behaviors for a broad range of mating or demographic groups (Grove, 2011; Potts et al., 2020). VSH strongly advocates for hominin adaptation in response to environmental instabilities rather than to a one comparatively stable habitat experienced over a prolonged period. Potts ( 1998a, 1998b) and Potts et al. (2020) found support for their VSH by examining the large mammal fossil fauna records from the southern Kenyan sites of Olorgesailie and Lainyamok, dated between 922 to 350 kya. Five prominent herbivore lineages went extinct during this period (Potts et al., 2020). The extinct forms include the zebra *Equus Oldowayensis*, the monkey *Theropithecus oswaldi*, the elephant *Elephas recki*, the hippo *Hippopotamus gorgeous*, and the pig genus *Metridiochoere*. Compared to the earliest members of their clades these species had massive bodies and possessed massive craniodental structures highly specialized for grazing (Potts, 1998b; Potts et al., 2020). Over time, the species' lineage grew bigger showing that it could cope with the environment by eating the abundant tough and coarse grasses (Potts et al., 2020). When grazing

grasses became scarce, the highly specialized *Theropithecus* competed with other versatile species but ultimately went extinct about 500 Kya (Potts, 1998b; Potts et al., 2020).

**Pulsed variability selection hypothesis (PVSH):** This is a slight variation to the VSH focusing on the role of short-scale extreme wet-dry climate phases (Maslin et al., 2015; Shultz & Maslin, 2013; Trauth et al., 2005, 2007). The hypothesis is based on the distinctive climate within EARS and lake levels acting as a driver of human evolution for the last 5 mya (Maslin et al., 2015; Shultz & Maslin, 2013; Trauth et al., 2005, 2007). Proponents of PVSH suggest that large lakes appeared and disappeared on a precession timescale following a sequence of alternating wet and dry conditions that caused significant vegetation shifts within the EARS (Shultz & Maslin, 2013). Several periods of deep lakes which existed between 4.6-4.4 mya, 4.0-3.9 mya, 3.6-3.3 mya, 3.1-2.9 mya, 2.7-2.5 mya, 2.0-1.7 mya, 1.1-0.9 mya, and 0.2-0 mya (Maslin et al., 2015; Trauth et al., 2015). They suggested further that the humid phases in East Africa were at 2.7- 2.5 mya, 1.8-1.6 mya, and 1-0.7 mya following the 400 kya eccentricity cycle (Shultz & Maslin, 2013). During these periods, changes in solar precision cycles increased the monsoonal system causing more rains in East Africa, thereby increasing the sizes of lakes (Maslin et al., 2015; Shultz & Maslin, 2013; Trauth et al., 2007). Increasing diatomaceous lake sediments document high lake levels during these times (Shultz & Maslin, 2013).

These expanded lakes would act as geographical barriers to hominin populations, allowing for diversification in diet and other adaptive behaviors across the region, resulting, at times, in speciation (Maslin et al., 2015). An excellent example of this is the occurrence of several hominin species, including *P. boisei*, *H. erectus*, *H. habilis*, and *H. rudolfensis*, during the period of maximum lake coverage at Koobi Fora (Kenya) around 1.9-1.8 mya (Shultz & Maslin, 2013). However, some authors (e.g., Warren et al., 2019) postulate that the degree of interspecific variability and extent to which these barriers acted as drivers of speciation is still up for debate.

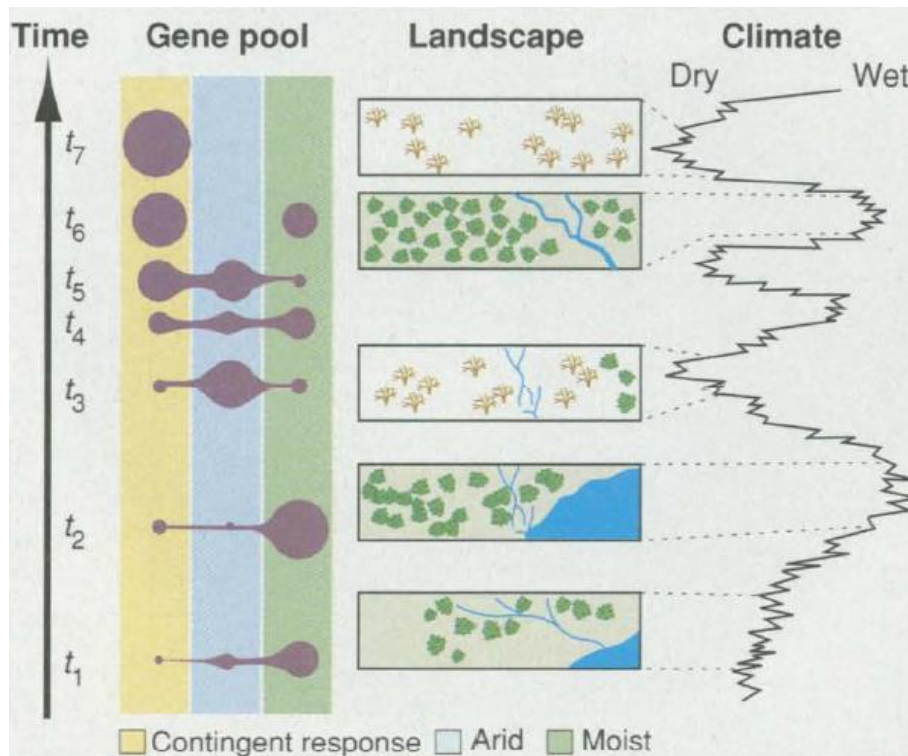


**Figure 1-3:** Hypothetical gene frequency fluctuation in response to varying environments to assess variability selection.

The right column shows environmental shifts reflected in the landscape at  $t_1$ , the lake is fed by river systems (wet conditions prevail) in open woodland. Following several extreme wet and dry periods, surface water disappears in  $t_7$ . The left column gene frequency fluctuations in response to varying environments. The size of the gene pool shows relative fitness in a specific time with response to habitat in: (a) features favored moist and extremely vegetated environments, (b) features preferred arid, open habitats, and (c) features that enable novel response and the ability to adapt and adjust to environmental change dominate  $t_5$  to  $t_7$ , Adapted from Potts (1996b:922).

### The Manyara Beds and Environmental Hypotheses

Regarding the reconstruction of early hominin habitats at the Manyara Beds, Potts' (1996b, 1998a, 1998b) VSH presents a model that better explaining hominins adaptation to varying environments. The VSH predicts that versatile hominins and other species will be found in varied habitats (Potts, 1998a, 1998b, 2002). The Manyara Beds near Makuyuni represent the period associated with the highest water level of the paleo-lake Manyara (Kaiser et al., 2010; Schwartz et al., 2012). Like other paleo-lakes within the EARS, the Manyara Beds exhibit various evidence of the paleo-lake Manyara's high and low water levels, therefore offering credible records for examining the VSH hypothesis. Using Potts (1996b, 1998b) model and an analysis of different lake levels (appearance and disappearance) it is possible to predict the relative periods in which certain organisms or behavior may yield higher fitness in dry open habitats, moist and wet habitats, or during recurrent changes in both conditions.



Drawing on phytolith remains from a detailed stratigraphic, this study has the potential to test VSH at the Manyara Beds. For instance, the C<sub>4</sub> vegetation reconstruction completed by Wolf et al. (2010) implies the presence of grasses mainly adapted to arid conditions. In contrast, phytolith analysis in this study can give a better record of vegetation indicators across local (during dry phases) and regional (e.g., fluvial transportation during wet periods) scales (Piperno, 2006; Potts et al., 2020; Rashid et al., 2019). In addition, phytoliths can discriminate the density on tree and grass cover in the paleolandscape. Finally, in a C<sub>4</sub> dominant environment, phytoliths can distinguish between the short grasses (Chloridoideae) adapted to warm and dry climates and the tall grasses (Panicoideae) that dominate in warm and humid areas (Barboni & Bremond, 2009; Potts et al., 2020). This discrimination helps to link past vegetation with water distribution in the paleolandscape (Barboni & Bremond, 2009; Bremond et al., 2008). In this manner, climatic fluctuations through time will be measured, which is essential for testing VSH. This study, therefore, will reveal how Acheulean tool-making hominins and the megagrazer populations in the Manyara Beds were able to cope with fluctuating habitats.

### **Significance**

This study will contribute to anthropological theory and the debate about the role played by aridity and seasonality in human evolution by advancing the current knowledge regarding variability selection hypothesis (Potts, 1996b, 1998a, 1998b, 2002). The VSH stresses the role of environmental instability as a driver for adaptations and extinction of some lineages (Potts, 1996b, 1998b). Despite the rarity of hominin remains, the Manyara Beds have archaeological localities exhibiting clear hominin occupation. There is no paleobotanical data for the Manyara Beds with which to examine climatic change and environmental fluctuation during the Middle Pleistocene. Unlike previous paleoecological studies of the Manyara Beds, the micro-botanical analysis in this study will provide a spatially and temporally fine-scale resolution of the paleoenvironment based on the identification of individual plant taxa. This will allow for a detailed reconstruction of the vegetation and provide information on seasonality and overall changes in aridity that occurred during the early Middle Pleistocene. These results will shed light on the adaptive micro-habitats of hominins and will help to support or refute Potts (1996b, 1998b, 2002) ideas for the VSH. Special emphasis will be given to any shifts between grasslands and woodlands, and the relationship between grassland development and climatic conditions (Bremond et al., 2008; Piperno, 2006).

Moreover, Acheulean tools dominate the archaeological records of the Early and Middle Pleistocene and existed in Africa and Eurasia for over a million years (Finkel & Barkai, 2018; Herries, 2011; Texier, 2018). Many paleoanthropologists and paleolithic archaeologists have focused on understanding how and when Acheulean tools originate (e.g., Finkel & Barkai, 2018; Gallotti &

Mussi, 2018; Herries, 2011; Texier, 2018), but, we know very little about how the Acheulean period ended. Many hypotheses have been proposed to explain the factors that led to the transition from larger cutting tools such as the hand axes and cleavers of the Acheulean Industry to the blades manufactured using the Levallois and the later point traditions of the Middle Stone Age (Herries, 2011). Climatic variability and its impact on resource distribution has been proposed to play a critical role in this technological transition (Grove et al., 2015; Potts et al., 2020). The phytolith data from this study will provide environmental data that will help characterize the environments of the latest Acheulean occupation at the Manyara Beds.

Finally, the study area is dated to 780,000 to 633,000 years ago, a timeframe that coincides with the emergence of *Homo heidelbergensis* around 800,000 to 700,000 years ago (Rightmire, 2001, 2004; Stringer, 2012). As *Homo heidelbergensis* is a putative ancestor of our own species, the data generated in this study will contribute to broad anthropological questions concerning the origins of *Homo sapiens*. In summary, a detailed paleoenvironmental record from the Manyara Beds will add to the current state of knowledge on the role of the East African Rift Valley lakes in human evolution, dispersal scenarios, and adaptation to increasingly arid and variable habitats.

## Literature Cited

- Albert, R. M., Bamford, M. K., & Cabanes, D. (2006). Taphonomy of phytoliths and macroplants in different soils from Olduvai Gorge (Tanzania) and the application to Plio-Pleistocene palaeoanthropological samples. *Quaternary International*, 148(1), 78–94.  
<https://doi.org/10.1016/j.quaint.2005.11.026>
- Alexandre, A., Meunier, J.-D., Lézine, A.-M., Vincens, A., & Schwartz, D. (1997). Phytoliths: Indicators of grassland dynamics during the late Holocene in intertropical Africa. *Palaeogeography, Palaeoclimatology, Palaeoecology*, 136(1–4), 213–229. [https://doi.org/10.1016/S0031-0182\(97\)00089-8](https://doi.org/10.1016/S0031-0182(97)00089-8)
- Bachofer, F., Quénéhervé, G., Hertler, C., Giemsch, L., Hochschild, V., & Maerker, M. (2018). Paleoenviromental Research in the Semiarid Lake Manyara Area, Northern Tanzania: A Synopsis. In C. Siart, M. Forbriger, & O. Bubenzer (Eds.), *Digital Geoarchaeology* (pp. 123–138). Springer International Publishing. [https://doi.org/10.1007/978-3-319-25316-9\\_8](https://doi.org/10.1007/978-3-319-25316-9_8)
- Bachofer, F., Quénéhervé, G., & Märker, M. (2014). The Delineation of Paleo-Shorelines in the Lake Manyara Basin Using TerraSAR-X Data. *Remote Sensing*, 6(3), 2195–2212.  
<https://doi.org/10.3390/rs6032195>
- Barboni, D. (2014). Vegetation of Northern Tanzania during the Plio-Pleistocene: A synthesis of the paleobotanical evidences from Laetoli, Olduvai, and Peninj hominin sites. *Quaternary International*, 322–323, 264–276. <https://doi.org/10.1016/j.quaint.2014.01.016>
- Barboni, D., & Bremond, L. (2009). Phytoliths of East African grasses: An assessment of their environmental and taxonomic significance based on floristic data. *Review of Palaeobotany and Palynology*, 158(1–2), 29–41. <https://doi.org/10.1016/j.revpalbo.2009.07.002>
- Bartlein, P. J., & Prentice, I. C. (1989). Orbital variations, climate and paleoecology. *Trends in Ecology & Evolution*, 4(7), 195–199. [https://doi.org/10.1016/0169-5347\(89\)90072-4](https://doi.org/10.1016/0169-5347(89)90072-4)
- Barton, H., Torrence, R., & Fullagar, R. (1998). Clues to Stone Tool Function Re-examined: Comparing Starch Grain Frequencies on Used and Unused Obsidian Artefacts. *Journal of Archaeological Science*, 25(12), 1231–1238. <https://doi.org/10.1006/jasc.1998.0300>
- Behrensmeyer, A. K., Todd, N. E., Potts, R., & McBrinn, G. E. (1997). Late Pliocene Faunal Turnover in the Turkana Basin, Kenya and Ethiopia. *Science*, 278(5343), 1589–1594.  
<https://doi.org/10.1126/science.278.5343.1589>
- Benito-Calvo, A., Barfod, D. N., McHenry, L. J., & de la Torre, I. (2014). The geology and chronology of the Acheulean deposits in the Mieso area (East-Central Ethiopia). *Journal of Human Evolution*, 76, 26–38. <https://doi.org/10.1016/j.jhevol.2014.08.013>

- Bennett, K. D. (1990). Milankovitch cycles and their effects on species in ecological and evolutionary time. *Paleobiology*, 16(1), 11–21. <https://doi.org/10.1017/S0094837300009684>
- Bremond, L., Alexandre, A., Wooller, M. J., Hély, C., Williamson, D., Schäfer, P. A., Majule, A., & Guiot, J. (2008). Phytolith indices as proxies of grass subfamilies on East African tropical mountains. *Global and Planetary Change*, 61(3–4), 209–224. <https://doi.org/10.1016/j.gloplacha.2007.08.016>
- Buck, L. T., & Stringer, C. B. (2014). *Homo heidelbergensis*. *Current Biology*, 24(6), R214–R215. <https://doi.org/10.1016/j.cub.2013.12.048>
- Buis, A. (2020, February). Milankovitch (Orbital) Cycles and Their Role in Earth’s Climate. *NASA’s Jet Propulsion Laboratory*.
- Cabanes, D., & Shahack-Gross, R. (2015). Understanding Fossil Phytolith Preservation: The Role of Partial Dissolution in Paleoecology and Archaeology. *PLOS ONE*, 10(5), e0125532. <https://doi.org/10.1371/journal.pone.0125532>
- Cabanes, D., Weiner, S., & Shahack-Gross, R. (2011). Stability of phytoliths in the archaeological record: A dissolution study of modern and fossil phytoliths. *Journal of Archaeological Science*, 38(9), 2480–2490. <https://doi.org/10.1016/j.jas.2011.05.020>
- Campisano, C. J. (2012). *Milankovitch Cycles, Paleoclimatic Change, and Human Evolution*. 4(5).
- Castañeda, I. S., Caley, T., Dupont, L., Kim, J.-H., Malaizé, B., & Schouten, S. (2016). Middle to Late Pleistocene vegetation and climate change in subtropical southern East Africa. *Earth and Planetary Science Letters*, 450, 306–316. <https://doi.org/10.1016/j.epsl.2016.06.049>
- Chandler-Ezell, K., Pearsall, D. M., & Zeidler, J. A. (2006). Root and Tuber Phytoliths and Starch Grains Document Manioc ( *Manihot Esculenta* ), Arrowroot ( *Maranta Arundinacea* ), and Llerén ( *Calathea* sp.) at the Real Alto Site, Ecuador. *Economic Botany*, 60(2), 103–120. [https://doi.org/10.1663/0013-0001\(2006\)60\[103:RATPAS\]2.0.CO;2](https://doi.org/10.1663/0013-0001(2006)60[103:RATPAS]2.0.CO;2)
- Cohen, A., Campisano, C., Arrowsmith, R., Asrat, A., Behrensmeyer, A. K., Deino, A., Feibel, C., Hill, A., Johnson, R., Kingston, J., Lamb, H., Lowenstein, T., Noren, A., Olago, D., Owen, R. B., Potts, R., Reed, K., Renaut, R., Schäbitz, F., ... Zinaye, B. (2016). The Hominin Sites and Paleolakes Drilling Project: Inferring the environmental context of human evolution from eastern African rift lake deposits. *Scientific Drilling*, 21, 1–16. <https://doi.org/10.5194/sd-21-1-2016>
- deMenocal, P. B. (2004). African climate change and faunal evolution during the Pliocene–Pleistocene. *Earth and Planetary Science Letters*, 220(1–2), 3–24. [https://doi.org/10.1016/S0012-821X\(04\)00003-2](https://doi.org/10.1016/S0012-821X(04)00003-2)
- Dominguez- Rodrigo, M., Serrallonga, J., Juan-Tresserras, J., Alcalá, L., & Luque, L. (2001). Woodworking activities by early humans: A plant residue analysis on Acheulian stone tools

- from Peninj (Tanzania). *Journal of Human Evolution*, 40(4), 289–299.  
<https://doi.org/10.1006/jhev.2000.0466>
- Donges, J. F., Donner, R. V., Trauth, M. H., Marwan, N., Schellnhuber, H.-J., & Kurths, J. (2011). Nonlinear detection of paleoclimate-variability transitions possibly related to human evolution. *Proceedings of the National Academy of Sciences*, 108(51), 20422–20427.  
<https://doi.org/10.1073/pnas.1117052108>
- Dupont, L. M., Caley, T., Kim, J.-H., Castañeda, I., Malaizé, B., & Giraudeau, J. (2011). Glacial-interglacial vegetation dynamics in South Eastern Africa coupled to sea surface temperature variations in the Western Indian Ocean. *Climate of the Past*, 7(4), 1209–1224.  
<https://doi.org/10.5194/cp-7-1209-2011>
- Esteban, I., De Vynck, J. C., Singels, E., Vlok, J., Marean, C. W., Cowling, R. M., Fisher, E. C., Cabanes, D., & Albert, R. M. (2017). Modern soil phytolith assemblages used as proxies for Paleoscape reconstruction on the south coast of South Africa. *Quaternary International*, 434, 160–179.  
<https://doi.org/10.1016/j.quaint.2016.01.037>
- Finkel, M., & Barkai, R. (2018). The Acheulean Handaxe Technological Persistence: A Case of Preferred Cultural Conservatism? *Proceedings of the Prehistoric Society*, 84, 1–19.  
<https://doi.org/10.1017/ppr.2018.2>
- Frost, S. R., Saanane, C., Starkovich, B. M., Schwartz, H., Schrenk, F., & Harvati, K. (2017). New cranium of the large cercopithecoid primate *Theropithecus oswaldi leakeyi* (Hopwood, 1934) from the paleoanthropological site of Makuyuni, Tanzania. *Journal of Human Evolution*, 109, 46–56. <https://doi.org/10.1016/j.jhevol.2017.05.007>
- Frost, S. R., Schwartz, H. L., & Giemsch, L. (2012). Refined age estimates and paleoanthropological investigation of the Manyara Beds, Tanzania. *Journal of Anthropological Sciences*, 90, 1–12.  
<https://doi.org/10.4436/jass.90001>
- Gallotti, R., & Mussi, M. (2018). Before, During, and After the Early Acheulean at Melka Kunture (Upper Awash, Ethiopia): A Techno-economic Comparative Analysis. In R. Gallotti & M. Mussi (Eds.), *The Emergence of the Acheulean in East Africa and Beyond* (pp. 53–92). Springer International Publishing. [https://doi.org/10.1007/978-3-319-75985-2\\_4](https://doi.org/10.1007/978-3-319-75985-2_4)
- Giemsch, L., Hertler, C., Märker, M., Quénéhervé, G., Saanane, C., & Schrenk, F. (2018). Acheulean Sites at Makuyuni (Lake Manyara, Tanzania): Results of Archaeological Fieldwork and Classification of the Lithic Assemblages. *African Archaeological Review*, 35(1), 87–106.  
<https://doi.org/10.1007/s10437-018-9284-4>

- Grass Phylogeny Working Group II. (2012). New grass phylogeny resolves deep evolutionary relationships and discovers C4 origins. *New Phytologist*, 193(2), 304–312.  
<https://doi.org/10.1111/j.1469-8137.2011.03972.x>
- Group, G. P. W., Barker, N. P., Clark, L. G., Davis, J. I., Duvall, M. R., Guala, G. F., Hsiao, C., Kellogg, E. A., & Linder, H. P. (2001). Phylogeny and Subfamilial Classification of the Grasses (Poaceae). *Annals of the Missouri Botanical Garden*, 88(3), 373. <https://doi.org/10.2307/3298585>
- Grove, M. (2011). Speciation, diversity, and Mode 1 technologies: The impact of variability selection. *Journal of Human Evolution*, 61(3), 306–319. <https://doi.org/10.1016/j.jhevol.2011.04.005>
- Grove, M., Lamb, H., Roberts, H., Davies, S., Marshall, M., Bates, R., & Huws, D. (2015). Climatic variability, plasticity, and dispersal: A case study from Lake Tana, Ethiopia. *Journal of Human Evolution*, 87, 32–47. <https://doi.org/10.1016/j.jhevol.2015.07.007>
- Hardy, B. L., Bolus, M., & Conard, N. J. (2008). Hammer or crescent wrench? Stone-tool form and function in the Aurignacian of southwest Germany. *Journal of Human Evolution*, 54(5), 648–662. <https://doi.org/10.1016/j.jhevol.2007.10.003>
- Hardy, B. L., & Garufi, G. T. (1998). Identification of Woodworking on Stone Tools through Residue and Use-Wear Analyses: Experimental Results. *Journal of Archaeological Science*, 25(2), 177–184. <https://doi.org/10.1006/jasc.1997.0234>
- Hart, T. C. (2011). Evaluating the usefulness of phytoliths and starch grains found on survey artifacts. *Journal of Archaeological Science*, 38(12), 3244–3253.  
<https://doi.org/10.1016/j.jas.2011.06.034>
- Hayes, E., Fullagar, R., Mulvaney, K., & Connell, K. (2018). Food or fiber craft? Grinding stones and Aboriginal use of *Triodia* grass (spinifex). *Quaternary International*, 468, 271–283.  
<https://doi.org/10.1016/j.quaint.2016.08.010>
- Herries, A. I. R. (2011). A Chronological Perspective on the Acheulian and Its Transition to the Middle Stone Age in Southern Africa: The Question of the Fauresmith. *International Journal of Evolutionary Biology*, 2011, 1–25. <https://doi.org/10.4061/2011/961401>
- Johnson, C. R., & McBrearty, S. (2012). Archaeology of Middle Pleistocene lacustrine and spring paleoenvironments in the Kapthurin Formation, Kenya. *Journal of Anthropological Archaeology*, 31(4), 485–499. <https://doi.org/10.1016/j.jaa.2012.05.001>
- Kaiser, T., Seiffert, C. C., Fiedler, L., Schwartz, H. L., Frost, S. R., & Nelson, S. V. (2010). Makuyuni, a new lower Palaeolithic hominid site in Tanzania. *Mitteilungen Hamburgisches Zoologischen Museum Institut*, 106, 69–110.
- Kaiser, T., Bromage, T. G., & Schrenk, F. (1995). Hominid Corridor Research Project update: New Pliocene fossil localities at Lake Manyara and putative oldest Early Stone Age occurrences at

- Laetoli (Upper Ndolanya Beds), northern Tanzania. *Journal of Human Evolution*, 28(1), 117–120. <https://doi.org/10.1006/jhev.1995.1010>
- Kealhofer, L., Torrence, R., & Fullagar, R. (1999). Integrating Phytoliths within Use-Wear/Residue Studies of Stone Tools. *Journal of Archaeological Science*, 26(5), 527–546. <https://doi.org/10.1006/jasc.1998.0332>
- Keller, C. M., Hansen, C., & Alexander, C. S. (1975). Archaeology and Paleoenvironments in the Manyara and Engaruka Basins, Northern Tanzania. *Geographical Review*, 65(3), 364. <https://doi.org/10.2307/213535>
- Kent, P. E. (1942). A Note on Pleistocene Deposits near Lake Manyara, Tanganyika. *Geological Magazine*, 79(1), 72–77. <https://doi.org/10.1017/S0016756800073532>
- Kingston, J. D., Hill, A., & Marino, B. D. (1994). Isotopic Evidence for Neogene Hominid Paleoenvironments in the Kenya Rift Valley. *Science*, 264(5161), 955–959. <https://doi.org/10.1126/science.264.5161.955>
- Kinyanjui, R. N. (2013). *Phytolith Analysis as a paleoecological tool for reconstructing Mid-Late Pleistocene environments in the Olorgesailie Basin, Kenya* [A thesis submitted to the Faculty of Science in fulfilment of the requirements for MSc. degree]. University of Witwatersrand.
- Kinyanjui, R. N. (2018). *Phytolith analysed to Compare Changes in Vegetation Structure of Koobi Fora and Olorgesailie Basins through the Mid-Pleistocene-Holocene Periods*. [A thesis submitted to the Faculty of Science in fulfilment of the requirements for Doctoral of Philosophy degree]. University of Witwatersrand.
- Lupien, R. L., Russell, J. M., Grove, M., Beck, C. C., Feibel, C. S., & Cohen, A. S. (2020). Abrupt climate change and its influences on hominin evolution during the early Pleistocene in the Turkana Basin, Kenya. *Quaternary Science Reviews*, 245, 106531. <https://doi.org/10.1016/j.quascirev.2020.106531>
- Maddux, S. D., Ward, C. V., Brown, F. H., Plavcan, J. M., & Manthi, F. K. (2015). A 750,000 year old hominin molar from the site of Nadung'a, West Turkana, Kenya. *Journal of Human Evolution*, 80, 179–183. <https://doi.org/10.1016/j.jhevol.2014.11.004>
- Madella, M., & Lancelotti, C. (2012). Taphonomy and phytoliths: A user manual. *Quaternary International*, 275, 76–83. <https://doi.org/10.1016/j.quaint.2011.09.008>
- Manzi, G. (2004). Human evolution at the Matuyama-Brunhes boundary. *Evolutionary Anthropology: Issues, News, and Reviews*, 13(1), 11–24. <https://doi.org/10.1002/evan.10127>
- Maslin, M. A., Shultz, S., & Trauth, M. H. (2015). A synthesis of the theories and concepts of early human evolution. *Philosophical Transactions of the Royal Society B: Biological Sciences*, 370(1663), 20140064. <https://doi.org/10.1098/rstb.2014.0064>

- McBrearty, S. (2001). The Middle Pleistocene of East Africa. In *Human roots: Africa and Asia in the Middle Pleistocene* (pp. 81–92). Western Academic and Specialist Press.
- McBrearty, S., & Brooks, A. S. (2000). The revolution that wasn't: A new interpretation of the origin of modern human behavior. *Journal of Human Evolution*, 39(5), 453–563.  
<https://doi.org/10.1006/jhev.2000.0435>
- Mercader, J., Bennett, T., Esselmont, C., Simpson, S., & Walde, D. (2009). Phytoliths in woody plants from the Miombo woodlands of Mozambique. *Annals of Botany*, 104(1), 91–113.  
<https://doi.org/10.1093/aob/mcp097>
- Mercader, J., Clarke, S., Bundala, M., Favreau, J., Inwood, J., Itambu, M., Larter, F., Lee, P., Lewiski-McQuaid, G., Mollel, N., Mwambwiga, A., Patalano, R., Soto, M., Tucker, L., & Walde, D. (2019). Soil and plant phytoliths from the *Acacia-Commiphora* mosaics at Oldupai Gorge (Tanzania). *PeerJ*, 7, e8211. <https://doi.org/10.7717/peerj.8211>
- Pearson, O. M. (2000). Postcranial remains and the origin of modern humans. *Evolutionary Anthropology: Issues, News, and Reviews*, 9(6), 229–247. [https://doi.org/10.1002/1520-6505\(2000\)9:6<229::AID-EVAN1002>3.0.CO;2-Z](https://doi.org/10.1002/1520-6505(2000)9:6<229::AID-EVAN1002>3.0.CO;2-Z)
- Piperno, D. R. (2006). *Phytoliths: A comprehensive guide for archaeologists and paleoecologists*. AltaMira Press.
- Piperno, D. R. (2009). Identifying crop plants with phytoliths (and starch grains) in Central and South America: A review and an update of the evidence. *Quaternary International*, 193(1–2), 146–159. <https://doi.org/10.1016/j.quaint.2007.11.011>
- Potts, R. (1996). Evolution and Climate Variability. *Science*, 273(5277), 922–923.  
<https://doi.org/10.1126/science.273.5277.922>
- Potts, R. (1998a). Environmental hypotheses of hominin evolution. *American Journal of Physical Anthropology*, 107(S27), 93–136. [https://doi.org/10.1002/\(SICI\)1096-8644\(1998\)107:27+<93::AID-AJPA5>3.0.CO;2-X](https://doi.org/10.1002/(SICI)1096-8644(1998)107:27+<93::AID-AJPA5>3.0.CO;2-X)
- Potts, R. (1998b). Variability selection in hominid evolution. *Evolutionary Anthropology: Issues, News, and Reviews*, 7(3), 81–96. [https://doi.org/10.1002/\(SICI\)1520-6505\(1998\)7:3<81::AID-EVAN3>3.0.CO;2-A](https://doi.org/10.1002/(SICI)1520-6505(1998)7:3<81::AID-EVAN3>3.0.CO;2-A)
- Potts, R. (2002). Complexity and adaptability in human evolution. In R. Boyd, M. Goodman, & A. S. Moffat (Eds.), *Probing human origins* (pp. 33–57). American Academy of Arts and Sciences.
- Potts, R. (2013). Hominin evolution in settings of strong environmental variability. *Quaternary Science Reviews*, 73, 1–13. <https://doi.org/10.1016/j.quascirev.2013.04.003>
- Potts, R., Dommain, R., Moerman, J. W., Behrensmeyer, A. K., Deino, A. L., Riedl, S., Beverly, E. J., Brown, E. T., Deocampo, D., Kinyanjui, R., Lupien, R., Owen, R. B., Rabideaux, N., Russell, J.



- M., Stockhecke, M., deMenocal, P., Faith, J. T., Garcin, Y., Noren, A., ... Uno, K. (2020). Increased ecological resource variability during a critical transition in hominin evolution. *Science Advances*, 6(43), eabc8975. <https://doi.org/10.1126/sciadv.abc8975>
- Potts, R., & Faith, J. T. (2015a). Alternating high and low climate variability: The context of natural selection and speciation in Plio-Pleistocene hominin evolution. *Journal of Human Evolution*, 87, 5–20. <https://doi.org/10.1016/j.jhevol.2015.06.014>
- Potts, R., & Faith, J. T. (2015b). Alternating high and low climate variability: The context of natural selection and speciation in Plio-Pleistocene hominin evolution. *Journal of Human Evolution*, 87, 5–20. <https://doi.org/10.1016/j.jhevol.2015.06.014>
- Rashid, I., Mir, S. H., Zurro, D., Dar, R. A., & Reshi, Z. A. (2019). Phytoliths as proxies of the past. *Earth-Science Reviews*, 194, 234–250. <https://doi.org/10.1016/j.earscirev.2019.05.005>
- Rightmire, G. P. (1996). The human cranium from Bodo, Ethiopia: Evidence for speciation in the Middle Pleistocene? *Journal of Human Evolution*, 31(1), 21–39. <https://doi.org/10.1006/jhevol.1996.0046>
- Rightmire, G. P. (2001). Patterns of hominid evolution and dispersal in the Middle Pleistocene. *Quaternary International*, 75(1), 77–84. [https://doi.org/10.1016/S1040-6182\(00\)00079-3](https://doi.org/10.1016/S1040-6182(00)00079-3)
- Rightmire, G. P. (2004). Brain size and encephalization in early to Mid-Pleistocene *Homo*. *American Journal of Physical Anthropology*, 124(2), 109–123. <https://doi.org/10.1002/ajpa.10346>
- Rightmire, G. P. (2008). *Homo* in the Middle Pleistocene: Hypodigms, variation, and species recognition. *Evolutionary Anthropology: Issues, News, and Reviews*, 17(1), 8–21. <https://doi.org/10.1002/evan.20160>
- Ring, U., Schwartz, H. L., Bromage, T. G., & Sanaane, C. (2005). Kinematic and sedimentological evolution of the Manyara Rift in northern Tanzania, East Africa. *Geological Magazine*, 142(4), 355–368. <https://doi.org/10.1017/S0016756805000841>
- Roach, N. T., Hatala, K. G., Ostrofsky, K. R., Villmoare, B., Reeves, J. S., Du, A., Braun, D. R., Harris, J. W. K., Behrensmeyer, A. K., & Richmond, B. G. (2016). Pleistocene footprints show intensive use of lake margin habitats by *Homo erectus* groups. *Scientific Reports*, 6(1), 26374. <https://doi.org/10.1038/srep26374>
- Ruffo, C. K., Birnie, A., & Tengnäs, B. (2002). *Edible wild plants of Tanzania*. Regional Land Management Unit/Sida.
- Schwartz, H., Renne, P. R., Morgan, L. E., Wildgoose, M. M., Lippert, P. C., Frost, S. R., Harvati, K., Schrenk, F., & Saanane, C. (2012). Geochronology of the Manyara Beds, northern Tanzania: New tephrostratigraphy, magnetostratigraphy and  $^{40}\text{Ar}/^{39}\text{Ar}$  ages. *Quaternary Geochronology*, 7, 48–66. <https://doi.org/10.1016/j.quageo.2011.09.002>

- Shakoor, S. A., Bhat, M. A., Mir, S. H., & Soodan, A. S. (2014). Investigations into Phytoliths as Diagnostic Markers for the Grasses (Poaceae) of Punjab. *Universal Journal of Plant Science*, 2(6), 107–122. <https://doi.org/10.13189/ujps.2014.020602>
- Shubi, A. (2016). *Geochemical and Petrographic Characterization of Lithic Artifacts from the Makuyuni Beds Locality 4, Tanzania, and Comparisons with Possible Source Materials* [B.A. Dissertation]. Macalester College Department of Geology.
- Shultz, S., & Maslin, M. (2013). Early Human Speciation, Brain Expansion and Dispersal Influenced by African Climate Pulses. *PLoS ONE*, 8(10), e76750. <https://doi.org/10.1371/journal.pone.0076750>
- Smith, G. M., Ruebens, K., Gaudzinski-Windheuser, S., & Steele, T. E. (2019). Subsistence strategies throughout the African Middle Pleistocene: Faunal evidence for behavioral change and continuity across the Earlier to Middle Stone Age transition. *Journal of Human Evolution*, 127, 1–20. <https://doi.org/10.1016/j.jhevol.2018.11.011>
- Sobolik, K. D. (1996). Lithic Organic Residue Analysis: An Example from the Southwestern Archaic. *Journal of Field Archaeology*, 23(4), 461–469. <https://doi.org/10.1179/009346996791973756>
- Stringer, C. (2012). The status of *Homo heidelbergensis* (Schoetensack 1908). *Evolutionary Anthropology: Issues, News, and Reviews*, 21(3), 101–107. <https://doi.org/10.1002/evan.21311>
- Stromberg, C. (2004). Using phytolith assemblages to reconstruct the origin and spread of grass-dominated habitats in the great plains of North America during the late Eocene to early Miocene. *Palaeogeography, Palaeoclimatology, Palaeoecology*, 207(3–4), 239–275. <https://doi.org/10.1016/j.palaeo.2003.09.028>
- Strömberg, C. A. E., Dunn, R. E., Crifò, C., & Harris, E. B. (2018). Phytoliths in Paleoecology: Analytical Considerations, Current Use, and Future Directions. In D. A. Croft, D. F. Su, & S. W. Simpson (Eds.), *Methods in Paleoecology* (pp. 235–287). Springer International Publishing. [https://doi.org/10.1007/978-3-319-94265-0\\_12](https://doi.org/10.1007/978-3-319-94265-0_12)
- Texier, P.-J. (2018). Technological Assets for the Emergence of the Acheulean? Reflections on the Kokiselei 4 Lithic Assemblage and Its Place in the Archaeological Context of West Turkana, Kenya. In R. Gallotti & M. Mussi (Eds.), *The Emergence of the Acheulean in East Africa and Beyond* (pp. 33–52). Springer International Publishing. [https://doi.org/10.1007/978-3-319-75985-2\\_3](https://doi.org/10.1007/978-3-319-75985-2_3)
- Trauth, M. H., Bergner, A. G. N., Foerster, V., Junginger, A., Maslin, M. A., & Schaebitz, F. (2015). Episodes of environmental stability versus instability in Late Cenozoic lake records of Eastern Africa. *Journal of Human Evolution*, 87, 21–31. <https://doi.org/10.1016/j.jhevol.2015.03.011>

- Trauth, M. H., Maslin, M. A., Deino, A. L., Strecker, M. R., Bergner, A. G. N., & Dühnforth, M. (2007). High- and low-latitude forcing of Plio-Pleistocene East African climate and human evolution. *Journal of Human Evolution*, 53(5), 475–486. <https://doi.org/10.1016/j.jhevol.2006.12.009>
- Trauth, M. H., Maslin, M. A., Deino, A., & Strecker, M. R. (2005a). Late Cenozoic Moisture History of East Africa. *Science*, 309(5743), 2051–2053. <https://doi.org/10.1126/science.1112964>
- Trauth, M. H., Maslin, M. A., Deino, A., & Strecker, M. R. (2005b). Late Cenozoic Moisture History of East Africa. *Science*, 309(5743), 2051–2053. <https://doi.org/10.1126/science.1112964>
- Tryon, C. A., McBrearty, S., & Texier, P.-J. (2006). Levallois Lithic Technology from the Kapthurin Formation, Kenya: Acheulian Origin and Middle Stone Age Diversity. *African Archaeological Review*, 22(4), 199–229. <https://doi.org/10.1007/s10437-006-9002-5>
- Vrba, E. S. (1985). Environment and evolution: Alternative causes of the temporal distribution of evolutionary events. *South African Journal of Science*, 81(5), 229–236.
- Vrba, E. S. (1988). Late Pliocene climatic events and hominid evolution. In *Evolutionary history of the “Robust” Australopithecines* (pp. 405–426). Routledge.
- Vrba, E. S. (1992). Mammals as a Key to Evolutionary Theory. *Journal of Mammalogy*, 73(1), 1–28. <https://doi.org/10.2307/1381862>
- Vrba, E. S. (1993). Turnover-pulsed, the red queen, and related topics. *American Journal of Science*, 239-A, 418–452.
- Warren, Hunter, L., Naidoo, N., Mavuso, S., Tommy, K., Molly, R., & Hlazo, N. (2019). Early hominins. In Beth, S., Nelson, K., Aguilera, K., & Braff, L. (Eds.), *Exploration: An open invitation to biological anthropology* (pp. 1–58). American Antropological Asociation.
- White, F. (1983). *The vegetation of Africa: A descriptive memoir to accompany the Unesco/AETFAT/UNSO vegetation map of Africa*. Unesco.
- Wolf, N. D., Nelson, S. V, Schwartz, H. L, Semprebon, G. M, Kaiser, T. M, & Bernor, R. L. (2010). Taxonomy and paleoecology of the Pleistocene Equidae from Makuyuni, northern Tanzania. *Palaeodiversity*, 3, 249–269.
- Zarrillo, S., Pearsall, D. M., Raymond, J. S., Tisdale, M. A., & Quon, D. J. (2008). Directly dated starch residues document early formative maize ( *Zea mays* L.) in tropical Ecuador. *Proceedings of the National Academy of Sciences*, 105(13), 5006–5011. <https://doi.org/10.1073/pnas.0800894105>

## **Chapter 2: What phytoliths are preserved in the modern soils in the vicinity of the Manyara beds, and how do they help inform those found in ancient assemblages?**

### **Abstract**

Phytoliths have greatly expanded our understanding of ancient landscapes and habitats. Studying phytoliths in paleosediments requires comparative data sets from the modern surface soil or plants to build models that help interpret ancient assemblages. As part of a larger study on the hominin-bearing Middle Pleistocene (0.780 to 0.633 Mya) Manyara Beds in Tanzania, this study examines phytolith production of the most common plants (n=21) and twenty-five modern surface soil phytolith samples from nearby Makuyuni village. Using Strömberg's (2003) classification and interpretation scheme, this study shows that the polyhedral epidermis morphotype is a strong indicator of *Commiphora* while *Acacia* is a rare producer of faceted blocky morphotypes. However, grass silica short cells are the most common phytolith morphotypes found in soil assemblages of the *Acacia-Commiphora* ecosystem. These results help to inform the taxonomy, preservation, and taphonomy of ancient sediments from the Manyara Beds by providing a referential baseline for studying phytoliths from the *Acacia-Commiphora* ecosystem, likely an important habitat for our hominin ancestors.

### **Introduction**

Studies of the past environments that our ancestors inhabited at Plio-Pleistocene sites in East Africa can be improved by incorporating macro- and microscopic plant remains (Albert et al., 2006; Barboni, 2014; Barboni et al., 1999, 2010; Barboni & Bremond, 2009; Esteban et al., 2017; Mercader et al., 2019; Potts et al., 2020; Rossouw & Scott, 2011; Yost et al., 2021). In the case of microscopic remains, pollen-bearing sediments are very rare. However, the chemistry and mechanical character of opal silica microfossils (phytoliths) allows them to survive better in dry environments and volcanic-rich sediments where fossil vertebrate tends to occur (Piperno, 2006). Therefore, phytoliths have a great potential to increase our understanding of the history of vegetation change in the past.

The usefulness of phytoliths as a source of paleoenvironmental data depends on the proper control of their production patterns, taxonomic significance, mode of dispersal, and the preservation of the assemblage in question (Albert et al., 2006; Cabanes & Shahack-Gross, 2015; Crifò & Strömberg, 2020; Piperno, 1985, 1991, 2006; Strömberg, 2003). The first two controls require detailed comparative collections on plants and the last two require studying phytolith assemblages in soils in the given region (Cabanes & Shahack-Gross, 2015; Piperno, 1985, 1991). Comparative collection is needed to distinguish diagnostic phytolith morphotypes that can be used for taxonomic

interpretation of the fossil assemblages (Barboni & Bremond, 2009; Neumann et al., 2017; Strömberg, 2004).

Phytoliths, however, suffer from the problems of multiplicity (plants produce more than one type) and redundancy (one morphotype is shared between plants) (Barboni & Bremond, 2009; Pearsall, 2016; Piperno, 2006; Rashid et al., 2019; Strömberg et al., 2018; Twiss et al., 1969). Multiplicity and redundancy complicate the taxonomic interpretation of phytoliths. As a result, only broader ecological groups can be established, such as woody dicots versus grasses or palms versus grasses. The redundancy problem can be reduced by examining variation in size, shape, and three-dimensional morphology (Piperno, 2006). At the same time, using a standardized classification system can efficiently recognize and separate taxonomic groups essential for paleoecological reconstruction (Neumann et al., 2017; Strömberg, 2004). The question remains: which finer morphological classification can improve taxonomic and ecological interpretations, and whether other phytolith researchers can recognize these variations?

The main challenge of many phytolith studies in Africa is the quest for diagnostic morphotypes that can be applied to reconstructing ancient vegetation (Neumann et al., 2017). Grass silica short cell phytoliths (GSSCs) are most diagnostic morphotypes. Since the initial classification of GSSCs according to their subfamilies: bilobate and cross=Panicoideae, saddle=Chloridoideae, and circular/oval rectangular=Pooideae by Twiss et al. (1969), many researchers globally, including Africa, follow this scheme with a slight modification depending on the study area, researcher, and the research questions at hand. As a result, the classification of GSSCs can differ. For example, saddle phytoliths are diagnostic of the Chloridoideae subfamily. In the initial classification by (Twiss, 1992; Twiss et al., 1969) saddles were not distinguished into different categories such as the “true saddle” and “collapsed saddle” because the three-dimensional morphology was not included (Piperno & Pearsall, 1998). Later on, others distinguished saddles into the true saddles recognised as “Chloridoid class” and collapsed saddle “Bambusoid class” (Barboni & Bremond, 2009; Neumann et al., 2009; Piperno, 2006; Piperno & Pearsall, 1998; Yost et al., 2018). Furthermore, “tall saddle” is described as saddles with convex faces slightly shorter than or equal to the length of the concave faces, which are also referred to as true saddle phytoliths produced by Chloridoideae grasses (Stromberg 2003; Kondo et al., 1994; Piperno and Pearsall., 1998). In Strömberg (2003), tall (wide) saddle is grouped within the true saddle morphotypes alongside the squat (long) saddles that occurs in high frequency in *Eragrostis* and represents Chloridoideae grasses. Piperno & Pearsall (1998) referred the same morphotypes as “tall saddle” in Strömberg (2003) as “tall saddle” and “squat saddles”. In East Africa, “true saddle” forms are defined as saddles with short/long convex edges, saddles symmetrical with concave and convex edged of the same length (Barboni & Bremond, 2009).

Very tall saddle width is over 15 micrometers, and collapsed saddles dominate Bambusoideae grasses (Piperno, 2006; Piperno & Pearsall, 1998; Strömberg, 2003; Yost et al., 2018). In East Africa, some Chloridoideae produce collapsed saddles (Barboni & Bremond, 2009) that are said to be diagnostic to Bambusoideae taxa in America (Strömberg, 2003). In contrast, Mercader et al. (2009) utilized the term "long saddle" instead of "collapsed saddle" to examine bamboo species in the Miombo woodlands of Central and East Africa. Another morphotype that is also confusing is "plateau saddle", which is abundant in the Arundinoideae grass subfamily, specifically species of *Phragmites*, but also occurs in numerous taxa of Chloridoideae, Aristidoideae, and Panicoideae (Neumann et al., 2017; Piperno, 2006). Because of this, Strömberg (2003) only assigns the plateaued saddle to the general PACMAD clade.

Another avenue where there is inconsistency is the micromorphological characters of "lobate" phytoliths, such as the length of the shank and shape of the outer margins of lobes in bilobates, (Barboni & Bremond, 2009; Fahmy, 2008; Neumann et al., 2017). Bilobates occurs in many Poaceae, and their taxonomic usefulness depends on knowledge of the local grass communities (Alexandre et al., 1997; Barboni et al., 1999; International Committee for Phytolith Taxonomy (ICPT) et al., 2019; Neumann et al., 2017; Piperno, 2006; Strömberg, 2003).

Similar trends are observed in non-grass phytoliths. Several studies have been conducted in Africa to clarify which morphotypes are diagnostic to trees and shrubs (Albert et al., 2015; Mercader et al., 2009, 2011, 2019; Neumann et al., 2017; Runge, 1999). Globular morphotypes and irregular shapes have been used by Runge (1999) as indicators of forest in the soils of Central African Forests. Neumann et al. (2009) used sclereids and globular morphotypes for woody plants in their early Holocene paleoenvironmental reconstruction of the Ounjougou site in Mali. In comparison, Mercader et al. (2009) included blocky, cylindroids, globular, and tabular forms as representatives of woody plants from the Miombo woodlands of Mozambique. Furthermore, Albert et al. (2006) utilized blocky parallelepiped phytoliths from Oldupai Gorge's surface soils to represent bark. The overall high representation of parallelepiped blocks in the soils and its bark phytolith has been questioned by Collura & Neumann (2017) because of the nature of the study area as an arid grassland with scattered trees. In addition, Collura & Neumann (2017) question the form of the woody phytolith reported by Dominguez- Rodrigo et al. (2001) from a 1.5 Ma Acheulean handaxe from Peninj. According to Collura & Neumann (2017), the image of the phytolith in Dominguez- Rodrigo et al. (2001: Fig.2) does not show a phytolith; instead, it is a polyhedral calcium oxalate crystal. Moreover, the woody tabular forms (e.g. tabular thin sinuate Fig. 6d, e, tabular elongate Fig. 4k, Cylindroid large Fig. 2j, tabular crenate Fig. 4i, and tabular psilate Fig. 4n) described in Mercader et al. (2009) are described as ELONGATE ENTIRE by the International Committee for Phytolith

Taxonomy (ICPT) (2019). These morphotypes correspond with Strömberg's (2003) smooth elongate class. According to the International Committee for Phytolith Taxonomy (ICPT) (2019), several modern groups produce the elongate entire, and its taxonomic affiliation is unknown.

From the above examples, it is obvious that the problem of using a finer classification system for Africa has yet to be solved, probably due to a high diversity and variability in plant phytolith morphotypes that are yet to be fully studied in modern African plants (Neumann et al., 2017; Piperno, 2006). As a result, when different authors are studying the same phytolith morphotypes, the results are often different. Therefore, a simpler classification system is necessary for a feasible paleoenvironmental reconstruction (Neumann et al., 2017; Strömberg, 2004). Consequently, this study utilizes Strömberg's (2003) classification and interpretive scheme to study modern phytolith assemblages from plants and soils in the *Acacia-Commiphora* ecosystem near the Manyara Beds in Northern Tanzania. Strömberg's (2003) classification scheme described and defined these morphotypes in more detail than previous authors. Therefore, it is easy to follow. It can be duplicated by researchers everywhere in the world. The modern-day *Acacia-Commiphora* ecosystem is relevant because the fossil fauna assemblage from the Manyara Beds has been interpreted as representing a relatively open habitat corresponding to the “*Acacia savanna*” environment (Kaiser et al., 2010:84).

The expansion of savanna grasslands, and open and closed wooded environments, which are the main components of the *Acacia-Commiphora* ecosystem landscape, is extremely important when it comes to the study of human evolution. Paleobotanical evidence indicates that the *Acacia-Commiphora* ecosystem emerged as early as 12 million years ago (Barboni et al., 2019; Bonnefille, 2010; Dominguez- Rodrigo et al., 2001). In Tanzania *Acacia* spp. pollens are reported to occur at early hominins sites Laetoli, Tanzania (3.7-3.5 Ma). Other pollens at Laetoli represent plant taxa such as Combretaceae, Anacardiaceae (*Rhus*), Capparidaceae (*Boscia*, *Meurua*), and herbs such as Solanaceae, Amarathaceae, and Labiatae, which form a significant part of the *Acacia-Commiphora* vegetation today (Bonnefille, 2010). Also, *Acacia* spp. pollens are reported to occur at the 1.76-1.5 Mya site of Peninj near Lake Natron associated with the presence of the genus *Homo* (Dominguez- Rodrigo et al., 2001).

Several modern phytolith studies of plants and surface soils have been conducted in Tanzania (Albert et al., 2015; Mercader et al., 2019). Albert et al. (2015) for instance, focused on phytoliths in soils from palm-related vegetation near Lake Manyara, Lake Eyasi, and Serengeti National Park, while Mercader et al. (2019) focused on the *Acacia-Commiphora* ecosystem near Olduvai Gorge. Together, they provide data on modern phytolith assemblages to reconstruct the hominin paleoecology at Olduvai Gorge, focusing on Bed I and Bed II ecology. In addition, Bremond

et al. (2008) conducted phytolith analysis in modern soil assemblages with the goal of tracing the dominant grass subfamilies and tree cover density from sites over the tropical mountains in East Africa, including Mount Rungwe and around Lake Masoko in Southern Tanzania. It is unclear, however, whether the classification schemes and/or plant species included in these studies can provide sufficient data for comparing the *Acacia-Commiphora* vegetation surrounding the Manyara Beds.

Using Strömberg's (2003) classification and interpretive scheme, this study characterizes phytolith assemblages from previous studied taxa *Acacia* spp., *Commiphora* spp., grasses *Aristida* spp., and *Sporobolus* spp. (previously reported in Mercader et al., 2019) and seventeen unstudied species of herbs, sedge, and tree/shrub species from the *Acacia-Commiphora* ecosystem in Northern Tanzania.

The following questions are addressed in this study:

- i. What are the phytolith morphotypes and plant functional types in the *Acacia-Commiphora* ecosystem surrounding the Manyara Beds?
- ii. Do phytolith assemblages from the topsoil reflect the vegetation types of the site?

Furthermore, I predict that GSSC phytoliths will be significantly more abundant in the *Acacia-Commiphora* ecoregion because they are more silicified than non-grass morphotypes that represent woody and herbaceous plants, most of which produce fewer and less silicified phytoliths.

## **Materials and Methods**

### **Study Area**

The study area is located near Makuyuni town (Figure 2-1). The climate of the study area is semi-arid, with an average annual rainfall of 651 mm (Bachofer et al., 2018). Rainfall follows a bimodal pattern: the first long rains occur between March and May, and the second short rains occur between November and January (Bachofer et al., 2018; Flores-Prieto et al., 2015). This low mean annual rainfall results in a sparsely vegetated semi-arid environment dominated by bushy grasslands (Bachofer et al., 2018; Maerker et al., 2015). The annual mean temperature is 26 °C (Bachofer et al., 2018; Flores-Prieto et al., 2015; Maerker et al., 2015).

The soils in the study area developed from varied lithological units. The basement complex is formed on Proterozoic quartzite and gneisses and is exposed by tectonic faults (Bachofer et al., 2018; Flores-Prieto et al., 2015; Ring et al., 2005; Schwartz et al., 2012). Some soils are rich in alkaline lavas such as alkali basalt, phonolite, nephelinite, and tuffs from explosive volcanism at Essimngori Hill. Carbonate volcanism and carbonate tephra deposits come from Ol Doinyo Lengai (90 km north of Makuyuni town) (Bachofer et al., 2018; Flores-Prieto et al., 2015; Ring et al., 2005;



Schwartz et al., 2012). There are also mudstones, siltstones, diatomites, marls, and tuffs eroded from the lacustrine and fluvial sediments of the Manyara Beds (Bachofer et al., 2018; Flores-Prieto et al., 2015; Ring et al., 2005; Schwartz et al., 2012; Wolf et al., 2010).

The study area is mapped as “scrublands” at the 1:50,000 scale by the Directorate of Overseas Surveys for the Republic of Tanganyika and Zanzibar (1969). In general, the modern vegetation of the study area belongs to the Somali-Maasai phytogeographical region comprised of thickets, woodlands, and grasslands, where *Acacia* and *Commiphora* are common (Ruffo et al., 2002; White, 1983). *Acacia* spp., *Acacia senegal*, *Balanite aegyptiaca*, *Combretum* spp., *Cordia monoica*, *Ficus* spp., *Grewia* spp., *Ziziphus* spp., *Barleria* spp., *Commiphora* spp., and *Hibiscus* spp., are among the common trees and shrubs (White, 1983). The common C<sub>4</sub> grasses are *Chloris* spp., *Panicum* spp., *Cenchrus* spp., *Andropogon* spp., *Aristida* spp., *Eragrostis* spp., and seasonal wet grasses *Cynodon dactylon* and *Sporobolus* spp. (Ruffo et al., 2002; White, 1983). Also, giant baobabs (*Adansonia digitata*) occur throughout the area, and candelabra *Euphorbia* and thickets made of *Sansevieria ehrebergii*, *Aloe* spp., *Cissus quadrangularis*, and *Sacostemma viminalis* are abundant (White, 1983).

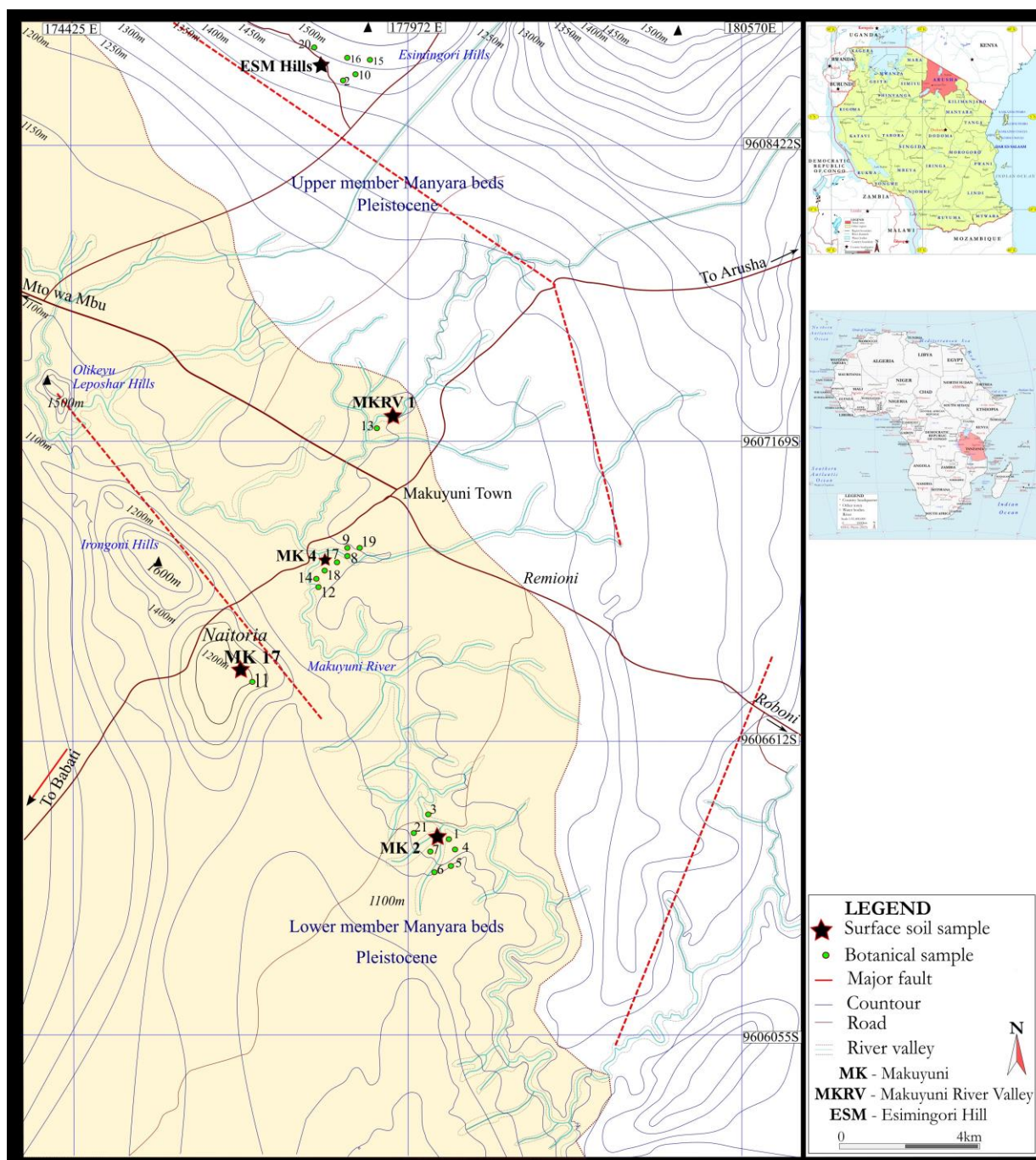


**Figure 2-1:** Map of the study area showing sites for botanical and surface soil collections.

Botanical samples include: 1. *Sporobolus consimilis*, 2. *Sporobolus ioclados*, 3. *Aristida adscensionis*, 4. *Chloris pycnothrix*, 5. *Chloris gayana*, 6. *Pennisetum* spp., 7. *Panicum coloratum*, 8. *Bothriochloa insculpta*, 9. *Centrus ciliaris*, 10. *Diheteropogon* spp., 11. *Brachiaria deflexa*, 12. *Acacia* spp., 13. *Solanum aculeatissimum*, 14. *Launaea cornuta*, 15. *Lochocarpus eriocalyx*, 16. *Zanthoxylum chalybeum*, 17. *Ecbolium revolutum*, 18. *Commiphora* spp., 19. *Grewia villosa*, 20. *Combretum zeyheri*, 21. *Cyperus rotundus*. Surface soil sites and vegetation types include: 1. MK 4 comprises bare soils with few grasses, herbaceous plants, and trees; 2. Open woodland with grasses, herbaceous plants, and shrubs at MK 2, 3. MK 17 has bare soil near grasses and shrubs; 4. MKRV 1 samples were collected near a dry river valley with patched trees, herbs, and grasses, and 5. Esimingori Hill includes woodland and bush grassland.

## Plant collection and extraction

Twenty-one plants were collected and analyzed for their phytoliths. All plants were collected in the field at the end of the growing season in 2021 to ensure the full deposition of phytoliths into plant tissues. Only mature and healthy plants were selected. Plant specimens included eleven grasses and ten non-grass species (Table 2-1, Figure 2-1). All plants were identified with the help of botanist Mr. Emanuel Mboya, who is affiliated with the Tropical Pesticides Research Institute and has extensive fieldwork experience and knowledge of plant identification in Northern Tanzania. Additional published sources were used, including the topographic map of Makuyuni town published by the Directorate of Overseas Surveys for Republic of Tanganyika and Zanzibar (1969), the vegetation of Africa map by White (1983), and the edible wild plants of Tanzania by Ruffo et al. (2002) to identify plants and their related microhabitats in the study area.

Plants were sampled using a hand pruning shear or by hand while wearing gloves. A whole plant comprising roots, flowers, stems, and leaves was collected for grass species. Only leaves and some parts of the stem were collected for non-grass plants, except for *Solanum aculeatissimum*, where both leaves and fruit were collected, and the sedge *Cyperus rotundus*, where the whole plant including the rhizomes and nuts was collected. After collection, the plant specimens were pressed between two pieces of paper to remove moisture and placed in a labeled paper bag for further drying and storage.

The specimens were processed at the University of Calgary Paleobotany Lab. Plant extraction followed the dry ash methods by Kooyman (2015), Pearsall (2016), and Piperno (2006). All grasses and non-grass specimens were cut into small pieces except for *Solanum aculeatissimum*, which was first separated into fruit and leaves, and *Cyperus rotundus*, which was split into rhizomes and leaves/stem. Plant samples were then washed with distilled water, followed by a sonic bath for 15 minutes using a Bransonic 220 sonicator to remove any adhering materials. After washing, each sample was placed in ceramic crucibles and ashed in a muffle furnace at 500°C for 8 hours. The recovered ash was weighed and transferred into a smaller beaker. Small amounts of hydrochloric acid (HCl) solution diluted to 10% and nitric acid (HNO<sub>3</sub>) at 3 normal solution were added simultaneously to remove carbonates and oxides and then washed into 15 mL centrifuge tubes with distilled water. Then, it was centrifuged three times at 3000 rev/min for 5 minutes and decanted. Then, hydrogen peroxide (H<sub>2</sub>O<sub>2</sub>) at 30% was added to remove organic materials, rinsed with distilled water, centrifuged three times at 3000 rev/min for 5 minutes, and dried overnight at 70°C.

A small amount of each dry sample was mounted on glass microscope slides using glycerol 50% so phytoliths could be rotated in the mount and sealed with nail polish. I counted one full slide for each species except for *Acacia* spp. and *Combretum zeyheri*, where a second slide was made due

to low phytolith recovery. For rich extracts, counts over 200 phytoliths were obtained (see Pearsall, 2016; Piperno, 2006). For plants with low counts, the morphotypes were described but not included in the overall statistical analysis. Samples were identified using a Leitz Laborlux 12 microscope at a magnification of 400x. Selected morphotypes were photographed using a microscope mounted Moticam 2500 (5.0 Pixel USB2.0) camera. Phytolith production was classified for non-grass plants following a scale by Wallis (2003) and McCune (2013): (NP) non-producer- No phytoliths observed, (R) rare-1 or 2 observed per slide, (U) uncommon- (3-30 per slide), (C) common-30-100 per slide, or (A) abundant >100 per slide.

**Table 2-1:** Plant species used in this study.

Sample #	Site	G.P. S/UTM 37	Genus species	Family	Subfamily	Plant part
1.	MK 2	E-0174398, N-9598450	<i>Sporobolus consimilis</i>	Poaceae	Chloridoideae	leaves, flowers, stem
2.	ESM	E-0174398, N-9598450	<i>Sporobolus ioclados</i>	Poaceae	Chloridoideae	Leaves, stem, flowers
3.	MK 2	E-0180432, N-9598679	<i>Aristida adscensionis</i>	Poaceae	Aristidoideae	Leaves, stem, flowers
4.	MK 2	E-0180530, N- 9598621	<i>Chloris pycnothrix</i>	Poaceae	Chloridoideae	Leaves, stem, flowers
5.	MK 2	E-0180527, N-9598624	<i>Chloris gayana</i>	Poaceae	Chloridoideae	Leaves, stem, roots
6.	MK 2	E-0180481, N-9598644	<i>Pennisetum</i> spp.	Poaceae	Panicoideae	Leaves, flowers, stem
7.	MK 2	E-0180481, N-9598644	<i>Panicum coloratum</i>	Poaceae	Panicoideae	Leaves, stem, roots
8.	MK 4	S 03° 33' 405", E 036° 05' 680"	<i>Bothriochloa insculpta</i>	Poaceae	Panicoideae	Leaves, stem, roots
9.	MK 4	S 03° 33' 357", E 36° 05' 628"	<i>Centhrus ciliaris</i>	Poaceae	Panicoideae	Leaves, flowers, stem
10.	ESM	E-0174398, N- 9598450	<i>Diheteropogon</i> spp.	Poaceae	Panicoideae	Leaves
11.	MK 17	E-0177004, N-9604742	<i>Brachiaria deflexa</i>	Poaceae	Panicoideae	Leaves, stem, flowers
12.	MK 4	E-0180523, N-9598734	<i>Acacia</i> spp.	Fabaceae	Mimosoideae	Leaves, flowers, stem
13.	MKRV1	E-0178831, N-9606452	<i>Solanum aculeatissimum</i>	Solanaceae		a. Leaves b. fruit
14.	MK 4	S-03° 33' 363", E-36° 05' 627"	<i>Launaea cornuta</i>	Asteraceae		Leaves, flowers, stem
15.	ESM	E-0174398, N-9598450	<i>Lochocarpus ericalyx</i>	Leguminosae		Leaves
16.	ESM	E-0174398, N-9598450	<i>Zanthoxylum chalybeum</i>	Rutaceae		Leaves
17.	MK 4	S- 03° 33' 395", E-36° 05' 626"	<i>Ecobolium revolutum</i>	Acanthaceae		Leaves, stem
18.	MK 4	E-018427, N- 9598684	<i>Commiphora</i> spp.	Burseraceae		Leaves
19.	MK 4	S-03° 33' 26", E-36° 05' 44"	<i>Grewia villosa</i>	Malvaceae		Leaves
20.	ESM	E-0174398, N-9598450	<i>Combretum zeyheri</i>	Combretaceae		Leaves
21.	MK 2	E-0180432, N- 9598681	<i>Cyperus rotundus</i>	Cyperaceae		a. Tuber, rhizomes b. Leaves and stem

## Surface soil and extraction

Topsoil samples were collected from five sites following Pearsall's (2016) pinch sampling method. Five composite samples were collected from a 10 x 10-meter area (Figure 2-2). In total, twenty-five surface soil samples (0-5 cm depth) were collected from Makuyuni River Valley Site 1 (MKRV 1), Esimingori Hill Site (ESM), Makuyuni Site 17 (MK 17), Makuyuni Site 2 (MK 2), and Makuyuni Site 4 (MK 4) (see Table 2-2, Figures 2-1 and 2-3). The upper topsoil was cleared of all litter during collection. Then the soil was collected using a trowel or by hand, while wearing gloves (a set of new gloves was worn every time during sampling), then each sample was bagged separately and labeled. The surrounding vegetation was noted, and soil color and other important landscape features were recorded.

Surface soil extraction procedures followed a combination of methods described in Kooyman (2015), Pearsall (2016), and Piperno (2006). First, the samples were sieved through a 0.25 mm geological sieve screen to remove root debris, coarse grain sand, and gravel. Three grams of sediment was placed in a 15 mL tube, and 10 mL of 0.1% ethylenediaminetetraacetic acid (EDTA) disodium salt dihydrate solution was added and mixed for 5 minutes using a Vortex mixer to suspend sediments. The samples were then centrifuged to settle coarse particles like sand and phytoliths while the clay remained suspended. The sample was then rinsed several times until they were mostly clear, indicating that clays had been removed. Then, enough hydrochloric acid (HCl) at 10% and nitric acid (HNO<sub>3</sub>) at 3 normal were added simultaneously to the sample until the whole sample was submerged to remove carbonates and clay oxide. The sample was then placed in a beaker filled with hot water for one hour to speed up the reaction. When the fizzing reaction ceased, the sample was washed three times with distilled water and centrifuged at 3000 rev/min for 5 minutes. Once the sample was acid-free, 30% hydrogen peroxide (H<sub>2</sub>O<sub>2</sub>) was added to eliminate organic matter; the sample was placed in a hot bath for one hour to speed up the reaction and rinsed three times. Then, separation of phytoliths from the heavy sediments was accomplished by adding 3 to 5 mL of sodium polytungstate (SPT) at a specific gravity of 2.3, then centrifuged at 3000 rev/min for 5 minutes. The final extract (suspended materials) containing phytoliths was transferred into a newly labeled 15 mL tube, washed with distilled water, and centrifuged twice at 3000 rev/min for 3 minutes and then dried in an oven for 24 hours, sometimes 48 hours, at 70°C temperature. After drying, a small portion (0.001 g) of the sediments was mounted on a microscope slide, then 2-3 drops of glycerine were added, mixed thoroughly, and coverslip edges were sealed using nail polish. I counted one slide for rich extracts and two slides for less rich extracts. Slides were examined at 400 x magnification. This resulted in a total count of 267 to 2378 phytoliths, depending on the sample.

**Table 2-2:** Descriptions of the five modern surface soil plots used in this study and the plants found growing on the soil plot.

Site	G.P.S	Vegetation	Main vegetation description
MK 4	E-0178375, N-9606415	Bare soils with few grasses, herbaceous plants, and trees	<i>Aristida</i> spp., <i>Cynodon dactylon</i> , <i>Aistida adscensionis</i> , <i>Launaea cornuta</i> , <i>Chloris</i> spp., <i>Cenchrus ciliaris</i> , <i>Sporobolus ioclados</i> , <i>Chloris gayana</i> , and <i>Bothriochloa insculpta</i> , <i>Ecbolium revolutum</i> , <i>Acacia</i> spp., <i>Acacia mellifera</i> , <i>Cissus quadrangularis</i> , <i>Sansevieria ehrenbergii</i> , <i>Justicia</i> spp., <i>Euphorbia hirta</i> , <i>Withania</i> spp., <i>Ocimum basilicum</i> , <i>Commiphora</i> spp., <i>Grewia villosa</i> , <i>Senna occidentalis</i> , and <i>Chlorophytum</i> spp.
MK 2	E-0180527, N-9598624	Open woodland with grasses, herbaceous plants, and shrubs	<i>Chloris pycnothrix</i> , <i>Bothriochloa insculpta</i> , <i>Chloris gayana</i> , <i>Sporobolus consimilis</i> , <i>Aristida</i> spp., <i>Panicum coloratum</i> , <i>Pennisetum</i> spp., <i>Acacia mellifera</i> , <i>Acacia tortilis</i> , <i>Barelia eranthemoides</i> , <i>Balanite aegyptiaca</i> , <i>Solanum incanum</i> , <i>Cordia</i> spp., <i>Acacia Senegal</i> , <i>Commiphora</i> spp., <i>Grewia villosa</i> , <i>Grewia bicolor</i> , <i>Capparis tomentosa</i> , and <i>Gutenbergia cordia</i> .
MK 17	E-0177004, N-9604742	Bare soil near grasses and shrubs	<i>Aristida</i> spp., <i>Brachiaria deflexa</i> , <i>Bothriochloa insculpta</i> , <i>Chloris pycnothrix</i> , <i>Chloris gayana</i> , <i>Croton dichogamus</i> , <i>Justicia</i> spp., <i>Phyllanthus maderaspatensis</i> , <i>Acacia drepanolobium</i> , <i>Acacia tortilis</i> , <i>Barleria eranthemoides</i> , <i>Balanite aegyptiaca</i> , and <i>Asparagus africanus</i> .
Makuyuni River Valley 1 (MKRV 1)	E-0177716, N-9606161	Near dry river valley with patched trees, herbs, and grasses	<i>Solanum aculeatissimum</i> , <i>Salvadora persica</i> , <i>Ricinus communis</i> , <i>Flueggea virosa</i> , <i>Grewia tembensis</i> , <i>Acacia tortilis</i> , <i>Commiphora</i> spp., <i>Sansevieria</i> spp., <i>Commiphora habessinica</i> , <i>Aristida</i> spp., <i>Brachiaria deflexa</i> , <i>Chloris</i> spp., <i>Sporobolus</i> spp., and <i>Cynodon dactylon</i>
Esimingori Hill (ESM)	E-0174398, N-9598450	Woodland and bush grassland	<i>Sporobolus Africana</i> , <i>Penissetum</i> spp., <i>Brachiaria deflexa</i> , <i>Bothriochloa insculpta</i> , <i>Aristida adscensionis</i> , <i>S. ioclados</i> , <i>Aristida</i> spp., <i>Diheteropogon</i> spp., <i>Chloris</i> spp., and <i>Eragostis</i> spp., <i>Lonchocarpus ericalyx</i> , <i>Acacia nilotica</i> , <i>Acacia tortilis</i> , <i>Commiphora habessinica</i> , <i>Acacia mellifera</i> , <i>Acacia</i> spp., <i>Dalbergia melanoxylon</i> , <i>Combretum zeyheri</i> , <i>Commiphora Africana</i> , <i>Commiphora</i> spp., <i>Zanthoxylum chalybeum</i> , <i>Combretum molle</i> , <i>Dalbeggia</i> spp., and <i>Ozoroa insignis</i>

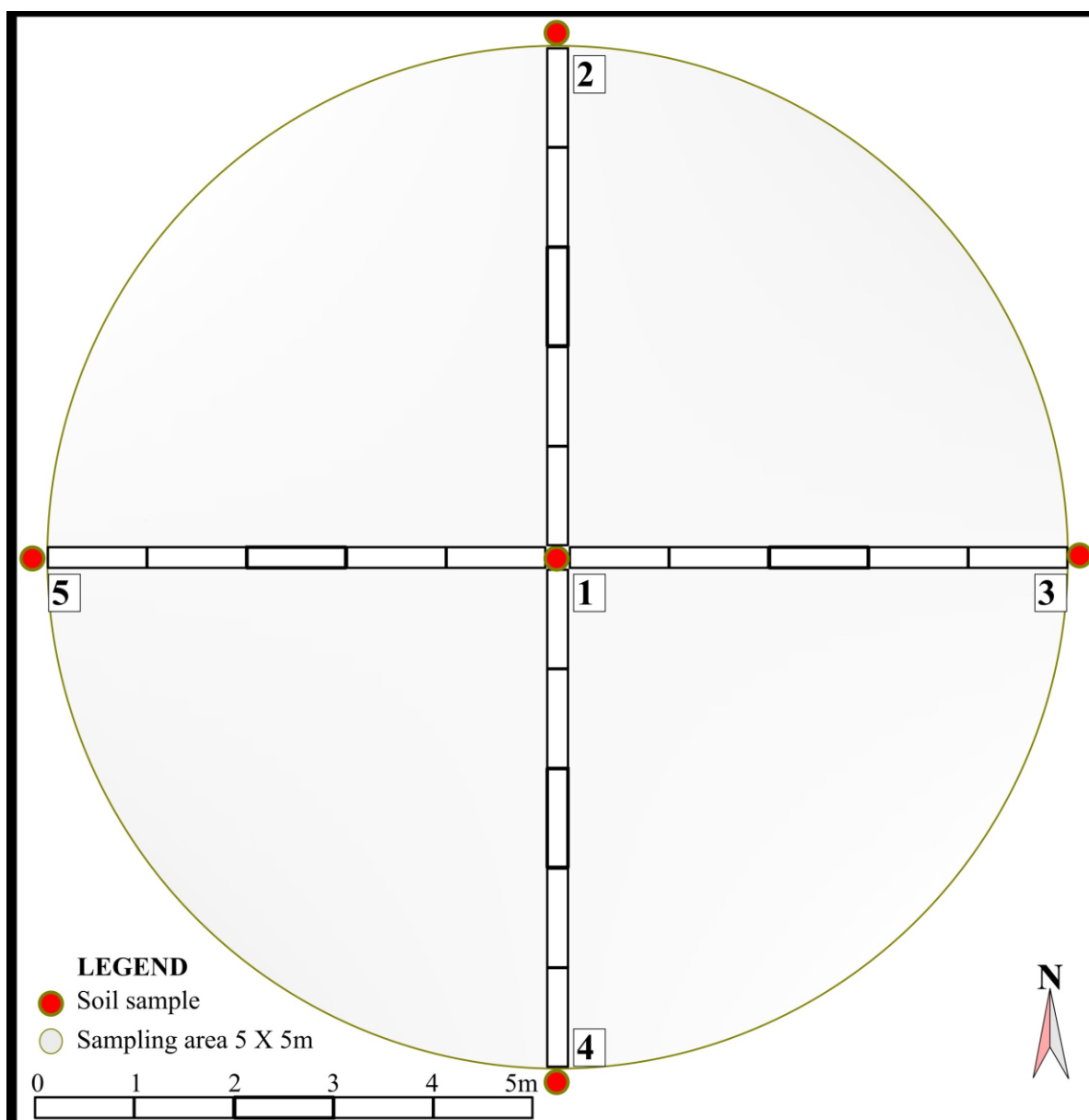


**Figure 2-2:** Surface soil plan showing the 10 x 10-meter pinch sampling.  
The first sample was collected at the center of the circle. The other four samples were taken 5 meters away at North, East, South and West points and pooled to create composite samples.





A.



B.



C.



D.



E.



F.

**Figure 2-3:** Photos of the study area showing the five soil sampling locations. A-B. Esimingori Hill (ESM) (A) shows the overall vegetation cover and (B) close detail of the sampling site; C. MK 17 site showing the nearby patch scrub vegetation; D. MK 4 site showing the patchy trees and shrub vegetation; E. MKRV 1 site sampled near a dry river channel. E. MK 2 sampling site.

## Statistical methods

Raw count data are presented in an Excel spreadsheet (Appendix A). Basic descriptive statistics, percentile values, and sums of frequencies were calculated and compared to understand the relationship and the range of variation within samples (Kennedy et al., 1996). Then, phytolith production in plants and site-specific assemblage variability were investigated further using multivariate statistical analyses such as the Normality test, one-way ANOVA test, and Kruskal-Wallis test to understand the data distribution and assess statistical significance. Correspondence analysis and cluster analysis were applied to the samples to understand the relationship between diagnostic phytolith morphotypes and taxonomic identification. All multivariate statistics were performed using PAST software.

A normality test was used to assess if the study samples were drawn from a normally distributed population (Legendre & Legendre, 1998; Mishra et al., 2019; Thode, 2002). The normality test determines parametric or non-parametric statistical tests should be used. The most popular tests for assessing normality are the Shapiro-Wilk and Kolmogorov-Smirnov tests; this study used the Shapiro-Wilk test (Legendre & Legendre, 1998; Thode, 2002). Shapiro-Wilk test is said to be the most powerful test in most situations; it helps to compare the sample's mean and the standard deviation for small sample sizes (<50) and larger samples (Mishra et al., 2019; Thode, 2002). The null hypothesis states that data are from normally distributed populations (Thode, 2002). When the p-value exceeds .05, the null hypothesis cannot be rejected, suggesting that data comes from a normally distributed population. Similarly, if the p-value is less than .05, the null hypothesis is rejected since the data is not normally distributed (Mishra et al., 2019; Thode, 2002).

The sample size of this study included three data sets. Since most of the data are not normally distributed, the one-way ANOVA test and non-parametric Kruskal-Wallis test were employed to assess the significant differences in the data when the assumptions of the ANOVA test were not met.

Correspondence analysis (CA) is among the ordination methods that present data in a graphical representation based on the similarity of sampling attributes in a resemblance space (Wildi, 2010). As an ordination method, CA works as a data reduction technique, and it helps to visualize patterns in multivariate data. Past phytolith researchers have used several ordination techniques, the most commonly used is Principal component analysis (PCA) (Barboni et al., 2007; Calla McNamee, 2012; Fredlund & Tieszen, 1994; Mercader et al., 2009, 2011; Rossouw & Scott, 2011), Cluster analysis (Mercader et al., 2009, 2011; Neumann et al., 2017); other methods used include Discriminant functional analysis (DFA), Non-metric multidimensional scaling (NMDS) (Crifò & Strömberg, 2021), and Canonical Correspondence analysis (CCA) (Neumann et al., 2017).

Principal component analysis (PCA) and Discriminant analysis (DA) require data to fit certain preconditions, such as the normal distribution of data (Legendre & Legendre, 1998; Neumann et al., 2017b). PCA, for instance, is sensitive to outliers; if data is highly skewed, the first few principal components will separate the extreme values from the rest of the sample units (Legendre & Legendre, 1998). Correspondence analysis is considered an alternative to PCA (Legendre & Legendre, 1998). Both techniques are eigen analysis-based approaches, rely on a single matrix, and are indirect gradient analysis methods. However, they are distinguished because PCA maximizes the variance explained by each axis, while CA maximizes the correspondence between species and sample scores. Neumann et al. (2017) postulated that the raw count data for phytolith data often follows the presence or absence of some morphotypes and, therefore, creates uneven distribution data. Therefore, CA is advantageous over PCA or DA because it can work better on data without preconditions. For this reason, CA is preferably used in this study.

Correspondence analysis (CA) is used to predict the factors that influence the composition of a dataset (Neumann et al., 2017). CA plots categories that are similar close to each other and shows which classes in the variables are related (Kennedy et al., 1996). Therefore, CA can help to deal with the major problems of multiplicity and redundancy and is a useful data exploration technique to identify phytolith morphotype relationships and environmental signatures (Neumann et al., 2017). In CA, the categories are plotted according to their scores, and the interpretation distances depend on the normalization (distribution of inertia over the row score and column scores) method used. The inertia column gives the total variance explained by each dimension in the model, while the singular value column gives the full scores of the eigenvalues (Doey & Kurta, 2011). Dimension 1 always explains the most variance of the model. In CA, eigenvalues and inertia are synonymous in that each axis has eigenvalues whose sum equals the cloud (mass of points) (Doey & Kurta, 2011). The values of the proportion of inertia columns give the percentage of the total variance that each dimension explains.

Correspondence analysis, however, suffers some setbacks; CA carries out simultaneous ordination of the rows and columns of the data matrix. Therefore, it can be difficult to draw inferences based on the association between these results in ordinations. Each axis is assumed to represent a specific environmental gradient. However, the second and higher axes can be distorted if the dataset spans long gradients. This distortion is called an arch (horseshoe) effect in CA. It also occurs in PCA. Axis extremes can be compressed such that the spacing between samples along an axis does not reflect the true difference in species composition (Legendre & Legendre, 1998; McCune et al., 2002; Wildi, 2010). The arch effect problem can be eliminated by detrended correlation analysis (DCA) (Doey & Kurta, 2011; Legendre & Legendre, 1998). However, detrending

CA creates another type of mathematical bias, so DCA is being used less frequently. The best option to interpret the arched form is the presence of an environmental gradient (Legendre & Legendre, 1998; McCune et al., 2002; Wildi, 2010). Inertia is often very strong at the first axis, and this allows the determination of environmental factors that originate from the gradients (Legendre & Legendre, 1998; McCune et al., 2002; Wildi, 2010)..

Cluster analysis is applied to create visualizable patterns that help during data interpretation. Cluster analysis is applied to classify data into observations based on group similarities or differences (Legendre & Legendre, 1998; McCune et al., 2002). Cluster analysis does not test hypotheses. Cluster analysis can be applied to any data set; it does not require underlying gradients or structure. Hierarchical agglomerative cluster using a single linkage (nearest neighbor) method using Euclidian Distance measure was applied in this study. The single linkage method considers the smallest distance. The problem with cluster analysis is that it creates chaining when single sample units are added to an existing group (groups are not combined); this is a common problem when using a single linkage grouping method (McCune et al., 2002).

## Results

The phytolith morphotype classification and interpretive scheme used in this study followed Strömberg's (2003) modern phytolith scheme, with minor modifications as shown in Table 2-3. The morphotype classification is grouped by grass silica short cells (GSSC), non-GSSC grass phytoliths, and non-grass phytolith morphotypes. Phytolith morphotypes are grouped according to tissues (e.g., mesophyll, epidermal, trichomes) and overall shape (e.g., elongates, spherical and sub-spherical bodies, Blo-bodies, etc.). Strömberg's (2003) classification scheme is organized with standardized terminologies for materials and ornamentation based on: (i) assignment of morphotype name and a code which is unique; for instance, code for bilobate is (BI), saddle (SA), epidermis cell (Epi), and so forth. A shorthand version is explained below; for the complete names and codes see Appendix B and for full morphotype descriptions, see Strömberg (2003). (ii) a description of the morphotype about how they look, (iii) discussion showing how the morphotype is similar to other morphotypes or can be distinguished, (iv) the origin in the plant, (v) photo, (vi) where it has been found in the modern reference collections or if it has been previously described, and (v) diagnostic morphotypes and their resulting plant functional types (PFT) for habitat reconstruction.

Table 3 summarizes the phytolith morphotype categories and representative plant functional type (PFT). These include: (i) palms (PALM-D) (ii) woody dicotyledons (DICOT-WO), (iii) woody and herbaceous dicotyledons (DICOT-GEN), (iv) phytoliths that are commonly found in several plant groups and therefore they are non-diagnostic of any taxonomic group (OTH), (v) common dicotyledons and other forest indicators (FI-GEN) such as palms, gymnosperms, ferns,

Marantaceae etc., (vi) morphotypes commonly found in conifers or monocots (CONI/MONO), (vii) morphotypes diagnostic to sedge (SEDGE), (viii) aquatic monocots (AQ-MONO), (ix) morphotypes that are abundant in grasses but also are commonly found in other monocots (GRASS/MONO-ND), and (x) morphotypes produced by grasses: grass silica short cells (GRASS), and diagnostic to grasses (GRASS-D).

The grass silica short (GSSCs) phytoliths are grouped further according to their subfamilies: (i) diagnostic early-diverging grasses (APPBO), (ii) general C<sub>3</sub> and C<sub>4</sub> Panicoideae, Arundinoideae, Chloridoideae, Micrairoideae, Aristidoideae, and Danthonioideae (PACMAD-GEN), (iii) diagnostic to panicoids (PANICOID), (iv) diagnostic to chloridoids (CHLORIDOID), (v) nondiagnostic pooids (POOID-ND), and (v) non-diagnostic GSSCs representing other grasses (OTHG).

Panicoids and Chloridoids are part of the PACMAD clade; however, they have diagnostic morphotypes that differentiate them from the rest of the subfamilies in the group. In this study, I used “other PACMADs” to refer to morphotypes found throughout the PACMAD clade and differentiate them from the panicoids and chloridoid-specific morphotypes.

CONI/MONO functional types are produced widely by conifers or other monocots; however, conifers are absent in my study area, therefore, the presence of morphotypes like Blo-3 Type A and Epi-8 comes from monocots.

**Table 2-3: Morphotype code and interpretive scheme used in this study.**  
For full details, see Appendix B.

<u>Grass short cell (GSSC) phytoliths</u> <b>General PACMAD clade</b> <i>PFT: other PACMADs</i> Symmetry B bilobate (BI-5) “simple lobate” Symmetry C bilobate (BI-6) “inverted” Symmetry D bilobate (BI-7) “almost panicoid” Polylobate with larger top (PO-3) Broken bilobate- BI-BR (BI5)/ BI-BR (BI-7)- (This thesis) <b>Panicoideae grasses</b> <i>PFT: PANICOID</i> Four-lobed cross with cross-shaped top (CR4-2) Three-lobed cross with cross-shaped top (CR3-2) Symmetry E bilobate (BI-8) “panicoid type” Irregular cross with cross shaped top (CRI-1) Perfect four-lobed cross (CR4-1) Polylobate with top and bottom same size (PO-4) <b>Chloridoideae grasses</b> <i>PFT: CHLORIOID</i> True saddle (SA-1) Crescentic conical rondel (CO-5) Cross-matchbox body with ears (CR4-10) <b>Non-diagnostic Pooideae grasses</b> <i>PFT: POOD-ND</i> Generic truncated rondel (CO-1) Crenate/trapeziform sinuate (CE-3) Crenate/trapeziform with symmetry D (CE-4) <b>Diagnostic Early diverging grasses-PFT:</b> APPBO Chusquared rondel with spiked top (CO-3) Collapsed saddle (SA-3)	<u>Non-diagnostic grass/monocots</u> <i>PFT: GRASS/MONO-ND</i> Rectangular plate (Blo-1) Spiny elongate (Epi-9) Pitted rod tracheary (Tra-8) Elongate with branched process (Epi-10)	<u>Woody and herbaceous dicots</u> <i>PFT: DICOT-GEN</i> Anticlinal epidermal (Epi-2) Polygonal epidermal (Epi-1) Crumped-up smooth elongate (Scl-11) Infilled parenchyma/honeycomb aggregate (M-2) Solid parenchyma/mesophyll cell (M-10) Dicotyledon stomata (St-1) Non-segmented armed trichome (Tri-3) Vesicular infilling-VI-sphere (VI-1) Smooth VI spheres and subspheres (CI-1) Large verrucate sphere (CI-3) Small pink sphere (CI-4)
	<u>Diagnostic grasses-Non GSSC phytoliths</u> <i>PFT: GRASS-D</i> Elongate with indented ends (Epi-11) Papillate elongate (Epi-12) Vertebral column body (mesophyll cell) -(M-7) Multilayered trichome (Ti-9) Bulliform keystone-shaped (Blo-10) Radiator shaped blocky/bulliform (Blo-9)	<u>Forest indicators</u> <i>PFT: FI-GEN</i> Hollow and infilled helical/helix tracheary (Tra-1) Worm like-infilled helix tracheary (Tra-2) Pilose-rugose sphere (CI-9) Small rugulose sphere (CI-7) Spongy mesophyll body (Scl-4) Elongate body with longitudinal facets (Scl-1) Short scl-1 (Scl-2) Parenchyma/honeycomb (M-1)
	<u>Monocots</u> <i>PFT: MONO</i> Faceted rectangular plate (Blo-3)- Type A Mesophyll tissue with straight files (M-5A) Monocotyledon stomata (St-4) Wavy elongate (Epi-8)	
	<u>Other morphotypes (non-diagnostic)</u> <i>PFT: OTH/UNKNOWN: Produced by many taxa</i> Smooth elongate (Elo-1) Thick trapezoidal “smooth elongate” (Elo-2) Faceted elongate (Elo-3) Smooth, cylindrical rod (Elo-7) Thickened rectangular plate (Blo-2)	
	<u>Diagnostic Commelinaceae</u> <i>PFT: COMMELINACEAE</i> Anisopler prismatic domed cylinder- (Pris-CI) (Eichhorn et al., 2010; Yost et al., 2018)	<u>Aquatic monocots</u> <i>PFT: AQ-MONO</i> Stellate parenchyma (rounded/ elongate) (SclF-7) Stellate parenchyma (SclF)
	<u>Diagnostic sedge</u> <i>PFT: SEDGE</i> Epidermal plate with conical bumps (Epi-6)	<u>Diagnostic palm</u> <i>PFT: PALM-D</i> Echinate sphere (CIm-2)
<u>Woody dicots</u> <i>PFT: DICOT-WO</i> MD Elongate (Elo-18) Large nodular sphere (CI-8) Compact, irregular S body (Scl-8) Multifaceted terminal tracheid (Scl-3)	<u>Other grasses</u> <i>PFT: OTHG</i> Small spiked rondel (CO-4)	

## Modern plant samples

### Phytoliths found in grasses

The studied assemblage has six species of the subfamily Panicoideae, four species of Chloridoideae, and one species of Aristidoideae. Grasses are prolific phytolith producers; in this study a total of 9310 phytoliths comprising 5871 GSSC and 3439 non-GSSC phytoliths were observed in the grass samples. Microphotographs of the selected morphotypes can be found in Appendix C.

#### Descriptive results: GSSC phytoliths and functional types

The bar chart (Figure 2-4) shows the diagnostic GSSCs observed in grass species and their resulting plant functional types (Figure 2-5). Figure 2-4 shows that *Sporobolus consimilis* and *Sporobolus ioclados* produce a high percentage of crescentic conical rondels (CO-5) and a few crosses, the matchbox body with ears (CR4-10) diagnostic to chloridoid plant functional type (Figure 2-4). *Chloris gayana* and *Chloris pynchothrix*, both produce a high percentage of true saddles (SA-1) (Figure 2-4), suggesting chloridoid plant functional type (Figure 2-5). True saddle (SA-1) is a hallmark of the Chloridoideae subfamily (Piperno, 2006; Strömberg, 2003; Yost et al., 2018). Also, a few matchbox crosses (CR4-10) are observed in *C. gayana*.

The six Panicoideae taxa in the study produce symmetry D bilobate (BI-7) “almost panicoid”, attributed to the general PACMAD clade (Figure 2-5). There is a small percentage of unique morphotypes diagnostic to Panicoideae, including polylobate with the top and bottom same size (PO-4), symmetry E bilobate (B1-8), the “panicoid type,” four-lobed crosses with near cross-shaped to cross-shaped top (CR4-2), perfect four-lobed cross (CR4-1), irregular cross with a close cross-shaped top (CR1-1), and three-lobed cross with a near cross-shaped top (CR3-2). Other morphotypes include the polylobate with a larger top (symmetry C) (PO-3) and symmetry B bilobate (B1-5), which occurs in other taxa, such as *Aristida adsceonis*, in this study.

Subfamily Aristidoideae includes one species, *Aristida adsceonis*, which produces symmetry B bilobate (BI-5) ‘simple bilobate’ and symmetry D bilobate (BI-7) “almost panicoid” (Figure 2-4). There is also a small presence of polylobate with a larger top (symmetry C) (PO-3); both represent the general PACMAD clade (Figure 2-5).

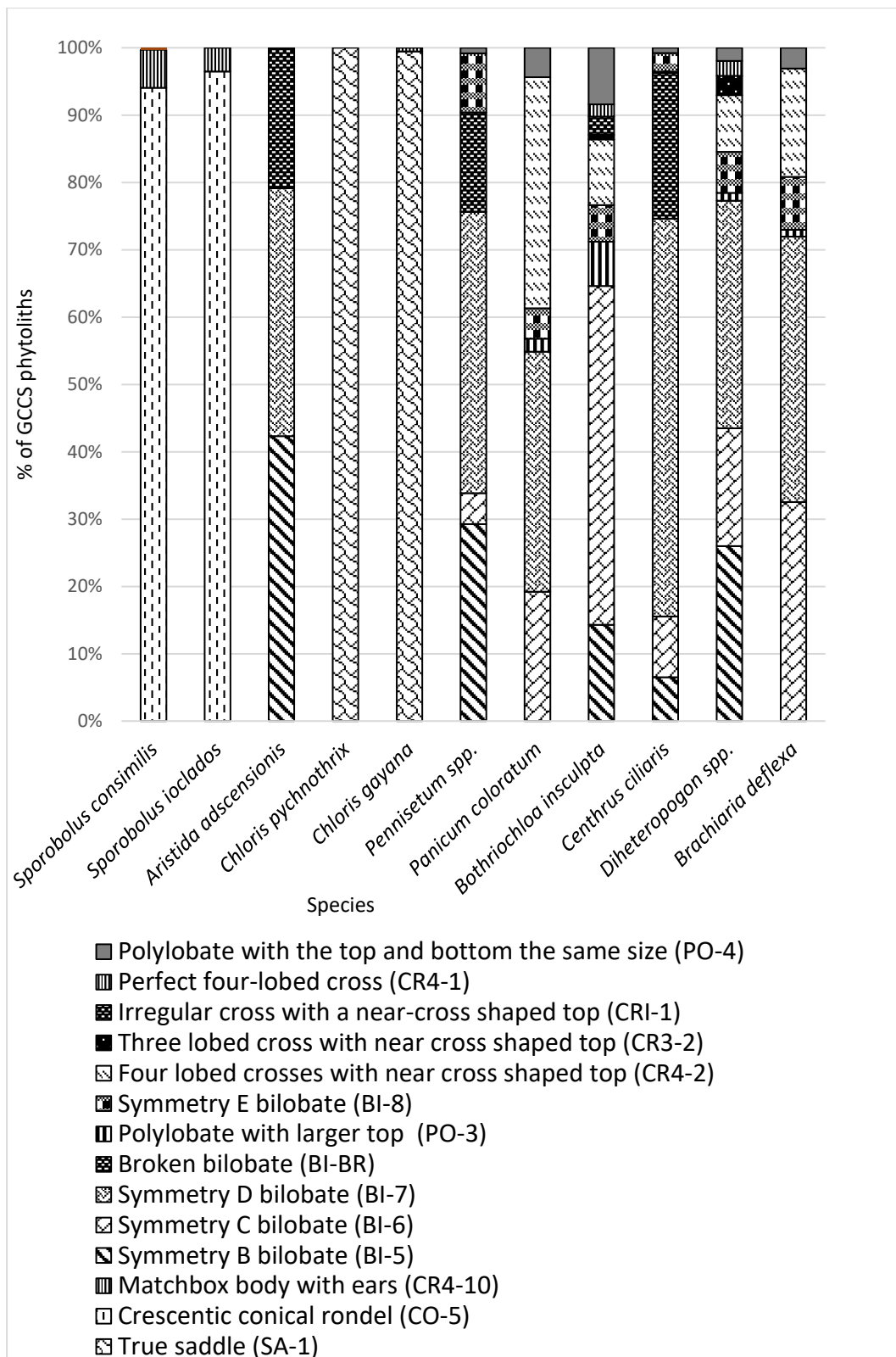


**Figure 2-4:** Percentage of grass silica short cell phytoliths in each grass species.



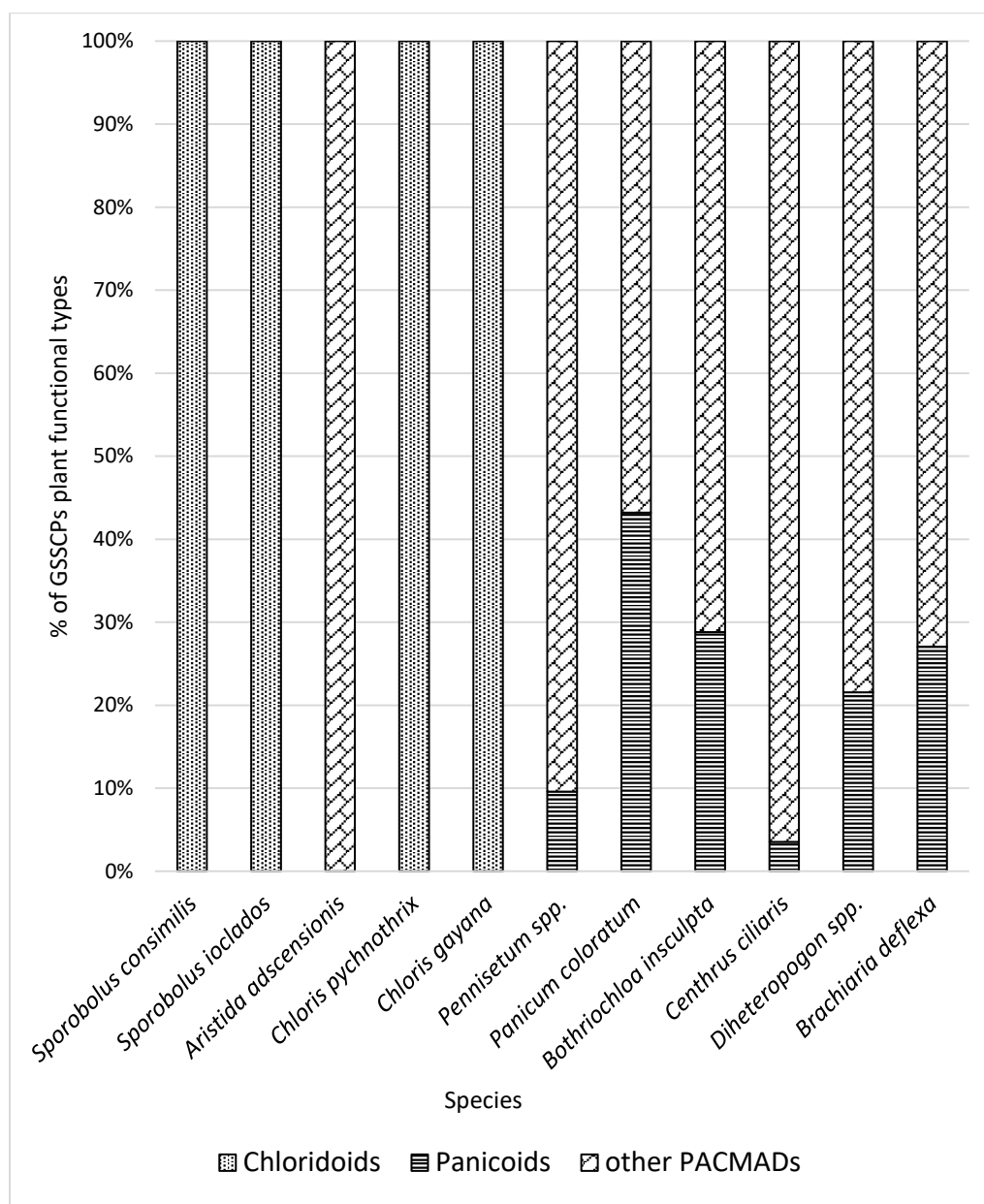


**Figure 2-5:** Percentage of plant functional types in species per diagnostic GSSC phytoliths.

### Statistical analysis

This study relied on 13 grass silica short cell phytoliths that can be assigned to a specific subfamily. Normality tests were applied to assess the distributions of the 13 morphotypes in species (n=11). The Shapiro-Wilk test results show that the data sample is not normally distributed (Table 2-4).

A non-parametric Kruskal-Wallis test was performed using a one-way ANOVA test for several samples. One-way ANOVA compares the medians of several univariate groups. The Kruskal-Wallis

test results show in all samples, there are no significant differences between the sample medians  
Chi-square=15.56, p (same)=0.05088 (Table 2-5)

**Table 2-4:** Normality test for grass species

	SA-1	CO-5	CR4-10	BI-5	BI-6	BI-7	PO-3	BI-8	CR4-2	CR3-2	CRI-1	CR4-1	PO-4
N	11	11	11	11	11	11	11	11	11	11	11	11	11
Shapiro-Wilk W	0.4897	0.4857	0.5559	0.7168	0.7829	0.7245	0.6927	0.8276	0.6436	0.4065	0.345	0.5003	0.8002
p(normal)	1.14E-06	1.02E-06	7.26E-06	0.000771	0.005597	0.000968	0.000377	0.02173	8.94E-05	1.17E-07	2.24E-08	1.53E-06	0.009478

**Table 2-5:** Kruskal-Wallis test for GSSC phytoliths

Kruskal-Wallis test for equal medians	
H (chi2):	15.56
Hc (tie corrected):	20.97
p (same):	0.05088
There is no significant difference between sample medians	

Results from Correspondence analysis: GSSC phytoliths

Correspondence analysis was performed for grass species (n=11) and phytolith morphotypes (n=13), with 76.59% of the loadings explained. In this study, Dimension 1 explains 38.40% of the total variance. Dimension 2 explains about 38.19% of the total variance. The distribution of phytolith morphotypes largely follows the subfamilies. In the biplot (Figure 2-6), there is a clear separation of the Chloridoideae from the rest of the subfamilies. Panicoideae and Aristidoideae seem to overlap.

#### Subfamily Chloridoideae

Crescentic conical rondels (CO-5), occasionally with horned decorations and matchbox cross (CR4-10), are exclusively present in *Sporobolus ioclados* and *S. consimilis*, which are loaded positively in Axis 2 (Figure 2-6). Crescentic conical rondels are markers for *Sporobolus* species (Barboni & Bremond, 2009; Strömberg, 2003; Yost et al., 2018).

*Chloris phychnothrix* and *C. gayana* load negatively on Axis 1 and 2 and are associated with true saddles, both squat and tall (SA-1). Saddles are regarded as the hallmark of the Chloridoideae subfamily worldwide (Mulholland, 1989; Neumann et al., 2017; Piperno, 2006; Piperno & Pearsall, 1998; Strömberg, 2003; Twiss et al., 1969; Yost et al., 2018). However, in East

Africa, *Sporobolus* and *Eragostis* occasionally produce rondels, which are rare in West Africa (Barboni & Bremond, 2009; Neumann et al., 2017; Yost et al., 2018).

#### Subfamily Panicoideae

The studied panicoid grasses show a larger diversity of bilobates, polylobates, and crosses, which are also abundant in some species. Some morphotypes dominate the whole subfamily, such as symmetry D bilobate (BI-7), also referred to as almost panicoid (see Strömberg, 2003). This morphotype occurs in close association with five panicoid species of *Pennisetum* sp., *Cenchrus ciliaris*, *Brachiaria deflexa*, *Diheteropogon* sp., and *Panicum coloratum*. Symmetry C bilobates (BI-6), which looks inverted, occur in all the six panicoid species. Cross morphotypes include the four-lobed crosses with near cross-shaped to cross-shaped top (CR4-2), irregular cross with near cross-shaped top (CR1-1), and three-lobed cross with near cross-shaped top (CR3-2) and are found exclusively in panicoid species in this study. This matches previous studies by (Barboni & Bremond, 2009; Brown, 1984; Fahmy, 2008; Neumann et al., 2017; Piperno, 2006; Twiss et al., 1969); Strömberg (2003) considers CR4-2, CR1-1, and CR3-2 as the hallmark of the Panicoideae subfamily (see also discussion by (Barboni & Bremond, 2009; Brown, 1984; Fahmy, 2008; Neumann et al., 2017; Piperno, 2006; Twiss et al., 1969). Bilobate symmetry B, also referred to as simple bilobate (Strömberg, 2003), occurs in three panicoid species of *Cenchrus ciliaris*, *Pennisetum* spp., and *Diheteropogon* spp.

#### Subfamily Aristidoideae

*Aristida adscencionis* loads negatively on axis 3. *A. adscencionis* is plotted together with the panicoid species. This overlap can be associated with the production of symmetry B bilobate (BI-5), which tends to have very long shanks and is linked to the symmetry D bilobates (BI-7) morphotypes in both subfamilies.

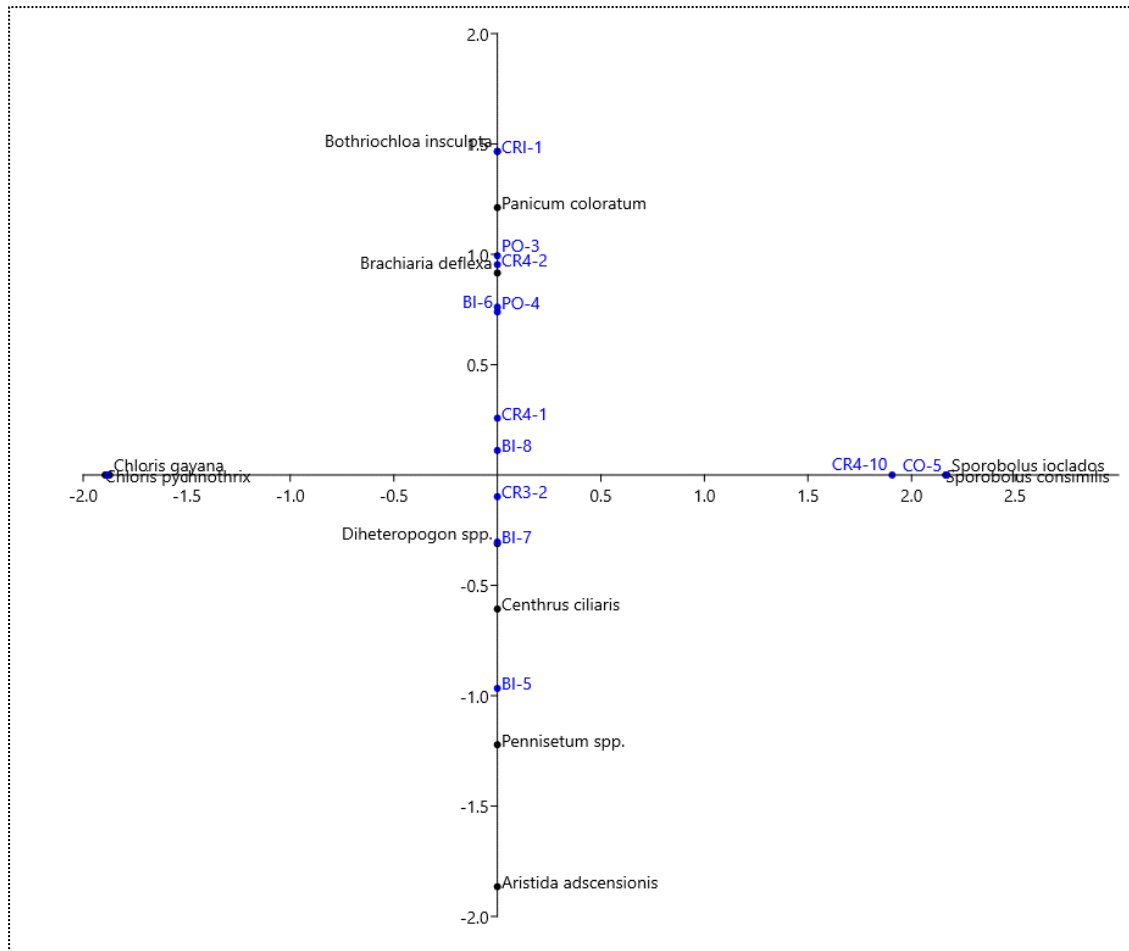


**Figure 2-6:** Correspondence analysis of diagnostic phytolith morphotypes in grass. Ordination diagram of axes 1-3.

#### Results from cluster analysis

Cluster analysis was performed on the plant functional types (PFTs) represented by each grass species. This was completed using Euclidean distance measure based on the nearest neighbor (also referred to as single linkage). The dendrogram (Figure 2-7) records two main groups: chloridoids and panicoids plus aristidoids. Within the chloridoids, the most similar species are *Chloris gayana* and *Chloris pychnothrix* due to the presence of the same morphotypes, true saddle (SA-1). *Sporobolus ioclados* is also grouped with the *Chloris* species due to the abundance of the cross “matchbox body with ears” also produced in *Chloris gayana*. *Sporobolus consimilis* is the most distinct of the chloridoids because it has higher production of the cross “matchbox body with ears” compared to *S. ioclados*.

In the second cluster *Aristida adscensionis* (Aristidoideae) is grouped with panicoid species and is closer to *Pennisetum* spp. and *Diheteropogon* spp., and it is also associated with *Centhrus*

*ciliaris*, and *Brachiaria deflexa*. The production of symmetry B bilobate (B1-5) and polylobate with a larger top (symmetry C) (PO-3) in Aristidoideae and Panicoideae causes the similarities between the two subfamilies in the cluster diagram. *Panicum coloratum* and *Bothriochloa insculpta* are slightly distinct from the rest of the panicoids due to the high number of phytolith morphotypes that are diagnostic of Panicoideae.

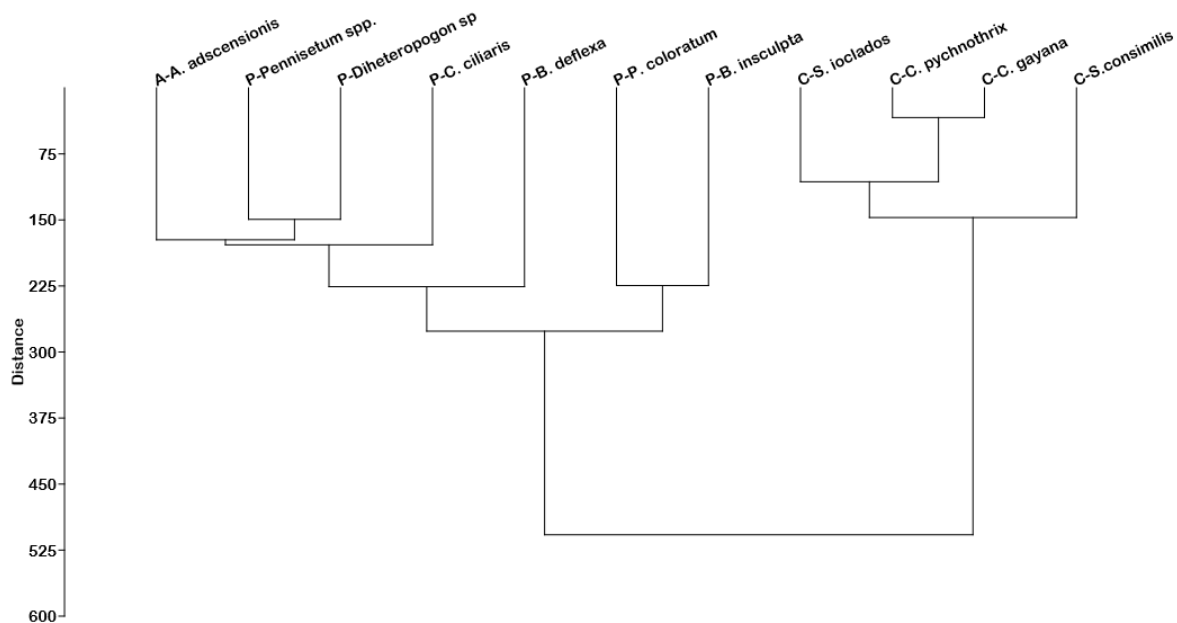


**Figure 2-7:** Hierarchical cluster dendrogram showing similarity of plant functional types for diagnostic GSSC phytoliths.

Dendrogram was generated using a Euclidean Distance similarity index based on the single linkage algorithm. Note the two distinct clusters: Chloridoideae (C) and Panicoideae (P) + Aristidoideae (A).

### Phytoliths found in non-grasses

Ten plants were sampled for this group, including trees, shrubs, herbs, and sedge.

Descriptive results shown in Table 2-6 provide raw data on the number of phytoliths recovered from these plants. See Appendix A for the detailed count of the selected morphotypes used in this category.

Descriptive results: phytoliths morphotypes abundance and plant functional types

Figure 2-8 shows the phytolith morphotypes that are found in each species. In Figure 2-9, these are collapsed into their larger functional groups. In Figure 2-9, *Acacia* spp. is linked to

morphotypes frequently occurring in monocotyledon plants (MONO). *Commiphora* spp., *Grewia villosa*, and *Launea cornuta* have the highest frequency of woody and herbaceous dicots (DICOT-GEN). *Ecbolium revolutum* is only linked to the unknown morphotype groups (OTH). *Lococarpus eriocalyx* and *Zanthoxylum chalybeum* have morphotypes that indicate the presence of woody and herbaceous dicots (DICOT-GEN) and forest indicators (FI-GEN). However, *Lococarpus eriocalyx* is unlike *Zanthoxylum chalybeum* in the presence of morphotypes that are diagnostic to woody dicots (DICOT-WO). Also, *Cyperus rotundus* has forest indicator morphotypes (FI-GEN) and the distinct epidermal plates of sedges, which are unique for this subfamily. On the other hand, *Solanum aculeatissimum* has a high frequency of the unknown morphotypes group (OTH), and a similar percentage of morphotypes that are diagnostic to woody and herbaceous dicots (DICOT-GEN), and forest indicators (FI-GEN).

**Table 2-6:** Phytolith production in non-grasses species.

(NP) non-producer- No phytoliths observed, (R) rare-1 or 2 observed per slide, (U) uncommon- (3-30 per slide), (C) common-30-100 per slide, or (A) abundant->100 per slide.

Species	Phytolith production				
	NP	R	U	C	A
<i>Acacia</i> spp.	-	1	-	-	-
<i>Solanum aculeatissimum</i>	-	-	-	43	-
<i>Launeae cornuta</i>	-	-	-	-	161
<i>Lochocarpus eriocalyx</i>	-	-	-	-	959
<i>Zanthoxylum chalybeum</i>	-	-	-	-	907
<i>Ecbolium revolutum</i>	-	-	14	-	-
<i>Combretum zeyheri</i>	0	-	-	-	-
<i>Commiphora</i> spp.	-	-	-	-	339
<i>Grewia villosa</i>	-	-	-	-	331
<i>Cyperus rotundus</i>	-	-	-	-	567
Total	0	1	14	43	3264

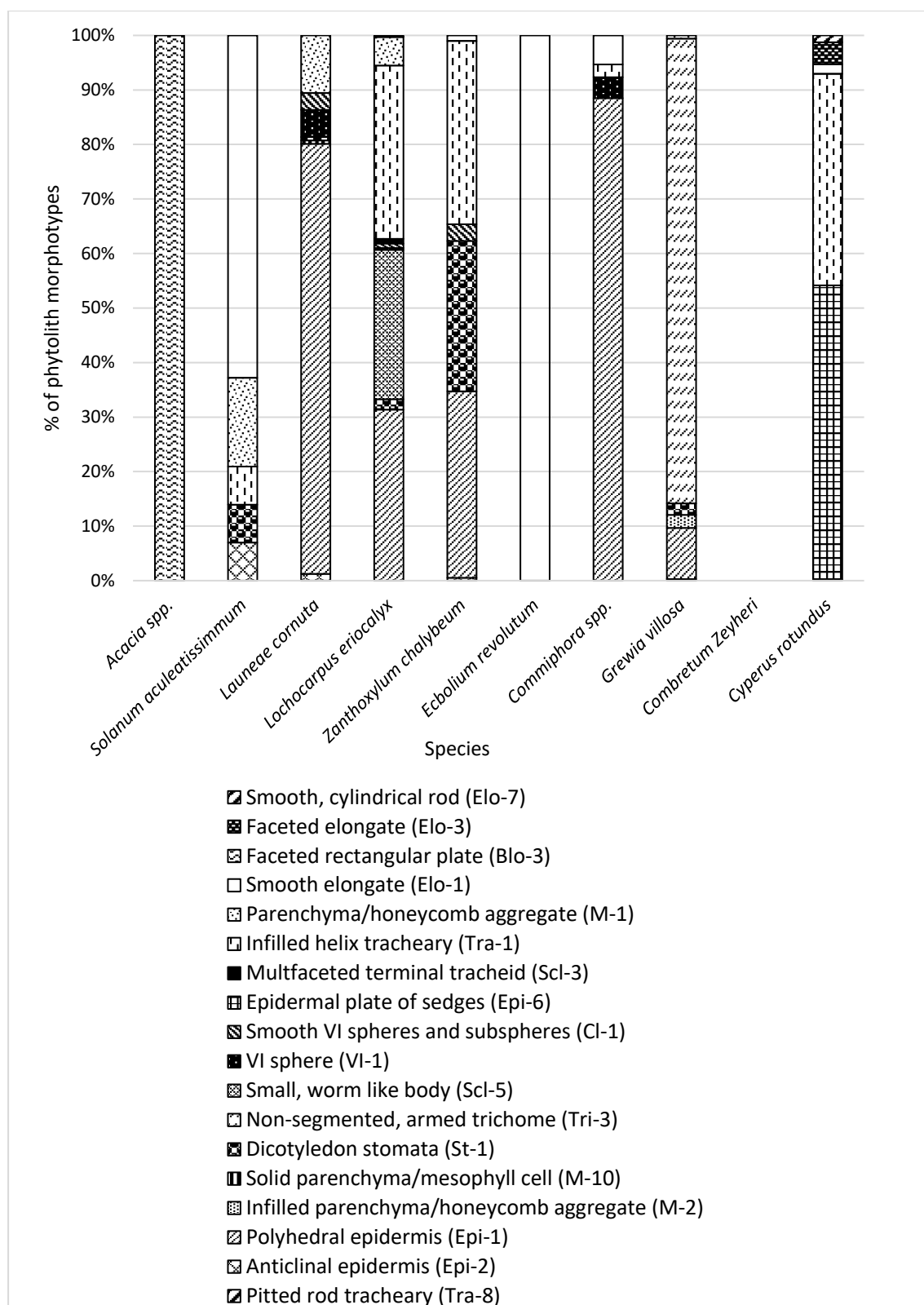


**Figure 2-8:** Percentage of phytoliths morphotypes per species.

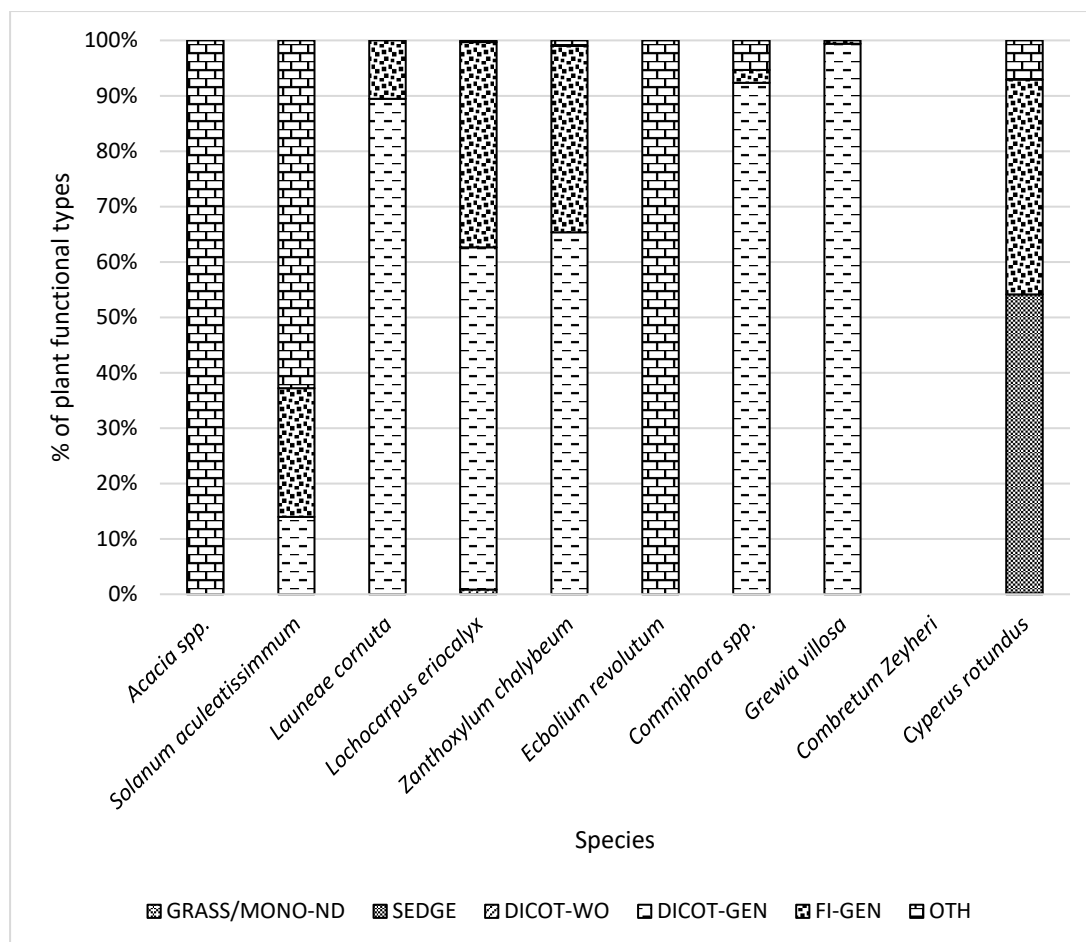


**Figure 2-9:** Percentage of plant functional types in non-grass plants per species.

### Statistical analysis

Normality tests using the Shapiro-Wilk test were applied to the diagnostic morphotypes ( $n=13$ ), and seven species were assigned specific plant functional types to examine if the data was normally distributed. Three species, *Acacia* spp., *Combretum zeyheri*, and *Ecbolium revolutum*, were not included since they do not have diagnostic morphotypes. Shapiro-Wilk suggests that the data is not normally distributed ( $p < 0.05$ ) except for one polyhedral epidermis (Epi-1), which is normally distributed with a  $p(\text{normal})$  value of 0.1343 (Table 2-7).

In general, the data is not normally distributed, so a non-parametric test, the Kruskal-Wallis test using one-way ANOVA, was used to assess the statistical significance of the sample. The Kruskal-Wallis's test (Table 2-8) for equal medians shows a substantial difference between the sample's medians.

Dunn's post hoc test (Table 2-9) shows that polyhedral epidermis (Epi-1) and infilled and hollow tracheid (Tra-1) are the most different from the rest of the morphotypes, also the median



values for dicotyledon stomata (St-1) are statistically difference to solid parenchyma/mesophyll cell (M-10).

**Table 2-7:** Normality test for diagnostic non-grass phytoliths

	Epi-2	Epi-1	M-2	M-10	St-1	Tri-3	Scl-5	VI-1	Cl-1	Epi-6	Scl-3	Tra-1	M-1
N	7	7	7	7	7	7	7	7	7	7	7	7	7
Shapiro-Wilk W	0.8542	0.7959	0.453	0.453	0.5075	0.453	0.453	0.7504	0.669	0.453	0.453	0.7342	0.6766
p(normal)	0.1343	0.0373	4.14E-06	4.14E-06	2.05E-05	4.14E-06	4.14E-06	0.01283	0.001686	4.14E-06	4.14E-06	0.008644	0.002047

**Table 2-8:** Kruskal-Wallis test for diagnostic non-grass phytoliths

Kruskal-Wallis test for equal medians	
H (chi2):	19
Hc (tie corrected):	24.78
p (same):	0.01591
There is a significant difference between sample medians	

**Table 2-9:** Dunn's post hoc values for non-grass phytoliths

	Epi-2	Epi-1	M-2	M-10	St-1	Tri-3	Scl-5	VI-1	Cl-1	Epi-6	Scl-3	Tra-1	M-1
Epi-2		0.08938	0.293	0.225	0.3989	0.3674	0.3613	0.9126	0.9677	0.3989	0.293	0.08406	0.9585
Epi-1	0.08938		0.005954	0.003591	0.3925	0.009321	0.009012	0.07053	0.08201	0.01101	0.005954	0.9776	0.09962
M-2	0.293	0.005954		0.8715	0.05807	0.8806	0.8897	0.3463	0.312	0.8352	1	0.00548	0.2698
M-10	0.225	0.003591	0.8715		0.03969	0.755	0.7638	0.2698	0.2408	0.7115	0.8715	0.003272	0.2057
St-1	0.3989	0.3925	0.05807	0.03969		0.081	0.07901	0.3404	0.3767	0.09158	0.05807	0.3767	0.4286
Tri-3	0.3674	0.009321	0.8806	0.755	0.081		0.9908	0.4286	0.3893	0.9539	0.8806	0.008565	0.3404
Scl-5	0.3613	0.009012	0.8897	0.7638	0.07901	0.9908		0.4219	0.383	0.9447	0.8897	0.008278	0.3346
VI-1	0.9126	0.07053	0.3463	0.2698	0.3404	0.4286	0.4219		0.9447	0.4631	0.3463	0.06616	0.8715
Cl-1	0.9677	0.08201	0.312	0.2408	0.3767	0.3893	0.383	0.9447		0.4219	0.312	0.07705	0.9263
Epi-6	0.3989	0.01101	0.8352	0.7115	0.09158	0.9539	0.9447	0.4631	0.4219		0.8352	0.01014	0.3705
Scl-3	0.293	0.005954	1	0.8715	0.05807	0.8806	0.8897	0.3463	0.312	0.8352		0.00548	0.2698
Tra-1	0.08406	0.9776	0.00548	0.003272	0.3767	0.008565	0.008278	0.06616	0.07705	0.01014	0.00548		0.09382
M-1	0.9585	0.09962	0.2698	0.2057	0.4286	0.3404	0.3346	0.8715	0.9263	0.3705	0.2698	0.09382	

## Results from correspondence analysis

*Acacia* spp. and *Combretum zeyheri* were excluded from the correspondence analysis because they are rare producers. *Ecbolium revolutum* is also excluded because it produces undiagnostic forms of smooth elongates (Elo-1). The CA results show 70.76% of the variation explained. The total of 40.95% of the variance is explained by axis 1. Axis two explains 29.8% of the variance.

In Figure 2-10, *Cyperus rotundus* is loaded positively on axis one associated with the morphotypes sedge epidermal plate (Epi-6) and helical tracheary element (Tra-1). *Grewia villosa* is also loaded negatively in Axis 2 and is related to non-segmented armed trichomes (Tri-3) and infilled parenchyma/ honeycomb aggregate (M-2) morphotypes.

*Solanum acueleatissimum*, *Launaea cornuta*, *Lochocarpus eriocalyx*, *Zanthoxylum chalybeum*, and *Commiphora* spp. are loaded positively on axis 1 and 2. *Launaea cornuta* is closely associated with parenchyma/honeycomb aggregate (M-1), solid parenchyma/mesophyll cell (M-10), and VI spheres (VI-1). *Zanthoxylum chalybeum* is associated with the polyhedral epidermis (Epi-1), dicotyledon-type stomata (ST-1), as well as hollow and infilled helix (helical tracheary element) (Tra-1).

*Commiphora* spp., and *Launaea cornuta* are closely linked to the polyhedral epidermis (Epi-1). In addition, *Solanum acueleatissimum* is near anticlinal epidermis (Epi-2) and dicotyledon-type stomata (ST-1). *Lochocarpus eriocalyx* is connected to sclereid body-compact, irregular S-body (Scl-8), hollow and infilled helix (helical tracheary element) (Tra-1), hollow and infilled helix (helical tracheary element) (Tra-1), parenchyma/honeycomb aggregate (M-1), and smooth VI spheres and sub spheres (CI-1).

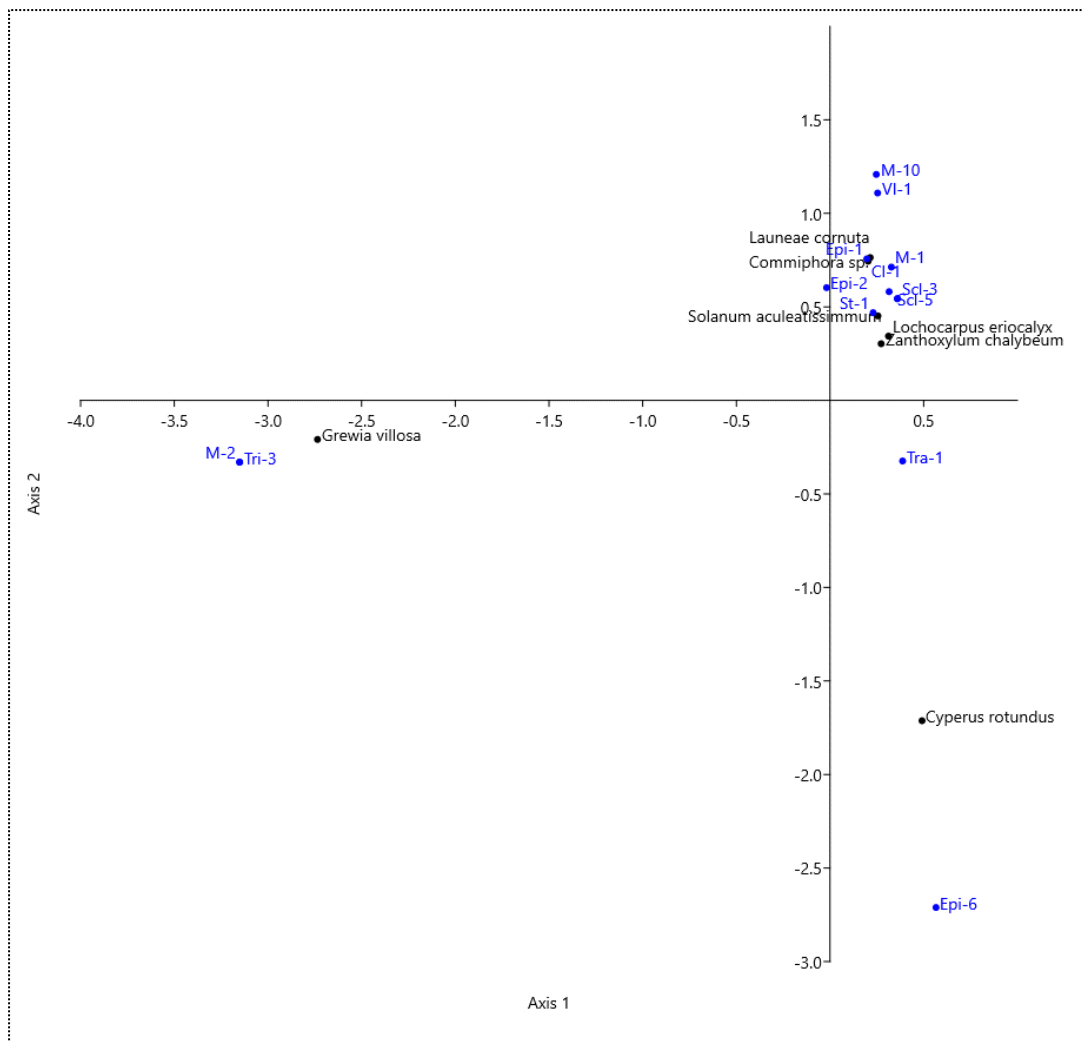


**Figure 2-10:** CA results of phytolith morphotypes in non-grass species. Ordination diagram of axis 1 and 2.

#### Cluster analysis: Non-grass phytolith morphotypes and plant functional types

Cluster analysis was performed to investigate if the broad plant functional types shown by each species can be differentiated from one another. Eight plant species were included except *Combretum zeyheri*, which did not yield any phytoliths, and *Acacia* spp., which had only one phytolith. Cluster analysis was performed using the Euclidean Distance measure and Single linkage algorithm. The dendrogram in Figure 2-11 shows similar patterns observed in the descriptive analysis. Herbs, sedge, trees, and shrubs occur in the same cluster (first cluster) because they share morphotypes non-diagnostic to any plant (unknown). *Launea cornuta*, *Commiphora* spp., and *Grewia villosa* share the production of morphotypes diagnostic to woody and herbaceous dicots (DICOT-GEN). The sedge, *Cyperus rotundus*, is distinct from the rest of the samples because it alone produces the epidermal plate with conical bumps morphotype that is diagnostic to Cyperaceous species. The trees and shrubs, *Lochocarpus eriocalyx*, and *Zanthoxylum chalybeum*, are in the second

cluster because they produce morphotypes that are diagnostic to woody dicots (DICOT-WO) and forest indicators (FI-GEN).

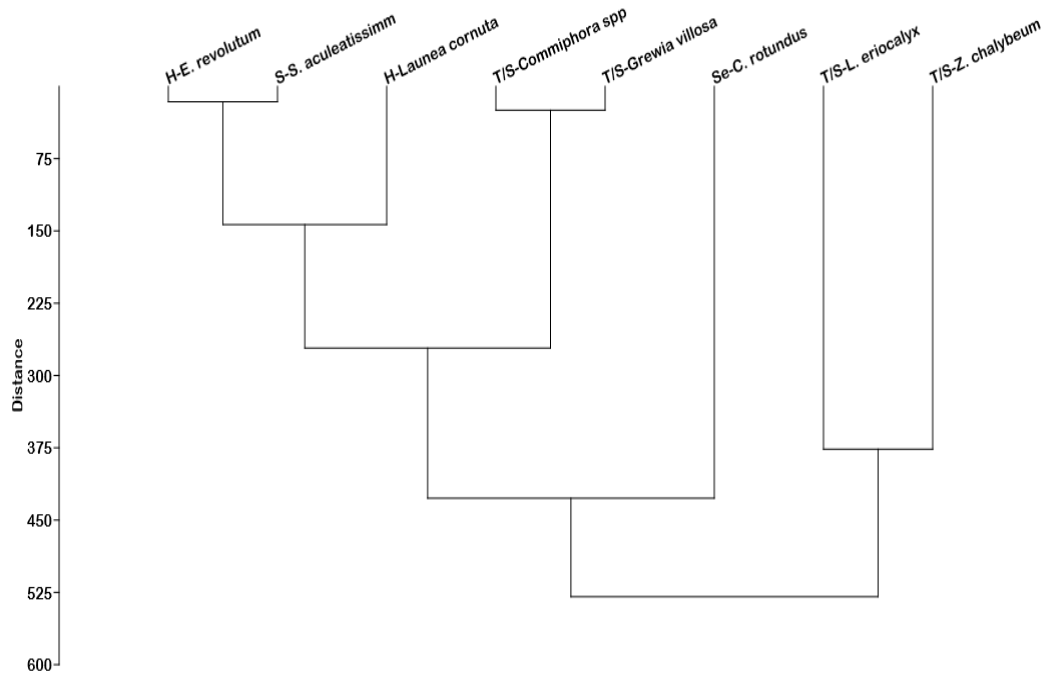


**Figure 2-11:** Cluster analysis of non-grass samples similarity of plant function types per diagnostic phytoliths.

Dendrogram created using Single Linkage Method and Euclidean Distance. H=herbs, S=shrubs, T/S=trees/shrub, and Se=Sedge.

### Surface soil phytoliths

Most phytoliths encountered in the surface soils were rondel, saddle, bilobate, polylobate, and cross morphotypes that come from grasses. Non-grass phytoliths included tracheary elements, spherical and subspherical bodies, and anisopolar prismatic domed cylinder bodies. Other forms include elongate (including the epidermal cells), trichomes, and blocky bodies (plates and chunks) that could have come from a variety of plants.

There is evidence of fragmentation and weathering effects on phytoliths, including pitting and break up. Many phytoliths, specifically broken bilobates, were observed from the Esimingori Hill samples. Broken bilobates that preserved 2/3 of their original form were counted and described as part of either symmetry B bilobate (simple lobate) BI-5 or symmetry D bilobate (almost Panicoid) BI-7, which added to the total number of phytoliths from the general PACMAD clade. Bilobates where

less than 2/3 was preserved were not counted because they are not diagnostic enough to be assigned to a specific form.

#### Results from descriptive analysis

Figure 2-12 shows the plant functional types observed at each site. Grass remains the most dominant vegetation type throughout the sampled sections. However, non-diagnostic monocots or grass, grass, monocots, forest indicators, woody dicots, woody and herbaceous dicots, and unknown morphotypes are also present (Figure 2-12). The vegetation at Esimingori Hill is woodland and bush grassland, while MK 2 is more open woodland with grasses, herbaceous plants, and shrubs. MKRV 1 site is near a dry river valley with patches of trees, herbs, and grasses. As a result, the Esimingori Hill site has the highest counts of grass phytoliths, followed by the MK 2 site. MKRV 1 has the lowest counts of the reconstructed plant functional types.

Bilobates, saddles, rondels, crosses, and polylobates characterize the surface soils of grass silica short cells. Bilobate morphotypes predominate at all sites, especially at Esimingori Hill, where they dominate the assemblage (Figure 2-13). Rondels and saddles also have the highest counts throughout the sections. MK 2 and MK 17 have the highest counts of cross morphotypes, while polylobates are rare throughout the sampled sections (Figure 2-13).

In terms of plant functional types displayed by the grass silica short cells, saddle, and rondel morphotypes indicate the presence of chloridoid grasses, and the bilobate morphotypes represent the other PACMADs (Figure 2-14). Panicoid-type morphotypes occur in a very small percentage, especially at the Esimingori Hill site. Esimingori Hill soil 4 has the highest counts of panicoid morphotypes than other samples. Different PACMAD morphotypes can be attributed to the presence of panicoid grasses and, to a small extent, aristidoids.

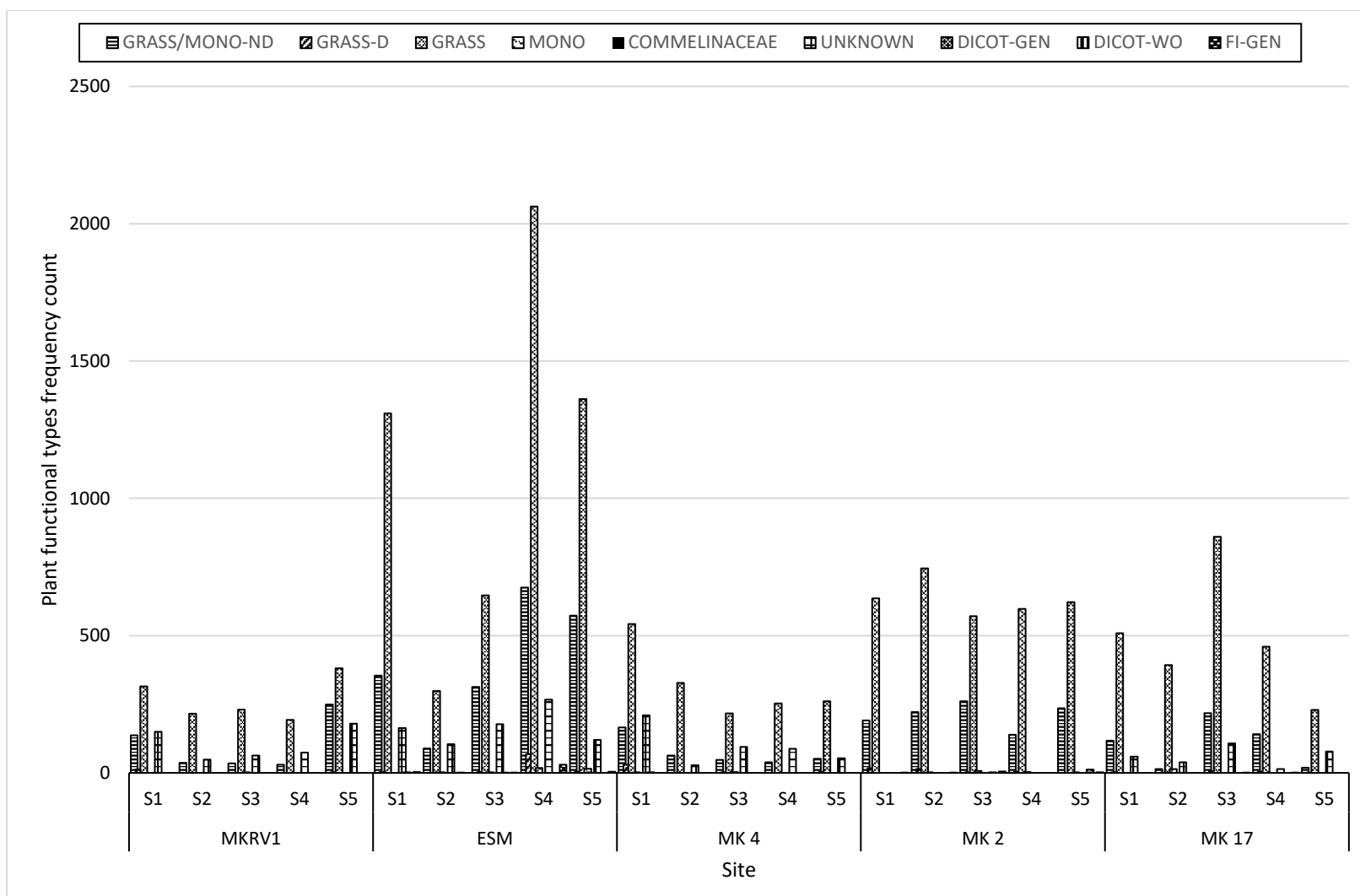


**Figure 2-12:** Count frequency of plant functional types represented by phytoliths at each site, broken down for the five samples.

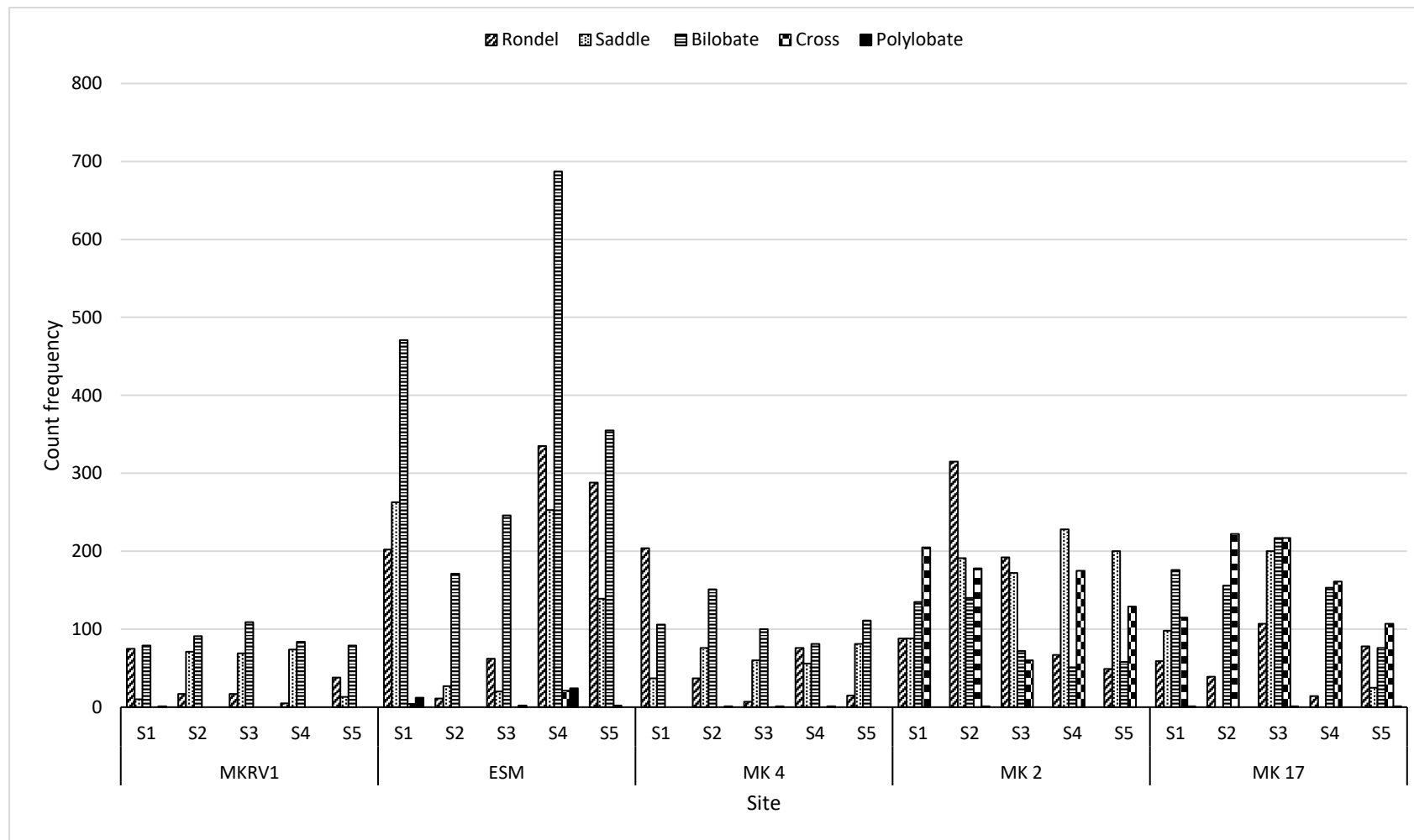


**Figure 2-13:** Count frequency of GSSC phytoliths per sample at each site.

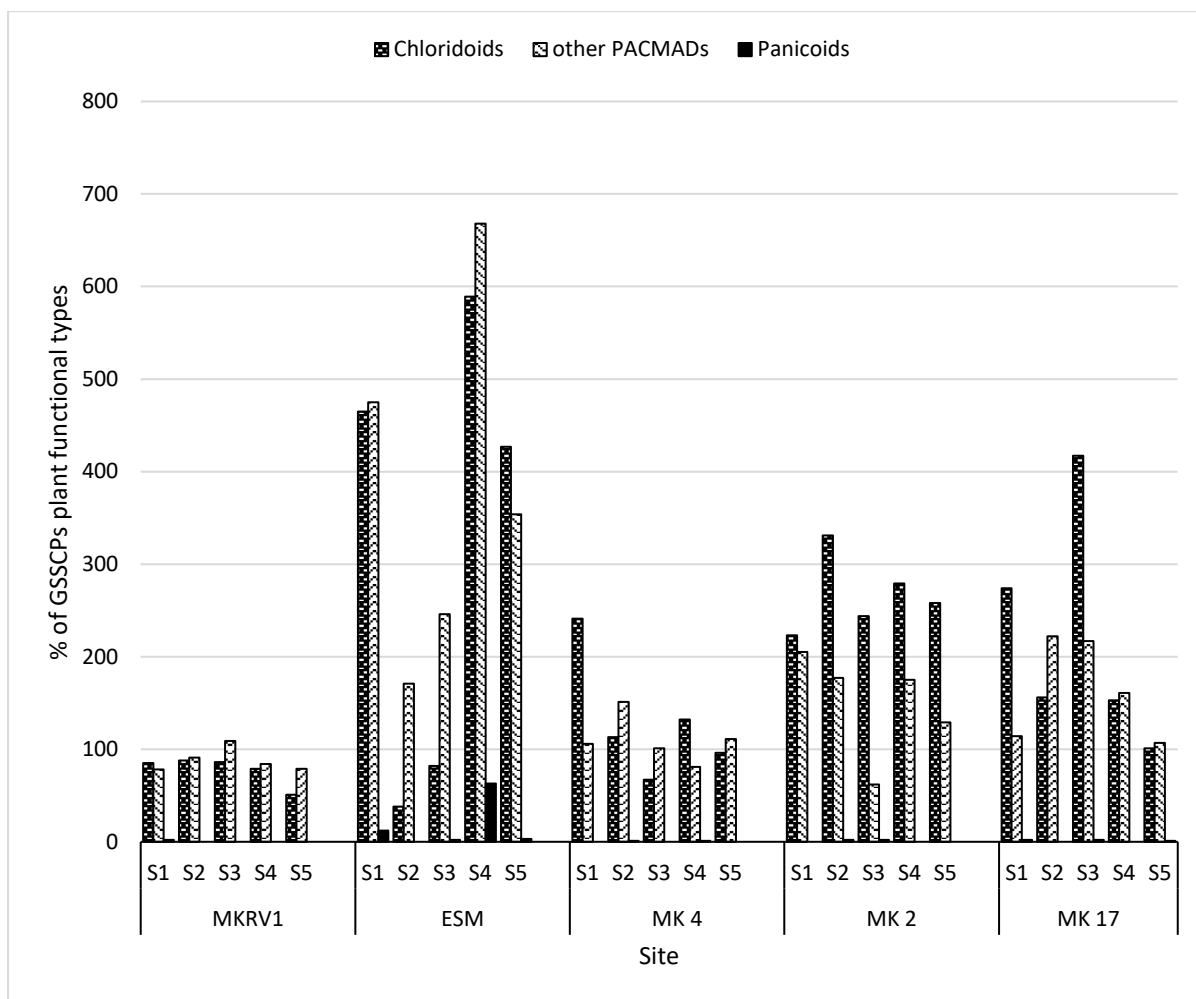


**Figure 2-14:** Count frequency of plant functional types represented by GSSC morphotypes per sample.

### Statistical analysis

The normality test, Shapiro-Wilk (Table 2-10) of the diagnostic phytoliths ( $n=16$ ) of the five sites show non-normal distributions. Individual morphotypes show that five morphotypes show normal distribution ( $p>0.05$ ), and eleven are not normally distributed ( $p<0.05$ ) (Table 2-10); as a result, the non-parametric test Kruskal-Wallis using ANOVA analysis was performed to assess the sample's significance. The Kruskal-Wallis test (Table 2-11) shows a significant difference between sample medians.

Dunn's post hoc test (Table 2-12) identified True saddle (SA-1), crescentic conical rondels (CO-5), and symmetry D bilobates (BI-7) as the most different morphotypes of the *Acacia-Commiphora* surface soils of the Manyara Beds.



**Table 2-10:** Normality test for diagnostic phytoliths morphotypes in surface soils

	SA-1	CO-5	CR4-10	BI-5	BI-6	BI-7	PO-3	BI-8	CR3-2	CR4-2	PO-4	CI-1	CI-3	Pris-CI	CI-8	Tra-1
N	5	5	5	5	5	5	5	5	5	5	5	5	5	5	5	5
Shapiro-Wilk W	0.9159	0.8291	0.5522	0.823	0.5522	0.9488	0.614	0.5895	0.7709	0.578	0.6969	0.6833	0.5522	0.7965	0.5522	0.7031
p(normal)	0.5035	0.137	0.000131	0.1231	0.000131	0.7289	0.000958	0.000452	0.04595	0.000312	0.008876	0.006353	0.000131	0.07586	0.000131	0.01033

**Table 2-11:** Kruskal-Wallis test for diagnostic morphotypes

Kruskal-Wallis test for equal medians	
H (chi2):	51.26
Hc (tie corrected):	54.3
p (same):	2.34E-06
There is a significant difference between sample medians	

**Table 2-12:** Dunn's post hoc test results

	SA-1	CO-5	CR4-10	BI-5	BI-6	BI-7	PO-3	BI-8	CR3-2	CR4-2	PO-4	CI-1	CI-3	Pris-CI	CI-8	Tra-1
SA-1		0.9777	0.000206	0.2566	0.0007	0.9219	0.01599	0.01862	0.000948	0.002109	0.01897	0.003419	0.000345	0.1217	0.000206	0.01726
CO-5	0.9777		0.000184	0.245	0.000632	0.9442	0.0148	0.01726	0.000858	0.001919	0.01759	0.003123	0.00031	0.1151	0.000184	0.01599
CR4-10	0.000206	0.000184		0.009961	0.7473	0.000139	0.1927	0.1743	0.6846	0.5239	0.1721	0.4328	0.8941	0.03046	1	0.1833
BI-5	0.2566	0.245	0.009961		0.02413	0.2177	0.2025	0.223	0.02993	0.05239	0.2257	0.073	0.01452	0.6795	0.009961	0.2126
BI-6	0.0007	0.000632	0.7473	0.02413		0.000487	0.3269	0.3	0.933	0.7527	0.2967	0.6439	0.85	0.0655	0.7473	0.3132
BI-7	0.9219	0.9442	0.000139	0.2177	0.000487		0.01217	0.01424	0.000665	0.001512	0.01452	0.002483	0.000236	0.09981	0.000139	0.01317
PO-3	0.01599	0.0148	0.1927	0.2025	0.3269	0.01217		0.9553	0.37	0.5059	0.9497	0.6043	0.2422	0.389	0.1927	0.9777
BI-8	0.01862	0.01726	0.1743	0.223	0.3	0.01424	0.9553		0.3409	0.4707	0.9944	0.5658	0.2204	0.4206	0.1743	0.9777
CR3-2	0.000948	0.000858	0.6846	0.02993	0.933	0.000665	0.37	0.3409		0.8172	0.3373	0.7053	0.7848	0.07878	0.6846	0.3553
CR4-2	0.002109	0.001919	0.5239	0.05239	0.7527	0.001512	0.5059	0.4707	0.8172		0.4664	0.8831	0.6141	0.1268	0.5239	0.4881
PO-4	0.01897	0.01759	0.1721	0.2257	0.2967	0.01452	0.9497	0.9944	0.3373	0.4664		0.5611	0.2177	0.4247	0.1721	0.9721
CI-1	0.003419	0.003123	0.4328	0.073	0.6439	0.002483	0.6043	0.5658	0.7053	0.8831	0.5611		0.5149	0.1677	0.4328	0.5849
CI-3	0.000345	0.00031	0.8941	0.01452	0.85	0.000236	0.2422	0.2204	0.7848	0.6141	0.2177	0.5149		0.04226	0.8941	0.2311
Pris-CI	0.1217	0.1151	0.03046	0.6795	0.0655	0.09981	0.389	0.4206	0.07878	0.1268	0.4247	0.1677	0.04226		0.03046	0.4046
CI-8	0.000206	0.000184	1	0.009961	0.7473	0.000139	0.1927	0.1743	0.6846	0.5239	0.1721	0.4328	0.8941	0.03046		0.1833
Tra-1	0.01726	0.01599	0.1833	0.2126	0.3132	0.01317	0.9777	0.9777	0.3553	0.4881	0.9721	0.5849	0.2311	0.4046	0.1833	

## Results from cluster analysis

The cluster analysis in Figure 2-15 shows similarities in the plant functional types resulting from the phytolith morphotypes identified at each site. In the dendrogram, samples from Esimingori Hill are the most distinct. These samples were collected from underneath trees and shrubs, and grasses were nearby. Esimingori Hill surface soils cluster alone because it has more phytoliths representing panicoid grasses, forest indicators (FI-GEN), and woody dicots (DICOT-WO). In the second cluster, samples from MK4 and MKRV1 are clustered together, and MK2 and MK17 are also relatively similar. These sites are within the same cluster because they have more phytoliths that are diagnostic to chloridoid grasses and other PACMADs.

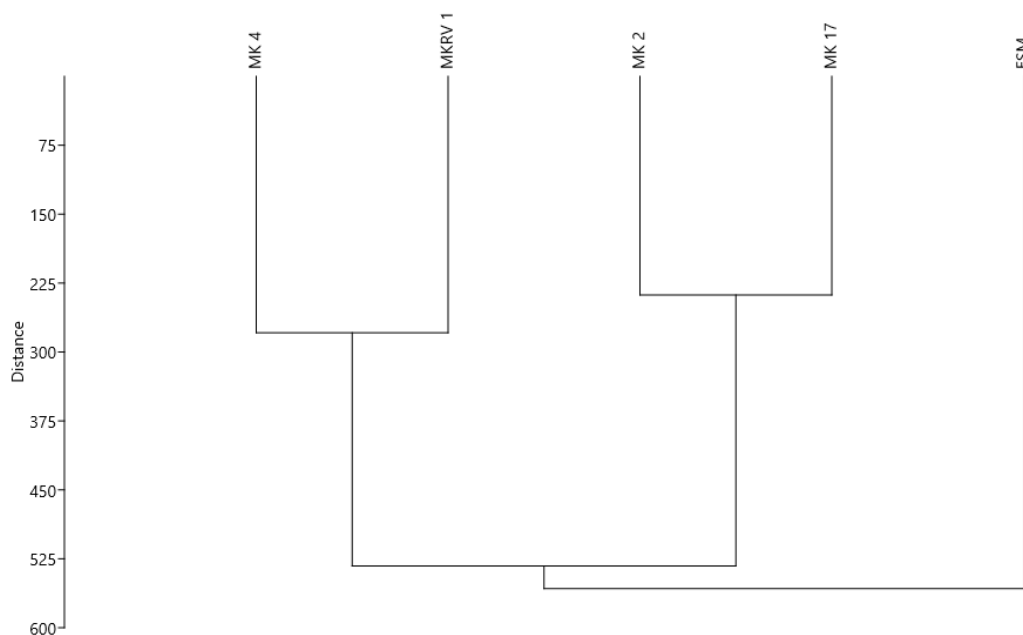


**Figure 2-15:** Cluster analysis of soil samples similarity of plant functional types per diagnostic phytoliths for each site.

Dendrogram created using the Single Linkage algorithm and Euclidean Distance metric.

## Results from correspondence analysis

Correspondence analysis was conducted to identify diagnostic phytoliths and their associated plant functional types ( $n=7$ ). 95.29% of the variance is explained. Axis 1 explains 72.07% of the total variation, while Axis 2 clarifies 23.22%. The biplot in Figure 2-18 shows that plant functional types from the MK 2 and Esimingori Hill (ESM) sites differ from the other three sites, MK 4, MKRV 1, and MK 17.

MK 2 site is loaded on the positive side in Axis 1 and 2 and is closely associated with Commelinaceae and herbaceous and woody dicots (DICOT-GEN). Samples from MK 2 were taken in a grassy area. The dominant grasses are *Chloris gayana* and *Chloris pycnothrix*, and other species include *Aristida* spp., *Sporobolus ioclados*, and *Bothriochloa insculpta*. The dominance of true saddles may be related to the presence of *Chloris gayana* and *Chloris pycnothrix* species at the site. Esimingori Hill site is loaded positively in Axis 1 and plotted closer to woody dicots (DICOT-WO), Panicoid grasses, and forest indicators (FI-GEN).

The panicoid phytoliths at the Esimingori Hill site can be associated with panicoids *Diheteropogon* spp., *Bothriochloa insculpta*, and *Penissetum* spp., growing on the site (see Table 2-2). Non-grass morphotypes such as the forest indicators infilled helix tracheid (Tra-1) could derive from *Lonchocarpus eriocalyx*, *Zanthoxylum chalybeum*, and *Commiphora* spp as shown in the modern plants analyzed in this study. The nodular large spheres (CI-8) for woody dicots (DICOT-WO) are difficult to explain; they might be associated with samples that were not included in this study or plants that are no longer growing at the site presently.

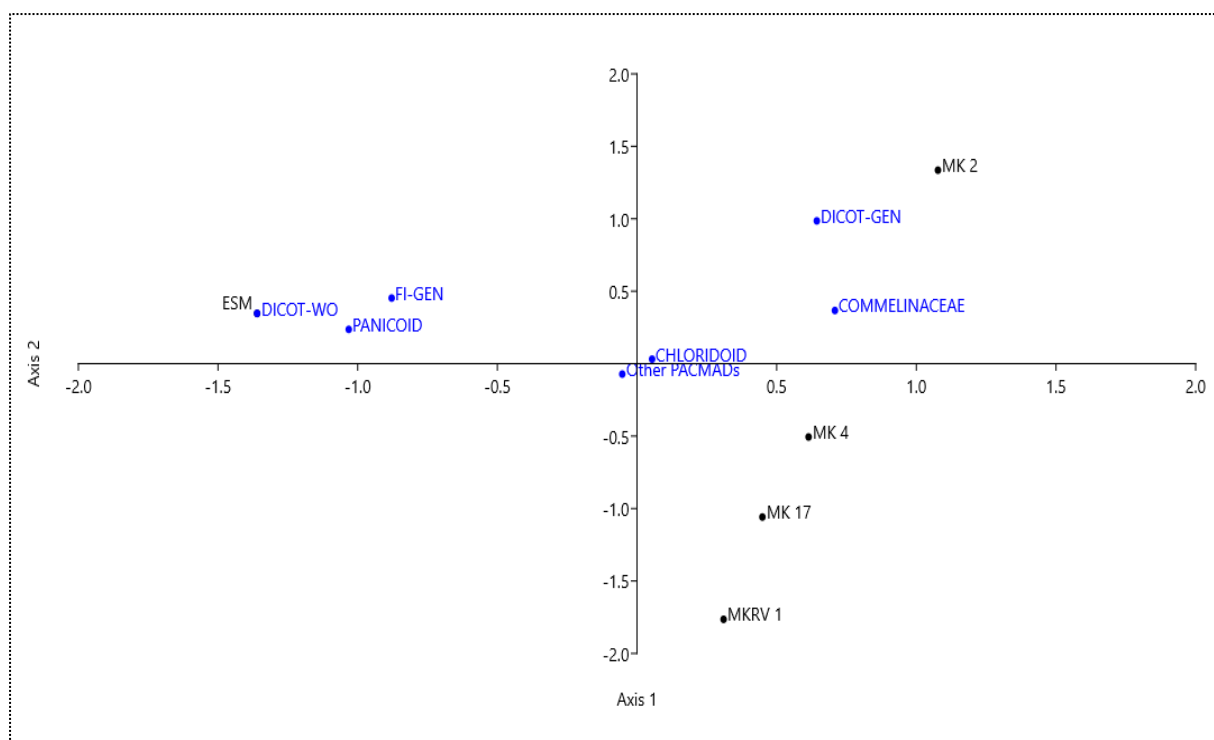


**Figure 2-16:** CA of sites (n=5) and functional groups (n=7).

## Discussion

### Phytoliths in modern plant samples

#### *Trees and shrubs*

The five trees and shrubs sampled show a range of phytolith production from non-producer to abundant (Table 2-4). The trees and shrubs in this assemblage share the production of infilled helical tracheid (Tra-1), dicotyledonous stomata, and polygonal epidermal cells (including a few anticlinal). It has been reported previously that dicot trees and shrubs produce polygonal and anticlinal (jigsaw puzzle) epidermis phytoliths (Bozarth, 1992; McNamee, 2014; Mercader et al., 2009; Strömberg, 2003). This study confirms the occurrence of these forms.

Results from CA analysis show *Grewia villosa* is distinguished from the rest of the trees and shrubs due to the production of non-segmented, armed trichomes (Tri-3) and infilled parenchyma/honeycomb (M-2). *Lochocarpus eriocalyx* is an abundant phytolith producer (Table 2-4) of polygonal epidermis (Epi-1), hollow and infilled helical tracheid (Tra-1), and sclereids compact irregular S body (Scl-8), smooth VI spheres and subspheres (Cl-1), dicotyledon stomata (ST-1), short sclereids (Scl-2), and parenchyma/honeycomb aggregate (M-1).

*Zanthoxylum chalybeum* is an abundant producer (Table 4) of polygonal epidermis (Epi-1), infilled helical tracheid (Tra-1), and dicotyledon stomata (ST-1). In addition, this species produces a small percentage of smooth VI spheres and subspheres (Cl-1) and anticlinal (jigsaw puzzle) epidermis (Epi-2).

*Commiphora* spp. was an abundant producer (Table 4) of polygonal epidermis (Epi-1). There is also the presence of VI spheres (VI-1) infilled helical tracheid (Tra-1). In a previous study by Mercader et al. (2019), four *Commiphora* species from Oldupai Gorge were included. One species is regarded as a low producer with a median of 104 phytoliths, and the other three are ranked very poor producers with a median value of 19 phytoliths.

*Acacia* spp. is a rare producer (Table 2-4) of blocky “faceted rectangular plate” (Blo-3A). *Acacia* spp. is an important tree in this ecosystem, and it is used as a source of food, timber, and medicine. Unfortunately, in my study it is a rare producer, confirming results by Mercader et al (2019). In that study, *Acacia mellifera* is very poor (rare) phytolith producer with an average of 19 phytoliths observed, while *Acacia nilotica* and *A. tortilis* are average producers, with a median of 104 phytoliths (Mercader et al., 2019). Mercader et al. (2009, 2019) examined phytolith morphotypes from varieties of *Acacia* species and revealed diverse morphotypes, including tabular forms, globular, hair base, blockies, and vessel morphotypes. However, the tabular forms (also referred to as ELONGATE ENTIRE) by the International Committee for Phytolith Taxonomy (ICPT) et al. (2019) and blocks occur in many plants. Therefore, they are non-diagnostic to plant taxa. Hair bases and vessels

have poor preservation in the soil, but they have high taxonomic value because they are diagnostic to different plant functional types widely produced among modern plants (International Committee for Phytolith Taxonomy (ICPT) et al., 2019). However, unlike hair base and vessel members, vessel laminate are also referred to as hollow and infilled helix tracheid (Tra-1) (Strömberg, 2003) can be preserved in soils and is used as the indicator of trees and shrubs. *Acacia* is a plant that people would love to identify in the paleontological record, but it may not be possible because they do not have unique morphotypes and are low producers.

#### *Sedge*

*Cyperus rotundus* leaves are abundant producers (Table 2-4) of an epidermal plate with conical bumps (also called Achene), diagnostic to the genus (Honaine et al., 2009; Majumder et al., 2020; Murungi & Bamford, 2020; Stevanato et al., 2019; Strömberg, 2003). The rhizome part of *Cyperus rotundus* contained many hollow and infilled helical tracheary (Tra-1) elements often found in high abundance in trees and shrubs. Infilled and hollow helical tracheid (Tra-1) are reported to occur in low-frequency in other Cyperaceae (Piperno, 2006; Strömberg, 2003). Honaine et al. (2009) referred to infilled and hollow helical tracheid morphotypes as cylindrical tracheids (Honaine et al., 2009).

#### *Herbs*

Herbs species in this study produce phytolith morphotypes, ranging from woody and herbaceous dicots, forest indicators, and unknown morphotypes produced by many taxa.

#### *Grasses*

Eleven species of grass were analyzed. The grass short-cell phytolith morphotypes saddles, bilobates, rondels, polylobates, and crosses were observed from subfamilies of Chloridoideae, Panicoideae, and Aristidoideae. The description of the short cells based on the planes of symmetry is explained in detail in Strömberg (2003). Other phytoliths include long cells, elongates, epidermal cells, trichomes (hairs), mesophyll, blocks, and tracheary elements (Piperno, 2006; Strömberg, 2003).

#### Subfamily Chloridoideae

This study confirms the abundance of squat saddle in the chloridoid species *Chloris gayana* and *Chloris pycnothrix* as the hallmark of the warm and dry-loving Chloridoideae subfamily (Neumann et al., 2017; Piperno & Pearsall, 1998, 1998; Strömberg, 2003; Twiss et al., 1969). This agrees with previous work showing that squat saddles represent 75% of phytolith types produced by West African *Chloris virgata* species (Neumann et al., 2017).

This study also confirms the presence of rondel morphotypes in chloridoid species from East Africa (Barboni et al., 1999; Barboni & Bremond, 2009; Strömberg, 2003; Yost et al.,

2018). *Sporobolus* species, *S. consimilis* and *S. ioclados* produce over 95% crescentic rondel. This agrees with Bamford et al.'s (2006) work that documented 95% of the phytoliths in *Sporobolus* species from Tanzania were of rondels. Barboni & Bremond (2009) also observed rondel morphotypes in the chloridoid species *Sporobolus consimilis*, *S. spicatus*, *Eragostis*, and *Urochondra setulosa* from East Africa. In terms of morphology, some are very small and look like a half-moon in the top view; from the side, some look horned/spooled (Barboni & Bremond, 2009; Strömberg, 2003; Yost et al., 2018). *Sporobolus* spp. crescentic rondel types are diagnostic to genus level; in East Africa there are no other grass phytoliths that are reported to be diagnostic to genus or species level (Barboni & Bremond, 2009; Strömberg, 2003; Yost et al., 2018).

#### Subfamily Panicoideae

Panicoideae produce a wide range of morphotypes, including bilobates, crosses, polylobates, and saddles (see also Barboni & Bremond, 2009; Brown, 1984; Fahmy, 2008; Gallego, 2004; Piperno, 2006; Twiss et al., 1969). However, some morphotypes are unique to the subfamily and therefore are diagnostic to panicoids, also referred to as the so-called “panicoid type” (Piperno, 2006; Strömberg, 2003; Twiss et al., 1969). There was a small percentage of panicoid-type bilobate-symmetry E bilobate (B1-8) in all of the panicoid species studied: *Panicum coloratum*, *Pennisetum* spp., *Brothriocloa insculpta*, *Cenchrus ciliaris*, *Diheterepogon* spp., and *Brachiaria deflexa*.

*Panicum coloratum* produces many four-lobed cross with a near cross-shaped top (CR4-2) (>200); there are also a small number of symmetry E bilobate (BI-8), and polylobate with top and bottom the same size (PO-4). *Panicum coloratum* was the only species with abundant panicoid morphotypes (see Strömberg, 2003). Similarly, Panicoideae species *Panicum* was observed to produce panicoid-type bilobates (Strömberg, 2003), crosses and polylobates. Perfect four-lobed crosses, four-lobed crosses with keeled shapes, and perfect three-lobed cross are abundant in *Panicum*, while four-lobed cross with near cross-shaped top are commonly found in *Zea mays*. All the panicoid species in this study observed to produces cross morphotypes except *Cenchrus ciliaris*. Also, the unique polylobates with the same size top and bottom (PO-4) occurs in all panicoids in this study; this agrees with Fahmy (2008) who suggested that polylobates and nodular bilobates are diagnostic markers for defining genera in the tribe Paniceae, such as *Brachiaria*, *Panicum*, *Pennisetum*, and *Setaria*.

Panicoid species in this study also produce bilobate and polylobate morphotypes that occur in other subfamilies. *Pennisetum* spp., *Brothriocloa insculpta*, *Cenchrus ciliaris*, and *Diheterepogon* spp. produce symmetry B bilobate (BI-5) “simple lobate,” also produced by *Aristida* spp. As a result, these morphotypes are placed in the general PACMAD clade. In

addition, *Panicum coloratum*, *Pennisetum* spp., *Centhrus ciliaris*, *Diheterepogon* spp., and *Brachiaria deflexa* produce a high number of symmetry D bilobate “almost panicoid,” and *Brothriocloa insculpta* is abundant in symmetry C bilobate “inverted”; all are indicative of the general PACMAD clade (Strömberg, 2003).

#### Subfamily Aristidoideae

The Aristidoideae species in this study (*A. adscensionis*) produces bilobates with very long shank and convex edges, also referred to as symmetry B “simple bilobate”. Mulholland (1989) reported the occurrence of similar morphotypes, bilobates with long shanks and saddle-like lobes, in *Aristida longiseta*. Similarly, Piperno (2006) observed the presence of simple bilobates with long, slim shafts connecting saddle-like (in a side view), rounded, or convex-edged end lobes in Aristidoideae species. Therefore, long-shank bilobates with saddle-like lobes are diagnostic of Aristidoideae. This study also observed rare polylobates with a larger top (PO-3) and abundant symmetry D bilobates in *A. adscensionis*. This agrees with Lalor (1995), who also observed bilobates with long shank and saddle-like lobes and nodular forms (also referred to as polylobates), and Strömberg (2003), who documented symmetry D bilobates in *A. adscensionis*. Other morphotypes, including sinuous, indented rondels, entire rondels, and saddles, show that redundancy of production between Aristidoideae, Chloridoideae, and Panicoideae is high (Barboni & Bremond, 2009; Neumann et al., 2017; Piperno, 2006). Because of this redundancy, long shank bilobate with no clear saddle-like forms of lobes should be treated with caution (Piperno, 2006) and are here included in the general PACMAD clade, as suggested by Strömberg (2003).

- i. What phytolith morphotypes and plant functional types are common in the *Acacia-Commiphora* ecosystem surrounding the Manyara Beds?

#### *The Acacia-Commiphora phytolith morphotypes*

The vegetation of the *Acacia-Commiphora* ecosystem ranges from wooded grassland to sparse bushland. The density of trees varies from high, forming a closed canopy, to scattered, creating an open grassland. The ecosystem ranges from dry subhumid to arid zones. Drought-tolerant plants characterize the vegetation of the *Acacia-Commiphora* Acacia ecosystem near the Manyara Beds, including *Acacia mellifera*, *Acacia tortilis*, *Combretum* spp., *Commiphora africana*, *Lococarpus eriocalyx*, *Balanite aegyptiaca*, *Acacia* spp., *Grewia* spp., *Cordia ovalis*, *Launea cornuta*, *Salvadora persica*, *Terminalia spinosa*, *Adansonia digitata*, *Acacia Senegal*, *Commiphora* spp., *Acacia senegal*, *Capparis tomentosa* and others (White, 1983).

The common grasses include species of *Aristida* spp., *Cynodon dactylon*, *Eragostis* spp., *Aistida adscensionis*, *Chloris* spp., *Centhrus ciliaris*, *Sporobolus ioclados*, *Sporobolus*



*consimilis*, *Panicum coloratum*, *Chloris*

*gayana*, *Pennisetum* spp., *Panicum* spp., *Brachiaria* spp., *Bothriochloa insculpta*, and others. Forbs include *Commelina* spp., *Ecbolium revolutum*, *Cissus quadrangularis*, *Sansevieria ehrenbergii*, *Euphorbia hirta*, and others. The sedge *Cyprus rotundus* occurs in muddy areas.

The correspondence analysis results (CA) for phytolith morphotypes (Figure 2-10) indicate that trees and shrubs in this study, including *Commiphora* spp., produced abundant epidermal cells (Epi-1), sclereids, mesophyll, and hair bases; however, most of these phytoliths are less silicified and therefore do not survive in soils. The *Acacia* spp. in this study is a rare producer of blocky (faceted rectangular plate) (Blo-3A); blocky morphotypes are not diagnostic to a specific taxon. CA results in Figure 2-16 demonstrate that Infilled helix tracheid and spheroid forms from trees and shrubs occur in the surface soils. Although in a very low abundance, they can be used as an indicator of these plants from the *Acacia-Commiphora* ecosystem. Grass short cell morphotypes saddles (squat) and rondels (crescentic/spool/horned) from chloridoid grasses and bilobates from “other PACMADs” (Figure 2-16) are abundant in the *Acacia-Commiphora* ecosystem (see also, Mercader et al., 2019). There are also sedge epidermal plates representing marsh areas of the *Acacia-Commiphora* landscape.

ii. Do phytolith assemblages from the topsoil reflect the vegetation types of the site?

To address this question, I examined phytolith morphotypes in surface soils from five sites to understand if the surface soils phytoliths match the vegetation. Vegetation types discussed here include:

1. Bare soils with few grasses, herbaceous plants, and trees for MK 4.
2. Open woodland with grasses, herbaceous plants, and shrubs for MK 2.
3. Bare soil near grasses and shrubs for MK 17.
4. Near dry river valley with patched trees, herbs, and grasses for MKRV 1.
5. Woodland and bush grasslands for Esimingori Hill site.

All soil samples are dominated by phytoliths from grass short cells (GSSC). Bilobate, rondels, and saddles are overrepresented in soils. Seven lobate classes were identified in soils: symmetry B bilobate (BI-5), symmetry C bilobate (BI-6), symmetry D bilobate (BI-7), polylobate with the top and bottom the same size (PO-4), symmetry E bilobate (BI-8), four-lobed crosses with near cross-shaped top (CR4-2), and polylobate with larger top (PO-3). The most dominant lobate type is symmetry D bilobate (BI-7), produced abundantly in the five panicoid species of *Pennisetum* spp., *Cenchrus ciliaris*, *Diheteropogon* spp., *Brachiaria deflexa*, and *Panicum coloratum* analyzed agrees with the presence of the general PACMAD clade seen at all five sites.

Crescentic conical rondels (CO-5) and horned rondels (Barboni & Bremond, 2009; Strömberg, 2003; Yost et al., 2018) are common in *Sporobolus* taxa and occur in soils where these species were found. True saddles occur abundantly in the soil samples and are abundant in *Chloris pychnothrix* and *Chloris gayana*. They are likely to originate from those two plants, and from *Cynodon dactylon* and *Eragostis* (see Barboni & Bremond, 2009; Mercader et al., 2019; Strömberg, 2003), which are also present in the study area. Among the panicoid type morphotypes, symmetry E bilobate and four-lobed crosses with near cross-shaped tops (CR4-2) are abundant in the surface soils from Esimingori Hill. CR4-2 also occur frequently in panicoid species *Panicum coloratum* (see also, Neumann et al., 2017a; Strömberg, 2003). At the same time, *Pennisetum* spp., *Brachiaria deflexa*, and *Diheteropogon* spp. have the highest counts of symmetry E bilobates. Still, this morphotype occurs, although to a small extent, in all panicoid species analyzed in this study. Polylobates with the larger top (PO-3) found in soils from Esimingori Hill match grass phytoliths from *Brachiaria deflexa*, *Panicum coloratum*, and *Pennisetum* spp., In summary, the short-cell phytoliths in the surface soils reflect well the grass species growing in the study area.

Symmetry D bilobate and true saddle are heavily reflected in the surface soils from MK 17, which is more open with a few patches of grasses. Symmetry D bilobate could be associated with the panicoid species *Brachiaria deflexa* and *Bothriochloa insculpta*, while the true saddle is linked to *Chloris pychnothrix* and *Chloris gayana* species. Crescentic conical rondels are strongly reflected at the MK 2 site and could be related to *Sporobolus consimilis* found at the site.

Forest indicator is reflected by the small presence of larger nodular spheres and infilled helical tracheid elements (Tra-1) in the surface soils, suggesting the presence of trees and shrubs at Esimingori Hill. Samples from Esimingori Hill were collected under trees and shrubs while soil samples at other sites were collected from under grasses. Large nodular sphere (CI-8) was not observed in the trees and shrubs species analyzed in this study but was found in soils. It is likely the species that produced these morphotypes were not sampled. Infilled helical tracheid is abundant in *Zanthoxylum chalybeum* and *Lococarpus eriocalyx* sampled from Esimingori Hill.

Spheroid phytoliths occur at a much lower frequency than GSSC and other morphotypes. Spherical and sub-spherical VI-spheres (CI-1) from MK 2 and MD-clump (CL-10) represent a forest indicator, while large verrucate spheres (CI-3) at MK 4 indicate the presence of woody and herbaceous dicots. Samples from MK 2 were collected near grasses and a few trees and shrubs. MD-clumps and larger verrucate spheres (CI-3) were not observed in the plant species analyzed in this study; they are probably being produced by other woody and herbaceous dicots not included in the studied assemblage or that is no longer there. Spherical and sub-spherical VI-sphere (CI-1)

morphotypes were observed in *Launeae cornuta*, *Zanthoxylum chalybeum*, and *Lococarpus eriocalyx*.

The distinctive phytoliths anisopolar prismatic domed cylindric produced by the members of the seeds of the monocotyledon herbs, Commelinaceae, occurs in surface soils surrounding the Manyara Beds. However, members of the genus Commelinaceae were not sampled in the modern plant assemblage. The Commelinaceae are widely distributed in tropical, subtropical, and warm temperate regions (Eichhorn et al., 2010). Commelinaceae species are valuable ecological and paleoecological indicators since they prefer damp habitats (Eichhorn et al., 2010). Also, they can be used in anthropogenic plant communities, especially in association with different cultivation practices (Eichhorn et al., 2010). In the case of this study, the presence of Commelinaceae species in the surface soil samples can likely be attributed to anthropogenic disturbance associated with farming in the study area, or it could be attributed to the humid climate.

The general pattern of phytolith types reported in other modern phytoliths studies in East Africa agrees with the patterns observed in this study, especially when it comes to the GSSC phytoliths (Albert et al., 2006, 2015; Bamford et al., 2006; Barboni et al., 1999; Barboni & Bremond, 2009; Kinyanjui, 2018; Mercader et al., 2019; Peppe et al., 2023). Despite using different classification schemes, these studies have identified that GSSCPs reflect the local plant communities in the study area (Albert et al., 2006, 2015; Bamford et al., 2006; Barboni et al., 1999; Barboni & Bremond, 2009; Kinyanjui, 2018; Mercader et al., 2019). Numerous studies have observed that chloridoid saddles, rondels (*Sporobolus* type), and non-chloridoid PACMAD bilobates are the most abundant morphotypes in soils (Albert et al., 2006, 2015; Bamford et al., 2006; Barboni & Bremond, 2009; Kinyanjui, 2018; Mercader et al., 2019). Compared to other studies, the soil samples from the Manyara Beds have poor preservation of woody morphotypes. Still, the occasional observation of spheroid morphotypes agrees with Mercader et al. (2019)'s documentation of globular forms at the *Acacia-Commiphora* soils of Oldupai Gorge, but they differ in the representations. Mercader et al.'s (2019) study saw a balance between woody and grass types, while in this study, the GSSC phytoliths are overrepresented at the surface soils of the Manyara Beds. This study also documents infilled tracheids in the surface soils representing the woody morphotypes, while the tabular forms previously considered as diagnostic to wood plants for Oldupai soils are considered non-diagnostic types under the (Strömberg, 2003) and (International Committee for Phytolith Taxonomy (ICPT) et al., 2019) classification scheme used in this study. Peppe et al. (2023) utilized a similar classification scheme (Stromberg 2023) to study modern assemblages and interpret the fossil assemblages from Early Miocene fossil sites (21-16 Ma) in Kenya and Uganda. Peppe et al. (2023) demonstrated the effectiveness of the classification scheme used in this study. They observed similar patterns of grass

assemblages and the distinctions between saddles of the C4 chloridoid and cross and bilobate forms of non-chloridoid PACMAD grasses in the fossil assemblages. Unlike my study, Peppe et al. (2023) included a broader range of environments and a broader ecological region from the evergreen forest of the Democratic Republic of Congo and Kakamega, which is significant in fossil assemblages. However, when comparing the modern assemblage from forest environments with grassy assemblages, most of the early Miocene sites that yielded phytoliths show a greater similarity with a C4-grass dominated habitats instead of forest assemblage from the Guineo-Congolian lowland rainforest.

#### *Taphonomic considerations*

As predicted, grass silica short cell phytoliths are more abundant than the less silicified cells like epidermal cells, specifically those from non-grasses plants (Epi-1 and Epi-2), stomata complexes (St-1), and mesophyll cells (M-1, M-2, M-5, and M-10); these were observed in the plant samples but are absent in the surface soils. Therefore, it is challenging to distinguish woodlands from grasslands using the surface soils from the surroundings of the Manyara Beds. This discrepancy between vegetation type and phytolith assemblages can be because some non-grass species do not produce phytoliths. For instance, *Combretum zeyheri* from Esimingori Hill did not make phytoliths; many non-grasses are non-producers (see Piperno, 2006). However, it is still possible to distinguish woodlands using the presence of certain morphotypes, like the various spherical forms and infilled helix tracheid representing woody dicots, woody and herbaceous dicots, and forest indicators.

Another reason for a low count of non-grass phytolith forms could be attributed to post-depositional alterations such as etching, which tends to affect forest indicator phytoliths more than GSSCPs, making them difficult to identify (Strömberg et al., 2018). Also, any plants recently removed by people or otherwise might be absent at the site, but their phytoliths are present. Finally, grass phytoliths are known to be better represented in soils than other plants because GSSCPs are compact and well-silicified compared to some non-grass morphotypes. Also, some grasses have a shorter life cycle than trees/shrubs and thus will be deposited in soils with a higher frequency (Albert et al., 2015; Piperno, 2006).

Therefore, certain phytolith morphotypes in soil should not simply be associated with their resistance to post-depositional factors; instead, other factors, such as the deposition duration and sedimentary level, should be considered as well. Also, it is acknowledged that phytolith preservation is often poor in disturbed areas and areas with scattered vegetation (Albert et al., 2015). Therefore, the lack of some phytolith morphotypes in surface soils is only sometimes related to their absence in the ecosystem. Albert et al. (2015) reported on the occurrence of low abundance phytolith

assemblages from modern palm-related vegetation and documented a low abundance of palm phytoliths compared to those found in paleoanthropological samples at Oldupai; instead, GSSCs were abundant in all their samples, and many do not correspond to the grass species growing at the sampling spot.

In addition, the post-depositional effects of weathering and breakage, specifically for broken bilobates, is observed in grass species *Aristida adscensionis*, *Penisetum* spp., and *Centhrus ciliaris*. In the surface soils, factors such as the naturally induced gully erosion at MK 4 (Maerker et al., 2015) and water transportation at sites such as Makuyuni River Valley (MKRV1) can remove the phytolith-rich layer. Also, these sites are occupied by people along with their domestic animals. Makuyuni is also within the migration corridors to Manyara and Ngorongoro National Parks, which most likely impacts MK2. Despite my efforts to sample areas with minimal disturbances, all these factors impact the soils and modern vegetation.

### Conclusions

This chapter was necessary to gain taphonomic control and define a classification scheme that is simple, more general and could be used globally despite the redundancy and multiplicity of phytolith morphotypes. Results of this study sets up a classification and interpretive scheme that will be used to analyze phytoliths from the ancient sediments of the Manyara Beds in Chapters 3 and 4.

Strömberg's (2003) phytolith classification scheme worked well for this assemblage. Through Strömberg's (2003) classification scheme, this study has demonstrated that the only phytoliths found in *Acacia* are faceted rectangular plates (Blo-3A) and the dominant phytoliths for *Commiphora* are polyhedral epidermal cells (Epi-1). However, these morphotypes have low taxonomic resolution.

This study found that in general, trees, shrubs, and herbs vary greatly in phytolith production. Diagnostic phytoliths in trees, herbs, and shrubs are hairs, tracheids, and polygonal epidermal cells. Epidermal cells and hairs are less useful due to poor preservation; as a result, woody and herbaceous dicot plant cover is poorly reflected in the surface soils of the Manyara Beds. The GSSC phytoliths bilobates symmetry D bilobates (indicative of the “other PACMADs), saddles, and rondels (crescentic/spool/horned) that represent chloridoids are the most common morphotypes at the *Acacia-Commiphora* vegetation. The GSSCPs assemblage from soils reflect the species growing in them today.

This study also observed that many of the phytolith forms created by modern plants at the study area can be identified in the soils beneath. Post-depositional processes such as weathering and breakage and anthropogenic processes such as overgrazing can remove phytolith rich soils as a result some phytolith morphotypes might be removed or there might be overrepresentation of other morphotypes.

## Literature Cited

- Albert, R. M., Bamford, M. K., & Cabanes, D. (2006). Taphonomy of phytoliths and macroplants in different soils from Olduvai Gorge (Tanzania) and the application to Plio-Pleistocene palaeoanthropological samples. *Quaternary International*, 148(1), 78–94.  
<https://doi.org/10.1016/j.quaint.2005.11.026>
- Albert, R. M., Bamford, M. K., & Esteban, I. (2015). Reconstruction of ancient palm vegetation landscapes using a phytolith approach. *Quaternary International*, 369, 51–66.  
<https://doi.org/10.1016/j.quaint.2014.06.067>
- Alexandre, A., Meunier, J.-D., Lézine, A.-M., Vincens, A., & Schwartz, D. (1997). Phytoliths: Indicators of grassland dynamics during the late Holocene in intertropical Africa. *Palaeogeography, Palaeoclimatology, Palaeoecology*, 136(1–4), 213–229. [https://doi.org/10.1016/S0031-0182\(97\)00089-8](https://doi.org/10.1016/S0031-0182(97)00089-8)
- Bachofer, F., Quénéhervé, G., Hertler, C., Giemsch, L., Hochschild, V., & Maerker, M. (2018). Paleoenvironmental Research in the Semiarid Lake Manyara Area, Northern Tanzania: A Synopsis. In C. Siart, M. Forbriger, & O. Bubenzer (Eds.), *Digital Geoarchaeology* (pp. 123–138). Springer International Publishing. [https://doi.org/10.1007/978-3-319-25316-9\\_8](https://doi.org/10.1007/978-3-319-25316-9_8)
- Bamford, M. K., Albert, R. M., & Cabanes, D. (2006). Plio-Pleistocene vegetation in the eastern palaeolake margin of Olduvai Gorge (Tanzania) and preliminary results from fossil macroplant and phytolith remains. *Quaternary International*, 148, 95–112.
- Barboni, D. (2014). Vegetation of Northern Tanzania during the Plio-Pleistocene: A synthesis of the paleobotanical evidences from Laetoli, Olduvai, and Peninj hominin sites. *Quaternary International*, 322–323, 264–276. <https://doi.org/10.1016/j.quaint.2014.01.016>
- Barboni, D., Ashley, G. M., Bourel, B., Arráiz, H., & Mazur, J.-C. (2019). Springs, palm groves, and the record of early hominins in Africa. *Review of Palaeobotany and Palynology*, 266, 23–41.  
<https://doi.org/10.1016/j.revpalbo.2019.03.004>
- Barboni, D., Ashley, G. M., Dominguez-Rodrigo, M., Bunn, H. T., Mabulla, A. Z. P., & Baquedano, E. (2010). Phytoliths infer locally dense and heterogeneous paleovegetation at FLK North and surrounding localities during upper Bed I time, Olduvai Gorge, Tanzania. *Quaternary Research*, 74(3), 344–354. <https://doi.org/10.1016/j.yqres.2010.09.005>
- Barboni, D., Bonnefille, R., Alexandre, A., & Meunier, J. D. (1999). Phytoliths as paleoenvironmental indicators, West Side Middle Awash Valley, Ethiopia. *Palaeogeography, Palaeoclimatology, Palaeoecology*, 152(1–2), 87–100. [https://doi.org/10.1016/S0031-0182\(99\)00045-0](https://doi.org/10.1016/S0031-0182(99)00045-0)

- Barboni, D., Bremond, L., & Bonnefille, R. (2007). Comparative study of modern phytolith assemblages from inter-tropical Africa. *Palaeogeography, Palaeoclimatology, Palaeoecology*, 246(2–4), 454–470. <https://doi.org/10.1016/j.palaeo.2006.10.012>
- Barboni, D., & Bremond, L. (2009). Phytoliths of East African grasses: An assessment of their environmental and taxonomic significance based on floristic data. *Review of Palaeobotany and Palynology*, 158(1–2), 29–41. <https://doi.org/10.1016/j.revpalbo.2009.07.002>
- Bonnefille, R. (2010). Cenozoic vegetation, climate changes and hominid evolution in tropical Africa. *Global and Planetary Change*, 72(4), 390–411. <https://doi.org/10.1016/j.gloplacha.2010.01.015>
- Bozarth, S. R. (1992). Classification of Opal Phytoliths Formed in Selected Dicotyledons Native to the Great Plains. In G. Rapp & S. C. Mulholland (Eds.), *Phytolith Systematics* (pp. 193–214). Springer US. [https://doi.org/10.1007/978-1-4899-1155-1\\_10](https://doi.org/10.1007/978-1-4899-1155-1_10)
- Bremond, L., Alexandre, A., Wooller, M. J., Hély, C., Williamson, D., Schäfer, P. A., Majule, A., & Guiot, J. (2008). Phytolith indices as proxies of grass subfamilies on East African tropical mountains. *Global and Planetary Change*, 61(3–4), 209–224. <https://doi.org/10.1016/j.gloplacha.2007.08.016>
- Brown, D. A. (1984). Prospects and limits of a phytolith key for grasses in the central United States. *Journal of Archaeological Science*, 11(4), 345–368. [https://doi.org/10.1016/0305-4403\(84\)90016-5](https://doi.org/10.1016/0305-4403(84)90016-5)
- Cabanes, D., & Shahack-Gross, R. (2015). Understanding Fossil Phytolith Preservation: The Role of Partial Dissolution in Paleoecology and Archaeology. *PLOS ONE*, 10(5), e0125532. <https://doi.org/10.1371/journal.pone.0125532>
- Calla McNamee. (2012). *Soil Phytolith Assemblages of the American Southwest: The Use of Historical Ecology in Taphonomic Studies* [Degree of Doctor of Philosophy]. University of Calgary.
- Collura, L. V., & Neumann, K. (2017). Wood and bark phytoliths of West African woody plants. *Quaternary International*, 434, 142–159. <https://doi.org/10.1016/j.quaint.2015.12.070>
- Crifò, C., & Strömberg, C. A. E. (2020). Small-scale spatial resolution of the soil phytolith record in a rainforest and a dry forest in Costa Rica: Applications to the deep-time fossil phytolith record. *Palaeogeography, Palaeoclimatology, Palaeoecology*, 537, 109107. <https://doi.org/10.1016/j.palaeo.2019.03.008>
- Directorate of Overseas Surveys for Republic of Tanganyika and Zanzibar. (1969). *Makuyuni (Tanganyika) Topographic Map*. [Topographic Map].
- Doey, L., & Kurta, J. (2011). Correspondence Analysis applied to psychological research. *Tutorials in Quantitative Methods for Psychology*, 7(1), 5–14. <https://doi.org/10.20982/tqmp.07.1.p005>

- Dominguez- Rodrigo, M., Serrallonga, J., Juan-Tresserras, J., Alcala, L., & Luque, L. (2001). Woodworking activities by early humans: A plant residue analysis on Acheulian stone tools from Peninj (Tanzania). *Journal of Human Evolution*, 40(4), 289–299.  
<https://doi.org/10.1006/jhev.2000.0466>
- Eichhorn, B., Neumann, K., & Garnier, A. (2010). Seed phytoliths in West African Commelinaceae and their potential for palaeoecological studies. *Palaeogeography, Palaeoclimatology, Palaeoecology*, 298(3–4), 300–310. <https://doi.org/10.1016/j.palaeo.2010.10.004>
- Esteban, I., De Vynck, J. C., Singels, E., Vlok, J., Marean, C. W., Cowling, R. M., Fisher, E. C., Cabanes, D., & Albert, R. M. (2017). Modern soil phytolith assemblages used as proxies for Paleoscape reconstruction on the south coast of South Africa. *Quaternary International*, 434, 160–179.  
<https://doi.org/10.1016/j.quaint.2016.01.037>
- Fahmy, A. G. (2008). Diversity of lobate phytoliths in grass leaves from the Sahel region, West Tropical Africa: Tribe Paniceae. *Plant Systematics and Evolution*, 270(1–2), 1–23.  
<https://doi.org/10.1007/s00606-007-0597-z>
- Flores-Prieto, E., Quénéhervé, G., Bachofer, F., Shahzad, F., & Maerker, M. (2015). Morphotectonic interpretation of the Makuyuni catchment in Northern Tanzania using DEM and SAR data. *Geomorphology*, 248, 427–439. <https://doi.org/10.1016/j.geomorph.2015.07.049>
- Fredlund, G. G., & Tieszen, L. T. (1994). Modern Phytolith Assemblages from the North American Great Plains. *Journal of Biogeography*, 21(3), 321. <https://doi.org/10.2307/2845533>
- Gallego, L. (2004). Phytolith Assemblages in Grasses Native to Central Argentina. *Annals of Botany*, 94(6), 865–874. <https://doi.org/10.1093/aob/mch214>
- Honaine, M. F., Zucol, A. F., & Osterrieth, M. L. (2009). Phytolith analysis of Cyperaceae from the Pampean region, Argentina. *Australian Journal of Botany*, 57(6), 512.  
<https://doi.org/10.1071/BT09041>
- International Committee for Phytolith Taxonomy (ICPT), Neumann, K., Strömberg, C. A. E., Ball, T., Albert, R. M., Vrydaghs, L., & Cummings, L. S. (2019). International Code for Phytolith Nomenclature (ICPN) 2.0. *Annals of Botany*, 124(2), 189–199.  
<https://doi.org/10.1093/aob/mcz064>
- Kaiser, T.M., Seiffert, C. C., Fiedler, L., Schwartz, H. L., Frost, S. R., & Nelson, S. V. (2010). Makuyuni, a new lower Palaeolithic hominid site in Tanzania. *Mitteilungen Hamburgisches Zoolischen Museum Institut*, 106, 69–110.
- Kennedy, R., Riquier, C., & Sharp, B. (1996). Practical Applications of Correspondence Analysis to Categorical Data in market Research. *Journal of Journal of Targeting Measurement and Analysis for Marketing*, 5, 56–70.



- Kinyanjui, R. N. (2018). *Phytolith analysed to Compare Changes in Vegetation Structure of Koobi Fora and Olorgesailie Basins through the Mid-Pleistocene-Holocene Periods*. [A thesis submitted to the Faculty of Science in fulfilment of the requirements for Doctoral of Philosophy degree]. University of Witwatersrand.
- Kooyman, B. (2015). Phytoliths: Preparation and Archaeological Extraction. In E. C. T. Yeung, C. Stasolla, M. J. Sumner, & B. Q. Huang (Eds.), *Plant Microtechniques and Protocols* (pp. 507–524). Springer International Publishing. [https://doi.org/10.1007/978-3-319-19944-3\\_28](https://doi.org/10.1007/978-3-319-19944-3_28)
- Legendre, P., & Legendre, L. (1998). *Numerical ecology* (2nd English ed). Elsevier.
- Maerker, M., Quénéhervé, G., Bachofer, F., & Mori, S. (2015). A simple DEM assessment procedure for gully system analysis in the Lake Manyara area, northern Tanzania. *Natural Hazards*, 79(S1), 235–253. <https://doi.org/10.1007/s11069-015-1855-y>
- Majumder, S., Mallick, T., & Ghosh, A. (2020). Morphological diversity of phytolith structures in six species of *Carex* L. and *Cyperus* L. (*Cyperaceae* Juss.) from West Bengal, India. *Biodiversitas Journal of Biological Diversity*, 21(8). <https://doi.org/10.13057/biodiv/d210808>
- McCune, J. L. (2013). *The long-term history of plant communities on southeastern Vancouver Island based on vegetation resurveys and phytolith analysis* [PhD Dissertation]. University of British Columbia.
- McCune, B., Grace, J. B., & Urban, D. L. (2002). *Analysis of ecological communities* (2nd printing). MjM Software Design.
- McNamee, C. (2014). *Soil Phytolith Assemblages of the American Southwest: The Use of Historical Ecology in Taphonomic Studies*. Library and Archives Canada = Biblioth que et Archives Canada.
- Mercader, J., Bennett, T., Esselmont, C., Simpson, S., & Walde, D. (2009). Phytoliths in woody plants from the Miombo woodlands of Mozambique. *Annals of Botany*, 104(1), 91–113. <https://doi.org/10.1093/aob/mcp097>
- Mercader, J., Bennett, T., Esselmont, C., Simpson, S., & Walde, D. (2011). Soil phytoliths from miombo woodlands in Mozambique. *Quaternary Research*, 75(1), 138–150. <https://doi.org/10.1016/j.yqres.2010.09.008>
- Mercader, J., Clarke, S., Bundala, M., Favreau, J., Inwood, J., Itambu, M., Larter, F., Lee, P., Lewiski-McQuaid, G., Mollel, N., Mwambwiga, A., Patalano, R., Soto, M., Tucker, L., & Walde, D. (2019). Soil and plant phytoliths from the *Acacia-Commiphora* mosaics at Oldupai Gorge (Tanzania). *PeerJ*, 7, e8211. <https://doi.org/10.7717/peerj.8211>

- Mishra, P., Pandey, C., Singh, U., Gupta, A., Sahu, C., & Keshri, A. (2019). Descriptive statistics and normality tests for statistical data. *Annals of Cardiac Anaesthesia*, 22(1), 67.  
[https://doi.org/10.4103/aca.ACA\\_157\\_18](https://doi.org/10.4103/aca.ACA_157_18)
- Mulholland, S. C. (1989). Phytolith shape frequencies in North Dakota grasses: A comparison to general patterns. *Journal of Archaeological Science*, 16(5), 489–511.  
[https://doi.org/10.1016/0305-4403\(89\)90070-8](https://doi.org/10.1016/0305-4403(89)90070-8)
- Murungi, M. L., & Bamford, M. K. (2020). Revised taxonomic interpretations of Cyperaceae phytoliths for (paleo)botanical studies with some notes on terminology. *Review of Palaeobotany and Palynology*, 275, 104189.  
<https://doi.org/10.1016/j.revpalbo.2020.104189>
- Neumann, K., Fahmy, A. G., Müller-Schneeßel, N., & Schmidt, M. (2017). Taxonomic, ecological and palaeoecological significance of leaf phytoliths in West African grasses. *Quaternary International*, 434, 15–32. <https://doi.org/10.1016/j.quaint.2015.11.039>
- Neumann, K., Fahmy, A., Lespez, L., Ballouche, A., & Huysecom, E. (2009). The Early Holocene palaeoenvironment of Ounjougou (Mali): Phytoliths in a multiproxy context. *Palaeogeography, Palaeoclimatology, Palaeoecology*, 276(1–4), 87–106.  
<https://doi.org/10.1016/j.palaeo.2009.03.001>
- Pearsall, D. M. (2016). *Paleoethnobotany*. Routledge. <https://doi.org/10.4324/9781315423098>
- Peppe, D. J., Cote, S. M., Deino, A. L., Fox, D. L., Kingston, J. D., Kinyanjui, R. N., Lukens, W. E., MacLachy, L. M., Novello, A., Strömberg, C. A. E., Driese, S. G., Garrett, N. D., Hillis, K. R., Jacobs, B. F., Jenkins, K. E. H., Kityo, R. M., Lehmann, T., Manthi, F. K., Mbua, E. N., ... McNulty, K. P. (2023). Oldest evidence of abundant C<sub>4</sub> grasses and habitat heterogeneity in eastern Africa. *Science*, 380(6641), 173–177. <https://doi.org/10.1126/science.abq2834>
- Piperno, D. R. (1985). Phytolith taphonomy and distributions in archeological sediments from Panama. *Journal of Archaeological Science*, 12(4), 247–267. [https://doi.org/10.1016/0305-4403\(85\)90032-9](https://doi.org/10.1016/0305-4403(85)90032-9)
- Piperno, D. R. (1991). The status of phytolith analysis in the American tropics. *Journal of World Prehistory*, 5(2), 155–191. <https://doi.org/10.1007/BF00974678>
- Piperno, D. R. (2006). *Phytoliths: A comprehensive guide for archaeologists and paleoecologists*. AltaMira Press.
- Piperno, D. R., & Pearsall, D. M. (1998). The Silica Bodies of Tropical American Grasses: Morphology, Taxonomy, and Implications for Grass Systematics and Fossil Phytolith Identification. *Smithsonian Contributions to Botany*, 85, 1–40. <https://doi.org/10.5479/si.0081024X.85>

- Potts, R., Dommain, R., Moerman, J. W., Behrensmeyer, A. K., Deino, A. L., Riedl, S., Beverly, E. J., Brown, E. T., Deocampo, D., Kinyanjui, R., Lupien, R., Owen, R. B., Rabideaux, N., Russell, J. M., Stockhecke, M., deMenocal, P., Faith, J. T., Garcin, Y., Noren, A., ... Uno, K. (2020). Increased ecological resource variability during a critical transition in hominin evolution. *Science Advances*, 6(43), eabc8975. <https://doi.org/10.1126/sciadv.abc8975>
- Rashid, I., Mir, S. H., Zurro, D., Dar, R. A., & Reshi, Z. A. (2019). Phytoliths as proxies of the past. *Earth-Science Reviews*, 194, 234–250. <https://doi.org/10.1016/j.earscirev.2019.05.005>
- Ring, U., Schwartz, H. L., Bromage, T. G., & Sanaane, C. (2005). Kinematic and sedimentological evolution of the Manyara Rift in northern Tanzania, East Africa. *Geological Magazine*, 142(4), 355–368. <https://doi.org/10.1017/S0016756805000841>
- Rossouw, L., & Scott, L. (2011). Phytoliths and Pollen, the Microscopic Plant Remains in Pliocene Volcanic Sediments Around Laetoli, Tanzania. In T. Harrison (Ed.), *Paleontology and Geology of Laetoli: Human Evolution in Context* (pp. 201–215). Springer Netherlands. [https://doi.org/10.1007/978-90-481-9956-3\\_9](https://doi.org/10.1007/978-90-481-9956-3_9)
- Ruffo, C. K., Birnie, A., & Tengnäs, B. (2002). *Edible wild plants of Tanzania*. Regional Land Management Unit/Sida.
- Runge, F. (1999). The opal phytolith inventory of soils in central Africa—Quantities, shapes, classification, and spectra. *Review of Palaeobotany and Palynology*, 107(1–2), 23–53. [https://doi.org/10.1016/S0034-6667\(99\)00018-4](https://doi.org/10.1016/S0034-6667(99)00018-4)
- Schwartz, H., Renne, P. R., Morgan, L. E., Wildgoose, M. M., Lippert, P. C., Frost, S. R., Harvati, K., Schrenk, F., & Sanaane, C. (2012). Geochronology of the Manyara Beds, northern Tanzania: New tepthrostratigraphy, magnetostratigraphy and  $^{40}\text{Ar}/^{39}\text{Ar}$  ages. *Quaternary Geochronology*, 7, 48–66. <https://doi.org/10.1016/j.quageo.2011.09.002>
- Stevanato, M., Rasbold, G. G., Parolin, M., Domingos Luz, L., Lo, E., Weber, P., Trevisan, R., & Galeazzi Caxambu, M. (2019). New characteristics of the papillae phytolith morphotype recovered from eleven genera of Cyperaceae. *Flora*, 253, 49–55. <https://doi.org/10.1016/j.flora.2019.03.012>
- Strömberg, C. A. E. (2003). *The Origin and Spread of Grass-dominated Ecosystem during the Tertiary of North America and How it Relates to Evolution of Hypsodont in Equids*. [PhD thesis]. University of California.
- Strömberg, C. A. E. (2004). Using phytolith assemblages to reconstruct the origin and spread of grass-dominated habitats in the great plains of North America during the late Eocene to early Miocene. *Palaeogeography, Palaeoclimatology, Palaeoecology*, 207(3–4), 239–275. <https://doi.org/10.1016/j.palaeo.2003.09.028>

- Strömberg, C. A. E., Dunn, R. E., Crifò, C., & Harris, E. B. (2018). Phytoliths in Paleoecology: Analytical Considerations, Current Use, and Future Directions. In D. A. Croft, D. F. Su, & S. W. Simpson (Eds.), *Methods in Paleoecology* (pp. 235–287). Springer International Publishing.  
[https://doi.org/10.1007/978-3-319-94265-0\\_12](https://doi.org/10.1007/978-3-319-94265-0_12)
- Thode, H. C. (2002). *Testing For Normality* (0 ed.). CRC Press.  
<https://doi.org/10.1201/9780203910894>
- Twiss, P. C. (1992). Predicted World Distribution of C3 and C4 Grass Phytoliths. In G. Rapp & S. C. Mulholland (Eds.), *Phytolith Systematics* (pp. 113–128). Springer US.  
[https://doi.org/10.1007/978-1-4899-1155-1\\_6](https://doi.org/10.1007/978-1-4899-1155-1_6)
- Twiss, P. C., Suess, E., & Smith, R. M. (1969). Morphological Classification of Grass Phytoliths. *Soil Science Society of America Journal*, 33(1), 109–115.  
<https://doi.org/10.2136/sssaj1969.03615995003300010030x>
- Wallis, L. (2003). An overview of leaf phytolith production patterns in selected northwest Australian flora. *Review of Palaeobotany and Palynology*, 125(3–4), 201–248.  
[https://doi.org/10.1016/S0034-6667\(03\)00003-4](https://doi.org/10.1016/S0034-6667(03)00003-4)
- White, F. (1983). *The vegetation of Africa: A descriptive memoir to accompany the Unesco/AETFAT/UNSO vegetation map of Africa*. UNESCO.
- Wildi, O. (2010). *Data analysis in vegetation ecology*. Wiley-Blackwell.
- Wolf, N. D., Nelson, S. V., Schwartz, H. L., Semperebon, G. M., Kaiser, T. M., & Bernor, R. L. (2010). Taxonomy and paleoecology of the Pleistocene Equidae from Makuyuni, Northern Tanzania. *Palaeodiversity*, 3, 249–269.
- Yost, C. L., Ivory, S. J., Deino, A. L., Rabideaux, N. M., Kingston, J. D., & Cohen, A. S. (2021). Phytoliths, pollen, and microcharcoal from the Baringo Basin, Kenya reveal savanna dynamics during the Plio-Pleistocene transition. *Palaeogeography, Palaeoclimatology, Palaeoecology*, 570, 109779. <https://doi.org/10.1016/j.palaeo.2020.109779>
- Yost, C. L., Jackson, L. J., Stone, J. R., & Cohen, A. S. (2018). Subdecadal phytolith and charcoal records from Lake Malawi, East Africa imply minimal effects on human evolution from the ~74 ka Toba supereruption. *Journal of Human Evolution*, 116, 75–94.  
<https://doi.org/10.1016/j.jhevol.2017.11.005>

### **Chapter 3: Were there any vegetation cover changes through time and space in the lower Manyara Beds? What kind of microhabitats were hominins using in the Lake Manyara region during the Middle Pleistocene?**

#### **Abstract**

The Manyara Beds have a substantial archaeological record and significant potential for investigating hominin adaptation to environmental variability in the Middle Pleistocene. Previous faunal and stable isotope studies suggest the occurrence of C<sub>4</sub> open grasslands. However, palaeobotanical data should be used to examine the relationship between vegetation and hominin activities in the paleo-lake Manyara landscape. Sixty-nine sediment samples from both archaeological and non-archaeological sites were analyzed for phytoliths. Results from archaeological site MK 4 revealed woody vegetation, palms, and C<sub>4</sub> grassland species, with abundant other PACMAD grasses, the dry adapted Chloridoideae, as well as a small percentage of Panicoideae, which prevails in warm and humid areas. There is also a presence of wetland taxa, sedges, the Commelinaceae, and aquatic monocots, suggesting that paleolandscape Manyara was well watered. The non-archaeological sites and archaeological site MK 17 revealed more open grassy conditions with scattered woody vegetation (palm and woody dicots). Overall, the region consisted of primarily C<sub>4</sub> grasslands made up of PACMAD grasses. These results indicate that varied habitats were available for the hominins at the Manyara Beds.

#### **Introduction**

The Manyara Beds are situated in the eastern Manyara Basin, a half-graben at the southern end of the Gregory Rift in Northern Tanzania (Figure 3-1) (Ring et al., 2005). The Manyara Beds sample a poorly studied stratigraphic interval in the Middle Pleistocene. The sediments lie above the Brunhes-Matuyama boundary below the Hollywood Tuff, and are thus estimated to be between 780,000 and 633,000 years old (Schwartz et al., 2012). The site's age overlaps with a major global climatic shift, the so called mid-Pleistocene transition marked by the intensification of glacial-interglacial climatic cycles that began 900 to 650 kya (Castañeda et al., 2016; Dupont et al., 2001; Grove et al., 2015; Maslin & Ridgwell, 2005). These climatic shifts coincided with the emergence of *Homo heidelbergensis*, which likely later gave rise to our own species, *Homo sapiens*, during the end of the Middle Pleistocene (Johnson & McBrearty, 2012; McBrearty & Brooks, 2000; Pearson, 2000; Rightmire, 1996; Stringer, 2012). This period also documents the technological transition from the larger cutting tools such as the hand axes and cleavers of the Acheulean Industry (Early Stone Age) to the Levallois technique manufactured blades, and later points, of the Middle Stone Age

approximately 500,000 years ago (Johnson & McBrearty, 2012; McBrearty, 2001; McBrearty & Brooks, 2000; Tryon et al., 2006).

Unfortunately, early Middle Pleistocene sites are sparse (Clark, 1987; Maddux et al., 2015; Potts, 2013; Rightmire, 1996, 2008). The Manyara Beds are among of the few sites that sample early Middle Pleistocene records and could potentially add to the existing knowledge concerning early hominin adaptations to environmental variability during this period (Frost et al., 2012; Kaiser et al., 2010; Wolf et al., 2010). Even though hominin remains are rare at these deposits, the Acheulean tools recorded from the Manyara Beds attest to hominin presence and exploitation of resources near the shores of ancient Lake Manyara (Giemsch et al., 2018; Kaiser et al., 2010).

The Manyara Beds are strategically important for examining the role of habitat change in human evolution because the deposits document evidence of numerous periods of environmental variability related to the enlargement and shrinkage of paleo-lake Manyara throughout the early Middle Pleistocene (Bachofer et al., 2018; Frost et al., 2012; Kaiser et al., 2010; Ring et al., 2005). Such changes to the lake's shorelines created lake flats and a succession of vegetation zones that provided complex mosaic habitats for hominin occupation and other animals starting the early Middle Pleistocene (Kaiser et al., 2010). Although previous studies have reconstructed the paleoecology of the fossiliferous sites at the Manyara Beds, these focused on materials collected from the surface, which have no spatial or temporal provenience (Bachofer et al., 2018; Kaiser et al., 2010; Kent, 1942; Ring et al., 2005; Schwartz et al., 2012).

Over the past two decades, novel approaches have been applied to the study of past environmental conditions at East African Plio-Pleistocene hominin sites (Albert et al., 2006; Albert, Bamford, Stanistreet, et al., 2015; Barboni et al., 1999; Barboni, 2014; Barboni & Bremond, 2009; Rossouw & Scott, 2011; Yost et al., 2021). Multi-proxy studies, including phytolith analysis, have demonstrated the value of paleobotanical records for providing detailed reconstruction of past environmental changes (Albert et al., 2006; Barboni, 2014; Potts et al., 2020; Rossouw & Scott, 2011; Yost et al., 2021).

This study utilizes plant micro-remains (phytoliths) from the Manyara Beds to examine the role of habitat change in this area. Although stable isotopic and faunal ecomorphology analyses have provided some information about the paleoenvironment at the Manyara Beds (Kaiser et al., 2010; Wolf et al., 2010), they can only indicate general vegetational types such as grassland, open woodland, or closed woodlands. Phytoliths, conversely, can corroborate those results and add specific detail because they can identify specific plant taxonomic group such as sedge, palms, Zingiberales, Commelinaceae and others (Pearsall, 2016; Piperno, 2006; Strömberg, 2003). At a C<sub>4</sub> grassland environment like that inferred for the Manyara Beds (Kaiser et al., 2010; Wolf et al., 2010),

phytoliths can further distinguish grasses that are adapted to warm and dry conditions (Chloridoideae) from wet and warm adapted grasses (Panicoideae) (Piperno, 2006; Strömberg et al., 2018). The reconstructed environment will help to understand how hominins and herbivores interacted with their surroundings and complement the previous isotopic and fauna composition studies (Frost et al., 2012; Kaiser et al., 2010; Wolf et al., 2010).

## Material and Methods

### Study Sites

Sediment for phytoliths analysis was collected in 2021 and 2022 from wall profiles at archaeological sites MK 4, MK 17, MK 2, and three non-archaeological sites throughout the Makuyuni River valley: MKRV 1, MKRV 2, and MKRV3, to evaluate hominin microhabitat preferences (Figure 3-1). The sampling approach combines spatial (horizontal) variation to understand preservation within and between sites and temporal (vertical) variation within the site to understand vegetation changes through time in the Manyara Beds. The archaeological sites were selected based on the previous report by Giemsch et al. (2018). The non-archaeological sites were selected based on the knowledge of geological exposures that expose the upper/lower member contact within the Makuyuni River Valley (Bachofer et al., 2018; Schwartz et al., 2012, 2012).

### Site stratigraphy

For age estimates, this study relied on site age models from already published data (Frost et al., 2012; Schwartz et al., 2012). This study focused on the uppermost 5.5-meter stratigraphic section of the lower member, just beneath the lower-upper member contact. A distinctive tephra layer (Hollywood tuff) occurs in the transition from the upper to lower member and is  $^{40}\text{Ar}/^{39}\text{Ar}$  dated to  $0.633 \pm 0.039$  Ma (Schwartz et al., 2012). The lower member is lacustrine in nature, grayish in color, and consists mainly of tuff, marls, siltstones, mudstones, and diatomites. Paleomagnetic dating shows that the top 6 meters of the lower member were deposited during the Bruhnes Normal Chron, and are therefore younger than 0.743 Ma (Schwartz et al., 2012). These two dates constrain the fossil and artifact-rich localities of MK 2 and MK 4 to be between 0.784 Ma and 0.633 Ma.

The location of MK 17 is not well known within the dated section. In 2008 a right proximal tibia fragment of *Theropithecus oswaldi leakeyi* (MK17.2008.1) was recovered on surface at MK 17 site, which could originate from the contact zone (0.784-0.633 Ma) since it is the most fossiliferous rich part of the Manyara Beds (Frost et al., 2017; Schwartz et al., 2012).

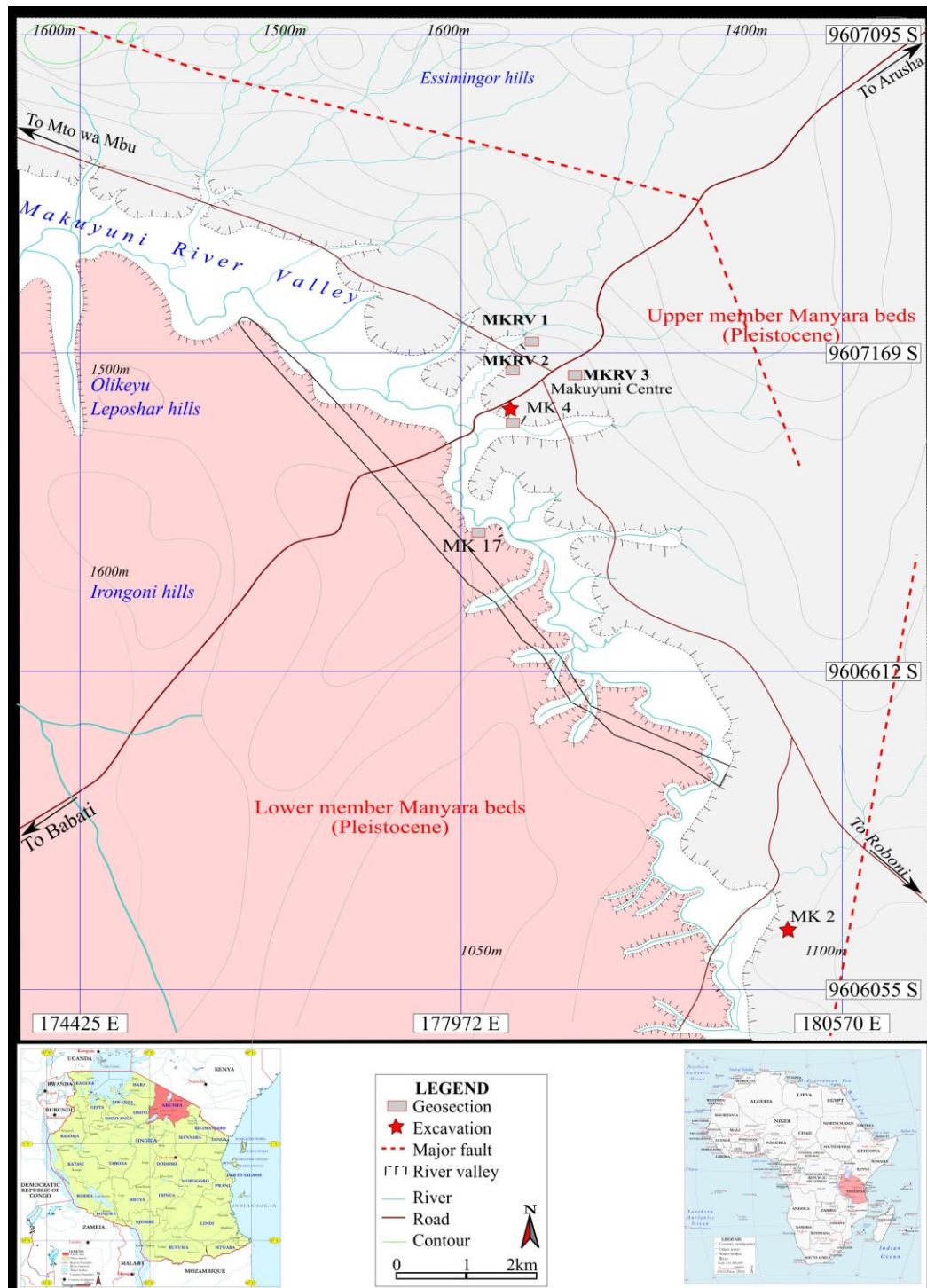


**Figure 3-1:** Map of the study area (Makuyuni town) showing the sampling sites in the Manyara Beds.



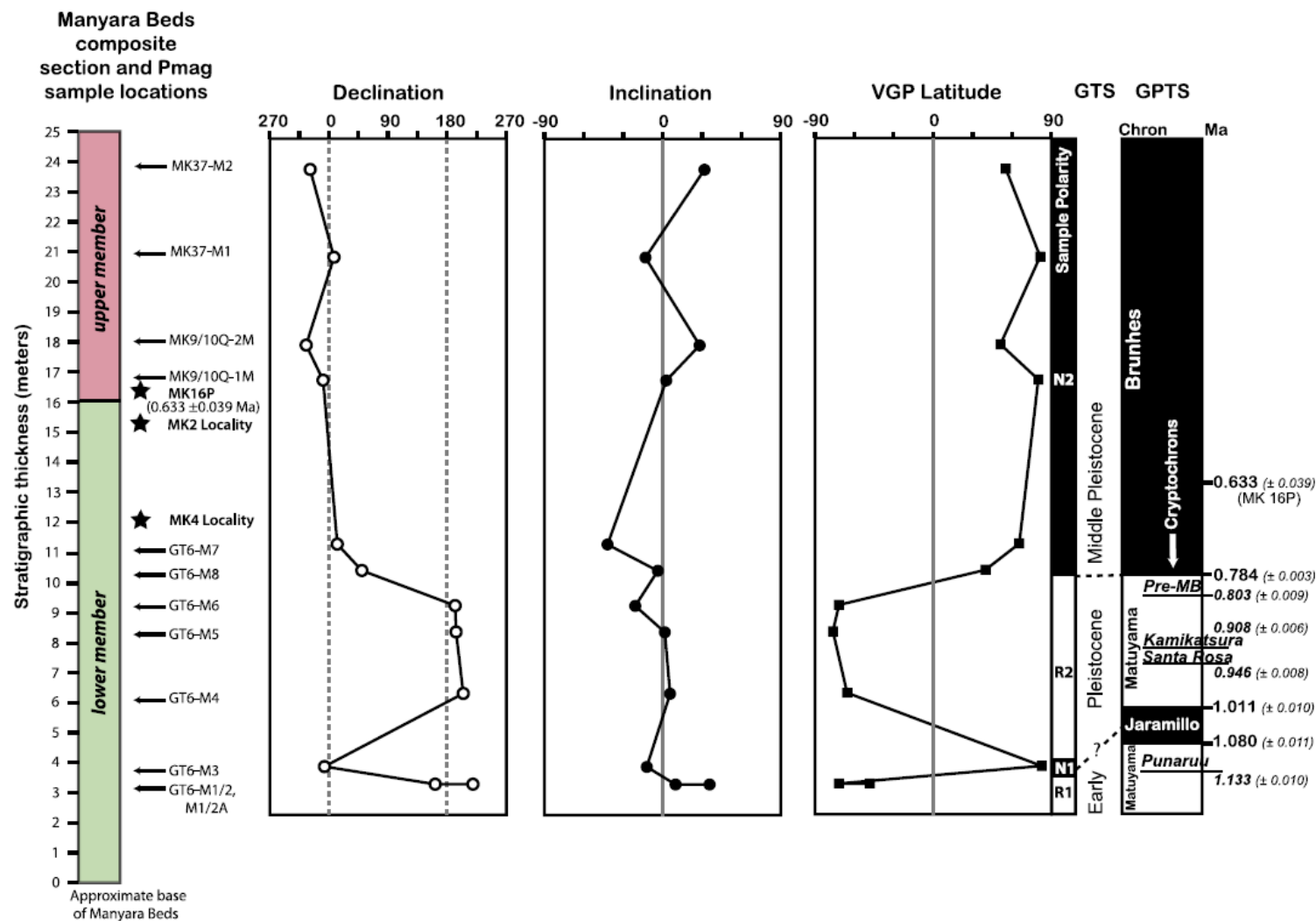


**Figure 3-2:** Correlation of Manyara Beds stratigraphy and magnetostratigraphy with the geological time scale and geomagnetic polarity time scale. Adopted from Schwartz et al. (2012:60, Fig 11).

## Identifying the target section

During sites selection and identifying sediment profiles for sampling beneath the contact of lower and upper member, I relied on age estimates and sites age models from already published data (Giemsch et al., 2018; Kaiser et al., 2010; Schwartz et al., 2012). A distinctively thick (and locally pumice rich) tuffaceous horizon (the Hollywood Tuff) occurs at or just above the contact of the between lower and upper members (Frost et al., 2012; Schwartz et al., 2012). This layer is widely distributed in north and northeast of Makuyuni Town at localities MK9/10, MK16, MK 19, and MK 37. The layer consists of thin beds of light-coloured volcanic ash interbedded with coarse to very coarse grained, poorly cemented, cross-bedded, grayish-orange pumice lapilli (Schwartz et al., 2012). The lithology of this layer is very distinctive (Schwartz et al., 2012).

South of the Makuyuni town the Hollywood Tuff is absent. But it is stratigraphically equivalent to the distinctively deep red to reddish-brown tephra deposit with minimal inputs of pumice informally named the Red Brick Tuff (Schwartz et al., 2012). The Red Brick Tuff is cemented by hematite, dolomite, calcite and/or zeolite, and it contains carbonate nodules, detrital grains and thin interbeds of pumice lapilli like those in the Hollywood Tuff. My sampling sites are in the south and northern of the Makuyuni town. At the southern part of the town the Hollywood Tuff is absent, however I was able to confidently recognize its equivalent tuff the Red Brick Tuff at all my sampling sites. I relied on Schwartz et al.'s (2012: Figures D and E) descriptions and photos to recognize the Red Brick Tuff. The Red Brick Tuff is often used by the local people, who quarry it for paving material (Schwartz et al., 2012). I was able to see various quarrying sites during my 2021 fieldwork and I have seen how local people at Makuyuni make and use the bricks to build their houses. Figure 3-3 shows the Red Brick Tuff identified in my 2021 fieldwork compared to Schwartz et al. (2012). The distinctiveness of this tuff made it possible to confidently identify the targeted section at all my sites except Geo-section 1, where it was not present. However, the layers in Geo-section 1 can be correlated to those of Geo-section 2 as explained in the next section.

Non-archaeological sites MKRV1 and MKRV2 were located towards the northeast side of the town where the “Hollywood Tuff” is present. Sampling at these sections targeted stratigraphic exposures where the upper member is shown by the light-coloured volcanic ash interbedded with coarse to very coarse-grained, poorly cemented, cross-bedded, grayish orange pumice lapilli always located at the base of the upper member (Schwartz et al., 2012). It is easy to identify because the large pieces of tephra are lightweight when picked from the unit. Also, I used Schwartz et al.'s (2012: Figure 4D) photograph description to identify “Hollywood Tuff” at my sites.

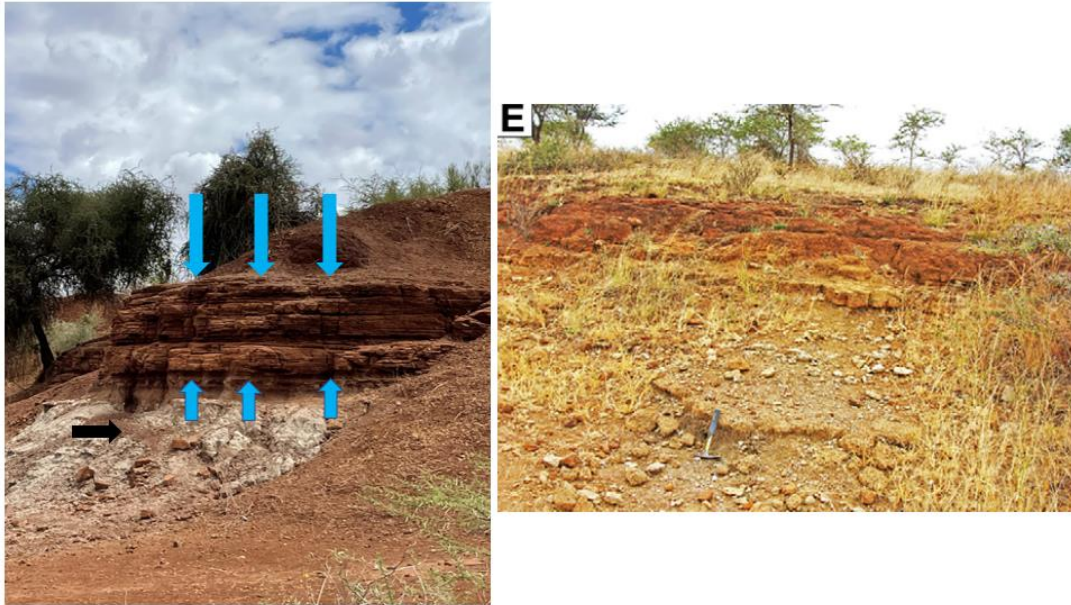


**Figure 3-3:** Left photograph shows the “Red Brick Tuff” observed near the Makuyuni River Valley (approximately 500 m from MK 4) during survey the 2021 fieldwork in this study. The Blue arrow shows the tuff and black shows the lower member grayish in colour. Right photo is Figure E from Schwartz et al. (2012) showing the Red Brick Tuff outcrop north of MK 101.

#### Sediment sampling


Following methods by Piperno (2006), samples were collected following natural stratigraphic layers in a fresh wall profile. At each section, a one-meter wide horizontal section of the profile was selected. Then the walls of natural profile exposures were scrapped clean with a trowel until each layer was clearly visible and sometimes picked to reveal an uncontaminated surface. Once revealed, new stratigraphic profiles (15 cm wide) of the fresh walls were prepared for detailed stratigraphic collection (Figure 3-4), and samples were collected. Sampling proceeded from the bottom to the top to avoid contamination. In each layer at least one sample was taken; in thicker layers samples were taken at 20 cm intervals. Sediment profiles were drawn for all geo-sections in the field. A Munsell color chart was used to identify each stratum's sediment structure and color (e.g. Table 3-1).

**Makuyuni Site 4 (MK 4; E-177037, S-9606663):** is located on the southwestern end of Makuyuni town close to a tributary of the Makuyuni River (Figure 3-1) (Kaiser et al., 2010). MK 4 covers about 2000 m<sup>2</sup> of area, and most artifacts and fossil remain from the Manyara Beds come from this site. The stratigraphic exposures at this site cover at least 4.5-5.5 meters above an active channel bed of the Makuyuni River. The stratigraphic unit comprises greenish to light grey lacustrine and terrestrial deposits dotted with thin marls and tuffaceous units (Kaiser et al., 2010). Samples were collected from two geo-sections: (i) MK4-GS1, which is located a 2-meter distance from excavation unit 1 and where 10 samples were collected (Table 3-1), and (ii) MK4-GS2, which is situated approximately 30 meters distance from MK4-GS1, where 17 samples were collected (Table 3-2) and. MK4-GS2 was

established in a sediment exposure nearby an active tributary of the Makuyuni River close to elephant remains. For more details see Kaiser et al. (2010).

At MK4-GS1 the Red Brick Tuff is not present, but I was able to correlate some layers in Geo-section 1 to those of Geo-section 2 (Figure 3-4). Layer 10 in both geo-sections are similar - fine silt clay grayish in color, and both have identical cultural remains: geo-section 2 has elephant remains and stone tools, and at geo-section 1, we found fragments of elephant tusks and a few lithic tools. In addition, Layer 9 in both geo-sections have light brown silty sandy clay deposits.


**Table 3-1:** Lithostratigraphic section for MK 4-Geo-section 1.

Sample number	Soil description and cultural materials	Top
L1-S10 (15 cm)	HUE 2.5Y 5/2 - Grayish brown soil silty sandy clay	
L2-S9 (30 cm)	HUE 2.5Y 3/2- Dark grayish brown fine silty clay with fauna and lithics	
L3-S8 (50 cm)	HUE 2.5Y 3/2- Dark grayish brown silty clay with fauna and lithics	
L4-S7 (70 cm)	HUE 2.5Y 3/2- Dark grayish brown silty clay with fauna and lithics	
L5-S6 (90 cm)	HUE 10Y 5/2- Grayish olive fine silty clay with fauna and lithics	
L6-S5 (110 cm)	HUE 2.5Y 4/3-Olive brown silty clay with fauna and lithics	
L7-S4 (130 cm)	HUE 5Y 7/1- Pale brown fine silty clay with fauna and lithics	
L8-S3 (150 cm)	HUE 5Y 6/2- Dark grey fine silty clay with fauna and lithics	
L9-S2 (170 cm)	HUE 2.5Y 6/2- Light brownish grey silty sandy clay with lithics	
L10-S1 (190 cm)	HUE 2.5Y 6/2- Light brownish grey fine silty clay with fauna	Bottom

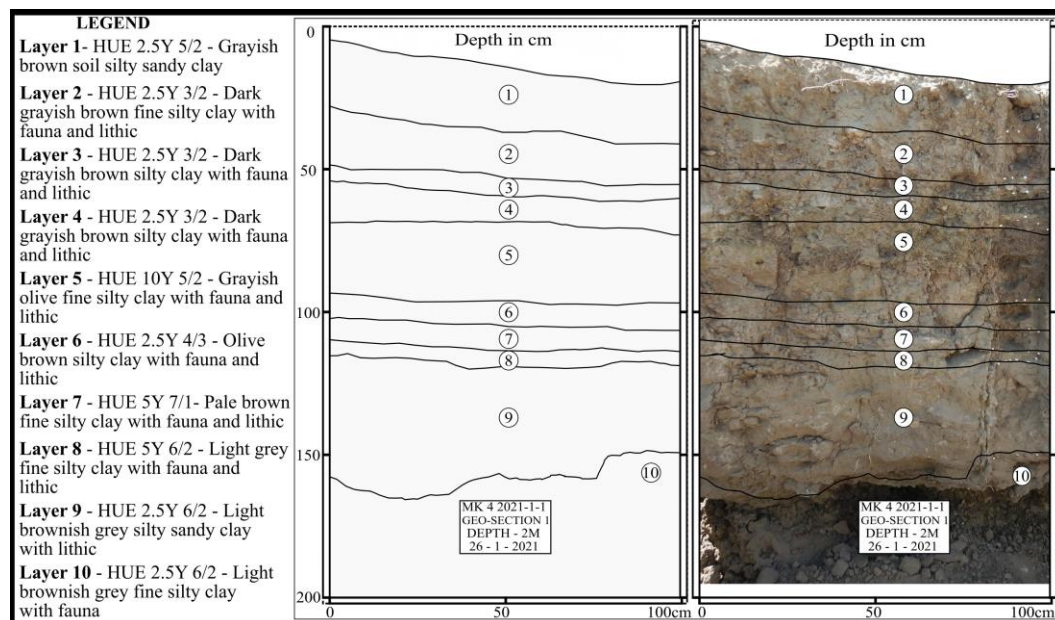



**Figure 3-4:** Geo-section 1 from MK 4 site showing column sampling 2 metres from excavation Unit 1.

**Table 3-2:** Lithostratigraphic sections for MK 4-Geo-section 2

Sample number	Soil Description and cultural materials	Top
L1-S17 (30 cm)	HUE 2.5Y 5/2 - Grayish brown silty sandy clay with roots	
L2-S16 (70 cm)	HUE 2.5Y 3/2- Dark grayish brown fine silty clay with small roots	
L3-S15 (110 cm)	HUE 2.5Y 3/2- Dark grayish brown silty clay	
L4-S14 (145 cm)	HUE 2.5Y 3/2- Dark grayish brown silty clay	
L5-S13 (175 cm)	HUE 10Y 5/2- Grayish olive fine silty clay	
L6-S12 (210 cm)	HUE 2.5Y 4/3-Olive brown silty clay	
L6-S11 (240 cm)		
L7-S10 (280 cm)	HUE 5Y 7/1- Pale brown fine silty clay	
L7-S9 (300 cm)		
L8-S8 (330 cm)	HUE 5Y 6/2- Light grey fine silty clay	
L9-S7 (370 cm)	HUE 2.5Y 6/2- Light brownish grey fine silty clay	
L9-S6 (390 cm)		
L10-S5 (400 cm)	HUE 2.5Y 6/2- Light brownish grey silty sandy clay soil with fauna and lithics	
L10-S4 (420 cm)		
L10-S3 (440 cm)		
L10-S2 (460 cm)		
L10-S1 (480 cm)		
	Bottom	


**Makuyuni Site 2 (MK 2; E-180463, S-9598646):** is located almost 12 km south of Makuyuni town, near an active channel of the Makuyuni River (Figure 3-1). At this site, the basin is underlain by nephelinite lavas and conglomerate exposures (Kaiser et al., 2010). Carbonate cement and microbial rinds on pebbles and cobbles are abundant in conglomerates (Kaiser et al., 2010; Ring et al., 2005). The lower member sediment exposures are an approximately 2 m sequence of natural profiles overlaid by a thin section (<3-5m) of the upper member brownish sandstones, separated by the Red Brick Tuff. At MK 2, a hominid left upper canine fragment (Makuyuni Homind 2) (MH2) was recovered nearby the lower member profile exposure. The tooth fragment consists of an incomplete root (Kaiser et al., 2010). Only 20 Acheulean tools are reported from the site (Giemsch et al., 2018). At MK 2, one 1 x 2-meter excavation unit was opened just beneath the contact of the lower and upper members. Excavation followed arbitrary levels at 20 cm intervals; we dug up to 1.7 m, but no fossil fauna or lithic tools were recovered from the excavation. After excavation, ten sediment samples (Table 3-3) were collected from nine identified layers in the excavation wall.

**Table 3-3:** Lithostratigraphic section for MK 2 Site.

Sample number	Sediment description	Top
L1-S10 (10 cm)	HUE 2.5Y 5/2- Greyish brown silty sandy clay	
L1-S9 (20 cm)		
L2-S8 (30 cm)	HUE 2.5Y 3/2- Dark greyish brown fine silty clay	
L3-S7 (50 cm)	HUE 2.5Y 3/2- Dark greyish brown silty clay	
L4-S6 (70 cm)	HUE 2.5Y 5/3- Olive silty clay	
L5-S5 (90 cm)	HUE 2.5Y 4/3- Olive brown fine silt clay	
L6-S4 (110 cm)	HUE 5Y 6/3- Pale olive brown silty sandy clay	
L7-S3 (130 cm)	HUE 5Y 7/1- Light grey fine silty clay	
L8-S2 (150 cm)	HUE 5Y 6/2- Light olive silty sandy clay	
L9-S1 (160 cm)	HUE 2.5Y 6/2- Light brownish grey silty sandy clay	Bottom

**Makuyuni site 17 (MK 17; E-177267, S-9605005):** is situated approximately 3 km southeast of the Makuyuni village and lies about 700 m south of one of the largest tributaries of the river. MK 17 exposes the lower-upper member contact zone and outcrops with upper and lower Manyara Beds. Kaiser et al. (2010) report the presence of Acheulean artifacts on the surface; none occur in stratigraphic layers. A similar observation is reported in Giemsch et al. (2018) 2008-2009 survey that revealed 10 Acheulean artifacts on the surface and other fossil fauna. Before this study, there was no paleoecological data that described the past environment of the MK 17 site. The sampled sections are devoid of cultural materials; however, I targeted areas with a clear transition from upper to lower members following the location of the presence of the “Red Brick Tuff.” Therefore, the sampled section is within the early Middle Pleistocene time frame. At MK 17, one geo-section was opened beneath the upper-lower member contact that exposed a 1.6-meter section of the lower member; eight samples were collected (Table 3-4).

**Table 3-4:** Lithological section for the MK 17 Site.


Sample number	Sediment description	Top
L1-S8 (15 cm)	HUE 2.5Y 5/2- Greyish brown sandy clay	
L2-S7 (30 cm)	HUE 2.5Y 3/2- Dark greyish brown fine silty clay	
L3-S6 (50 cm)	HUE 2.5Y 3/2- Dark greyish brown silty clay	
L4-S5 (70 cm)	HUE 2.5Y 5/3- Olive silty clay	
L5-S4 (80 cm)	HUE 2.5Y 4/3- Olive brown fine silt clay	
L6-S3 (90 cm)	HUE 5Y 6/3- Pale olive brown silty sandy clay	
L7-S2 (130 cm)	HUE 5Y 7/1- Light grey, fine silty clay soil	
L8-S1 (150 cm)	HUE 5Y 6/2- Light olive silty sandy clay	Bottom

**Makuyuni River Valley Sites (MKRV):** Three sections were mapped, and sediments were collected along the Makuyuni River (see Figure 3-4). At these sites, no archaeological or paleontological materials have ever been documented or mapped. These sites were mapped during the 2021 and 2022 fieldwork.


MKRV 1 (E-0177004, S-9604742) had a stratigraphic exposure of about 4 meters of the uppermost portions of the lower member. Ten layers were identified, and ten sediment samples were taken from the identified stratigraphic profile exposures (Table 3-5). At MKRV 2 (E-0177814, S-9606979), there was 1.8 m of Lower Member sediments exposed; six samples were collected (Table 3-6).

MKRV 3 (E-0177278, S-7607478) is about 500 meters from the current checkpoint entrance the Makuyuni town center, close to an active channel of the Makuyuni River. This site's lower member sediment exposures cover about 1.8 meters beneath the lower-upper member contact zone. Seven layers were identified, where seven sediment samples for phytolith analysis were collected (Table 3-7).


**Table 3-5:** Lithological section for the MKRV-1 Site.

Sample number	Sediment description	Top
L1-S10 (15 cm)	HUE 2.5Y 5/2- Greyish brown silty sandy clay with roots	
L2-S9 (40 cm)	HUE 2.5Y 3/2- Dark greyish brown fine silty clay with small roots	
L3-S8 (70 cm)	HUE 2.5Y 3/2- Dark greyish brown silty clay	
L4-S7 (110cm)	HUE 2.5Y 5/3- Olive brown silty clay	
L5-S6 (130 cm)	HUE 2.5Y 4/3- Olive brown fine silt clay	
L6-S5 (160 cm)	HUE 5Y 6/3- Pale olive brown silty sandy clay	
L7-S4 (200 cm)	HUE 5Y 7/1- Light grey fine silty clay	
L8-S3 (230 cm)	HUE 5Y 6/2- Light olive silty sandy clay	
L9-S2 (260 cm)	HUE 2.5Y 6/2- Light brownish grey silty sandy clay	
L10-S1 (270 cm)	HUE 5Y 5/2- Olive grey fine silty clay	
		Bottom

**Table 3-6:** Lithological section for the MKRV-2 Site.

Sample number	Sediment description	Top
L1-S7 (15 cm)	HUE 2.5Y 5/2- Greyish brown silty sandy clay	
L2-S6 (30 cm)	HUE 2.5Y 3/2- Dark greyish brown fine silty clay	
L3-S5 (60 cm)	HUE 2.5Y 3/2- Dark greyish brown silty clay	
L4-S4 (80 cm)	HUE 2.5Y 5/3- Olive silty clay	
L5-S3 (110 cm)	HUE 2.5Y 4/3- Olive brown silt clay	
L6-S2 (130 cm)	HUE 5Y 6/3- Pale olive brown silty sandy clay	
L7-S1 (150 cm)	HUE 5Y 7/1- Light grey fine silty clay	
		Bottom

**Table 3-7:** Lithological section for the MKRV 3 Site.

Sample number	Sediment description	Top
L1-S7 (15 cm)	HUE 2.5Y 5/2- Greyish brown silty sandy clay	
L2-S6 (30 cm)	HUE 2.5Y 3/2- Dark greyish brown fine silty clay	
L3-S5 (45 cm)	HUE 2.5Y 3/2- Dark greyish brown silty clay	
L4-S4 (80 cm)	HUE 2.5Y 5/3- Olive brown silty clay	
L5-S3 (100 cm)	HUE 2.5Y 4/3- Olive brown fine silt clay	
L6-S2 (130 cm)	HUE 5Y 6/3- Pale olive brown silty sandy clay	
L7-S1 (160 cm)	HUE 5Y 7/1- Light grey fine silty clay	Bottom



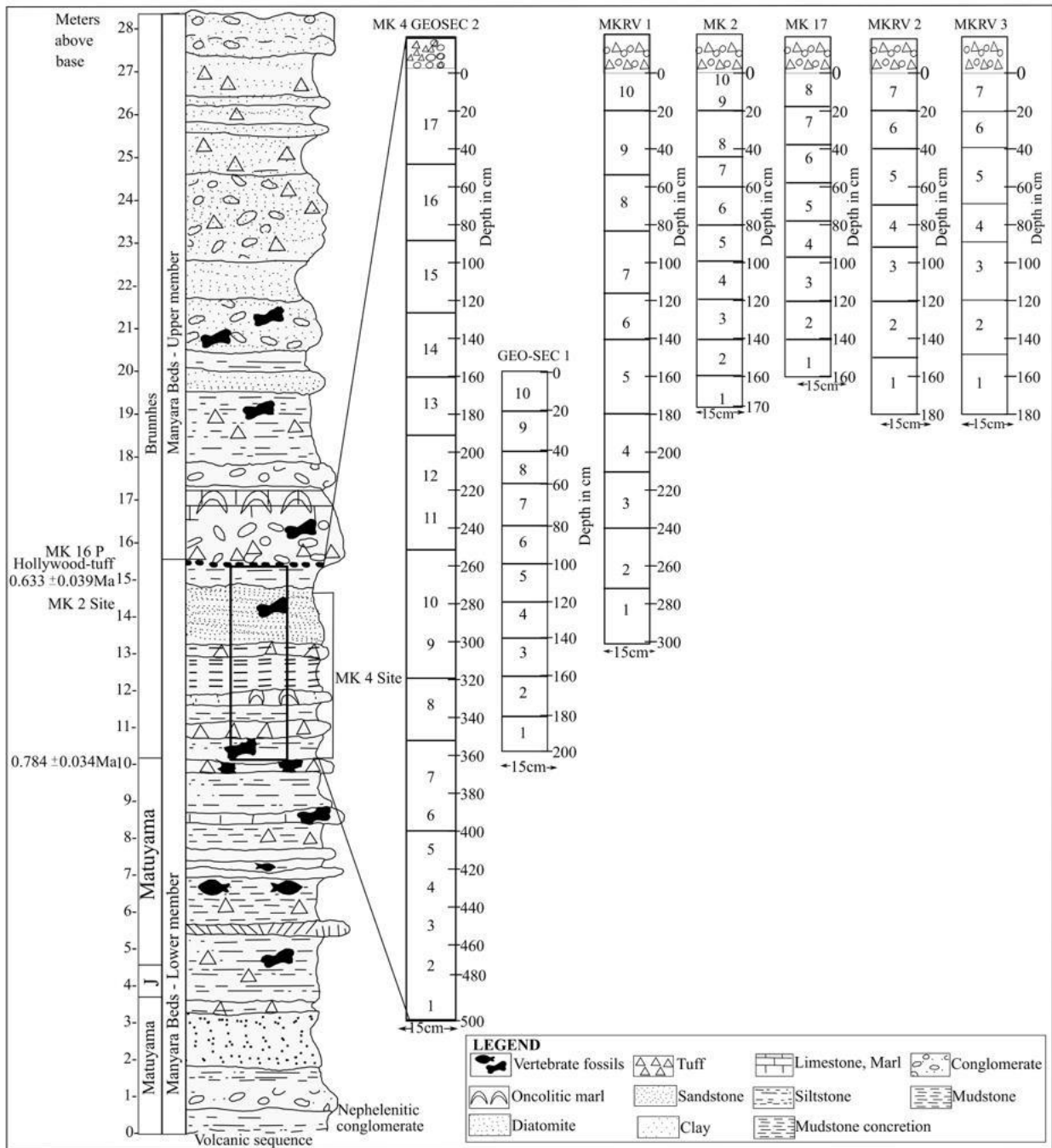


**Figure 3-5:** Generalized stratigraphic column of the Manyara Beds near Makuyuni town showing the sampling sections in relation to 6-metre section of the uppermost part of the lower member and the upper-lower member contact (which is either the Hollywood Tuff or laterally equivalent Red Brick Tuff).

Modified from Frost et al. (2012), Schwartz et al. (2012) and Wolf et al. (2010). The numbers in columns represent sediment samples.

## Phytolith extraction and analytical procedures

Extraction procedures followed a combination of the methods of Pearsall (2016) and Kooyman (2015). All phytolith extractions were conducted at the Paleobotany Lab, University of Calgary. In the lab, sediment samples were ground using a ceramic mortar and pestle to remove clay clumps and then sieved through a 125µm sieve to remove large sandy particles. Then 3 grams of sediment was placed in a 15 mL centrifuge tube, then filled with 10 mL of 0.1% ethylenediaminetetraacetic acid (EDTA) disodium salt dihydrate was added, and vortexed for five minutes to disperse clay then centrifuged at 3000 rev/min for one minute and decanted. Then, it was filled with distilled water and washed multiple times at 3000 rev/min for one minute until the clay is removed.

After that, enough (until the sample was submerged) hydrochloric acid (HCl) at 10% and nitric acid (HNO<sub>3</sub>) at 3-normal were added simultaneously to remove carbonates and clay oxides. The sample was then placed in a hot bath for one hour to accelerate the reaction and centrifuged three times at 3,000 rev/min for 3 minutes to remove acids. Then, enough 30% hydrogen peroxide (H<sub>2</sub>O<sub>2</sub>) was added to remove organic matter. Once the fizzing ceased, the sample was placed in a hot bath for one hour to speed up the reaction, then washed with distilled water three times at 3,000 rev/min. Then, phytoliths were separated by adding 3 to 5 mL of sodium polyngstungate with a specific gravity of 2.3; the sample was centrifuged at 3,000 rev/min for five minutes. The supernatant containing phytoliths was decanted, placed into newly labeled vials, and dried overnight at 70°C.

However, the sample extracted from SPT had soil suspended, resulting in a higher extract weight with many silt particles mixed with phytoliths, impeding visualizing during microscopic counting (see Pearsall, 2016). To obtain a clean extract, the SPT extracts were floated a second time using zinc bromide at the specific gravity of 2.38 in the Strömberg lab at the University of Washington, United States of America. The resulting phytolith extract was dried in an oven at 70°C until all water evaporated, usually between 1 to 2 days. After drying, 0.001 g of phytolith extract was mounted to a 2-inch microscope slide using glycerol (see Pearsall, 2016), and nail polish was used to seal the microscope slide with glycerol; a subset of slides were mounted permanently using Meltmount.

The samples were analyzed at a magnification of 400x and 1000x using a Leitz Labor lux 12 microscope at the University of Calgary and a Nikon Eclipse 80i microscope with an attached DS-Fi1 camera at the University of Washington. The number of phytoliths counted depends on the questions a researcher is attempting to answer (Piperno, 2006; Strömberg, 2009; Zurro, 2018). It has been suggested by some authors that a count of 200 phytoliths is statistically robust (Piperno, 2006;

Strömberg, 2009; Zurro, 2018). Therefore, an entire slide was scanned until a minimum count of 200 diagnostic phytoliths was reached (Pearsall, 2016; Piperno, 2006; Strömberg, 2009) or until the material was exhausted (Barboni et al., 2010). I counted one slide for samples with high yields and sometimes up to three slides per sample with low phytolith density to reach the total of 200 diagnostic phytoliths counted (see also, Albert & Bamford, 2012; McCune & Pellatt, 2013; Zurro, 2018). Selected morphotypes were photographed using a microscope-mounted Moticam 2500 (5.0 Pixel USB2.0) and DS-Fi1 camera.

### **Phytolith morphotypes and taxonomic interpretation**

This study used the classification and interpretive scheme used in Strömberg's (2003) work, augmented with subsequent data (Crifò & Strömberg, 2021; Strömberg, 2003; Strömberg et al., 2018) and the reference collections from the modern plants and soil from the surroundings of the Manyara Beds (Chapter 2). Accordingly, phytoliths were grouped into diagnostic phytoliths/key indicator morphotypes representing broad plant functional types (PFTs). The diagnostic morphotypes used to study fossil assemblages include those that can reveal key forest indicators versus grassland or closed versus open vegetation, especially in tropical regions. Phytoliths from Poaceae (grasses), forest indicators (including palms, herbaceous and dicot woody plants, woody dicots), and wetland indicators (sedges, Commelinaceae, and other aquatic monocots) are used as key indicators to interpret fossil assemblages (Table 3-8) (Piperno, 2006; Strömberg, 2003, 2004).

Poaceae includes the grass silica short cell phytoliths (GSSCs), which are classified into three broad categories: rondels (crescentic conical rondels, *Chusquae*, and generally truncated rondels), lobates (bilobate, crosses and polylobates), and saddles. Rondels are associated with C<sub>3</sub> grasses of the subfamilies Oryzoideae, Danthonoideae, and Pooideae (Barboni & Bremond, 2009; Piperno, 2006; Strömberg, 2003; Yost, 2019) but are also common in C<sub>4</sub> taxa such as the Chloridoideae (Bamford et al., 2006; Barboni & Bremond, 2009; Strömberg, 2003; Yost, 2019) and Panicoideae (Barboni & Bremond, 2009; Piperno, 2006). Saddles are characteristics of C<sub>4</sub> chloridoid grasses, and lobates are characteristic of C<sub>4</sub> panicoid grasses. Redundancy is high within the grass families and as a result, some morphotypes can only be assigned to the general PACMAD clade, which includes Chloridoideae and Panicoideae as well as Aristidoideae (Piperno, 2006; Strömberg, 2003).

Panicoids, Aristidoids, and chloridoids are part of the general PACMAD grasses, but they have diagnostic morphotypes that allow me to identify them specifically. Other PACMAD subfamilies cannot be distinguished from their phytoliths. I utilize the term "general PACMADs" to distinguish panicoid, aristidoids, and chloridoid morphotypes from the rest of the general clade (which includes subfamilies Panicoideae, Arundinoideae, Chloridoideae, Micrairoideae, Aristidoideae, and Danthonoideae).

## Statistical analysis

Descriptive and multivariate analysis were employed to assess if vegetation changes through time could be differentiated by the phytolith assemblages. Multivariate analyses included cluster analysis, correspondence analysis (CA), a test for Normality, and Kruskal-Wallis test using plant functional types, performed using Paleontological Statistics (PAST) software to visualize similarities in the environmental reconstructions and helped compare the environmental change through time and space at the Manyara Beds.

In addition, two indices were used in this study to evaluate changes in vegetation structure: the forest cover ratio (FI-t ratio) (Crifò & Strömberg, 2021; Strömberg, 2003, 2009) and the aridity index ( $I_{ph}$ ) (Alexandre et al., 1997; Barboni et al., 1999; Bremond et al., 2008; Rashid et al., 2019). FI-t ratio tracks the relative changes between grasses and non-grasses (forest indicators). The FI-t is comparable to the D/P ratio used by Alexandre et al. (1997) to track the density of forests in tropical regions but varies in that it includes all phytolith morphotypes produced by taxa indicative of forest habitats (i.e. palms, woody dicots, forest indicators, woody and herbaceous dicots, and Zingiberales) instead of only ligneous dicotyledons (globular phytoliths) and is expressed as percentage instead of a true ratio (Strömberg, 2003). The forest indicators morphotypes include all forms (such as epidermal polygons, various tracheary elements, sclerenchyma, cystoliths, various decorated globulars) diagnostic of woody and herbaceous dicotyledons, ferns, gymnosperms, and non-grass monocots such as palms (Aracaceae) and gingers and grass short cell silica phytoliths (Strömberg, 2003).

The FI-t=total sum of different forest indicators used here as (DICOT-GEN+FI-GEN+PALM+DICOT-WO). FI-t ratio around or below 50% indicates a shift towards more open vegetation, such as savanna or woodland.

The FI-t ratio is defined as:  $FI-t \text{ ratio (\%)} = FI-t / (FI-t + GSSC) \times 100$

The aridity index ( $I_{ph}$ ) assesses aridity by examining the relative proportion of chloridoid grasses of  $C_4$  in the assemblage (Diester-Haas et al., 1973).  $I_{ph}$  is the percentage of Chloridoideae short cells relative to the sum of Chloridoideae and Panicoideae (Alexandre et al., 1997; Barboni et al., 1999; Bremond et al., 2008). High values (>30%) of  $I_{ph}$  suggest the dominance of Chloridoideae short grasses adapted to dry climatic conditions (Alexandre et al., 1997; Barboni et al., 1999). Low  $I_{ph}$  values (<30%) indicate dominance by Panicoideae, which are the tall-grass savanna adapted to humid climates or availability of high moisture (Alexandre et al., 1997; Barboni et al., 1999).

The  $I_{ph}$  index is defined as:  $I_{ph} \text{ (\%)} = \text{Chloridoid} / (\text{Chloridoid} + \text{Panicoide} + \text{Other PACMADs}) \times 100$

**Table 3-8:** Lists of phytolith types included in this study

include phytolith-based functional types, producing taxa, vegetation types for which they are diagnostic, and ecology adapted from (Crifò & Strömberg, 2021 p4; Strömberg, 2003), with slight modifications from Eichhorn et al. (2010) and (Yost, 2019).

Phytolith types	PFT	PTF full name	Producing taxa	Vegetation type	Climate preference
Non-GSSCs	Palm	Palms	Arecaceae	FI	Mostly wet, tropical
	Woody dicots	Woody dicotyledons	Woody dicotyledon angiosperms	FI	various
	Other FI	Other forest indicators	Woody and herbaceous dicotyledons	FI	various
Non-GSSCs (Wetland indicators)	Commelinaceae	Commelinaceae	Commelinaceae	Wetlands	Mostly wet, warm temperate, tropical, and subtropical Eichhorn et al. (2010) and (Yost, 2019).
	SEDGE	Sedge	Cyperaceae	Wetland	closer proximity with water or wet soils
	AQ-MONO	Aquatic monocots	Cyperaceae	Wetland	closer proximity with water or wet soils
GSSCs	APPBO	Bambusoideae, Oryzoideae, and early diverging grasses (C <sub>3</sub> )	Bambusoideae, Oryzoideae, and early diverging grasses in subfamilies Anomochlooideae, Puelioideae, and Pharoideae	FI (wetlands)	Mostly wet, tropical- temperate

	POOID-ND	Non-diagnostic Pooideae (C <sub>3</sub> )	Mainly Pooideae, but possibly redundancy in PACMADs	Mainly open habitat	Arid, temperate
	CHLOR	Chloridoideae (C <sub>4</sub> )	Chloridoideae	Open habitat	Arid, warm-tropical
	PANI	Panicoideae (C <sub>3</sub> & C <sub>4</sub> mostly C <sub>4</sub> )	Panicoideae	Mostly Open habitat, some closed habitats	Relatively wet, tropical
	PACMAD	Panicoideae, Arundinoideae, Chloridoideae, Micrairoideae, Aristidoideae, and Danthonoideae (C <sub>3</sub> and C <sub>4</sub> )	Panicoideae, Arundinoideae, Chloridoideae, Micrairoideae, Aristidoideae, and Danthonoideae	Mostly Open habitat, some closed habitats	Wet-arid, warm tropical
	OTHG	Other grasses	Unknown/ multiple grass taxa	N/A	N/A

## Results

### Phytolith assemblages: site-based results

Phytolith preservation and recovery from sediments in the Lower Manyara Beds varied from excellent to none. Among the 69 samples, 19 did not produce any phytoliths. Intervals where no phytoliths were recovered could be associated with silica dissolution in volcanic-rich layers (Stromberg et al., 2018). For samples that yielded phytoliths, preservation of phytoliths was good, but etching was observed. Even though there is some etching and breakage, fragile phytoliths such as anticlinal epidermis, sedges, and stellate parenchyma are still present. There is some damage to lobate phytoliths, but some of them can still be identified following the Strömberg (2003) scheme by their level of symmetry and be assigned to their specific class and eventually a subfamily.

A total of 43 phytoliths morphotypes were observed (Figure 3-6; Appendix A). Table 3-9 represents functional types, FI-t ratio, and aridity index resulting from the observed phytolith morphotypes.

In addition to phytoliths, other micro-botanical remains observed include diatoms. Diatoms are rare at the Manyara Beds (n=18), occurring only at archaeological site MK 4 (Appendix A). Although no detailed identification has been made in these silica remains, diatoms commonly indicate the presence of aquatic habitats from freshwater to marine (Carballeira & Pontevedra-Pombal, 2020; Stoermer & Smol, 2001; Taffs et al., 2017), and in this case surely indicate fresh water.

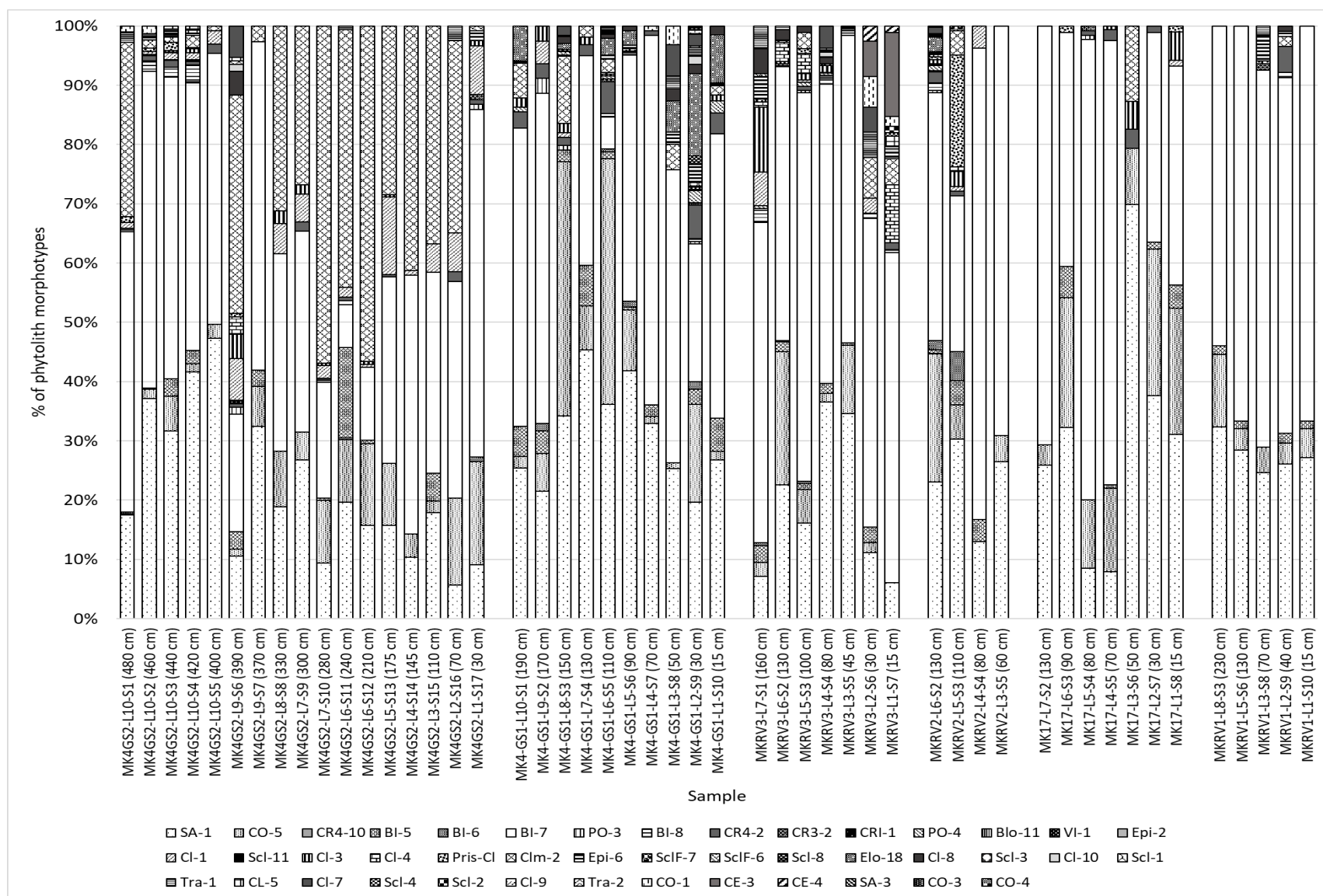


**Figure 3-6:** Percentage of phytolith morphotypes at each site's sample.



**Table 3-9:** Phytolith recovery per sample, listed by plant functional type.

For individual morphotype data see Appendix A. FI-t ratio and  $I_{ph}$  index are listed for each sample.

SAMPLE	GSSC-TOT	FI-TOT	Wetland	Chloridoids	Panicoids	PACMADs	Pooid-ND	Pooid-D	APPBO	OthG	$I_{ph}$ index (%)	FI-t ratio (%)
MK4GS2-L10-S1 (480 cm)	264	127	4	70	2	188	4	0	0	0	27%	32%
MK4GS2-L10-S2 (460 cm)	443	14	3	178	12	247	6	0	0	0	41%	3%
MK4GS2-L10-S3 (440 cm)	1558	62	23	617	46	886	9	0	0	0	40%	4%
MK4GS2-L10-S4 (420 cm)	712	36	4	323	27	358	4	0	0	0	46%	5%
MK4GS2-L10-S5 (400 cm)	127	4	0	65	2	60	0	0	0	0	51%	3%
MK4GS2-L9-S6 (390 cm)	62	108	1	20	1	41	0	0	0	0	32%	64%
MK4GS2-L9-S7 (370 cm)	144	4	0	58	0	86	0	0	0	0	40%	3%
MK4GS2-L8-S8 (330 cm)	85	53	0	39	0	46	0	0	0	0	46%	38%
MK4GS2-L7-S9 (300 cm)	85	42	0	40	2	43	0	0	0	0	47%	33%
MK4GS2-L7-S10 (280 cm)	112	164	0	55	2	55	0	0	0	0	49%	59%
MK4GS2-L6-S11 (240 cm)	171	143	1	96	4	71	0	0	0	0	56%	46%
MK4GS2-L6-S12 (210 cm)	86	117	0	60	0	26	0	0	0	0	70%	58%
MK4GS2-L5-S13 (175 cm)	151	109	0	68	1	82	0	0	0	0	45%	42%
MK4GS2-L4-S14 (145 cm)	73	53	0	18	0	55	0	0	0	0	25%	42%
MK4GS2-L3-S15 (110 cm)	62	44	0	21	0	41	0	0	0	0	34%	42%
MK4GS2-L2-S16 (70 cm)	72	51	0	25	2	45	0	0	0	0	35%	41%
MK4GS2-L1-S17 (30 cm)	107	12	2	32	2	73	0	0	0	0	30%	10%
MK4-GS1-L10-S1 (190 cm)	221	34	1	70	9	142	0	0	0	0	32%	13%
MK4-GS1-L9-S2 (170 cm)	74	5	0	22	2	50	0	0	0	0	30%	6%
MK4-GS1-L8-S3 (150 cm)	416	95	4	395	7	14	0	0	0	0	95%	19%
MK4-GS1-L7-S4 (130 cm)	156	5	0	85	3	68	0	0	0	0	54%	3%
MK4-GS1-L6-S5 (110 cm)	752	60	9	637	56	59	0	0	0	0	85%	7%
MK4-GS1-L5-S6 (90 cm)	472	16	5	257	3	212	0	0	0	0	54%	3%
MK4-GS1-L4-S7 (70 cm)	255	0	0	87	2	164	2	0	0	0	34%	0%
MK4-GS1-L3-S8 (50 cm)	75	18	2	25	0	47	3	0	0	0	35%	19%
MK4-GS1-L2-S9 (30 cm)	1462	461	66	720	172	545	12	1	9	3	50%	24%

MK4-GS1-L1-S10 (15 cm)	173	24	1	56	11	106	0	0	0	0	32%	12%
MKRV3-L7-S1 (160 cm)	147	55	10	20	6	121	0	0	0	0	14%	27%
MKRV3-L6-S2 (130 cm)	673	43	3	324	3	346	0	0	0	0	48%	6%
MKRV3-L5-S3 (100 cm)	258	25	2	62	4	192	0	0	0	0	24%	9%
MKRV3-L4-S4 (80 cm)	750	63	2	310	15	425	0	0	0	0	41%	8%
MKRV3-L3-S5 (45 cm)	518	2	0	240	6	272	0	0	0	0	46%	0%
MKRV3-L2-S6 (30 cm)	96	21	0	15	1	64	6	10	0	0	19%	18%
MKRV3-L1-S7 (15 cm)	147	34	2	11	3	102	3	28	0	0	9%	19%
MKRV2-L7-S1 (150 cm)	0	0	0	0	0	0	0	0	0	0	-	-
MKRV2-L6-S2 (130 cm)	970	64	8	465	44	461	0	0	0	0	48%	6%
MKRV2-L5-S3 (110 cm)	88	11	24	44	1	43	0	0	0	0	50%	11%
MKRV2-L4-S4 (80 cm)	52	2	0	7	0	45	0	0	0	0	13%	4%
MKRV2-L3-S5 (60 cm)	68	0	0	21	0	47	0	0	0	0	31%	0%
MKRV2-L2-S6 (30 cm)	0	0	0	0	0	0	0	0	0	0	-	-
MKRV2-L1-S7 (15 cm)	0	0	0	0	0	0	0	0	0	0	-	-
MK17-L8-S1(150 cm)	0	0	0	0	0	0	0	0	0	0	-	-
MK17-L7-S2 (130 cm)	58	0	0	17	0	41	0	0	0	0	29%	0%
MK17-L6-S3 (90 cm)	95	0	1	52	0	43	0	0	0	0	55%	0%
MK17-L5-S4 (80 cm)	130	0	0	26	2	102	0	0	0	0	20%	0%
MK17-L4-S5 (70 cm)	163	1	0	36	3	124	0	0	0	0	22%	1%
MK17-L3-S6 (50 cm)	52	11	0	50	2	0	0	0	0	0	96%	17%
MK17-L2-S7 (30 cm)	178	0	0	111	2	65	0	0	0	0	62%	0%
MK17-L1-S8 (15 cm)	96	6	1	54	0	42	0	0	0	0	56%	6%
MKRV1-L10-S1 (270 cm)	0	0	0	0	0	0	0	0	0	0	-	-
MKRV1-L9-S2 (260 cm)	0	0	0	0	0	0	0	0	0	0	-	-
MKRV1-L8-S3 (230 cm)	139	0	0	62	0	77	0	0	0	0	45%	0%
MKRV1-L7-S4 (200 cm)	0	0	0	0	0	0	0	0	0	0	-	-
MKRV1-L6-S5 (160 cm)	0	0	0	0	0	0	0	0	0	0	-	-
MKRV1-L5-S6 (130 cm)	81	0	0	26	0	55	0	0	0	0	32%	0%
MKRV1-L4-S7 (110cm)	0	0	0	0	0	0	0	0	0	0	-	-

MKRV1-L3-S8 (70 cm)	175	3	9	54	2	119	0	0	0	0	31%	2%
MKRV1-L2-S9 (40 cm)	111	3	1	34	6	71	0	0	0	0	31%	3%
MKRV1-L1-S10 (15 cm)	81	0	0	26	0	55	0	0	0	0	32%	0%

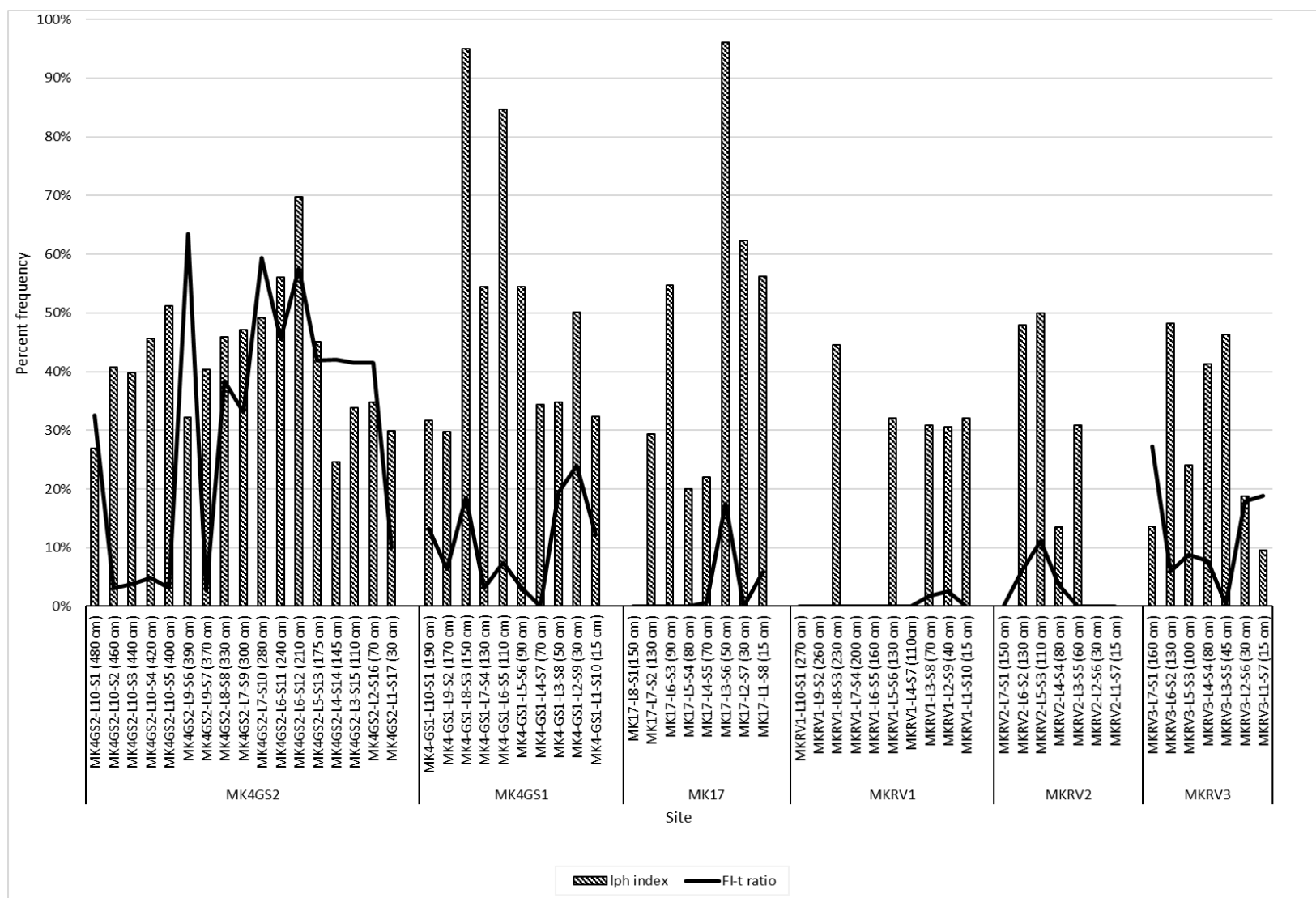


**Figure 3-7:** Comparison of the FI-t ratio and  $I_{ph}$  index for the archaeological and non-archaeological sites at the Manyara Beds.

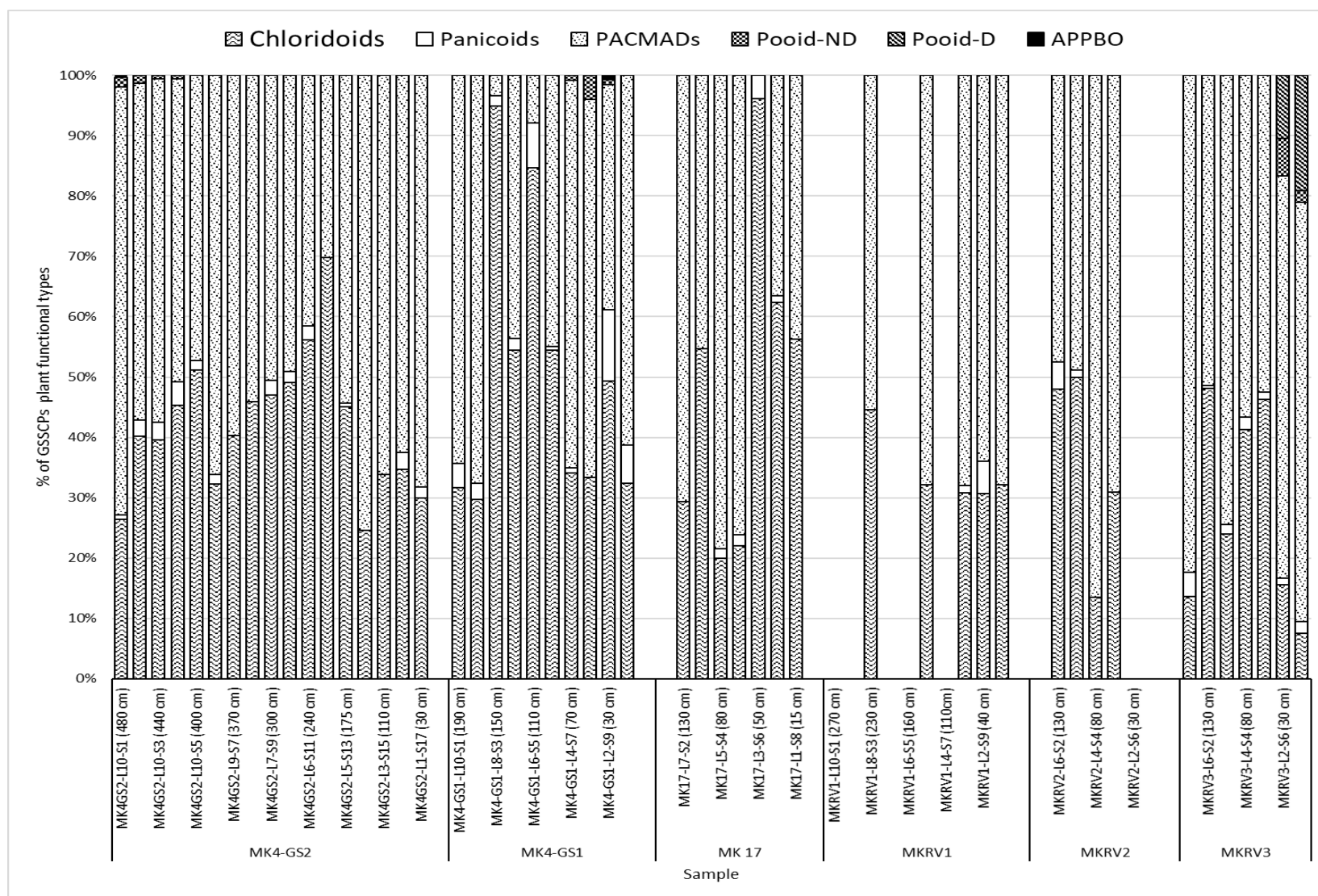


**Figure 3-8:** Percentage of GSSC phytolith categories per sample.

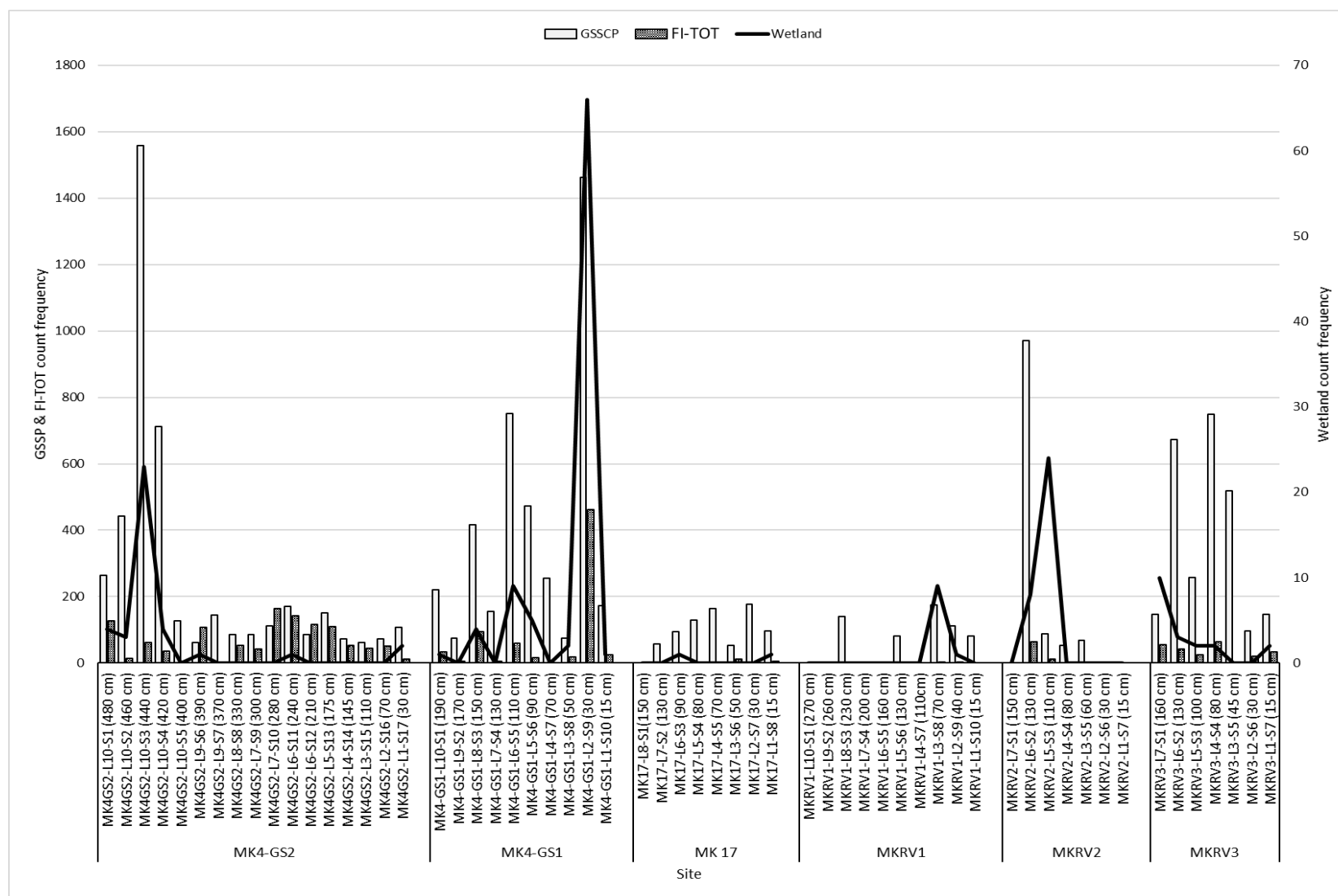


**Figure 3-9:** Count frequency of plant functional types.  
Bars represent grass and forest indicators, while the line tracks wetland indicators.

## Archaeological sites

*MK4-GS1.*

**Phytolith morphotypes:** The ten samples from MK4-GS1 were all well preserved, with high phytolith recovery comprising thirty-two morphotypes (Appendix A; see Fig. 3-10 for representative morphotypes). GSSC bilobates (especially symmetry D bilobates) (BI-7), true saddles (SA-1), and crescentic rondels (CO-5) are the most abundant. Polylobate (PO-4, PO-3), panicoid-type bilobate (BI-8), and crosses (CR4-10, CR4-2, CR4-2, CR1-1) also occur but at a very low frequency. Phytoliths from woody trees and shrubs include echinate spheroids (CIm-2) and MD elongates (Elo-18); there is also a small presence of epidermis (Epi-2), infilled helix tracheids (Tra-1), smooth VI spheres and subspheres (CI-1), compound sphere (CI-5), large nodular spheres (CI-8), verrucate (CI-3) and rugose spheres (CI-9). Sedge epidermal plates (Epi-6), anisopolar prismatic domed cylinder (Pris-CI), and stellate parenchyma represents (ScIf-6, ScIf-7) the wetland morphotypes (Figure 3-6).

**Phytolith indices:** All samples have low FI-t ratio (<50%) indicating an open area where grasses are the dominant vegetation (Figure 3-7, Table 3-9). Also, high  $I_{ph}$  values (>30%) is recorded for all samples indicating dry conditions.

**Environmental interpretation:** These phytolith assemblages document extensive grasslands. The grass assemblages shift from the dominance of general C<sub>3</sub> and C<sub>4</sub> warm wet and dry adapted PACMAD morphotypes to warmer and drier loving C<sub>4</sub> chloridoid grasses (Figure 3-8, Table 3-9). The humid-loving panicoids have a very small input. Sample number MK4-GS1-L2-S9 (30 cm) has the highest proportion of wetland indicators Cyperaceae (sedge) and a small percentage of Commelinaceae (Table 3-9, Figure 3-9), suggesting proximity to the water sources. This level (Appendix A) also documents the highest number of diatoms (n=9), further supporting the presence of wet environments (see Taffs et al., 2017). The higher  $I_{ph}$ , indicates the occurrence drier conditions, however the presence of sedge at this age zone (MK4-GS1-L2-S9 (30 cm)) can be an indicator of paleoenvironmental change that indicates a gradual return to a wet climate at MK 4 (Murungi & Bamford, 2020; Piperno, 2006; Stevanato et al., 2019). These wetlands would support diverse plants, including grasses, woody dicots, and other forest indicators, such as palms, forest indicators, and woody and herbaceous dicots (Figure 3-9). These ecological units support my initial prediction for occurrence of grasslands and woodlands/gallery forests during the periods of lake contractions when a series of formations of lake flats allow the succession of plants.

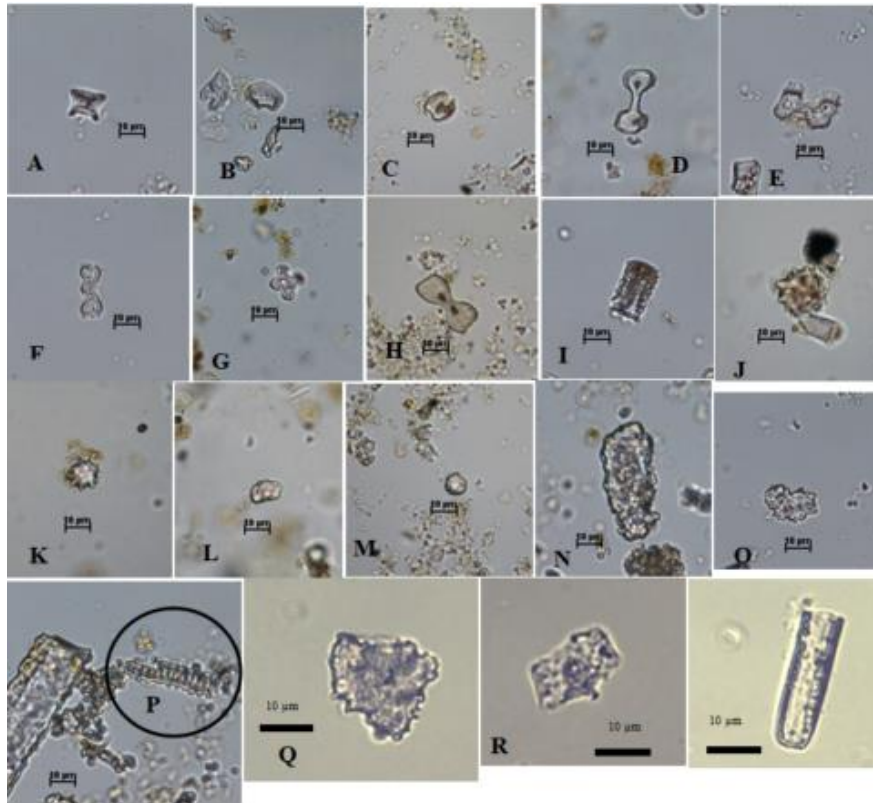


**Figure 3-10:** Selected distinctive and diagnostic phytoliths recovered from MK4-GS1 site. (A-B) Conical rondels diagnostic to  $C_4$  Chloridoideae grasses. (A) Horned rondel and (B) Crescentic rondel. (C) True saddle typical of  $C_4$  Chloridoideae grasses. (D-E)  $C_4$  and  $C_3$  “other PACMAD” bilobates. (D) Symmetry B bilobate (simple bilobate) and (E) Symmetry D bilobate “almost panicoid”. (F-H)  $C_4$  Panicoideae morphotypes: (F) polylobate with top and bottom the same size, (G) four-lobed crosses with almost cross-shaped top, and (H) symmetry E bilobate “panicoid type”. (I) Anisopolar cylinder with a psilate prismatic flat end and decorated diagnostic to  $C_3$  Commelinaceae (see Eichhorn et al., 2010). (J-K) echinate spheres diagnostic to palms (Aracaceae). (L-M) woody and herbaceous dicots: (L) small pink sphere and (M) smooth VI spheres. (N-P) forest indicators: (N) MD clump, (O) small rugulose sphere, and (P) infilled helical tracheid. (Q) Compact irregular sclereid body diagnostic of woody dicots. (R) epidermis cell for sedge (Cyperaceae) with conical bumps surrounding the central papilla. (S) diatom

#### *MK4-GS2.*

**Phytolith morphotypes:** The 17 samples from MK4-GS2 were all productive with higher phytolith recovery. Twenty-seven morphotypes were observed (Appendix A; see Fig. 3-11 for representative morphotypes); by grouping the phytolith morphotypes into plant functional types, the results show that grassy phytoliths occupy a large portion of the assemblage. The GSSC symmetry D bilobates (BI-7) “almost panicoid”, true saddles (SA-1), and crescentic rondels (CO-5) have the highest counts. Other GSSCs morphotypes such as polylobates (PO-4, PO-3), crosses (CR4-10, CR4-2, CR4-2, CR1-1), and other bilobates-symmetry C (BI-6) symmetry B (BI-5), and symmetry E (BI-8) were present in



much lower percentages. The dominant forest indicators are palm echinate spheroids from layer 2 (S-16) through 8 (S-8), which is reduced at layer 10 (Sample 5 through 2) and appeared again at layer 10-sample1. Other non-grass phytoliths, such as tracheids (Tra-1), spheroids (Cl), and sclereids (Scl), are rare throughout the section (Appendix A). Wetland indicators include a small percentage of sedge epidermal plate with conical bumps (Epi-6) and anisopolar prismatic domed cylinder (Pris-Cl) (Figure 3-6).

**Phytolith indices:** The FI-t ratio (>50%) documents three phases of closed vegetation signifying the presence of more trees and shrubs, mostly attributed to palm echinate spheroids. The rest of the samples have low FI-t ratio indicating open conditions (Figure 3-7, Table 3-9). Most samples throughout the section have high  $I_{ph}$  values (>30%), representing the dominance of C<sub>4</sub> chloridoid grasses and arid local conditions. But there are two phases of low aridity represented by samples L4-S14 (145 cm) and L-10-S1 (480 cm), indicating the presence of humid conditions (Figure 3-7, Table 3-9).

**Environmental interpretation:** The environment at MK4-GS2 was dominated by grasses. The low FI-t ratio and higher aridity values supports the general structure of vegetation as an open habitat with C<sub>4</sub> chloridoid grasses, except for three layers: L6-S12 (210 cm), L7-S10 (280 cm), and L9-S6 (390 cm), which had more closed vegetation (Figure 3-7, Table 3-9). Descriptive results (Figure 3-8) show that the GSSC phytoliths alternate from being dominated by C<sub>4</sub> arid-loving chloridoids phytoliths and the C<sub>3</sub> and C<sub>4</sub> general PACMAD grasses. The panicoid-type phytoliths are reduced significantly and completely disappeared at age zone (370 cm) layer 9, layer 8 (330 cm), layer 6 (210 cm), layer 4 (145 cm), and layer 3 (110 cm) (Figure 3-8). Forest indicators, especially palm, continue throughout the section except at the topmost layer (age zone level 20 cm), where the forest elements completely disappear (Figure 3-9, Table 3-9). The palm type indicates a relatively warm and humid climate prevailing throughout the 5-meter section. Wetland indicators such as diatoms, sedges and aquatic monocots are rare throughout the section; however, Commelinaceae taxa are abundant at zone 440 cm (L10-S3) (Figure 3-9, Table 3-9), suggesting the occurrence of wetland/damp habitat (Eichhorn et al., 2010; Yost, 2019).

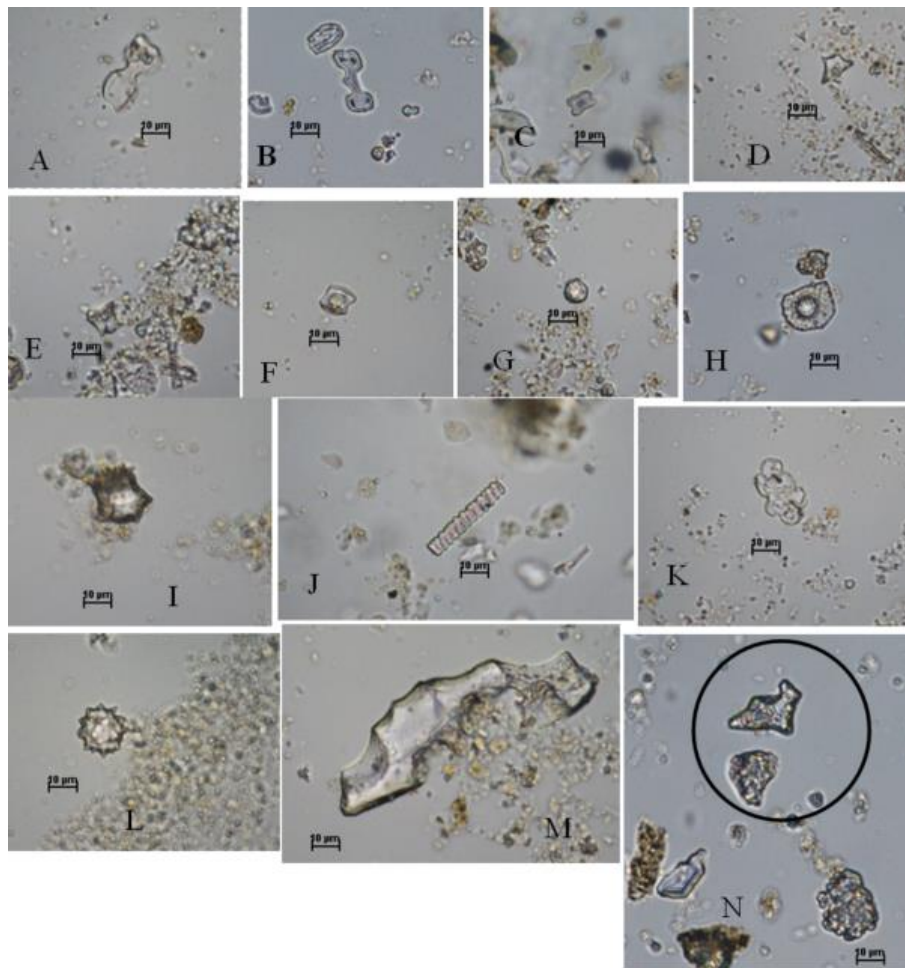


**Figure 3-11:** Selected distinctive and diagnostic phytoliths recovered from MK4-GS2.

A-F. Grasses (Poaceae): (A). symmetrical D bilobate (almost panicoid) diagnostic to C<sub>4</sub> and C<sub>3</sub> “other PACMAD” clade. (B-C) C<sub>4</sub> Panicoideae grasses morphotypes: (B) polylobate with top and bottom the same size and (C) four lobed crosses with almost cross shaped top. (D-E). conical rondel morphotypes: (D) horned rondel diagnostic to C<sub>4</sub> Chloridoideae grasses, and (E) *Chusquea* with spiked top diagnostic to Bambusoideae. (F) true saddle morphotype indicative of C<sub>4</sub> Chloridoideae. (G) smooth VI sphere diagnostic to woody and herbaceous dicots. (H) sedge (Cyperaceae) epidermis plate with conical bump.

(I) Anisopolar cylinder with a psilate prismatic domed end diagnostic to C<sub>3</sub> Commelinaceae (see Eichhorn et al., 2010). (J-M) Forest indicators (trees and shrubs) : (J) infilled helical tracheid, (K) compound sphere forest indicators, (L) echinate sphere diagnostic to palms (M) large faceted sclereid body diagnostic of non-grass plants. (N) stellate parenchyma (sclereid) diagnostic of aquatic monocotyledons.

#### MK 17

**Phytolith morphotypes:** Seven samples of the eight collected from MK 17 yielded phytoliths. Eleven morphotypes were identified from MK 17. Grass phytoliths dominate the assemblage (Appendix A; see Fig. 3-12 for representative morphotypes), largely the GSSCs symmetry D bilobate (BI-7), true saddles (SA-1), and crescentic rondel (CO-5). Crosses, polylobate, and panicoid-type bilobate are very rare throughout the section. Forest indicators are rare at this site, shown by a small portion of

verrucate (CL-3) and smooth spheres (CL-1) (attributed to woody and herbaceous dicots) and echinate spheres (CLm-2) from the small portion of forest indicators observed in sample MK 17-L1-S8 (15 cm) and MK 17-L3-S6 (80 cm) (Figure 3-6). Wetland indicators are nearly absent; only a small percentage of anisopolar prismatic cylinder (Pris-Cl) from Commelinaceae are present.

**Phytolith indices:** The low FI-t values suggests the presence of more open environments dominated by grasslands (Figure 3-7, Table 3-9). The higher  $I_{ph}$  values in layers 3, 2, and 1 support the increase of C<sub>4</sub> chloridoid grasses and drier conditions. Two phases of low aridity are documented at sample numbers L4-S5 (70 cm) and L5-S4 (80 cm), implying a reduction of aridity-loving chloridoid grasses and a transition to humid settings.

**Environmental interpretation:** Descriptive results show GSSCs shift from being chloridoid-dominated to generally PACMAD-dominated. In addition, sample MK17-LS-S6 (50 cm) is notable for the very high proportion of C<sub>4</sub> chloridoid grass phytoliths but with few panicoids and the “other PACMAD” group is absent (Figure 3-8, Table 3-9). The three phases of low aridity suggest the presence of humid conditions, while the rest of the samples are dominated by chloridoid grasses and hence signify arid conditions locally. The low FI-t ratio at MK 17 indicates open conditions dominated by grasses, however descriptive results show the presence of a few scattered trees and shrubs represented by palms and woody herbaceous dicots (Figure 3-9, Table 3-9).

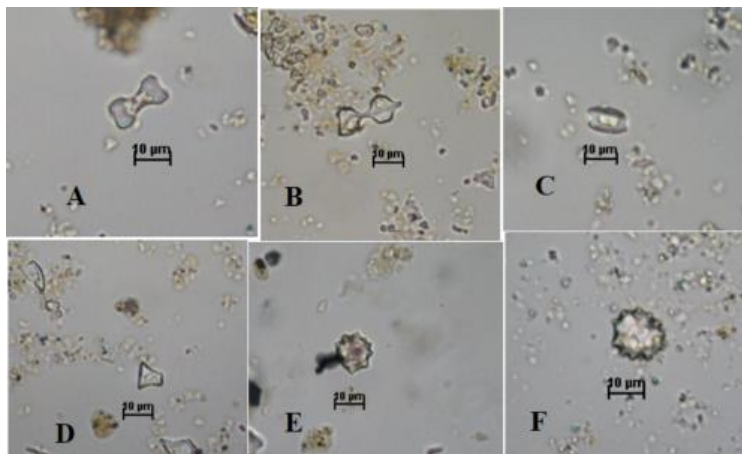


**Figure 3-12:** Selected key phytoliths from Site MK 17.

A-D. Grasses (Poaceae): (A). symmetrical D bilobate (almost panicoid) diagnostic to C<sub>4</sub> and C<sub>3</sub> “other PACMAD” clade. (B) broken polylobate with larger top-symmetry C type. (C-D). C<sub>4</sub> Chloridoideae types: (C) true saddle and (D) rondel type. (E-F). Echinate sphere diagnostic of palms.

## Non-Archaeological sites

### MKRV 1

**Phytolith morphotypes:** From the ten samples collected at MKRV 1, only five (Sample L1-S10, L2-S9, L3-S8, L5-S6, and L8-S3) yielded phytoliths (Appendix A; see Fig. 3-13 for representative morphotypes). Twelve phytolith morphotypes were identified. From top to bottom, GSSC symmetry D bilobates (BI-7) dominate the assemblage, followed by true saddles (SA-1) and rondels (CO-5). Other GSSC phytoliths, such as polylobate (PO), cross (CR), and panicoid-type bilobate (BI-8), are rare throughout the section (Figure 3-6). Very few arboreal morphotypes, echinate spheres (CI-m-2), large nodular spheres (CI-5), helix tracheids (Tra-1), wetland indicators, anisopolar prismatic domed cylinders (Pris-CI), and sedge epidermal plates occur (Epi-6).

**Phytolith indices:** The low values of the FI-t ratio suggest the presence of more open conditions where grasslands are the dominant vegetation; this is supported further by the high  $I_{ph}$  values (>30%) throughout the section (Figure 3-7, Table 3-9), indicating the dominance of  $C_4$  chloridoid grasses and dry conditions.

**Environmental interpretation:** The low FI-t ratio throughout the section indicates an open formation where trees and shrubs are scarce. Figure 3-8 displays the abundance of general PACMAD grasses, followed by phases dominated by dry-loving  $C_4$  chloridoids. Panicoids are also present in a small amount at layers 3 and 2. Nevertheless, the high  $I_{ph}$  values (>30%) throughout the section (Figure 3-7, Table 3-9) indicate an increased contribution of phytoliths from  $C_4$ -Chloridoideae grasses hence suggesting drier local conditions. Layer 3 (age zone 70 cm), in particular, has more wetland indicators sedge and Commelinaceae (Figure 3-9; Table 3-9). However, the absence of diatoms at this site (Appendix A) indicates vegetation growing near water sources.

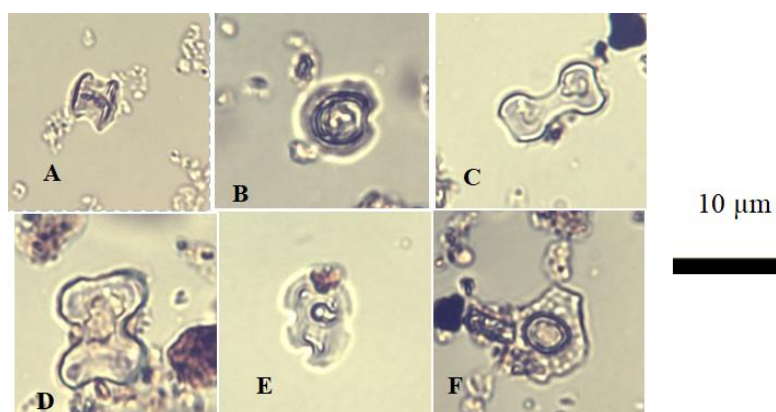


**Figure 3-13:** MKRV 1 selected distinctive phytolith morphotypes.

A-E. Grasses (Poaceae), A-B.  $C_4$  Chloridoideae (A) true saddle and (B) crescentic conical rondel (*Sporobolus* type). (C-D) Symmetrical D bilobate (almost panicoid) diagnostic of  $C_4$  and  $C_3$  PACMAD clade. (E) four-lobed crosses with an almost cross-shaped top diagnostic of  $C_4$  Panicoideae grasses. (F) sedge (Cyperaceae) epidermis plate with a conical bump.

**Phytolith morphotypes:** Only four of this site's seven samples were productive. Twenty-five phytolith morphotypes were identified from the assemblage (Appendix A; see Fig. 3-14 for representative morphotypes). The GSSC phytoliths symmetry D bilobates (BI-7), true saddle (SA-1), and crescentic rondels (CO-5) are the most common phytoliths throughout the section (Figure 3-6). Other GSSC morphotypes include a small percentage of the panicoid-type bilobate (BI-8), polylobate (PO), and cross (CR). Forest indicators such as anticlinal epidermis (Epi-2), large verrucate sphere (CI-3), small pink sphere (CI-4), and echinate spheres (CI-m-2) infrequently occur (Figure 3-6). The wetland indicators stellate parenchyma (ScIF-7) and anisopolar prismatic domed cylinder (Pris-CI) comprise a small portion of the morphotypes.

**Phytolith indices:** Three samples have low FI-t values, representing the dominance of grasslands, and very high (>30%)  $I_{ph}$  values, indicating the dominance of  $C_4$  chloridoid grasses. Only one phase of low aridity (13%) occurs indicating wet conditions (Figure 3-7, Table 3-9).

**Environmental interpretation:** The low FI-t ratio indicates open habitats dominated by grasslands, especially the prevalence of  $C_4$  chloridoids as shown by the low aridity values. Results shows grassland shifts from the dominance of varied PACMADs at the younger layers to the arid-adapted chloridoid grasses (Figure 3-8; Table 3-9). Chloridoid grasses are abundant at layers 6 and 5 and are significantly reduced at layer 4, then increase again at layer 3 (Figure 3-8; Table 3-9). Wetland indicators Commelinaceae and aquatic monocots occur at layers 6 and 5; sedge is completely absent at this site (Figure 3-9, Table 3-9). Closed vegetation is present, based on the rare presence of palm, woody dicots, and woody and herbaceous dicots at layer 6 age zone level 130 cm and layer 5 (110 cm).

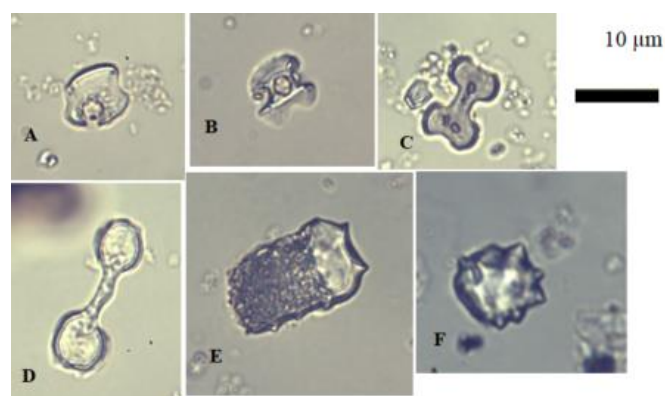


**Figure 3-14:** Key phytolith morphotypes from MKRV 2.

(A) True saddle, diagnostic to  $C_4$  Chloridoideae grasses. (B) three-lobed crosses with almost cross-shaped top diagnostic to  $C_4$  Panicoideae grasses. (C-D)  $C_4$  and  $C_3$  "other PACMAD" clade (C). symmetrical D bilobate (almost panicoid) and (D) symmetry B bilobate (simple lobate). (E) Anisopolar cylinder with a psilate prismatic domed end diagnostic to  $C_3$  Commelinaceae (see Eichhorn et al., 2010). (F) Forest indicators, echinate sphere, an indicator of palms.

**Phytolith morphotypes:** The seven samples from this site were productive and rich with diverse phytolith types. Thirty phytolith morphotypes were identified from this site (Appendix A; see Fig. 3-15 for representative morphotypes). GSSC symmetry D bilobate (BI-7) dominates the phytoliths assemblages, followed by true saddles (SA-1), and crescentic rondels (CO-5) (Figure 3-6). Other GSSC phytoliths including bilobate (symmetry C, B, and E), cross, polylobates, generic truncated rondel (CO-1), and crenates (CE-4 and CE-3) occur in a very small percentage. Arboreal morphotypes include scalloped blocky (Blo-11), smooth VI sphere and subspheres (CI-1), verrucate spheres (CI-3), small pink spheres (CI-4), infilled helix tracheid (Tra-1), compound sphere (CI-5), rugose sphere (CI-8), spongy mesophyll (Scl-3), and short sclereid (Scl-1), all of which occur in a very small percentage (Figure 3-6). The wetland morphotypes sedge epidermal plate (Epi-6), anisopolar cylinder (Pris-CI), and stellate parenchyma (SclF-6) are also present, although in a very low frequency.

**Phytolith indices:** The FI-t ratio is very low, suggesting the presence of an open grassland environment. Throughout the section, there are three low aridity phases ( $I_{ph} < 30\%$ ) that document humid conditions (Figure 3-7, Table 3-9). Four arid phases occur, reflecting the dominance of  $C_4$  chloridoid grasses in the phytolith assemblage and, hence, the prevalence of dry local conditions.

**Environmental interpretation:** Like other sites in the Manyara Beds, the phytoliths and low FI-t ratio in this sample show a predominantly open grassland environment. The GSSCs show changes through time at younger layers 1 and 2, the warm, dry, and wet adapted general PACMAD grasses increase, and a significant reduction of dry-loving chloridoid grasses. There is a slight increase of chloridoid grasses at Layer 3 and a sharp decrease at Layer 5, followed by an increase of chloridoid grasses at Layer 6 and then reduction at Layer 7 (Figure 3-8; Table 3-9). This shift in chloridoid grasses is mirrored by the high  $I_{ph}$  values ( $>30\%$ ) at layers 6, 5, 4, and 3 suggesting the prevalence of chloridoid grasses and arid local conditions (Figure 3-7; Table 3-9). Layers 7, 2, and 1 have low  $I_{ph}$  values, implying the occurrence of moist local conditions. A small percentage of humid-loving panicoid grasses occurs throughout the section. Also, the occurrence of non-diagnostic pooid morphotypes at younger layers can be attributed to PACMAD taxa (Crifò & Strömberg, 2021; Mulholland, 1989). The presence of sedge, Commelinaceae, and aquatic monocots shows a small percentage of wetland indicators (Figure 3-9; Table 3-9).



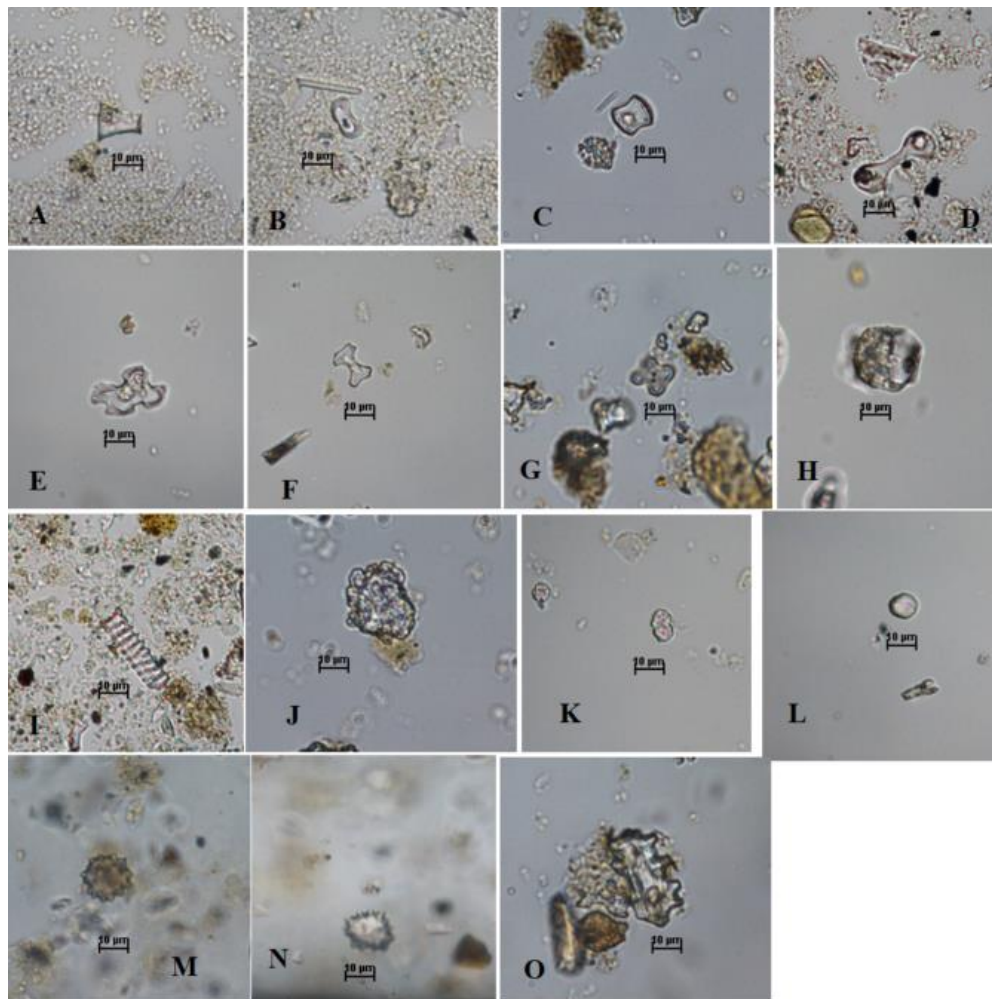


**Figure 3-15:** Selected distinctive and diagnostic phytoliths recovered from MKRV 3  
 (A). rondel type (B-C). C<sub>4</sub> Chloridoideae morphotypes (B) crescentic conical rondel and (C) true saddle.  
 (D-E) C<sub>4</sub> and C<sub>3</sub> “other PACMAD” bilobates (D) Symmetry B bilobate (simple bilobate) and (E) Symmetry D bilobate (almost panicoid).  
 (F-G) C<sub>4</sub> Panicoideae morphotype (F). symmetry E bilobate (panicoid type), and (H). four-lobed crosses with almost cross-shaped tops.  
 (H) Anisopolar cylinder with a psilate prismatic top is flat and decorated end diagnostic to C<sub>3</sub> Commelinaceae (see Eichhorn et al., 2010).  
 (I-J) Forest indicators (trees and shrubs), (J) infilled helical tracheid (forest indicators), (K) large nodular sphere, an indicator of woody dicots.  
 (K-L) Woody and herbaceous dicots (L). small pink sphere and (M). smooth VI spheres.  
 (M-N) The echinate sphere is diagnostic to palms.  
 (O) Stellate parenchyma indicative of aquatic monocotyledonous.

## Results from Statistical analysis

One sample test was performed for aridity and Ft-ratio to test the significance of the data using a t-test. Results for the forest ratio (Table 3-10) and aridity index (Table 3-11) show the mean values are significant difference.

Plant functional type data are not normally distributed (Shapiro-Wilk test; Table 3-12). Consequently, a Kruskal-Wallis test was used to assess variance. Table 3-13 shows that, in all samples, there is a significant difference between sample medians. Dunn's post hoc test was used to determine where the difference originated. Results show significant differences in the median values for the abundance of the plant's functional groups for grasses, which look more different than others. Aquatic and forest indicators do not seem to differ (Table 3-14).

**Table 3-10:** Ft-ratio t-test values

Sample mean:	15.36
Difference:	15.36
95% conf. interval:	(10.26 20.46)
t :	6.0524
p (same mean):	1.94E-07
Means are significantly different	

**Table 3-11:** Aridity index t-test values

Sample mean:	41.38
Difference:	41.38
95% conf. interval:	(36.16 46.6)
t :	15.931
p (same mean):	5.16E-21
Means are significantly different	



**Table 3-12:** Normality table for plants functional types for all samples (n=50)

	Sedges	Commelinaceae	Aquatic monocots	Woody and herbaceous dicots	Woody dicots	Forest indicators	Palms	Chloridoideae	Panicoids	other PACMADs	Diagnostic pooids	Early diverging grasses-APPBO
N	50	50	50	50	50	50	50	50	50	50	50	50
Shapiro-Wilk W	0.2259	0.3767	0.2798	0.749	0.2056	0.3689	0.6254	0.6459	0.3637	0.6539	0.189	0.1254
p(normal)	8.86E-15	2.92E-13	2.91E-14	7.02E-08	5.75E-15	2.40E-13	4.73E-10	9.96E-10	2.11E-13	1.35E-09	4.07E-15	1.13E-15

**Table 3-13:** Kruskal-Wallis value for the samples

Kruskal-Wallis test for equal medians	
H (chi2):	292.2
Hc (tie corrected):	345.7
p (same):	1.93E-67
There is a significant difference between sample medians	

**Table 3-14:** Dunn's post hoc value for plants functional types

	Sedges	Commelinaceae	Aquatic monocots	Woody and herbaceous dicots	Woody dicots	Forest indicators	Palms	Chloridoids	Panicoids	other PACMADs	Diagnostic pooid	Early diverging grasses-APPBO
Sedges		0.8672	0.09736	0.000247	0.4288	0.2898	0.000312	8.86E-21	0.000824	2.18E-22	0.0961	0.04711
Commelinaceae	0.8672		0.068	0.000468	0.5326	0.3727	0.000586	4.25E-20	0.001487	1.12E-21	0.06706	0.03135
Aquatic monocots	0.09736	0.068		1.02E-07	0.01432	0.0066	1.42E-07	3.55E-28	5.67E-07	4.65E-30	0.995	0.7433
Woody and herbaceous dicots	0.000247	0.000468	1.02E-07		0.004047	0.009129	0.9517	1.32E-08	0.748	1.30E-09	9.83E-08	1.59E-08
Woody dicots	0.4288	0.5326	0.01432	0.004047		0.7892	0.004894	1.15E-17	0.01067	3.84E-19	0.01408	0.005493
Forest indicators	0.2898	0.3727	0.0066	0.009129	0.7892		0.01088	1.13E-16	0.02226	4.16E-18	0.006476	0.002335
Palms	0.000312	0.000586	1.42E-07	0.9517	0.004894	0.01088		9.27E-09	0.7943	8.92E-10	1.37E-07	2.26E-08
Chloridoids	8.86E-21	4.25E-20	3.55E-28	1.32E-08	1.15E-17	1.13E-16	9.27E-09		1.92E-09	0.701	3.31E-28	8.88E-30
Panicoids	0.000824	0.001487	5.67E-07	0.748	0.01067	0.02226	0.7943	1.92E-09		1.68E-10	5.48E-07	9.83E-08
other PACMADs	2.18E-22	1.12E-21	4.65E-30	1.30E-09	3.84E-19	4.16E-18	8.92E-10	0.701	1.68E-10		4.33E-30	1.03E-31
Diagnostic pooid	0.0961	0.06706	0.995	9.83E-08	0.01408	0.006476	1.37E-07	3.31E-28	5.48E-07	4.33E-30		0.748
Early diverging grasses-APPBO	0.04711	0.03135	0.7433	1.59E-08	0.005493	0.002335	2.26E-08	8.88E-30	9.83E-08	1.03E-31	0.748	

## Results from Cluster Analysis

One common similarity in the environment for all sites is the abundance of GSSC saddles and rondels from Chloridoideae and bilobates representing the “other PACMADs.” There are also small variations in the environment displayed by the presence of morphotypes that are diagnostic to palms, woody dicots, woody and herbaceous dicots, forest indicators, aquatic monocots, sedges, and the Commelinaceae.

In Figure 3-16 sample MK4-GS2-L10-S3 (440 cm) is the most distinct, a position driven by having the highest number of symmetry D bilobates representing the “other PACMADs” and chloridoid saddles. This sample also has more panicoid-type crosses, polylobates, and bilobates. There is also a high number of Commelinaceae representing the wetlands. Sample MK4-GS1-L2-S9-S2 (30 cm) is also distinct; it has more phytolith morphotypes that are diagnostic to “other PACMADs” and chloridoid grasses. MK4-GS1-L2-S9-S2 (30 cm) also has the highest counts of panicoids and wetland indicators epidermal plate for sedges, implying the phases when the site was near water sources at MK 4. MK4-GS1-L8-S3 (150 cm) and MK4-GS1-L6-S5 (110 cm) are also distinct from the rest by having more chloridoid morphotypes, saddles, and rondels.

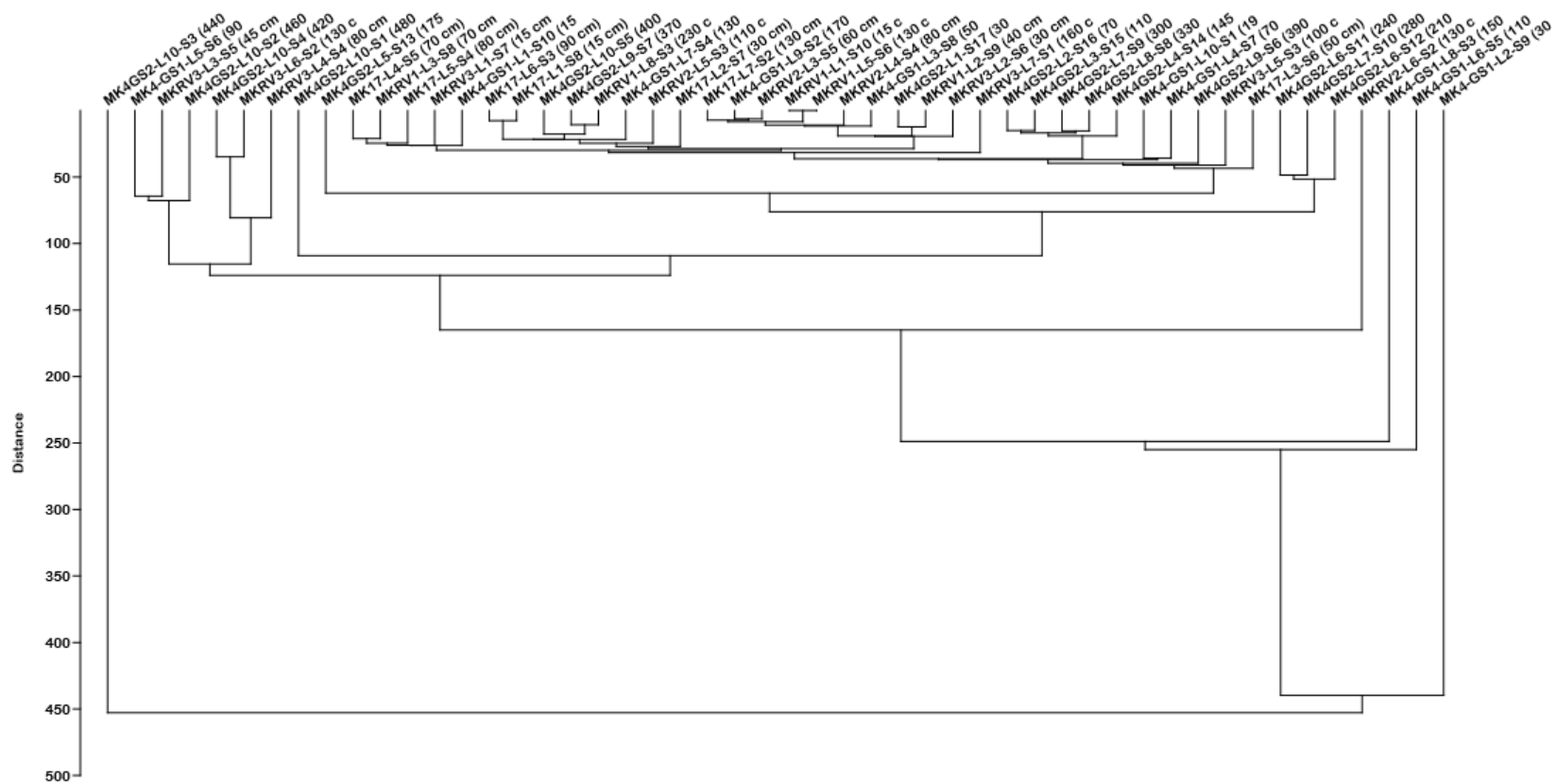


**Figure 3-16:** Cluster dendrogram showing similarity values of environment using the Single Linkage method based on Euclidean distance from the Manyara Bed Samples (n=50).

## Results from Correspondence analysis

Results of the plant functional types (n=12) per diagnostic phytolith morphotypes (n=43) are plotted in Figure 3-17 for each site' sample (n=50). In the biplot, 55.17% of the loadings are explained. Axis 1 presents 37.42% of the total variance (inertia), and Axis 2 represents 17.75% of the inertia.

In general, samples from all sites are clustered on the positive side of Axis 1 and 2. CA analysis observes similar trends to cluster analysis; MK4GS2-L10-S1 (480 cm) is closely linked to other PACMADs grasses and Commelinaceae. Sites from MK4 are plotted in close association with forest indicators of palms, woody and herbaceous dicots, forest indicators, and woody dicots. Four samples from MK4-GS2: MK4GS2-L4-S14 (145 cm), MK4GS2-L5-S13 (175 cm), MKGS2-L2-S16 (70 cm), and MKGS2-L7-S9 (300 cm) are plotted on the positive side of Axis 2 and the negative side of Axis 1 in a close association with woody and herbaceous dicot. Samples MK4GS2-L8-S8 (330 cm), MK4GS2-L6-S11 (240 cm), MKGS2-L7-S10 (280 cm), and MK4GS2-L6-S12 (210 cm) are in a close association with palms, while MK4GS2-L3-S15 (110 cm) is linked to other grass and bambusoid grasses.

Also, five samples from MKGS1 are plotted on the positive side of Axis 1. MK4-GS1-L1-S10 (15 cm) and MK4-GS1-L3-S8 (50 cm) are plotted close to chloridoid and aquatic monocot; MK4-GS1-L6 (110 cm) is linked to panicoid and forest indicator, while MK4-GS1-L2-S9 (30 cm) is associated with sedge and woody dicot.



## Discussion

### *Paleoenvironmental reconstruction*

From the results above, an open grassland environment, with a major presence of C<sub>4</sub> Chloridoideae grasses, has been dominant throughout most of the time interval studied. The presence of C<sub>4</sub> grasses agrees with previous paleoecological research (Frost et al., 2012; Kaiser et al., 2010) that shows the persistence of specialized mega-grazer mammal species such as the horses *Equus* and *Eurygnathohippus* and the baboon *Theropithecus oswaldi*. However, the phytoliths results offer more details on the vegetation reconstructions through the identification of plant taxa. This study documents vegetation heterogeneity, composed of a variety of Poaceae (wet and dry loving grasslands), palms (Arecaceae), woody dicots, woody and herbaceous dicots, forests, and wetland resources including Cyperaceae (sedges), Commelinaceae, and other aquatic monocots in different proportions and different areas. Phytolith results show that vegetation was more diverse and species-rich than what has been interpreted from fauna and isotopic data (Frost et al., 2012, 2017; Kaiser et al., 2010; Wolf et al., 2010). This supports my initial prediction that terrestrial vegetation such as gallery forests, woodlands, and grasslands represent periods when the lake contracts. This further aligns with Ring et al. (2005) suggestions that the lower member of the Manyara Beds represents a Pleistocene regression phase.

The grasslands at the Manyara Beds change through time. Some samples are dominated by dry C<sub>4</sub> chloridoids and others by the general PACMAD clade, including the C<sub>3</sub> and C<sub>4</sub> warm, humid, and dry PACMAD grasses. The moisture-loving panicoid grasses seems to be rare at the Manyara Beds (Figure 3-8). This low percentage of panicoid-type and dominance of “other PACMAD” phytoliths is consistent with the results obtained from the modern surface soils in Chapter 2 of this study. However, we cannot rule out the fact that panicoids produced some of the other PACMAD morphotypes. The problem of redundancy in GSSCs remains a major challenge. As a result, some forms in this study can only be assigned to a group-level terminology such as PACMAD, which challenges taxonomic interpretations. It is currently difficult to correlate the individual proportions of GSSC phytoliths, especially the bilobates, to each of the PACMAD subfamilies (Panicoideae, Arundinoideae, Chloridoideae, Micrairoideae, Aristidoideae, and Danthonoideae).

All samples have high percentage of symmetry D bilobates representing C<sub>3</sub> and C<sub>4</sub> warm dry and wet adapted PACMADs and crescentic/horned/spool rondels and saddles of the drought-adapted short grasses of savannas C<sub>4</sub> Chloridoids (Albert et al., 2006; Barboni & Bremond, 2009; Piperno, 2006; Strömberg, 2003). The modern reference study in Chapter 2 is significant to overcome this PACMAD dilemma. My modern reference collection results show that the chloridoid genus *Sporobolus* produces many crescentic/spool/horned rondels, while *Chloris* produces true

saddles (Albert et al., 2006; Barboni & Bremond, 2009; Piperno, 2006; Strömberg, 2003). The aristidoid, *Aristida* spp. makes symmetry B bilobates. In contrast, the panicoid taxa produce a high number of symmetry D bilobates, as well as a good amount of symmetry C bilobate and symmetry B bilobates that other members of the PACMAD clade make (see Strömberg, 2003). My modern plant reference collections show that the chloridoids surrounding the Manyara Beds do not produce the bilobates forms found in the “general” PACMAD clade. From what I know about this area's modern grasses, most panicoid species produce symmetry D, C, and B bilobates, while aristidoids make symmetry B bilobates (see also, Strömberg, 2003). Consequently, in my fossil assemblage I have a chloridoid-dominated environment and other taxa. Therefore, the high percentage of symmetry D bilobates, followed by symmetry C and a small amount of symmetry B bilobates in the fossil assemblage indicate that the environment is shifting away from chloridoid-dominated to some other kind of grasses; possibly panicoids and to a small extent aristidoids.

Grasses are excellent environmental indicators because of their short lifespans: their expansion and contraction often follow climate shifts (Barboni & Bremond, 2009; Neumann et al., 2009; Novello & Barboni, 2015; Piperno, 2006; Strömberg, 2003; Twiss, 1992; Twiss et al., 1969). The aridity index shows the dominance of drier conditions (Figure 3-7) with very short humid phases at both the archaeological and non-archaeological sites. FI-t ratio supports the dominance of grasslands at the Manyara Beds. However, at MK 4, the FI-t ratio documents three phases of closed woodlands suggesting a high density of trees and shrubs (Figure 3-7). In arid areas like the early Middle Pleistocene at the Manyara Beds, the heterogeneity of vegetation at the landscape could be increased by the surface water (rivers, lakes) and groundwater springs, which may permit the occurrence of forests locally (Albert et al., 2009a; Albert, Bamford, & Esteban, 2015; Barboni et al., 2019; Novello et al., 2017). Correspondence analysis (Figure 3-17), demonstrates vegetation at MK 4 consisting of woody and herbaceous dicots, woody dicots, and palm phytoliths, indicating riparian/gallery forests with high water tables linked to warm and humid environments (Albert et al., 2009a; Albert, Bamford, & Esteban, 2015; Barboni et al., 2019). This supports Kaiser et al's (2010) interpretation that the Manyara Beds bovid communities indicate a mixture of open and closed woodlands. In addition, Commelinaceae, Cyperaceae (sedge), and other aquatic monocots are important elements of the wetland environment occurring at archaeological site MK 4. These groups also occur to a small extent at non-archaeological sites (Figure 3-6 and 3-9), suggesting the Manyara Beds grasslands were well-watered.

### *Taphonomy*

The lower member sediments lie unconformably above the deeply weathered volcanic basement, while the upper-lower member contact is considered conformable (Wolf et al., 2010).



The stratigraphic levels of the lower member indicate low sedimentation rates characterized by extensive bioturbated deposits (Kaiser et al., 2010; Wolf et al., 2010). The higher degree of carnivore tooth marks, fragmentation, root marks, insect marks, rodent gnawing, and weathering in the fossil fauna assemblages suggests extensive surface exposure before burial (Kaiser et al., 2010; Wolf et al., 2010). Extensive surface exposures imply that the lacustrine deposits of the lower Manyara Beds might undergo several episodes of erosion. Erosion might impact phytolith preservation; phytoliths can be removed or added to a specific assemblage, leading to overrepresentation or underrepresentation of some phytolith morphotypes, or to partial destruction or alteration, rendering phytoliths impossible to identify. In general, there is an overrepresentation of grass short silica cell phytoliths such as bilobates, saddles, and rondels, with an underrepresentation of dicots (woody and herbaceous), sedges, and other aquatic monocots across all sites (e.g., Hyland et al., 2013; Strömberg et al., 2018).

#### *Phytolith representation and microhabitats*

Regarding phytolith representation, I expected to see shifts in wetland indicators such as sedges and other aquatic monocots following my initial predictions in Chapter 1. However, these morphotypes are not well represented in the fossil assemblages. Several studies have shown that grasses, palm, and woody dicot globular forms are more resistant to dissolution, while sedge phytoliths are fragile and underrepresented (Albert, Bamford, & Esteban, 2015; Albert, Bamford, Stanistreet, et al., 2015b; Albert et al., 2006; Piperno, 2006; Strömberg, 2003). Monocots, including grasses, are prolific producers, unlike many woody and herbaceous dicots. Because of their durability and short life span, they tend to dominate the soil phytoliths even in an environment where grasses are scarce or absent (Chapter 2; Albert, Bamford, & Esteban, 2015; Barboni et al., 1999; Barboni & Bremond, 2009; Piperno, 2006). The abundance of grass phytoliths in fossil soils tends to bias paleoenvironmental interpretations towards a more grass-dominated ecosystem, even though other plants like trees, shrubs, and forbs might be present (Albert, Bamford, & Esteban, 2015; Piperno, 2006). Palm echinate spheres and woody/leaves phytoliths are resistant and preserve well, but in reduced numbers (Albert, Bamford, & Esteban, 2015; Albert et al., 2009b; Barboni et al., 2019; Piperno, 2006; Strömberg et al., 2018). In addition, the volcanic-rich sediments in eastern Africa can intensify the problem of dissolution and etching of phytoliths, causing additional taphonomic bias (Albert et al., 2006; Albert & Bamford, 2012).

Phytolith from the Manyara Beds suggests periods when the lake was far from the sites. The presence of wetland indicators (diatoms, sedges, and other aquatic monocots) with grasslands and other forest indicators like palms suggests that during the early Middle Pleistocene Manyara Beds had a lot of water sources despite the prevalence of arid conditions. In northern Tanzania,

paleoenvironmental reconstructions at the Pleistocene Oldupai Gorge sites revealed similar types of environments with palms, sedge, dicots, and grasses occurring at upstream areas rich in water resources at Oldupai Gorge Bed I sites FLK Zinj, FLK North, and HWK East below Tuff IF (Albert & Bamford, 2012) and lowermost Bed II paleosurfaces at sites HWKEE, VEK, and HWKE (Albert et al., 2009a). Palm pollen indicating the presence of *Phoenix reclinata* was documented at the FLKN site in Bed I deposits below Tuff ID and IF (Bonnefille, 1984). The palms *Phoenix reclinata* and *Hyphaene petersiana* currently occur at Lake Manyara and Eyasi (Albert, Bamford, & Esteban, 2015).

Albert, Bamford, & Esteban (2015) have shown that palms have different niches in the same ecosystem. At Lake Manyara, for example, *Phoenix* occurs beneath the tree canopy of the spring forest. At the same time, *Hyphaene* is dominant in open, dry grounds, but in both areas, grasses (Poaceae) and aquatic herbs (wetlands) *Typha*, *Phragmites*, ferns, and Cyperaceae species are abundant (Albert, Bamford, & Esteban, 2015). These landscapes are reported to have a higher input of grass phytoliths than palms and other woody and herbaceous dicots; representation of sedge and other aquatic monocot phytoliths is also poor (Albert, Bamford, & Esteban, 2015). Presently, the vegetation surrounding the Manyara Beds is characterized by semi-arid savanna formed by scrubland and wooded grassland with *Acacia* and *Commiphora* (Kaiser et al., 2010; Rohde & Hilhorst, 2001; White, 1983) as well as several shrubs. At the Manyara Beds, palms are absent today but can be found near the Lake Manyara shorelines (Albert, Bamford, & Esteban, 2015). The phytolith records from the Manyara Beds (with sedge, palm, grasses, and dicots) likely reflect similar vegetation to what occurs today at the palm-dominated landscape near the present-day Lake Manyara shoreline. After all, the lower member of the Manyara Beds near Makuyuni village represents the maximum extent and the highest level of Lake Manyara, when the lake size was almost four times larger than its modern size (Bachofer et al., 2018).

#### *Hominin habitat preferences*

The phytolith record of the Manyara Beds bolsters previous studies by giving more details on the vegetation that attracted *Homo* populations during the early Middle Pleistocene (Frost et al., 2012; Giemsch et al., 2018; Kaiser et al., 2010). The identification of sedge, palm, grassy, Commelinaceae, and dicot plant resources helps to explain the presence of artifacts at the lower-upper member contact, signifying hominin exploitation of the landscape along the shorelines of the paleolake Manyara (Frost et al., 2012; Giemsch et al., 2018; Kaiser et al., 2010). The archaeological site MK 4 is different from the rest of the sites. The other archaeological site, MK 17, looks like non-

archaeological sites, and matches previous interpretations by Kaiser et al. (2010) that the Middle Pleistocene environment resembles the present *Acacia* savanna environment in the study area.

The phytolith assemblages in this study follow my initial prediction that hominins use environments near lake shores during the transgression period where varied terrestrial plants populated the lake flat deposits. The phytolith assemblages at MK4 show a varied environment covered with an abundance of forests with palms, woody dicotyledons, woody and herbaceous dicotyledons, grasses, and wetlands (shown by sedge, aquatic monocotyledons, and  $C_3$  Commelinaceae taxa). These ecological units could have offered freshwater resources and plant foraging opportunities for early hominins. Palm and other forest landscapes probably had rivers, streams, and channels that would have offered drinkable water to hominins and shade, allowing them to occupy these ecological units as home bases for stone tool manufacturing and refuge from predators (Albert et al., 2009a; Barboni et al., 2019; Blumenschine & Masao, 1991; Blumenschine & Peters, 1998). Hominins would have acquired food resources like nuts from palms, seeds and young leaf shoots from grasses, stalks and rhizomes from sedges (see Chapter 4) and engaged in hunting activities in the nearby savanna grasslands and probably occasionally scavenging from carnivore prey near the lake shores (Blumenschine & Peters, 1998). These results support previous ideas that stone tools near the lower-upper member contact display hominin's exploitation of the varied ecological resources near the paleo-Lake Manyara (Frost et al., 2012; Giemsch et al., 2018; Kaiser et al., 2010).

### Conclusions

This study provides the first paleobotanical data for the Manyara Beds with which to examine the relationship between vegetation and hominin activities in the paleo-lake Manyara landscape. Phytolith data in this study improves previous environmental reconstructions by providing more detail. Phytolith analysis confirms the openness of the environment; the landscape is mostly grassland throughout the early Middle Pleistocene with scattered trees and shrubs.

This study demonstrates the persistence of  $C_4$  vegetation through space and time in the Manyara Beds, as previously thought. But it also shows that there is more variation in the mesic and xeric  $C_4$  and  $C_3$  PACMAD grasses, including short-grass savanna and mesic tall savanna grasses, which fluctuated throughout the early Middle Pleistocene. Environmental evaluation from phytolith assemblage shows higher diversity in habitats at the Manyara Beds. Wetland phytoliths suggest that plenty of water sources were available in the environment; palm and forests could have offered food (e.g., nuts, edible leaves, and fruits), sedges could have offered edible rhizomes and stalks, grasses could have offered bedding materials at the home bases and food from seeds and young leaves. This

study fills gaps in our knowledge that helps us understand why some sites like MK 4 were preferred by hominins at the Manyara Beds.

### Literature cited

- Albert, R. M., & Bamford, M. K. (2012). Vegetation during UMBI and deposition of Tuff IF at Olduvai Gorge, Tanzania (ca. 1.8 Ma) based on phytoliths and plant remains. *Journal of Human Evolution*, 63(2), 342–350. <https://doi.org/10.1016/j.jhevol.2011.05.010>
- Albert, R. M., Bamford, M. K., & Cabanes, D. (2006). Taphonomy of phytoliths and macroplants in different soils from Olduvai Gorge (Tanzania) and the application to Plio-Pleistocene palaeoanthropological samples. *Quaternary International*, 148(1), 78–94. <https://doi.org/10.1016/j.quaint.2005.11.026>
- Albert, R. M., Bamford, M. K., & Cabanes, D. (2009). Palaeoecological significance of palms at Olduvai Gorge, Tanzania, based on phytolith remains. *Quaternary International*, 193(1–2), 41–48. <https://doi.org/10.1016/j.quaint.2007.06.008>
- Albert, R. M., Bamford, M. K., & Esteban, I. (2015). Reconstruction of ancient palm vegetation landscapes using a phytolith approach. *Quaternary International*, 369, 51–66. <https://doi.org/10.1016/j.quaint.2014.06.067>
- Albert, R. M., Bamford, M. K., Stanistreet, I., Stollhofen, H., Rivera-Rondón, C., & Rodríguez-Cintas, A. (2015). Vegetation landscape at DK locality, Olduvai Gorge, Tanzania. *Palaeogeography, Palaeoclimatology, Palaeoecology*, 426, 34–45. <https://doi.org/10.1016/j.palaeo.2015.02.022>
- Alexandre, A., Meunier, J.-D., Lézine, A.-M., Vincens, A., & Schwartz, D. (1997). Phytoliths: Indicators of grassland dynamics during the late Holocene in intertropical Africa. *Palaeogeography, Palaeoclimatology, Palaeoecology*, 136(1–4), 213–229. [https://doi.org/10.1016/S0031-0182\(97\)00089-8](https://doi.org/10.1016/S0031-0182(97)00089-8)
- Bachofer, F., Quénéhervé, G., Hertler, C., Giemsch, L., Hochschild, V., & Maerker, M. (2018). Paleoenviromental Research in the Semi-arid Lake Manyara Area, Northern Tanzania: A Synopsis. In C. Siart, M. Forbriger, & O. Bubenzer (Eds.), *Digital Geoarchaeology* (pp. 123–138). Springer International Publishing. [https://doi.org/10.1007/978-3-319-25316-9\\_8](https://doi.org/10.1007/978-3-319-25316-9_8)
- Bamford, M. K., Albert, R. M., & Cabanes, D. (2006). Plio-Pleistocene vegetation in the eastern palaeolake margin of Olduvai Gorge (Tanzania) and preliminary results from fossil macroplant and phytolith remains. *Quaternary International*, 148, 95–112.

- Barboni, D. (2014). Vegetation of Northern Tanzania during the Plio-Pleistocene: A synthesis of the paleobotanical evidences from Laetoli, Olduvai, and Peninj hominin sites. *Quaternary International*, 322–323, 264–276. <https://doi.org/10.1016/j.quaint.2014.01.016>
- Barboni, D., Ashley, G. M., Bourel, B., Arráiz, H., & Mazur, J.-C. (2019). Springs, palm groves, and the record of early hominins in Africa. *Review of Palaeobotany and Palynology*, 266, 23–41. <https://doi.org/10.1016/j.revpalbo.2019.03.004>
- Barboni, D., Ashley, G. M., Dominguez-Rodrigo, M., Bunn, H. T., Mabulla, A. Z. P., & Baquedano, E. (2010). Phytoliths infer locally dense and heterogeneous paleovegetation at FLK North and surrounding localities during upper Bed I time, Olduvai Gorge, Tanzania. *Quaternary Research*, 74(3), 344–354. <https://doi.org/10.1016/j.yqres.2010.09.005>
- Barboni, D., Bonnefille, R., Alexandre, A., & Meunier, J. D. (1999). Phytoliths as paleoenvironmental indicators, West Side Middle Awash Valley, Ethiopia. *Palaeogeography, Palaeoclimatology, Palaeoecology*, 152(1–2), 87–100. [https://doi.org/10.1016/S0031-0182\(99\)00045-0](https://doi.org/10.1016/S0031-0182(99)00045-0)
- Barboni, D., & Bremond, L. (2009). Phytoliths of East African grasses: An assessment of their environmental and taxonomic significance based on floristic data. *Review of Palaeobotany and Palynology*, 158(1–2), 29–41. <https://doi.org/10.1016/j.revpalbo.2009.07.002>
- Blumenschine, R. J., & Masao, F. T. (1991). Living sites at Olduvai Gorge, Tanzania? Preliminary landscape archaeology results in the basal Bed II lake margin zone. *Journal of Human Evolution*, 21(6), 451–462. [https://doi.org/10.1016/0047-2484\(91\)90095-D](https://doi.org/10.1016/0047-2484(91)90095-D)
- Blumenschine, R. J., & Peters, C. R. (1998). Archaeological predictions for hominid land use in the paleo-Olduvai Basin, Tanzania, during lowermost Bed II times. *Journal of Human Evolution*, 34(6), 565–608. <https://doi.org/10.1006/jhev.1998.0216>
- Bonnefille, R. (1984). Palynological research at Olduvai Gorge. *National Geographic Society Research Report*, 17, 227–243.
- Bremond, L., Alexandre, A., Wooller, M. J., Hély, C., Williamson, D., Schäfer, P. A., Majule, A., & Guiot, J. (2008). Phytolith indices as proxies of grass subfamilies on East African tropical mountains. *Global and Planetary Change*, 61(3–4), 209–224. <https://doi.org/10.1016/j.gloplacha.2007.08.016>
- Carballeira, R., & Pontevedra-Pombal, X. (2020). Diatoms in Paleoenvironmental Studies of Peatlands. *Quaternary*, 3(2), 10. <https://doi.org/10.3390/quat3020010>
- Castañeda, I. S., Caley, T., Dupont, L., Kim, J.-H., Malaizé, B., & Schouten, S. (2016). Middle to Late Pleistocene vegetation and climate change in subtropical southern East Africa. *Earth and Planetary Science Letters*, 450, 306–316. <https://doi.org/10.1016/j.epsl.2016.06.049>

- Clark, J. D. (1987). Transitions: *Homo erectus* and the Acheulian: the Ethiopian sites of Gadeb and the Middle Awash. *Journal of Human Evolution*, 16(7–8), 809–826.  
[https://doi.org/10.1016/0047-2484\(87\)90025-X](https://doi.org/10.1016/0047-2484(87)90025-X)
- Crifò, C., & Strömberg, C. A. E. (2021). Spatial patterns of soil phytoliths in a wet vs. dry neotropical forest: Implications for paleoecology. *Palaeogeography, Palaeoclimatology, Palaeoecology*, 562, 110100. <https://doi.org/10.1016/j.palaeo.2020.110100>
- Diester-Haas, L., Schrader, H. J., & Thiede, J. (1973). Sedimentological and paleoclimatological investigations of two pelagicooze cores off Cape Barbas, North-West Africa. 'Meteor' *Forschungs-Ergeb, Reihe C* 16, 19–66.
- Dupont, L. M., Donner, B., Schneider, R., & Wefer, G. (2001). Mid-Pleistocene environmental change in tropical Africa began as early as 1.05 Ma. *Geology*, 29(3), 195.  
[https://doi.org/10.1130/0091-7613\(2001\)029<0195:MPECIT>2.0.CO;2](https://doi.org/10.1130/0091-7613(2001)029<0195:MPECIT>2.0.CO;2)
- Eichhorn, B., Neumann, K., & Garnier, A. (2010). Seed phytoliths in West African Commelinaceae and their potential for palaeoecological studies. *Palaeogeography, Palaeoclimatology, Palaeoecology*, 298(3–4), 300–310. <https://doi.org/10.1016/j.palaeo.2010.10.004>
- Frost, S. R., Saanane, C., Starkovich, B. M., Schwartz, H., Schrenk, F., & Harvati, K. (2017). New cranium of the large cercopithecoid primate *Theropithecus oswaldi leakeyi* (Hopwood, 1934) from the paleoanthropological site of Makuyuni, Tanzania. *Journal of Human Evolution*, 109, 46–56. <https://doi.org/10.1016/j.jhevol.2017.05.007>
- Frost, S. R., Schwartz, H. L., & Giemsch, L. (2012). Refined age estimates and paleoanthropological investigation of the Manyara Beds, Tanzania. *Journal of Anthropological Sciences*, 90, 1–12.  
<https://doi.org/10.4436/jass.90001>
- Giemsch, L., Hertler, C., Märker, M., Quénéhervé, G., Saanane, C., & Schrenk, F. (2018). Acheulean Sites at Makuyuni (Lake Manyara, Tanzania): Results of Archaeological Fieldwork and Classification of the Lithic Assemblages. *African Archaeological Review*, 35(1), 87–106.  
<https://doi.org/10.1007/s10437-018-9284-4>
- Grove, M., Lamb, H., Roberts, H., Davies, S., Marshall, M., Bates, R., & Huws, D. (2015). Climatic variability, plasticity, and dispersal: A case study from Lake Tana, Ethiopia. *Journal of Human Evolution*, 87, 32–47. <https://doi.org/10.1016/j.jhevol.2015.07.007>
- Johnson, C. R., & McBrearty, S. (2012). Archaeology of Middle Pleistocene lacustrine and spring paleoenvironments in the Kapthurin Formation, Kenya. *Journal of Anthropological Archaeology*, 31(4), 485–499. <https://doi.org/10.1016/j.jaa.2012.05.001>

- Kaiser, T.M., Seiffert, C. C., Fiedler, L, Schwartz, H. L, Frost, S. R, & Nelson, S. V. (2010). Makuyuni, a new lower Palaeolithic hominid site in Tanzania. *Mitteilungen Hamburgisches Zoolischen Museum Institut*, 106, 69–110.
- Kent, P. E. (1942). A Note on Pleistocene Deposits near Lake Manyara, Tanganyika. *Geological Magazine*, 79(1), 72–77. <https://doi.org/10.1017/S0016756800073532>
- Kooyman, B. (2015). Phytoliths: Preparation and Archaeological Extraction. In E. C. T. Yeung, C. Stasolla, M. J. Sumner, & B. Q. Huang (Eds.), *Plant Microtechniques and Protocols* (pp. 507–524). Springer International Publishing. [https://doi.org/10.1007/978-3-319-19944-3\\_28](https://doi.org/10.1007/978-3-319-19944-3_28)
- Maddux, S. D., Ward, C. V., Brown, F. H., Plavcan, J. M., & Manthi, F. K. (2015). A 750,000 year old hominin molar from the site of Nadung’a, West Turkana, Kenya. *Journal of Human Evolution*, 80, 179–183. <https://doi.org/10.1016/j.jhevol.2014.11.004>
- Maslin, M. A., & Ridgwell, A. J. (2005). Mid-Pleistocene revolution and the ‘eccentricity myth.’ *Geological Society, London, Special Publications*, 247(1), 19–34. <https://doi.org/10.1144/GSL.SP.2005.247.01.02>
- McBrearty, S. (2001). The Middle Pleistocene of East Africa. In *Human roots: Africa and Asia in the Middle Pleistocene* (pp. 81–92). Western Academic and Specialist Press.
- McBrearty, S., & Brooks, A. S. (2000). The revolution that wasn’t: A new interpretation of the origin of modern human behavior. *Journal of Human Evolution*, 39(5), 453–563. <https://doi.org/10.1006/jhev.2000.0435>
- McCune, J. L., & Pellatt, M. G. (2013). Phytoliths of Southeastern Vancouver Island, Canada, and their potential use to reconstruct shifting boundaries between Douglas-fir forest and oak savannah. *Palaeogeography, Palaeoclimatology, Palaeoecology*, 383–384, 59–71. <https://doi.org/10.1016/j.palaeo.2013.05.003>
- Mulholland, S. C. (1989). Phytolith shape frequencies in North Dakota grasses: A comparison to general patterns. *Journal of Archaeological Science*, 16(5), 489–511. [https://doi.org/10.1016/0305-4403\(89\)90070-8](https://doi.org/10.1016/0305-4403(89)90070-8)
- Murungi, M. L., & Bamford, M. K. (2020). Revised taxonomic interpretations of Cyperaceae phytoliths for (paleo)botanical studies with some notes on terminology. *Review of Palaeobotany and Palynology*, 275, 104189. <https://doi.org/10.1016/j.revpalbo.2020.104189>
- Neumann, K., Fahmy, A., Lespez, L., Ballouche, A., & Huysecom, E. (2009). The Early Holocene palaeoenvironment of Ounjougou (Mali): Phytoliths in a multiproxy context. *Palaeogeography, Palaeoclimatology, Palaeoecology*, 276(1–4), 87–106. <https://doi.org/10.1016/j.palaeo.2009.03.001>

- Novello, A., & Barboni, D. (2015). Grass inflorescence phytoliths of useful species and wild cereals from sub-Saharan Africa. *Journal of Archaeological Science*, 59, 10–22.  
<https://doi.org/10.1016/j.jas.2015.03.031>
- Novello, A., Barboni, D., Sylvestre, F., Lebatard, A.-E., Paillès, C., Bourlès, D. L., Likius, A., Mackaye, H. T., Vignaud, P., & Brunet, M. (2017). Phytoliths indicate significant arboreal cover at Sahelanthropus type locality TM266 in northern Chad and a decrease in later sites. *Journal of Human Evolution*, 106, 66–83. <https://doi.org/10.1016/j.jhevol.2017.01.009>
- Pearsall, D. M. (2016). *Paleoethnobotany*. Routledge. <https://doi.org/10.4324/9781315423098>
- Pearson, O. M. (2000). Postcranial remains and the origin of modern humans. *Evolutionary Anthropology: Issues, News, and Reviews*, 9(6), 229–247. [https://doi.org/10.1002/1520-6505\(2000\)9:6<229::AID-EVAN1002>3.0.CO;2-Z](https://doi.org/10.1002/1520-6505(2000)9:6<229::AID-EVAN1002>3.0.CO;2-Z)
- Piperno, D. R. (2006). *Phytoliths: A comprehensive guide for archaeologists and paleoecologists*. AltaMira Press.
- Potts, R. (2013). Hominin evolution in settings of strong environmental variability. *Quaternary Science Reviews*, 73, 1–13. <https://doi.org/10.1016/j.quascirev.2013.04.003>
- Potts, R., Dommain, R., Moerman, J. W., Behrensmeyer, A. K., Deino, A. L., Riedl, S., Beverly, E. J., Brown, E. T., Deocampo, D., Kinyanjui, R., Lupien, R., Owen, R. B., Rabideaux, N., Russell, J. M., Stockhecke, M., deMenocal, P., Faith, J. T., Garcin, Y., Noren, A., ... Uno, K. (2020). Increased ecological resource variability during a critical transition in hominin evolution. *Science Advances*, 6(43), eabc8975. <https://doi.org/10.1126/sciadv.abc8975>
- Rashid, I., Mir, S. H., Zurro, D., Dar, R. A., & Reshi, Z. A. (2019). Phytoliths as proxies of the past. *Earth-Science Reviews*, 194, 234–250. <https://doi.org/10.1016/j.earscirev.2019.05.005>
- Rightmire, G. P. (1996). The human cranium from Bodo, Ethiopia: Evidence for speciation in the Middle Pleistocene? *Journal of Human Evolution*, 31(1), 21–39.  
<https://doi.org/10.1006/jhev.1996.0046>
- Rightmire, G. P. (2008). *Homo* in the Middle Pleistocene: Hypodigms, variation, and species recognition. *Evolutionary Anthropology: Issues, News, and Reviews*, 17(1), 8–21.  
<https://doi.org/10.1002/evan.20160>
- Ring, U., Schwartz, H. L., Bromage, T. G., & Sanaane, C. (2005). Kinematic and sedimentological evolution of the Manyara Rift in northern Tanzania, East Africa. *Geological Magazine*, 142(4), 355–368. <https://doi.org/10.1017/S0016756805000841>
- Rohde, R., & Hilhorst, T. (2001). A profile of environmental change in the Lake Manyara Basin, Tanzania. *Drylands Programme, IIED*, 109, 1–27.



- Rossouw, L., & Scott, L. (2011). Phytoliths and Pollen, the Microscopic Plant Remains in Pliocene Volcanic Sediments Around Laetoli, Tanzania. In T. Harrison (Ed.), *Paleontology and Geology of Laetoli: Human Evolution in Context* (pp. 201–215). Springer Netherlands.  
[https://doi.org/10.1007/978-90-481-9956-3\\_9](https://doi.org/10.1007/978-90-481-9956-3_9)
- Schwartz, H., Renne, P. R., Morgan, L. E., Wildgoose, M. M., Lippert, P. C., Frost, S. R., Harvati, K., Schrenk, F., & Saanane, C. (2012). Geochronology of the Manyara Beds, northern Tanzania: New tephrostratigraphy, magnetostratigraphy and  $^{40}\text{Ar}/^{39}\text{Ar}$  ages. *Quaternary Geochronology*, 7, 48–66. <https://doi.org/10.1016/j.quageo.2011.09.002>
- Stevanato, M., Rasbold, G. G., Parolin, M., Domingos Luz, L., Lo, E., Weber, P., Trevisan, R., & Galeazzi Caxambu, M. (2019). New characteristics of the papillae phytolith morphotype recovered from eleven genera of cyperaceae. *Flora*, 253, 49–55.  
<https://doi.org/10.1016/j.flora.2019.03.012>
- Stoermer, E. F., & Smol, J. P. (Eds.). (2001). *The diatoms: Applications for the environmental and earth sciences* (1. paperback ed). Cambridge University Press.
- Stringer, C. (2012). The status of *Homo heidelbergensis* (Schoetensack 1908). *Evolutionary Anthropology: Issues, News, and Reviews*, 21(3), 101–107.  
<https://doi.org/10.1002/evan.21311>
- Strömberg, C. A. E. (2003). *The Origin and Spread of Grass-dominated Ecosystem during the Tertiary of North America and How it Relates to Evolution of Hypsodont in Equids*. [PhD thesis]. University of California.
- Strömberg, C. A. E. (2004). Using phytolith assemblages to reconstruct the origin and spread of grass-dominated habitats in the great plains of North America during the late Eocene to early Miocene. *Palaeogeography, Palaeoclimatology, Palaeoecology*, 207(3–4), 239–275.  
<https://doi.org/10.1016/j.palaeo.2003.09.028>
- Strömberg, C. A. E. (2009). Methodological concerns for analysis of phytolith assemblages: Does count size matter? *Quaternary International*, 193(1–2), 124–140.  
<https://doi.org/10.1016/j.quaint.2007.11.008>
- Strömberg, C. A. E., Dunn, R. E., Crifò, C., & Harris, E. B. (2018). Phytoliths in Paleoecology: Analytical Considerations, Current Use, and Future Directions. In D. A. Croft, D. F. Su, & S. W. Simpson (Eds.), *Methods in Paleoecology* (pp. 235–287). Springer International Publishing.  
[https://doi.org/10.1007/978-3-319-94265-0\\_12](https://doi.org/10.1007/978-3-319-94265-0_12)
- Taffs, K. H., Saunders, K. M., & Logan, B. (2017). Diatoms as Indicators of Environmental Change in Estuaries. In K. Weckström, K. M. Saunders, P. A. Gell, & C. G. Skilbeck (Eds.), *Applications of*

- Paleoenvironmental Techniques in Estuarine Studies* (Vol. 20, pp. 277–294). Springer Netherlands. [https://doi.org/10.1007/978-94-024-0990-1\\_11](https://doi.org/10.1007/978-94-024-0990-1_11)
- Tryon, C. A., McBrearty, S., & Texier, P.-J. (2006). Levallois Lithic Technology from the Kapthurin Formation, Kenya: Acheulian Origin and Middle Stone Age Diversity. *African Archaeological Review*, 22(4), 199–229. <https://doi.org/10.1007/s10437-006-9002-5>
- Twiss, P. C. (1992). Predicted World Distribution of C3 and C4 Grass Phytoliths. In G. Rapp & S. C. Mulholland (Eds.), *Phytolith Systematics* (pp. 113–128). Springer US. [https://doi.org/10.1007/978-1-4899-1155-1\\_6](https://doi.org/10.1007/978-1-4899-1155-1_6)
- Twiss, P. C., Suess, E., & Smith, R. M. (1969). Morphological Classification of Grass Phytoliths. *Soil Science Society of America Journal*, 33(1), 109–115. <https://doi.org/10.2136/sssaj1969.03615995003300010030x>
- White, F. (1983). *The vegetation of Africa: A descriptive memoir to accompany the Unesco/AETFAT/UNSO vegetation map of Africa*. Unesco.
- Wolf, N. D., Nelson, S. V., Schwartz, H. L., Semperebon, G. M., Kaiser, T. M., & Bernor, R. L. (2010). Taxonomy and paleoecology of the Pleistocene Equidae from Makuyuni, northern Tanzania. *Palaeodiversity*, 3, 249–269.
- Yost, C. L. (2019). *Phytoliths and microcharcoal from East African Lake sediments used to reconstruct Plio-Pleistocene vegetation and hydroclimate* [PhD thesis]. The University of Arizona.
- Yost, C. L., Ivory, S. J., Deino, A. L., Rabideaux, N. M., Kingston, J. D., & Cohen, A. S. (2021). Phytoliths, pollen, and microcharcoal from the Baringo Basin, Kenya reveal savanna dynamics during the Plio-Pleistocene transition. *Palaeogeography, Palaeoclimatology, Palaeoecology*, 570, 109779. <https://doi.org/10.1016/j.palaeo.2020.109779>
- Yost, C. L., Jackson, L. J., Stone, J. R., & Cohen, A. S. (2018). Subdecadal phytolith and charcoal records from Lake Malawi, East Africa imply minimal effects on human evolution from the ~74 ka Toba supereruption. *Journal of Human Evolution*, 116, 75–94. <https://doi.org/10.1016/j.jhevol.2017.11.005>
- Zurro, D. (2018). One, two, three phytoliths: Assessing the minimum phytolith sum for archaeological studies. *Archaeological and Anthropological Sciences*, 10(7), 1673–1691. <https://doi.org/10.1007/s12520-017-0479-4>

## **Chapter 4: What phytoliths are preserved on stone tools?**

### **Abstract**

This research examined phytolith residues on the small flake lithic assemblage (Series 2) from the Manyara Beds in Northern Tanzania. The Series 2 lithic assemblages consist of flakes, scrapers, points, core scrapers, and cores obtained from excavation at the MK 4 site. One hundred and six stone tools with their adhering matrix and 20 sediment samples collected from underneath some stone tools (control samples) were collected from the 2021 excavation unit and were examined for their phytolith residues. Ten control samples were analyzed and all were devoid of phytoliths. The absence of phytoliths in the control samples suggests that phytoliths found adhering to stone tools represent tool use. Phytoliths were found on 10 artifacts, indicating that at least some of these tools were used to process grasses including both the dry adapted Chloridoideae and humid adapted Panicoideae. Phytoliths from herbaceous plants include sedge (Cyperaceae) and Commelinaceae, palms (Arecaceae), unknown woody and herbaceous dicots, other forest indicators, and unknown forms. These results are further supported by the general environmental reconstruction of the site where C<sub>4</sub> grasses were the dominant vegetation coupled with scattered trees, shrubs, and wetland taxa, suggesting early hominins' exploitation of resources found at their home base.

### **Introduction**

Archaeology aims to study past lifeways and the history of humankind using material remains (Renfrew & Bahn, 2000). Material remains are comprised of every conceivable substance on earth; if humans used, touched, cooked, ate, built with, modified, or created it, it falls within the bounds of the archaeological quest seeking to understand why people lived in a certain way, why they created those behavioral patterns, and how their lifeways and material culture emerged the way they did (Renfrew & Bahn, 2000; Zurro & Gadekar, 2023). Unfortunately, most of the materials used and consumed by prehistoric societies, especially during the Pleistocene period, were perishable, making it difficult to reconstruct past economies. Chipped stones and debitage represent one of the most abundant artifacts of the Pleistocene period that are preserved and can carry important clues to understanding prehistoric lifeways (Chazan, 2013; Guibert-Cardin et al., 2022; Renfrew & Bahn, 2000). Lithic artifacts are the product of complex behaviors involving carefully selecting raw materials, then designing, shaping, utilizing, and subsequently discarding them (Renfrew & Bahn, 2000).

Over the past forty years, archaeological methodologies and techniques have developed to include new techniques, such as residue analysis of lithic tools, to establish the relationship between

humans and their environments (Hayes et al., 2018; Kealhofer et al., 1999; Kooyman et al., 1992; Pearsall, 2016; Piperno, 2006). Residue analysis on prehistoric stone tools started in North America with the work of Briuer (1976) that included microscopic usewear developed in the early 1960's by the PhD work of Sergai Semenov (Semenov & Semenov, 1970). Residue analysis can identify many microscopic residues such as starch granulate, stellate hairs, pollens, calcium oxalate crystals, raphides, cell walls, cell lumen, tracheids, fibre tips, spiral vessels, and hair vessels phytoliths, as well as starch grains (Hayes et al., 2018; Kealhofer et al., 1999; Pearsall, 2016). Regarding the interpretation of residue results at archaeological sites, some researchers have proposed approaches that include analysis of immediate adjacent soil samples to verify the residue results on tools were not from contamination (Kooyman et al., 1992; M. E. Newman et al., 1993; M. Newman & Julig, 1989). Archaeological studies on residue analysis improved in the 1980s, following the development of methods to include scanning electron microscope with energy dispersive X-ray spectroscopy (EDS) (Croft, 2021).

Phytoliths have been used to understand stone tool function and to identify the types of plants being processed in archaeological assemblages (Barton et al., 1998; Fullagar et al., 2006; Kealhofer et al., 1999, 1999; Pearsall, 2016; Piperno, 2006). There have been numerous studies in the literature reporting phytolith residues from chipped stones at Late Pleistocene, Early Holocene, and Neolithic sites (Barton et al., 1998; Field et al., 2020; Fullagar et al., 2006; Hayes et al., 2018, 2021). But plant residues, including phytoliths, are challenging to isolate and usually very scarce (Zurro & Gadekar, 2023). In addition, archaeological deposits and sediments contain diverse organic matter that might transfer to artifacts and contaminate them (Hart, 2011; Pearsall, 2016; Pearsall et al., 2004; Piperno, 2006; Zurro & Gadekar, 2023). This becomes an even greater challenge for more ancient assemblages.

In Africa, two studies have documented phytolith residues on Early and Middle Pleistocene sites: Dominguez- Rodrigo et al. (2001) reported the presence of *Acacia* phytoliths from a 1.7-1.5 million year old (Ma) Acheulean handaxe, suggesting woodworking at the Peninj site in Tanzania. However, the results of this paper have been questioned by Collura & Neumann (2017). Phytoliths from sediments at the series of rock shelters at Pinnacle Point 13B cave that revealed complex behavior by Middle Stone Age hominins, including intentional plant gathering for firewood and possibly bedding (Albert & Marean, 2012; Esteban et al., 2018). This evidence shows the potential of phytolith residues, especially from chipped stone, for understanding the function of stone tools and hominin exploitation of plant resources within their landscape deep into the Pleistocene.

## The Manyara Beds and their Lithic Assemblages

This study aims to document phytolith residues from lithic artifact assemblage from the Middle Pleistocene Manyara Beds in Northern Tanzania. The Manyara Beds in Northern Tanzania preserve records of ancient Lake Manyara shorelines inhabited by a group of early *Homo*, probably within the broad range of *H. heidelbergensis sensu lato (s.l.)* during the early part of the Middle Pleistocene period, approximately 780,000 to 633,000 years ago (Frost et al., 2012, 2017; Schwartz et al., 2012). Although hominin remains are rare in the Manyara Beds (limited only to two very fragmented fossils), their occupation is documented by numerous stone tools assigned to the Early Late Acheulean industry (Giemsch et al., 2018). The full regional extension of the Manyara Beds is unknown, but the known exposures cover approximately 125km<sup>2</sup> surrounding Makuyuni town (Figure 4-1) (Kaiser et al., 2010). The Manyara Beds are numbered into numerous 'MK areas' (after the village name 'Makuyuni'), which range from meter to kilometer scale areas and contain fossil vertebrates, lithic artifacts, and geological features (Kaiser et al., 2010).

The available literature on the archaeological finds at the Manyara Beds has established two lithic inventories: (i) Series 1, derived from surface collections and dominated by handaxes and cleavers made of volcanic rocks, and (ii) Series 2, derived from excavation and comprised of small flaked quartz and basalt tools (Kaiser et al., 2010). Both raw materials (quartz and basalt) occur in the immediate vicinity, from sources located from 5 to 20 kilometer away from the site (Kaiser et al., 2010).

The Series 1 lithic inventory occurs at numerous sites within the Manyara Beds, including MK 4, MK 123, MK 91, MK 101, MK 2, and MK 17; the Series 2 lithic assemblage occurs mainly at site MK 4 (Giemsch et al., 2018; Kaiser et al., 2010). Kaiser et al. (2010) proposed that the difference between the two assemblages could be chronological or that the Series 2 assemblage at MK4 represents evidence of a special economy. However, the chronological difference must be confirmed since small tools assemblages such as scrapers and drills tend to occur at long-term Acheulean campsites where handaxes and cleavers are the dominant artifacts (Chazan, 2013; Giemsch et al., 2018; Guibert-Cardin et al., 2022).

Makuyuni Site 4 (MK4) is also rich in fossil fauna, but their association with the stone tools is unclear. Several studies have found that fossil fauna from MK 4 exhibits a high incidence of carnivore tooth marks. Hence, they may represent a "carnivore attrition assemblage" (Kaiser et al., 2010:69). The absence of recognizable evidence of hominin activity in the accumulated fossil assemblage and the fact that lithic tools occur at the same levels suggest that MK 4 represents a palimpsest where hominin lithic tools occur in areas where fossil fauna accumulate naturally (Kaiser et al., 2010). Bachofer et al. (2018) proposed that the fossil fauna and lithic tools were deposited in different

archaeological layers under different conditions. The fauna is related to the harder rock formations that are left behind when the shorelines recede in the higher parts of the fluvial terrace systems, and the tools are associated with sediments deposited closer to the paleolake shoreline and the paleo-river network (Bachofer et al., 2018).

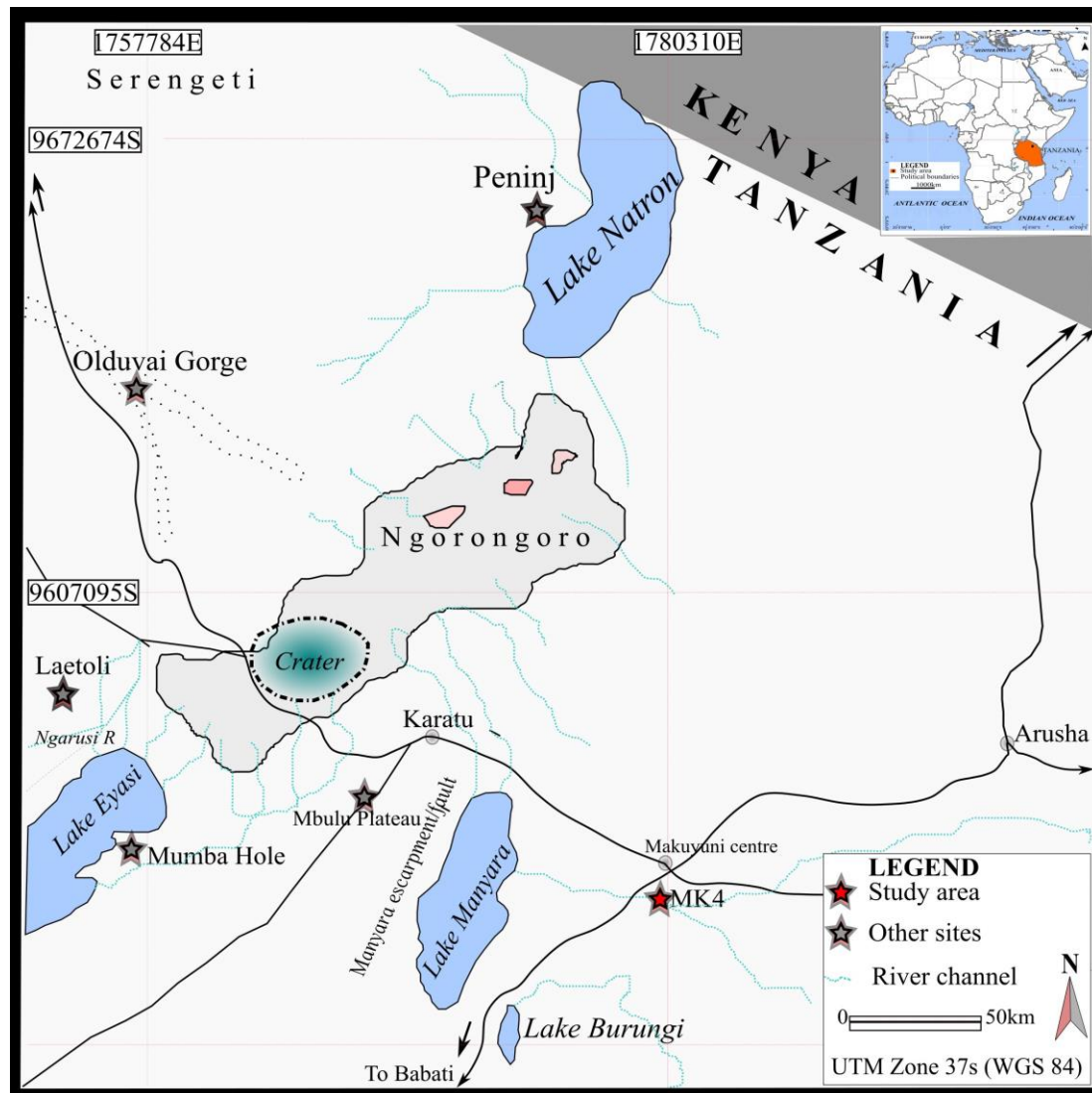


**Figure 4-1:** Map of Arusha region showing the location of the study area of the Manyara Beds near Makuyuni Town in association to other archaeological sites in Northern Tanzania.

## Materials and methods

### Study Area

The largest number of fossils and artifacts from the Manyara Beds were recovered from MK 4 (Giemsch et al., 2018; Kaiser et al., 2010; Wolf et al., 2010). The MK 4 site covers about 2000 m<sup>2</sup>. The site occurs near an active tributary of the Makuyuni River at the southwest end of the town (Giemsch et al., 2018; Kaiser et al., 2010).

MK 4 sediments include both lower and upper Manyara Beds deposits (Figure 4-3), with archaeological remains confined to the uppermost part of the lower Manyara Beds, which consist mostly of sandstones (Kaiser et al., 2010). The most abundant fossil remains at the site include bovids (Antilopini, Hippotragini, Bovini, Reduncini), equids (*Equus* and *Eurygnathohipus*), and suids (*Nyanzachoerus kanamensis*, *Metridiochoerus andrewsi*, *Metridiochoerus compactus*, and *Phachoecorus* sp). Other fossils include Cichlidae, Osteichthyes, Chelonidae, Crocodilia, Giraffidae, *Hippopotamus*, *Ceratotherium*, *Elephas*, Carnivora (presumably *Panthera*), Thryonomyidae (Rodentia), Cercopithecidae, and Hominidae (Primates) (Kaiser et al., 2010).

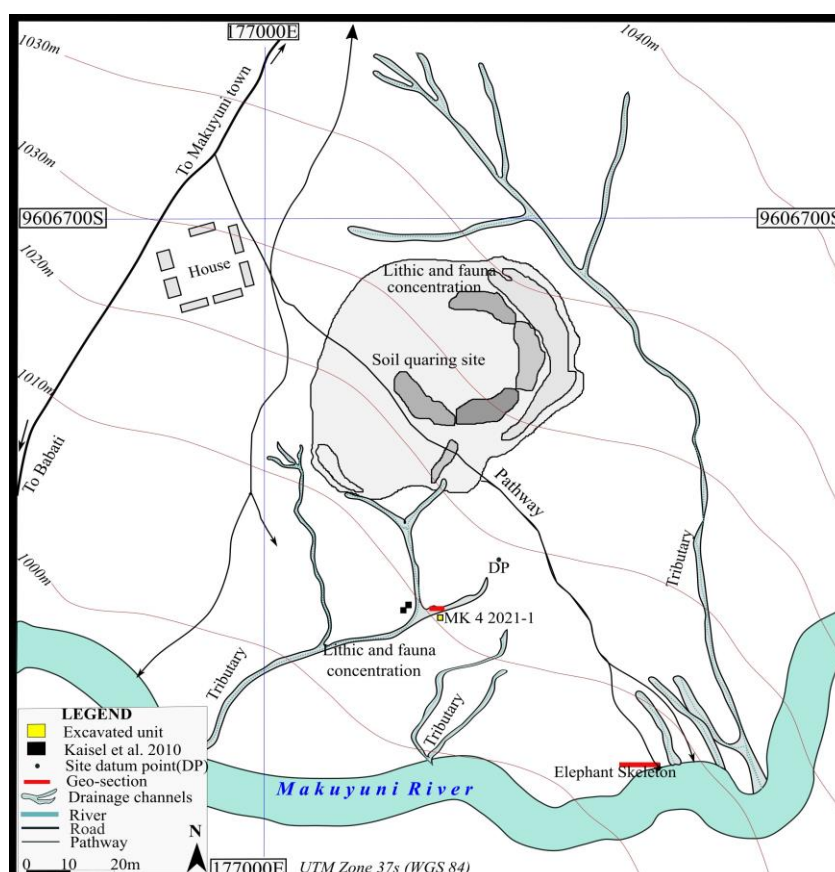


**Figure 4-2:** Map of MK4 showing the location of the 2021 excavation unit.

The two geo-sections, and Kaiser et al.'s (2010) excavation unit (modified from Kaiser et al. (2010)).

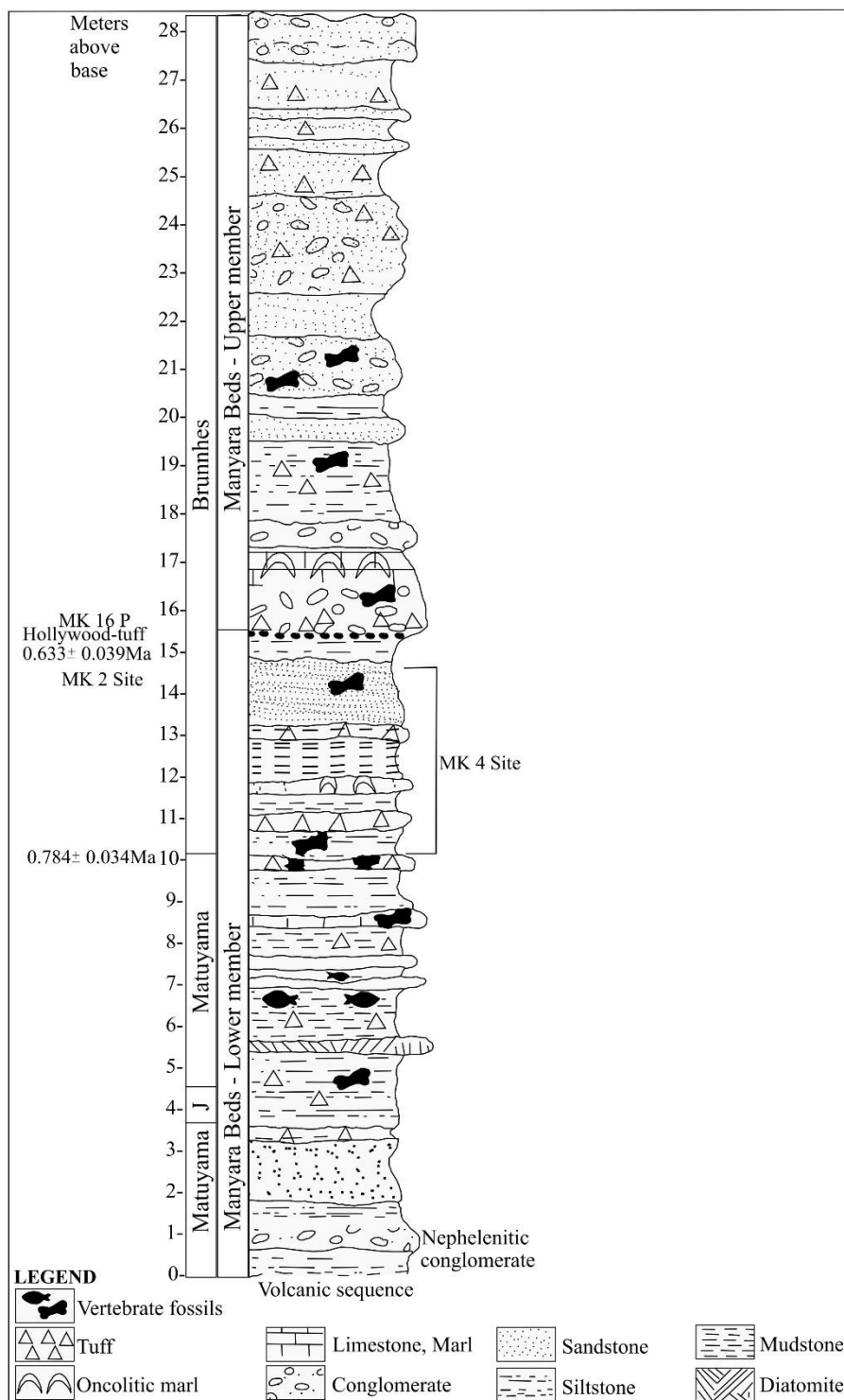


**Figure 4-3:** The generalized stratigraphic column of the Manyara Beds. Modified from Wolf et al. (2010) and Schwartz et al. (2012).



## Excavation

The 2021 excavation site is located almost 2.5 meters from Kaiser et al.'s (2010) excavation site (Figure 4-2). Both excavation sites are located between 4.5 to 5.5 meters above the active channel bed of the Makuyuni River. In both excavations, the stratigraphic exposures consist of at least 4-5 meters of greenish to light grey lacustrine sediments with marls and tuffaceous units (Figure 4-2).

The 2021 excavation was carried out near a natural stratigraphic profile. The area has three intersected gullies that create a scarp, forming a natural profile exposure. This area was selected based on previous knowledge of its artifact-rich excavations conducted by the University of Dar es Salaam Field Schools in 2014 and 2015 reported in Bundala (2015), as well as Kaiser et al. (2010).

A 2 by 2 meter excavation unit was established at the site in 2021 to recover artifacts and fossils. The excavation unit was divided into four squares, namely A1, A2, B1, and B2 (Figure 4-4). Excavation followed arbitrary levels of 10 cm, allowing great control over artifact provenience, and samples were collected and labeled according to the squares. All artifacts used for this study were collected from layer 3 (depth 50-70 cm). Layer 3, comprised of compact mudstone with carbonate nodules, was the most productive layer, with numerous artifacts scattered across space that can provide insight into the possible use of the area. A second 2 by 2 meter excavation unit was opened to trace the continuation of the fossil-rich layer (Figure 4-4), but only squares C1 and D1 were excavated from the extension unit. Artifact depth was taken using a total station. Excavation concluded at a sterile layer at 2 meters depth. Once each unit was finished, soil profiles were drawn along the two walls (Figure 4-5).

Excavation Unit 1 was located about 2 meters away from Geo-section 1, which is located on an adjacent gully of natural exposure and is analyzed in Chapter 3. Phytolith samples from Geo-section 1 form an important control on the archaeological phytoliths recovered from tools, because the same layer was sampled in both areas. Layer 3 in Geo-section 1 can be correlated to Layer 3 (the artifact-rich layer) in excavation Unit 1. The similarities are based on:

1. Careful depth measurements from the same reference point, Layer 3 in geosection 1 depth is between 50 to 70 cm, like Layer 3 in unit 1 (50-70 cm).
2. Matching soil color, both are silty clay dark grayish brown.
3. Both have cultural materials, lithic, and fauna.
4. The carbonate nodules in Unit 1, layer 3 are comparable to those in geo-section 1 layer 3.

I expect to see more and variety of phytoliths in an environmental sample, while as on artifacts, I anticipate seeing fewer phytoliths and of a very specific representing one or just a small number of taxa.

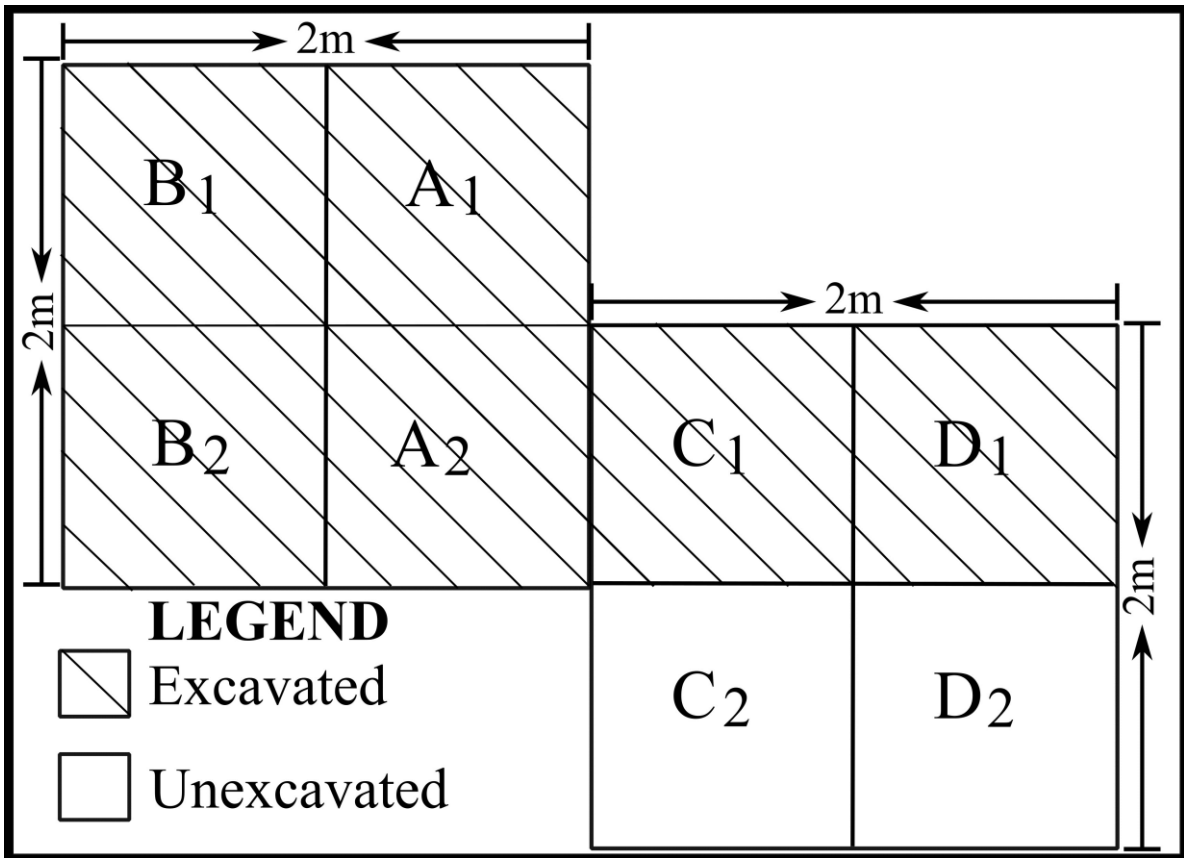
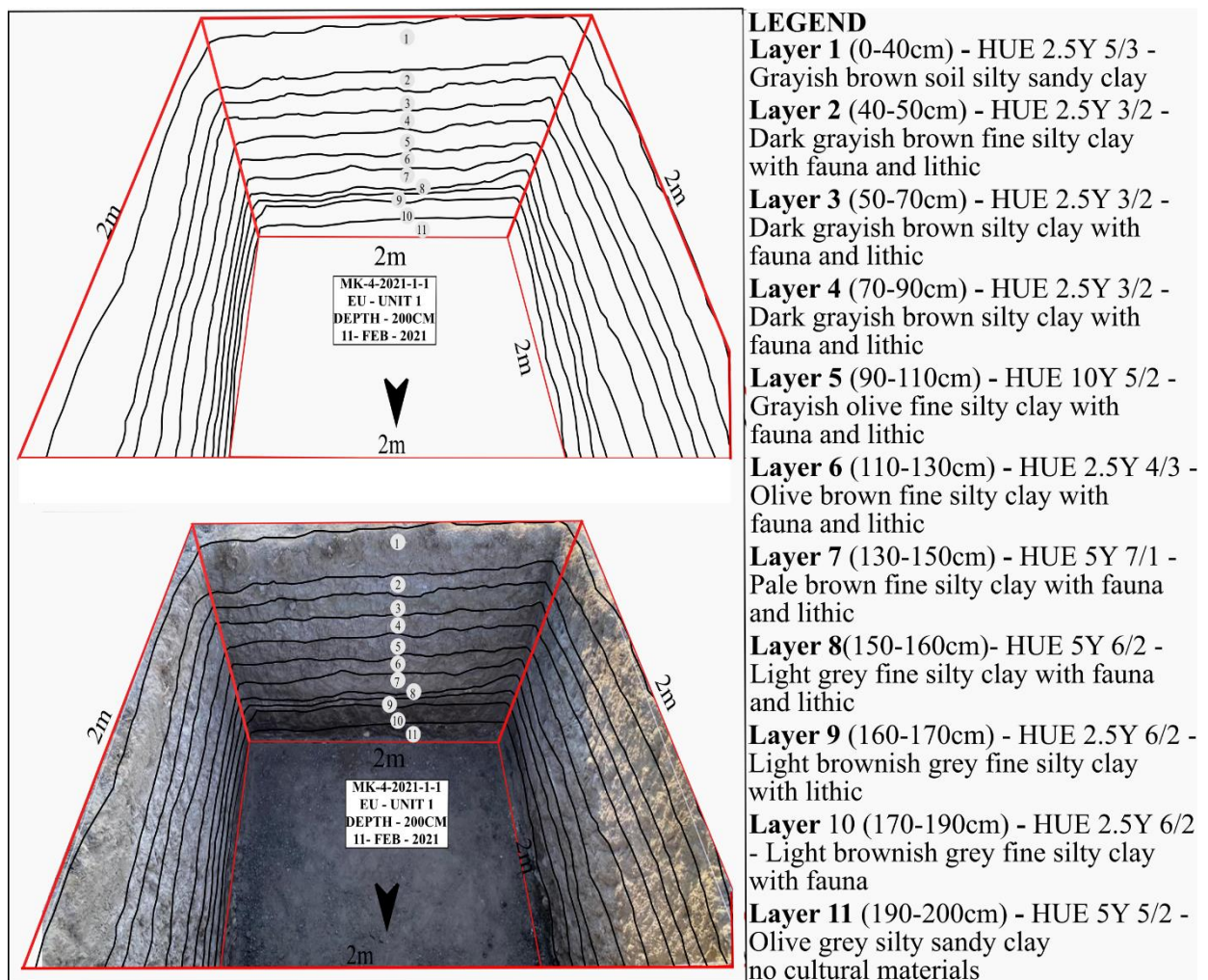


Figure 4-4: Excavation plan at MK 4.



**Figure 4-5:** Wall profile showing the eleven layers identified from the first 2 by 2 unit after excavation (Unit A/B). All stone tools analyzed in this study for phytolith residues came from Layer 3. EU=Excavation Unit.

#### Sampling methods

The main methodological concern is the authenticity of the phytolith residues. At many archaeological sites, there are high incidences of contact between stone tools and other materials that could transfer phytoliths onto stone tools (Barton et al., 1998; Kealhofer et al., 1999; Pearsall, 2016). The problem becomes more acute at sites where phytolith recovery is expected to be low, the likelihood that a phytolith comes from contamination is higher.

Piperno (2006) and Pearsall (2016) present comprehensive reviews of the best practices for researchers attempting to recover authentic phytoliths residues from artifacts, and many researchers utilizes these methods (Barton et al., 1998; Chandler-Ezell et al., 2006; Fullagar et al., 2006; Hart, 2011; Kealhofer et al., 1999; Pearsall et al., 2004). To collect lithic artifacts for microbotanical study, I followed Piperno's (2006) methods. Artifacts were removed from the ground

using starch-free plastic gloves and immediately placed in plastic bags. A new pair of gloves and alcohol wipes were used to clean the tip of the trowel after collecting every sample to avoid cross-contamination (Hart, 2011; Pearsall, 2016; Piperno, 2006). Once the artifact was removed from the ground, control sediments (if applicable) were collected from directly beneath and around the margin of the artifact within 5-10 cm of the tool. These samples are useful to compare against phytolith assemblages from the artifacts (see Piperno, 2006). This was designed as a control to assess the distinctive association of the artifact residue assemblages by comparing phytolith residues from soil samples directly associated with artifacts and those derived from the same archaeological context. The control sample helps to establish whether any microbotanical remains found on stone tool surfaces are qualitatively or quantitatively distinct from those in the general cultural background or environment (Barton et al., 1998; Hart, 2011; Kealhofer et al., 1999; Piperno, 2006).

#### Artifact collection

Artifacts found in situ, if diagnostic to either core or flake, were collected immediately using the protocol described above. A total of 106 (Table 4-1) and twenty control samples (underneath sediments) were collected from Layer 3.

All bagged artifacts were placed in clean buckets with covered tops to avoid contamination and transported to our field camp. Artifacts recovered from the sieve were placed in a single bag per square unit at every level and were not used for residue analysis. Twenty control samples (Table 4-3) of sediments underlying 20 different tools in squares A1, B1, B2, C1, and D1 were collected and bagged separately.

Exportation procedures focused on ensuring limited handling to avoid further contamination during transportation of artifacts used to study residues. This was achieved by placing all the selected artifacts in a separate sealed bucket from the sediments. After obtaining all the transportation and clearing permits, the buckets were sealed with a Government of Tanzanian seal. Then, all samples were transported to Canada for lab analysis.

**Table 4-1:** Summary of the archaeological assemblage from Layer 3.

Square	Tools (N)	Tool Type		Raw Material	
		Flake	Core	Quartz	Basalt
A1	26	13	13	18	8
A2	10	2	8	5	5
B1	50	23	27	39	11
B2	15	4	11	8	7
C1	2	1	1	1	1
D1	3	3	0	2	1
<b>Totals</b>	<b>106</b>				

### Phytolith extraction

#### Control samples

I followed approaches by Pearsall (2016) and Piperno (2006) to test whether the residues extracted from the artifact could be presumed associated with tool use. I analyzed control sediments collected from directly beneath the artifacts and compared qualitative or quantitative patterns distinctive from those found in artifact residue. I proposed that if phytoliths were left on artifacts in the context of use, then phytolith assemblage in the artifact residue sample should significantly differ from the control samples. Likewise, the similarities between artifact residues and the sediments underneath would imply that phytoliths became associated with artifacts after deposition. This hypothesis was tested by comparing phytolith assemblage from artifact residues with the control sediment samples (site soil sample). Due to time constraints, only ten of the twenty control samples were analyzed for phytolith content. Four of these sediment samples came from underneath artifacts that yielded phytoliths: MK4-2021-B1-14, MK4-2021-B1-46, MK4-2021-B1-66, and MK4-2021-B1-87.

Phytoliths from the control sediments were extracted at the Paleobotany Lab at the University of Calgary. In the lab, two grams of sediment from each sample was placed in a 15 mL tube and subjected to acid treatment by adding 10 mL of 0.1% ethylenediaminetetraacetic acid (EDTA) disodium salt dihydrate solution to remove clay. Since our lab did not have an automatic shaker, the sample was mixed by hand and vortexed for five minutes. The sample was then left in EDTA for 24 hours, then washed three times using distilled water. The sample was then washed multiple times with distilled water at 3,000 rev/min for one minute until the sample was less cloudy signifying that clay was removed.

After that, enough 10% hydrochloric acid (HCl) and nitric acid (HNO<sub>3</sub>) diluted to 3 Normal solution were added simultaneously until the sample was full submerged to remove inorganic matter and clay oxides. After fuzzing ceased, the sample was placed in a beaker containing boiled water (hot bath) to speed up the reaction for one hour. The samples were then washed with distilled water at 3,000 rev/min for three minutes, then the supernatant was decanted to remove acids; this was repeated three times. Then, organic matter was removed by adding 30% H<sub>2</sub>O<sub>2</sub> solution and placed in a hot bath for one hour. The samples were again centrifuged three times at 3,000 rev/min to remove hydrogen peroxide. Phytoliths were floated by adding 3 to 5 mL of sodium polytungstate (SPT) with a specific gravity of 2.3 to separate them from heavy minerals. The samples were then centrifuged at 3,000 rev/min for 5 minutes. Then, the light materials containing phytoliths were separated from the heavy minerals, and the supernatant containing phytoliths was decanted and placed into newly labeled vials and dried overnight at 70°C. The phytolith residue was then dried, and three slides from each sample (n=10 samples and 30 slides) were mounted on a microscope slide using glycerine.

#### Artifacts

Extraction of artifact residue samples was conducted at the Ancient DNA lab (with HEPA-filtered air) at the University of Calgary to avoid contamination with other samples. Some researchers sample only a small portion of the artifact for residue analysis (see Piperno, 2006 for more details). In this study, the entirety of each artifact was sampled because each of the artifacts measured no more than 10 cm in length. Residue extraction followed methods by Pearsall (2016) with slight modifications to minimize handling and avoid contamination across samples.

Artifacts were not brushed of adhering dirt. Instead, the stone tools were soaked in individual beakers for 24 hours until the loose sediments dislodged. The stone tools were removed and rinsed with water in a spray bottle until all loose sediments were removed. The dislodged sediments were then concentrated into smaller volumes in 50 mL tubes by centrifuging the tubes at 3,000 rev/min for 2 minute and decanting the supernatant liquid. This sediment (Sediment Cycle 1) was reserved for future research, but not analyzed for phytoliths as part of this study.

Then, the artifact was placed into a new beaker for sonicate cleaning. Enough distilled water to cover the artifact was added, and then the beaker was placed in an ultrasonic bath using a Bransonic 220 sonicator for 20 minutes. The stone tool was then removed and rinsed with water in a spray bottle until all loose sediments are removed. The sediments were concentrated in a 15 mL centrifuge tube. Recovered sediments from Sediment Cycle 2 weighed

between 0.2 g and 0.001 g. Sediment cycle 2 sediments were processed further to recover phytoliths following the procedure described for control samples above.

### Counting and Classification

After drying, a small portion of phytolith residue was mounted on a microscope slide using glycerin and Meltmount to make permanent slides. Microscope inspection, identification, and counting were done using a polarized light microscope, either the Leitz Labor lux 12 (University of Calgary) or Nikon Eclipse 80i (University of Washington) microscope at 400x magnification. Two slides were examined for artifact residues (Sediment Cycle 2 extracts) and three for each control sample. The goal of making more than one slide was to achieve the minimum count of 200 grains which is statistically analyzable (Albert & Bamford, 2012; Pearsall, 2016; Piperno, 2006; Zurro, 2018). Representative morphotypes were photographed using a microscope-mounted Moticam 2500 (5.0 Pixel USB2.0) and DS-Fi1 camera.

Morphological identification was based on Strömberg's (2003) classification and interpretation scheme supplemented by later publications in Stromberg (2004), Strömberg et al. (2018), and Crifò & Strömberg (2021), other publications (Eichhorn et al., 2010; Piperno, 2006; Yost et al., 2018), and augmented by modern reference collections from the study area (Chapter 2 in this study). When possible, the morphotype terminology follows the International Code for Phytoliths Nomenclature (ICPN 2.0) (International Committee for Phytolith Taxonomy (ICPT) et al., 2019).

This study used the following plant functional types: (i) non-diagnostic (unknown); (ii) dicots (plants that have two "seed" leaves) such as trees, shrubs, and some herbaceous; (iii) monocotyledons (plants that have one "seed" leaves) such as grasses, palms, and sedge; (iv) diagnostic to palms, (v) indicative of forests, (vi) represents Commelinaceae (Eichhorn et al., 2010; Yost et al., 2018), (vii) sedge, (viii) diagnostic to grass specifically the short cells silica such as bilobate, saddle, rondel, and polylobate (vii) and some are non-diagnostic to grasses or other monocots (grass/mono-ND) (Table 4-2).

The PACMAD grasses include the Panicoideae, Arundinoideae, Chloridoideae, Micrairoideae, Aristidoideae, and Danthonioideae. Some short cell morphotypes are only diagnostic to the more inclusive clade (PACMAD) level. Chloridoideae and Panicoideae are part of the PACMAD clade but they have their own sets of unique morphotypes that allow me to specifically identify them. Lobates (cross, bilobate, and polylobate) are assigned to Panicoideae, while saddles and spooled/horned/crescentic rondels are diagnostic of the Chloridoideae grasses (Twiss et al., 1969; Twiss 1992). In due regards, this study utilises the term "other PACMADs" to differentiate general PACMADs morphotypes from the ones that are specific to chloridoids and panicoids.

**Table 4-2:** Morphotype classes used in this study

After Strömberg 2003, and later studies in Strömberg 2004; Strömberg et al., 2018.

<b>Phytolith morphotype</b>	<b>Taxonomic interpretation/plant functional type</b>
Echinate sphere (CIm-2)	Palm
MD-clump (CI-10)	Trees and shrubs-forests
Small pink sphere (CI-4)	Woody and herbaceous dicots
Smooth VI sphere and subsphere (CI-1)	Woody and herbaceous dicots
Anisopolar prismatic domed cylinder (Pris-CI)	Commelinaceae
Rondel (crescentic/spooled/horned) (CO-5)	C <sub>4</sub> Chloridoideae
Saddle (SA-1)	C <sub>4</sub> Chloridoideae
Cross -Four lobed cross with near a cross shaped top (CR4-1)	Panicoideae (C <sub>4</sub> & C <sub>3</sub> mostly C <sub>4</sub> )
Bilobate- symmetry E bilobate (BI-8)	Panicoideae (C <sub>4</sub> & C <sub>3</sub> mostly C <sub>4</sub> )
Polylobate-with top and bottom same size (PO-4)	Panicoideae (C <sub>4</sub> & C <sub>3</sub> mostly C <sub>4</sub> )
Polylobate-with larger top (PO-3)	C <sub>4</sub> & C <sub>3</sub> "Other PACMADs"
Bilobate <ul style="list-style-type: none"> <li>• symmetry D bilobate (BI-7)</li> <li>• symmetry C bilobate (BI-6)</li> <li>• Symmetry B bilobate (BI-5)</li> </ul>	C <sub>4</sub> & C <sub>3</sub> "other PACMADs"
Trichome (Tri-8)	Non-diagnostic grass/monocot
Spiny elongate (Epi-9)	Non diagnostic grass/monocot
Smooth elongate (Elo-1)	Unknown
Thick rectangular plate (Blo-2)	Unknown



## Results

### Results from control samples

Ten control samples were analyzed. Even though three slides were prepared and counted per sample, the control sediments did not yield any phytoliths (Table 4-3). The fact that sediments underneath yielded no phytoliths even after examining three slides from each sample strongly suggests that the phytoliths recovered from artifact residues cannot be interpreted as contamination.

**Table 4-3:** Sediments sample beneath artifacts (control samples).  
Twenty samples were collected, but only ten were analyzed. None of the analyzed samples preserved phytoliths.

Sample #	Layer	Depth (cm)	Phytoliths: NA-Not applicable
MK4-2021-B1-5	Layer 3	-59.235	NA
MK4-2021-B1-14	Layer 3	-59.178	0
MK4-2021-A1-19	Layer 3	-57.63	0
MK4-2021-C1-21	Layer 3	-58.92	0
MK4-2021-B1-23	Layer 3	-59.162	NA
MK4-2021-C1-24	Layer 3	-57.485	0
MK4-2021-B2-25	Layer 3	-57.788	0
MK4-2021-B1-29	Layer 3	-57.74	NA
MK4-2021-B1-31	Layer 3	-59.235	NA
MK4-2021-B1-33	Layer 3	-59.165	NA
MK4-2021-B1-46	Layer 3	-59.217	0
MK4-2021-B1-48	Layer 3	-59.145	NA
MK4-2021-B1-56	Layer 3	-59.14	NA
MK4-2021-B1-66	Layer 3	-59.143	0
MK4-2021-A1-74	Layer 3	-59.636	NA
MK4-2021-A1-77	Layer 3	-59.057	0
MK4-2021-D1-80	Layer 3	-58.94	0
MK4-2021-B1-87	Layer 3	-59.254	0
MK4-2021-B1-92	Layer 3	-59.178	NA
MK4-2021-B1-106	Layer 3	-59.149	NA

## Results from stone tools residues

Most of the Sediment Cycle 2 samples did not yield any phytoliths, and those that did had low phytolith recovery, as expected. Only ten tools had identifiable phytoliths adhering to them (Table 4-4). As a result, this study is more qualitative than quantitative.

The assignment of tools into categories (Table 4-4) was done after all the residues had been extracted and the external surface of the tool was visible. I relied on Kaiser et al. (2010), which describes the small lithic tools found at MK4 during previous excavations. I also consulted other literature on lithic analysis (e.g., Balme & Paterson, 2006; Renfrew & Bahn, 2000; Shea, 2013) that describe tool types in more detail. I used the following categories:

1. A **flake** is a piece of stone removed from the core. Its characteristics include an interior(ventral) and exterior (dorsal) surface, a striking platform at one end, ripples, and sometimes a bulb of percussion on the ventral surface.
2. **Scrapers** are flakes with at least one unifacially retouched edge that is less than 70 degrees (obtuse) working edge. Cutting tools (also referred to as knives) have steep cutting edges, usually more than 70 degrees (acute working edge). It is also different from a chopper in terms of size; choppers are unifacial large-sized pebble tools that have two or more deep flake scars that create sharp cutting edges, and the butt end is blunt or rounded.
3. Pounding/**hammerstones** are artifacts shaped by percussion. Hammerstones are usually spherical or subspherical and weigh less than 2 kg. Their most distinctive feature are convex or flat concentrations of crushing and other damage resulting from their use.
4. The **core** is the parent mass from which flakes are removed.
5. **Core tools** (core scrapers) are cores on which retouches have been applied on one or more edges.

**Table 4-4:** List of Manyara Bed artifacts that yielded phytoliths (n = 10)

Artifact/sample #	Artifact description	Wear/edge description	Possible use
MK4-2021-B1-14	Core made of basalt. The surface is pitted/grooved, showing pounding use.	Grooved surface	Pounding/Hammer stone
MK4-2021-B1-46	Quartz flakes with sharp edges can be used for cutting.	Sharp edges	Scraper
MK4-2021-B1-66	Basalt core with flake scars shaped to create sharp cutting edges that can be used as core scraper.	Roundish edge/dull	Core scraper
MK4-2021-A1-67	Basalt core roundish like river cobble	Roundish and grooved surface	Pounding/hammer stone
MK4-2021-B1-71	Basalt core with multiple flake scars creating sharp cutting edges	Sharp edges	Core scraper
MK4-2021-B1-87	Quartz flake with sharp cutting edges.	Sharp edges	Scraper
MK4-2021-A1-98	Quartz core with multiple flake scars edges creating sharp cutting edges.	Sharp edges	Core scraper
MK4-2021-B2-101	Basalt core with multiple flake scars creating sharp cutting edges.	Dull edges	Core scraper
MK4-2021-B1-104	Quartz core with multiple flake scars forming sharp cutting edges.	Sharp edges	Core scraper
MK4-2021-B1-105	Quartz core with sharp cutting edges	Sharp edges	Core scraper

Most of the artifacts that yielded phytolith residues come from a single 1 x 1 m square unit B1 (n=7), which was the most artifact rich excavation square, with just one tool from each of squares A1 and B2 yielding phytoliths. Squares A2, D1, and C1 did not yield tools with phytoliths. Herbaceous morphotypes recovered from tools include sedge (Cyperaceae) and Commelinaceae, arboreal taxa including palm (Arecaceae), unknown woody and herbaceous dicots, forest indicators, and plants that are non-diagnostic grasses/monocotyledonous taxa as well as the 'other' morphotype group, which are non-diagnostic to any plant group (Table 4-5, Figure 4-6). The phytolith assemblage includes three types of grass short cell morphotypes: those representing the general C<sub>3</sub> and C<sub>4</sub> PACMADs, C<sub>4</sub> dry adapted Chloridoideae, and humid loving Panicoideae (Table 4-6, Figure 4-7).

**Table 4-5:** Phytoliths found on ten stone tools.

These data represent functional groups. For detailed data on exactly which morphotypes were found, see Appendix A.

Artifact number/sample #	Tool Type	Raw Material	Grass	Palm	Unknown	Sedge	Non-diagnostic grass/monocot	Wood & herbaceous dicot	Commelinaceae	Forest indicators	Totals
MK4-2021-B1-14	Core	Basalt	68	0	18	0	14	0	0	0	100
MK4-2021-B1-46	Flake	Quartz	18	1	16	0	0	0	0	1	36
MK4-2021-B1-66	Core	Basalt	5	0	13	0	1	0	0	0	19
MK4-2021-A1-67	Core	Basalt	67	1	17	2	15	3	0	0	105
MK4-2021-B1-71	Core	Basalt	4	1	12	0	5	0	0	0	22
MK4-2021-B1-87	Flake	Quartz	2	0	9	0	2	0	0	0	13
MK4-2021-A1-98	Core	Quartz	4	0	2	0	1	0	0	0	7
MK4-2021-B2-101	Core	Basalt	11	1	14	0	4	0	1	0	31
MK4-2021-B1-104	Core	Quartz	5	0	4	0	3	0	0	0	12
MK4-2021-B1-105	Core	Quartz	6	0	3	0	4	0	0	0	13

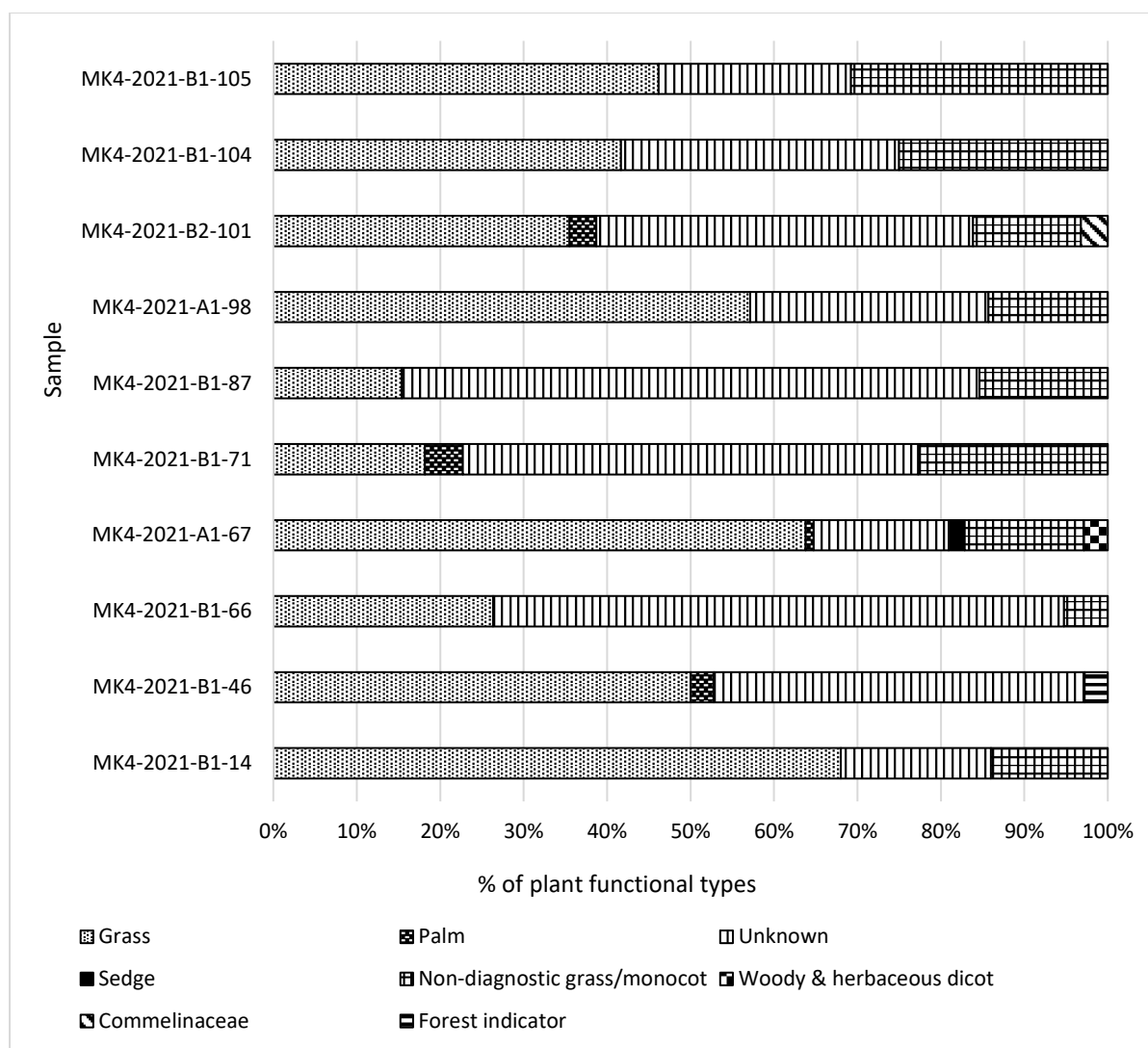


**Figure 4-6:** Phytolith frequencies per artifact.

**Table 4-6:** Grass phytoliths found on each artifact.

For detailed data on exactly which morphotypes were found, see Appendix A.

Artifact/sample #	Tool Type	Raw Material	Chloridoids	Panicoids	Other PACMADs	Total
MK4-2021-B1-14	Core	Basalt	38	0	30	68
MK4-2021-B1-46	Flake	Quartz	9	1	8	18
MK4-2021-B1-66	Core	Basalt	1	0	4	5
MK4-2021-A1-67	Core	Basalt	30	1	36	67
MK4-2021-B1-71	Core	Basalt	1	0	3	4
MK4-2021-B1-87	Flake	Quartz	1	0	1	2
MK4-2021-A1-98	Core	Quartz	1	0	3	4
MK4-2021-B2-101	Core	Basalt	3	0	8	11
MK4-2021-B1-104	Core	Quartz	0	0	5	5
MK4-2021-B1-105	Core	Quartz	0	0	6	6

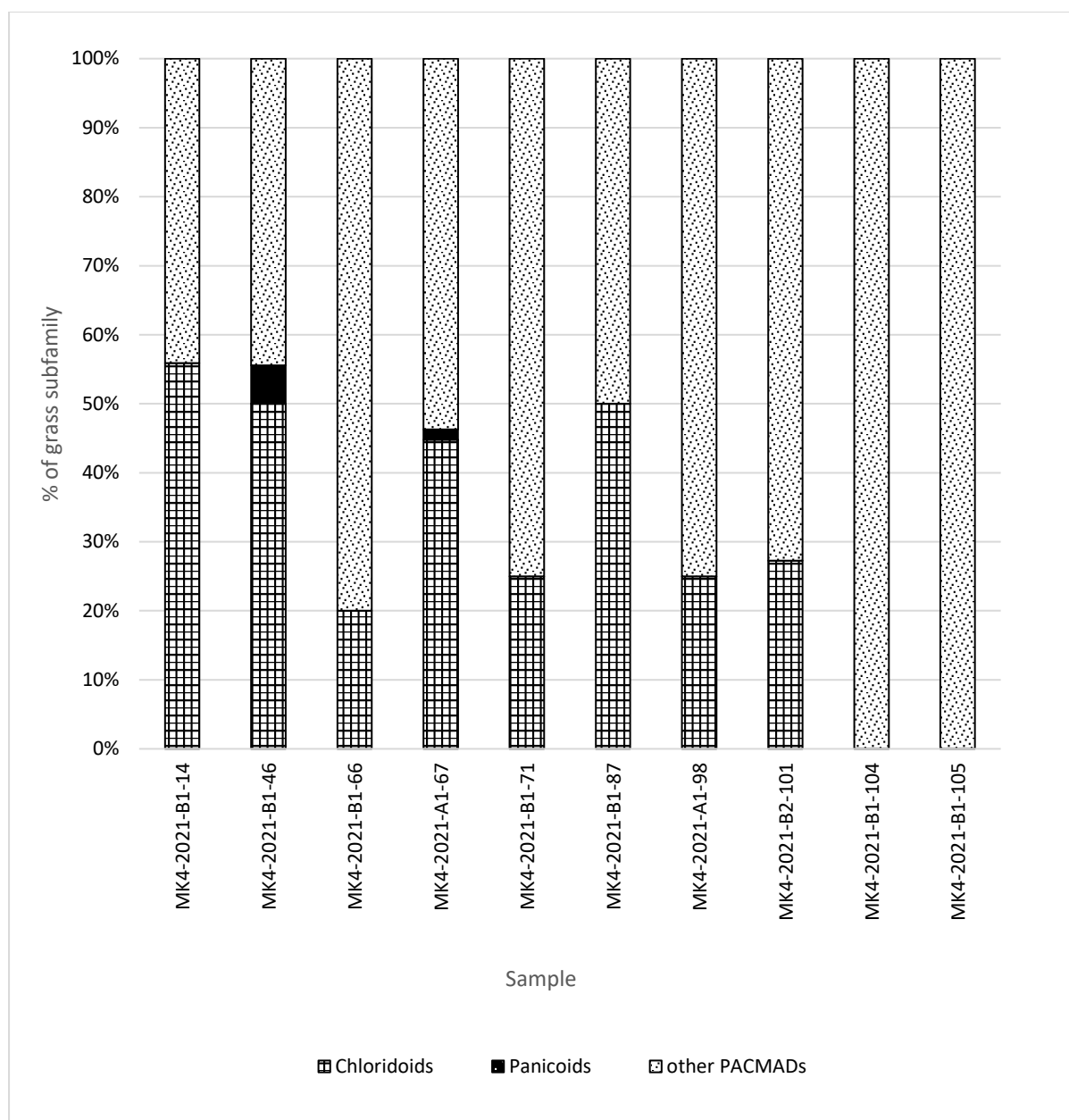


**Figure 4-7:** Frequencies of grass phytoliths found on all artifacts that produced phytoliths.

*Artifact # MK4-2021-B1-14*

MK4-2021-B1-14 is a basalt core with a pitted and grooved surface that was likely used as a grinding or pounding tool (Table 4-4). This artifact yielded the highest phytolith count ( $\geq 100$ ). This artifact's phytoliths assemblage is characterized by 68% grasses (Table 4-5, Figure 4-6), which includes true saddles and crescentic rondels from the warm and arid-loving short grasses, the chloridoids (56%), and bilobates from the "other PACMADs" (44%) (Table 4-6, Figure 4-7). There are also epidermal cells and spindle-shaped infilled trichomes that are non-diagnostic to grasses or other monocotyledonous plants (18%). Finally, there are non-diagnostic smooth elongates (14%). Smooth elongates are commonly found in many kinds of plants, including grasses, palms, sedges, and woody dicots (Table 4-5, Figure 4-6). Given the nature of the phytolith assemblage, Artifact #14 was probably used as an instrument for scraping grass piths, soft woody tissue, and other plants or pounding grasses and other monocots.

*Artifact # MK4-2021-B1-46*

MK4-2021-B1-46 is a quartz flake with sharp cutting edges that was likely used as a scraper (Table 4-4). The phytoliths observed are 50% grasses (Table 4-5, Figure 4-6), including true saddles and crescentic rondels from chloridoids, bilobates representing "other PACMAD" grasses, and crosses from humid-adapted tall panicoid grasses (Table 4-6, Figure 4-7). Woody phytoliths include spheroid echinates from palms (3%) and MD-clump representing forests (3%). Finally, faceted rectangular plates and smooth elongates are present, which can be produced by any plant (44%) (Table 4-5, Figure 4-6). The phytolith assemblage suggests using this flake tools to scrape or cut hard woody tissues, grass piths, and leaves.

*Artifact # MK4-2021-B1-66*

MK4-2021-B1-66 is a basalt core with multiple flake scars forming sharp edge and it was probably used as core scraper (Table 4-4). The phytoliths assemblage from this sample is comprised of 68% smooth elongates produced by many plant taxa (Table 4-5, Figure 4-6). Grass phytoliths make up 26% of the assemblage including bilobates (other PACMAD grasses; 80%) and crescentic rondels (chloridoid grasses; Table 4-6, Figure 4-7). Other morphotypes observed include epidermal cell spiny elongates that are non-diagnostic and can represent grass or monocotyledon plants (Table 4-5, Figure 4-6). All these phytolith morphotypes occurs in grasses, suggesting the use of this tool as a core scraper for scraping grass piths or grinding grasses as a whole plant or just leaves.

*Artifact # MK4-2021-A1-67*

MK4-2021-A1-67 is a basalt core with sharp edges (Table 4-4). This artifact had higher phytolith counts ( $\geq 100$ ). This artifact's phytolith assemblage was made up of 64% grasses (Table 4-5,

Figure 4-6), including true saddles and crescentic conical rondels (chloridoid grasses; 45%) and bilobates (“other PACMAD” grasses; 45%). Panicoids are represented by a small fraction of bilobates (1%; Table 4-6, Figure 4-7). Other morphotypes include 16% smooth elongates from unknown plant taxa (Table 4-6, Figure 4-7). Spindle-shaped trichomes and epidermal long-cell spiny elongate are also present and produced by monocotyledonous plants or grasses (14%). Woody plants are shown by woody and herbaceous dicots smooth VI spheres, small pinky spheres (3%), and echinate spheres representing palms (1%). Wetland plants are shown by the presence of 2% sedge epidermal plates (also known as a polygonal achene), which occur in the leaves and/or culm (Murungi & Bamford, 2020; Piperno, 2006; Stevanato et al., 2019). The residues from this artifact suggest scraping and pounding of siliceous-rich monocots and dicots.

*Artifact # MK4-2021-B1-71*

MK4-2021-B1-71 is a basalt core with multiple flake scars, creating a sharp cutting edge, that could be used as core scraper (Table 4-4). The phytolith assemblage observed for MK4-2021-B1-71 comprises 55% smooth elongates produced by many taxa (other plants) (Table 4-5, Figure 4-6). Grass phytoliths consist of 18% of the assemblage, including crescentic conical rondels (chloridoids; 25%) and bilobates (from any PACMAD grass; 75%) (Table 4-6, Figure 4-7). The artifact's diagnostic phytoliths suggest scraping silicious grasses.

*Artifact # MK4-2021-B1-87*

MK4-2021-B1-87 is a quartz flake with sharp edge (Table 4-4). Phytolith morphotypes observed in this sample include 69% smooth elongate morphotypes produced by other plant categories. Grass morphotypes make up 15% of the assemblage (Table 4-5, Figure 4-6), including true saddles (chloridoids; 50%) and bilobates produced by any member of the “other PACMAD” clade (50%) (Table 4-6, Figure 4-7). Spiny elongates produced by grasses or other monocots comprise of 15% the assemblage (Table 4-5, Figure 4-6). The residue assemblage from this artifact likely originates from a single source, possibly from the grass subfamilies presented by the observed short cell phytoliths. This artifact was probably used to cut or scrape grass piths and leaves.

*Artifact # MK4-2021-A1-98*

MK4-2021-A1-98 is a quartz core with multiple flake scars making sharp edges that can be used as a core scraper (Table 4-4). Compared to other artifacts, MK4-2021-A1-98 had the lowest phytolith count (n=7). The phytolith assemblage is made up of 57% grasses (Table 4-5, Figure 4-6), including the bilobates (“other PACMAD” clade; 75 %) 25% crescentic conical rondels (Chloridoideae; Table 4-6, Figure 4-7). There are also smooth elongates representing 29% of other plants and spindle-shaped infilled trichomes that are non-diagnostic to grasses and other monocots (14%)



(Table 4-5, Figure 4-6). Spindle-shaped trichomes occur only in monocots, while smooth elongates are found in many plant families, including grasses. The phytolith assemblages likely come from a single source: grasses that produce all these morphotypes.

*Artifact # MK4-2021-B2-101*

MK4-2021-B2-101 is a basalt with multiple flake scars creating sharp edges that can be utilized as a core scraper (Table 4-4). The phytoliths observed are made up of both C<sub>3</sub> and C<sub>4</sub> grasses and C<sub>3</sub> monocots (Table 4-5, Figure 4-6). The morphotypes include 45% undiagnostic smooth elongates. Grasses represent 35% of the assemblage, comprising bilobates (“other PACMAD” clade; 73%), and true saddle morphotypes diagnostic to the short chloridoid grasses (27%; Table 4-6, Figure 4-7). 14% of the assemblage comprises spindle-shaped trichomes, found in monocotyledonous plants. Also, there are anisopolar prismatic cylinders diagnostic of the C<sub>3</sub> herbaceous monocots (Commelinaceae; 3%) and spheroid echinates diagnostic to palms (3%) (Table 4-5, Figure 4-6). The residue assemblage from Artifact #101 suggests use of this artifact as a core scraper for cutting and scraping a range of plant materials.

*Artifact # MK4-2021-B1-104*

MK4-2021-B1-104 is a quartz core with multiple flake scars creating sharp edges that could be used as a core scraper (Table 4-4). This artifact’s phytolith assemblage comprised 42% grasses, including bilobates (“other PACMADs”; Table 4-6, Figure 4-7). Other morphotypes include 33% smooth elongates representing other plants, and spindle-shaped trichomes are often found in monocots (25%) (Table 4-5, Figure 4-6). All these morphotypes can originate from the “other PACMAD” grasses, suggesting that Artifact #104 was used to scrape or grind grasses.

*Artifact # MK4-2021-B1-105*

MK4-2021-B1-105 is a quartz core with sharp cutting edges that can be used as a core scraper (Table 4-4). The phytoliths observed for MK4-2021-B1-105 comprise 46% grasses (Table 4-5, Figure 4-6) including bilobates from “other PACMAD” grasses (Table 4-6, Figure 4-7). There is also the presence of smooth elongates representing indeterminate forms (23%) and spindle-shaped trichomes that come from monocots (31%) (Table 4-5, Figure 4-6). Like MK4-2021-B1-104 this phytolith assemblage suggests using Artifact #105 for scraping grasses.

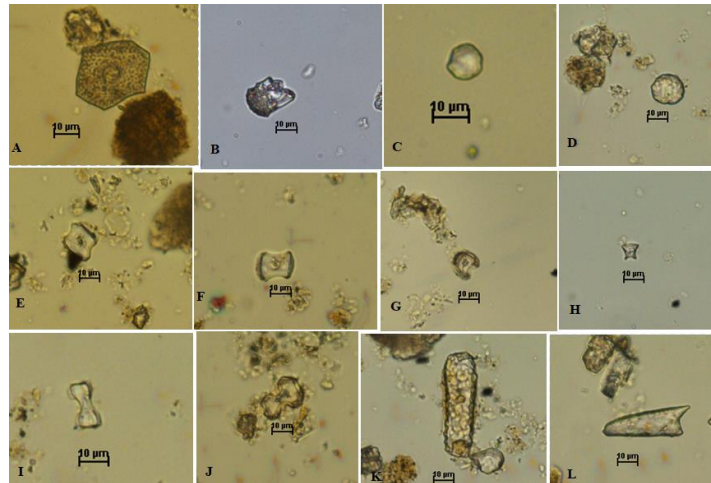


**Figure 4-8:** Selected diagnostic phytoliths found in stone tool residues.

A. Sedge epidermal plate with central cone. B. Anisoipolar prismatic cylinder with broken end, diagnostic to C<sub>3</sub> Commelinaceae. C. Smooth VI sphere, diagnostic to woody and herbaceous dicots. D. Small pink sphere, diagnostic to woody and herbaceous dicots. E-F. True saddle morphotypes indicative of C<sub>4</sub> Chloridoideae grasses. G-H. C<sub>4</sub> Chloridoideae grasses conical rondel morphotypes: G, crescentic conical rondel and H, horned rondel. I-J. Symmetrical D bilobate (almost panicoid) diagnostic to PACMADs. K. pitted smooth elongate from unknown. L. spindle-shaped trichome non-diagnostic to grasses and other monocotyledon plants.

### Testing for the Authenticity of Artifact Residues

In addition to control samples taken directly under a subset of artifacts, the authenticity of the artifact-derived phytoliths can be tested by comparing artifact-derived phytoliths with those recovered from the same layer in Geo-section 1 (#MK4-GS1-L3). Layer 3 in Geo-section 1 had among the lowest phytolith recovery from the whole section (n=224 phytoliths), suggesting a period of disturbance or removal of sediment-rich phytoliths by other agents. As expected, there are more phytoliths in the real sediment samples than in the sediments adhering to the tools (see Figure 4-9). There is also a much greater diversity of phytolith morphotypes from the sediments, suggesting that MK4-GS1-L3 is capturing a wide range of the vegetation present instead of the limited set of phytoliths observed from the artifacts. Finally, the two assemblages look different; there is a much higher percentage (>20%) of non-diagnostic grass or monocots forms in the sediment sample, which are rare on the tools, suggesting they are not plants that hominins are targeting. In addition, there are more phytoliths representing palms, sedges, and forest indicators in sediments, which are also rare on the tools. When they do occur, they represent just one or two phytoliths.

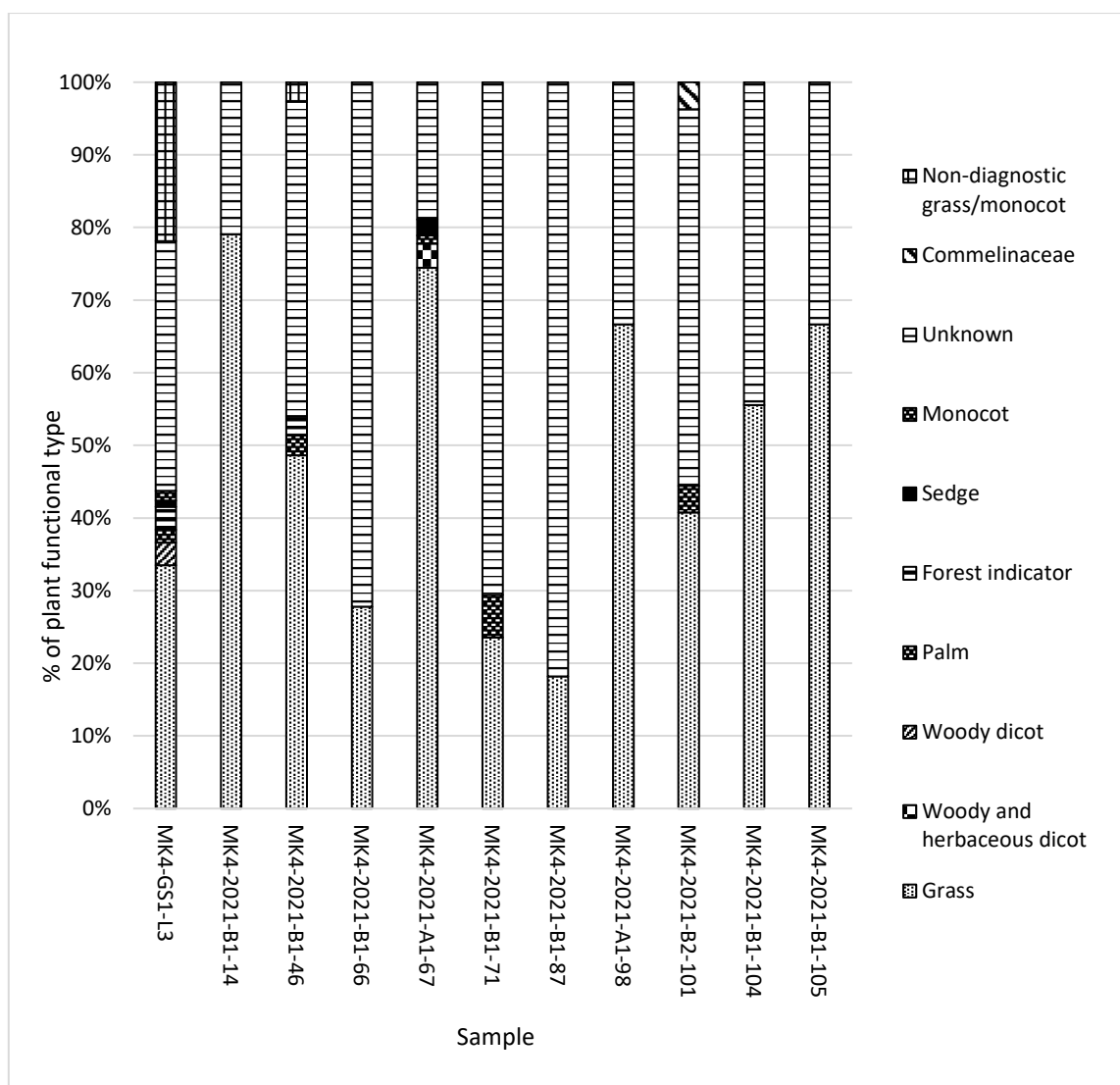


**Figure 4-9:** Comparison of phytolith assemblages from Geo-section 1 sample #MK4-GS1-L3 and artifacts.

## Discussion and Interpretation

### *Overview of the findings*

The phytoliths observed suggest early hominin exploitation of plant resources at the Manyara Beds during the Early Middle Pleistocene period. The absence of phytoliths on the control samples and the presence of a different mixture of grasses on the tools than in the Geo-section (Layer 3) implies that the occurrences of grass residues from artifacts are not a result of natural factors such as transfer from sediments.

My results show that *Homo* at the Manyara Beds exploited grass plant resources when it might have seemed more likely that they were exploiting dicots. The grass assemblages from tools contain distinctive grass morphotypes (see Figure 4-8), including bilobates originating from the leaf part or glumes of PACMAD grasses (many forms); rondels and saddles that come from short C<sub>4</sub> chloridoids that prefer dry conditions, and the panicoid (C<sub>4</sub> and C<sub>3</sub>) bilobates found in tall panicoid grasses that would have flourished in warmer and wetter conditions (Barboni & Bremond, 2009; Mulholland, 1989; Pearsall, 2016; Piperno, 2006).

Other rare phytoliths found adhering to tools include sedge epidermal phytoliths, originating from the leaf or achene (fruit) part of cyperaceous plants (Murungi & Bamford, 2020; Piperno, 2006; Stevanato et al., 2019) and dicotyledons spheres that are likely to originate from the leaf, wood, or bark of woody or herbaceous dicots (Collura & Neumann, 2017; Piperno, 2006; Strömberg, 2003). There are also echinate spheres from palms, known to be produced everywhere in the plant body, including the nut shells (Albert et al., 2009; Pearsall, 2016; Piperno, 2006). Finally, phytoliths from general monocots and indeterminate types are produced by many plant taxa.

### *Artifact Use*

The range of phytoliths found adhering to tools suggests that artifacts were used for various activities, including grinding, pounding, and scraping silicious, woody, and soft plants. The basalt cores that had adhering palm phytoliths were presumably used for nut-cracking at the home base. A focus on plant exploitation at MK 4 might help explain why MK 4 has the unique Series 2 lithic assemblage. They were using these tools for plant processing that did not require a handaxe, therefore justifying why the tools at MK 4 are different. Grass processing (such as grinding, crushing, cleaning, or scraping piths), sedge (cutting stalks and pith), and cracking nuts would not have required large cutting tools (see Dominguez- Rodrigo et al., 2001). Therefore, these simple tools, such as flakes, cores, and choppers at the MK 4 Site, would have been more suited to carrying out plant processing tasks. This aligns with the assumption that the small tool kit assemblage (Series 2) may represent a distinct assemblage or 'special economy' (Kaiser et al., 2010). These results,

however, are preliminary, and we cannot say explicitly that Series 2 stone tools were associated solely with plant exploitation.

#### *Grasses and their potential uses*

Globally, there are many ways in which grasses are currently consumed, often serving as a source of nutrition. As foods, grass seeds, and young pith/leaves can be consumed raw or ground to make cooking flour. Medicinal use of grasses includes charms, ritual cleansing, and treatments against intestinal parasites, ingestions, profuse menstruation, colds, bruises, dysmenorrhoea, and teething troubles (Gebashe et al., 2019, 2020; Hayes et al., 2018).

Contemporary hunter-gatherers and small-scale societies reveal a wealth of information on the consumption and use of grasses (Alt et al., 2022; Hayes et al., 2018). These societies collected grasses for matting and bedding, starting fires, making containers for storing and transporting food and goods, food medicine, and for other uses (Alt et al., 2022; Hayes et al., 2018). In most cases, grasses are collected roughly in proportion to their availability in the immediate vicinity of the sites. In Australia, ethnohistorical evidence shows the use of pounding tools by Australian Aboriginals to process the grass *Triodia spinifex* seeds for food, fiber, hafting adhesive, fire, figurines, medicine, nets, shelter, and other purposes (Hayes et al., 2018). As a medicine, a whole plant of *Triodia pungens* is crushed and mixed with termitaria (the clay casing of termite nests) and a little water; the resulting liquid is drunk to promote the health of mothers and their newborn babies (Hayes et al., 2018). Panicoid species such as *Cenchrus ciliaris* are commonly used as pain alleviation in South Africa and dysmenorrhea (relief for menstrual cramps) in South Africa (Gebashe et al., 2019). *C. ciliaris* is also used as diuretic drugs and emollients (balms) in Asian countries (Katewa & Jain, 2003). The panicoid species *Imperata cylindrica* is used to treat intestine diseases in South Africa and Malaysia (Gebashe et al., 2019, 2020). Chloridoid species include roots of *Eragrostis plana* used to treat menorrhagia, for more details see (Gebashe et al., 2019 p. 304).

As a source of nutrition, grasses provide about 40% of human nutritional needs, comprising most of the important food resources such as corn (*Zea mays*), sugarcane (*Saccharum officinarum*), pearl millet (*Cenchrus americanus*), rice (*Oryza sativa*), wheat (*Triticum aestivum*), and sorghum (*Sorghum bicolor*) (*Sorghum bicolor*) (Alt et al., 2022; Frisk et al., 2023). Aside from cultivated grasses, wild grasses are widely used as a food source globally, especially during dry periods. The utilization of wild grasses has been documented at various sites in Northern Africa during the 19<sup>th</sup> century, where grains of wild grasses formed a major part of their food and are still collected today, specifically in drought periods where their availability became critical for survival (Harlan, 1989a). In northern Africa, several Paniceae species named *acha*, *kasha*, or *kreb*, sold at the local markets (Harlan, 1989a; Le Moyne et al., 2023). *Kreb* includes a mixture of small Paniceae grains,

including *Panicum*, *Brachiaria*, and *Echinochloa* (such as *E. pyramidalis* *E. stagnina*) Klee et al. (2000). Another example comes from the southern coast of Iceland, where the seeds of lyme grass (*Elymus arenarius*) were used to make flour for cakes, porridge, and soup during the early 18th century (Gudmundsson, 1996).

#### *Evidence for grass consumption and use by ancient hominins*

The abundance of C<sub>4</sub> grass phytoliths in the artifact residues is not a surprise when considering the evolutionary history of our ancestors and their diet (Cerling et al., 2011; Henry et al., 2012; Paine et al., 2018; Ungar & Sponheimer, 2011). The hypothesis that our ancestors fed on C<sub>4</sub> plant-based foods in a wooded grassland savanna environment is not new (Cerling et al., 2011; Ungar & Sponheimer, 2011). Numerous studies have attempted to explain how C<sub>4</sub> plants (either grasses, sedge, or both) contributed to hominins' diet and how they were utilized (Alt et al., 2022; Paine et al., 2018; Peters & Vogel, 2005; van der Merwe et al., 2008). Grasses and sedges contain several parts that can be consumed as food, including tubers, rhizomes, and culms in sedges and seeds and leaves (including blade, collar, and sheath) in grasses (Gebashe et al., 2019; Hayes et al., 2021; Paine et al., 2018). There are various lines of evidence including stable carbon isotopes, dental microwear, hominin dental and facial anatomy, and microbotanical analysis on dental calculus demonstrating that hominins incorporated C<sub>4</sub> plants in their diets (Cerling et al., 2011; Levin et al., 2015; Ungar & Sponheimer, 2011).

Stable isotope analysis of tooth enamel tells us that from around 3.7 million years ago, some hominins were consuming C<sub>4</sub> plants (Alt et al., 2022; Cerling et al., 2011, 2013; Ungar & Sponheimer, 2011; van der Merwe et al., 2008). The consumption of C<sub>4</sub>-derived food increased through time, culminating with *Paranthropus boisei* (2.0-1.4 Ma), whose diet comprised mainly (75-80%) of C<sub>4</sub> foods (Alt et al., 2022; Cerling et al., 2011; Ungar & Sponheimer, 2011; van der Merwe et al., 2008). But it seems to be typical in *Australopithecus* and the early members of the genus *Homo*, *H. habilis* and *H. rudolfensis*, and later *Homo* (*H. erectus*) (Patterson et al., 2019; Schoeninger, 2014; Ungar & Sponheimer, 2011). Stable carbon isotopes clearly show that early hominins are consuming C<sub>4</sub> plants during the early Pleistocene (Alt et al., 2022; Patterson et al., 2019; Schoeninger, 2014; Ungar & Sponheimer, 2011). While there is a lack of evidence on what hominins were consuming during the Middle Pleistocene, they likely continued to do so. Microbotanical remains, starch, and phytoliths document grass consumption at Late Pleistocene sites. Starch granules recovered from chipped (core tools and scrapers) and ground stone tools from a Middle Stone Age site in Mozambique document evidence of grass seeds consumption by *early Homo sapiens* around 105,000 years ago (Mercader, 2009). In addition, Madella et al. (2002) report on the abundance of

inflorescence grass phytoliths at Imud cave (Israel) associated with the consumption and intentional collection of grass seeds by Neanderthals.

Phytolith remains also provide further direct evidence of C<sub>4</sub> (sedges and grass) and C<sub>3</sub> (trees, shrubs, and herbs) consumption by our earliest ancestors (Henry et al., 2012). Henry et al. (2012) document the feeding behavior of *Australopithecus sediba* (2 million years ago) specimens from South Africa by examining phytoliths in their dental calculus. Thirty-eight phytoliths were recovered from *A. sediba*, suggesting consumption of leaf, fruit, wood, or bark dicots, bulliform phytoliths from grasses, sedges, palms, or monocotyledonous plants, and other phytoliths from indeterminate plants (Henry et al., 2012). However, many dicot phytoliths indicate that *A. sediba* preferred to consume C<sub>3</sub> foods with a small percentage of the broadly available C<sub>4</sub> resources.

Underground storage organs (USOs) from sedges could have been a source of C<sub>4</sub> input for hominins since they would be unavailable to most herbivores (Peters & Vogel, 2005; van der Merwe et al., 2008). It has been proposed that hominins would have access to these nutrient-rich USOs using digging sticks, offering a new feeding niche for exploitation year-round (Peters & Vogel, 2005; van der Merwe et al., 2008). Among the edible sedge species are *Cyperus denudatus* and *Cyperus dives*, which grow in grasslands of floodplains, and *Cyperus papyrus*, a C<sub>4</sub> sedge that grows in shallow water. *Cyperus papyrus* grows up to 4 meters tall; the culms have a soft white rind about 0.5 cm thick, the interior is about 2 to 3 cm diameter, and is often chewed by people in South Africa (van der Merwe et al., 2008). The culm of *C. papyrus* is chewy and has a pleasant taste, while the rhizome is rich in starch and more fibrous. van der Merwe et al. (2008) report a *C. papyrus* nutritional analysis showing that papyrus rhizomes and culm have more carbohydrates than raw potato (*Solanum tuberosum*) tuber. Papyrus is considered a good source for a C<sub>4</sub> plant diet by *P. boisei* since they are abundant in near wetland areas, a preferred habitat for early hominins (van der Merwe et al., 2008).

Moreover, a study by Macho (2014) on the feeding behavior of yellow baboons (*Papio cynecephalus*) at Amboseli National Park in Kenya, provides insight into *P. boisei* diet on the edible bulbous tubers from sedges. Macho (2014) propose that like the yellow baboons, *P. boisei* would have eaten the sedge *Cyperus esculentus* by choosing the grass bulb at the base of the grass blade. According to Macho (2014) tiger nuts, sedge *Cyperus esculentus* and/or *Cyperus rotundus* are rich in starches, and are highly abrasive when consumed raw, and that would have explained the abrasion and wear and tear that is seen in *P. boisei* teeth.

Other cultural uses of grasses for making fire and bedding have been documented using microbotanical remains and micromorphological studies of sediments from cultural layers at several sites in the Middle Stone Age sites in Africa and Middle Paleolithic sites in Europe (Albert & Marean, 2012; Cabanes et al., 2010; Wadley et al., 2011). Phytolith analysis from the Pinnacle Point 13B

(South Africa) cave preserved a high abundance of C<sub>3</sub>, with very few C<sub>4</sub> grasses from burnt layers belonging to the leaves, stems, and inflorescences (Albert & Marean, 2012). A micromorphological study from the Middle Stone Age site Sibudu rock shelter (South Africa) shows successions of the hearth, dumped sediments, and bedding layers, gives a clear case of evidence for bedding areas where dicotyledonous, sedge, and grass phytoliths have been detected for making the bedding structures around 77,000 years ago (Wadley et al., 2011). Nadel et al. (2004) reported on a 23,000-year-old grass-bedding preparations using leaves and stems by fisher-hunter-gathers societies in the Upper Paleolithic site of Ohalo II site in Israel. Cabanes et al. (2010) reported the preparations of grass bedding by Neanderthals from a Middle Paleolithic site, Esquilleu Cave in Spain. Additional evidence comes from ethnographic data that shows modern hunter-gatherers, and horticultural societies who live in rock shelters use grasses to make bedding (Galanidou, 1997, 2000).

### **Conclusions**

This study establishes a direct connection between the stone tools and the plant taxa species available at the site. The durability of phytoliths allows the possibility of recovering information from older sites where starch and macrobotanical residues are no longer preserved (Dominguez-Rodrigo et al., 2001; Kealhofer et al., 1999; Pearsall, 2016; Rossouw & Scott, 2011; Stromberg, 2004). The absence of phytoliths from the sediments beneath the stone tools demonstrates that phytoliths were not introduced onto the surface of stone tools because of post-depositional processes. The phytoliths adhering to tools provide information on the types of plants used by early hominins at the Manyara Beds during the early Middle Pleistocene period (0.78-0.633 million years ago). It would be an interesting question to pursue in future research, with more detailed studies and quantitative analysis to understand the patterns of residue distribution in the artifacts and possibly use wear analysis to collaborate these results.

A variety of phytoliths are recovered but are dominated by grass phytoliths. This is a novel finding that, while initially surprising, fits with much other paleodietary research on early hominins. Moreover, the staple foods that many humans consume come from grasses. The evolution of our earliest ancestors is said to have a strong correlation with the emergence of grasslands during the Miocene period (Dominguez- Rodrigo et al., 2001; Peppe et al., 2023). In addition, ethnohistorical and ethnographic evidence shows how modern societies incorporate wild grasses into their diet, use them for medicine, make shelters and bedding, extract fibers, cordage, and other purposes.



## Literature Cited

- Albert, R. M., & Bamford, M. K. (2012). Vegetation during UMBI and deposition of Tuff IF at Olduvai Gorge, Tanzania (ca. 1.8 Ma) based on phytoliths and plant remains. *Journal of Human Evolution*, 63(2), 342–350. <https://doi.org/10.1016/j.jhevol.2011.05.010>
- Albert, R. M., Bamford, M. K., & Cabanes, D. (2009). Palaeoecological significance of palms at Olduvai Gorge, Tanzania, based on phytolith remains. *Quaternary International*, 193(1–2), 41–48. <https://doi.org/10.1016/j.quaint.2007.06.008>
- Albert, R. M., & Marean, C. W. (2012). The Exploitation of Plant Resources by Early *Homo sapiens*: The Phytolith Record from Pinnacle Point 13B Cave, South Africa: phytoliths from Pinnacle Point 13B cave, South Africa. *Geoarchaeology*, 27(4), 363–384. <https://doi.org/10.1002/gea.21413>
- Alt, K. W., Al-Ahmad, A., & Woelber, J. P. (2022). Nutrition and Health in Human Evolution—Past to Present. *Nutrients*, 14(17), 3594. <https://doi.org/10.3390/nu14173594>
- Bachofer, F., Quénéhervé, G., Hertler, C., Giemsch, L., Hochschild, V., & Maerker, M. (2018). Paleoenvironmental Research in the Semiarid Lake Manyara Area, Northern Tanzania: A Synopsis. In C. Siart, M. Forbriger, & O. Bubenzer (Eds.), *Digital Geoarchaeology* (pp. 123–138). Springer International Publishing. [https://doi.org/10.1007/978-3-319-25316-9\\_8](https://doi.org/10.1007/978-3-319-25316-9_8)
- Barboni, D., & Bremond, L. (2009). Phytoliths of East African grasses: An assessment of their environmental and taxonomic significance based on floristic data. *Review of Palaeobotany and Palynology*, 158(1–2), 29–41. <https://doi.org/10.1016/j.revpalbo.2009.07.002>
- Barton, H., Torrence, R., & Fullagar, R. (1998). Clues to Stone Tool Function Re-examined: Comparing Starch Grain Frequencies on Used and Unused Obsidian Artefacts. *Journal of Archaeological Science*, 25(12), 1231–1238. <https://doi.org/10.1006/jasc.1998.0300>
- Balme, J., & Paterson, A. (Eds.). (2006). *Archaeology in practice: A student guide to archaeological analyses* (1. publ). Blackwell.
- Briuer, F. L. (1976). New Clues to Stone Tool Function: Plant and Animal Residues. *American Antiquity*, 41(4), 478–484. <https://doi.org/10.2307/279013>
- Cabanes, D., Mallol, C., Expósito, I., & Baena, J. (2010). Phytolith evidence for hearths and beds in the late Mousterian occupations of Esquilleu cave (Cantabria, Spain). *Journal of Archaeological Science*, 37(11), 2947–2957. <https://doi.org/10.1016/j.jas.2010.07.010>
- Cerling, T. E., Manthi, F. K., Mbua, E. N., Leakey, L. N., Leakey, M. G., Leakey, R. E., Brown, F. H., Grine, F. E., Hart, J. A., Kaleme, P., Roche, H., Uno, K. T., & Wood, B. A. (2013). Stable isotope-based diet reconstructions of Turkana Basin hominins. *Proceedings of the National Academy of Sciences*, 110(26), 10501–10506. <https://doi.org/10.1073/pnas.1222568110>

- Cerling, T. E., Mbua, E., Kirera, F. M., Manthi, F. K., Grine, F. E., Leakey, M. G., Sponheimer, M., & Uno, K. T. (2011). Diet of *Paranthropus boisei* in the early Pleistocene of East Africa. *Proceedings of the National Academy of Sciences*, 108(23), 9337–9341. <https://doi.org/10.1073/pnas.1104627108>
- Chandler-Ezell, K., Pearsall, D. M., & Zeidler, J. A. (2006). Root and Tuber Phytoliths and Starch Grains Document Manioc ( *Manihot Esculenta* ), Arrowroot ( *Maranta Arundinacea* ), and Llerén ( *Calathea sp.*) at the Real Alto Site, Ecuador. *Economic Botany*, 60(2), 103–120. [https://doi.org/10.1663/0013-0001\(2006\)60\[103:RATPAS\]2.0.CO;2](https://doi.org/10.1663/0013-0001(2006)60[103:RATPAS]2.0.CO;2)
- Chazan, M. (2013). Butchering with small tools: The implications of the Evron Quarry assemblage for the behaviour of *Homo erectus*. *Antiquity*, 87(336), 350–367. <https://doi.org/10.1017/S0003598X00048997>
- Collura, L. V., & Neumann, K. (2017). Wood and bark phytoliths of West African woody plants. *Quaternary International*, 434, 142–159. <https://doi.org/10.1016/j.quaint.2015.12.070>
- Crifò, C., & Strömberg, C. A. E. (2021). Spatial patterns of soil phytoliths in a wet vs. dry neotropical forest: Implications for paleoecology. *Palaeogeography, Palaeoclimatology, Palaeoecology*, 562, 110100. <https://doi.org/10.1016/j.palaeo.2020.110100>
- Croft, S. (2021). *Lithic residue analysis: A review and guide to techniques*. BAR Publishing.
- Dominguez- Rodrigo, M., Serrallonga, J., Juan-Tresserras, J., Alcalá, L., & Luque, L. (2001). Woodworking activities by early humans: A plant residue analysis on Acheulian stone tools from Peninj (Tanzania). *Journal of Human Evolution*, 40(4), 289–299. <https://doi.org/10.1006/jhev.2000.0466>
- Eichhorn, B., Neumann, K., & Garnier, A. (2010). Seed phytoliths in West African Commelinaceae and their potential for palaeoecological studies. *Palaeogeography, Palaeoclimatology, Palaeoecology*, 298(3–4), 300–310. <https://doi.org/10.1016/j.palaeo.2010.10.004>
- Esteban, I., Marean, C. W., Fisher, E. C., Karkanas, P., Cabanes, D., & Albert, R. M. (2018). Phytoliths as an indicator of early modern humans plant gathering strategies, fire fuel and site occupation intensity during the Middle Stone Age at Pinnacle Point 5-6 (south coast, South Africa). *PLOS ONE*, 13(6), e0198558. <https://doi.org/10.1371/journal.pone.0198558>
- Field, J., Summerhayes, G., Luu, S., Coster, A., Ford, A., Mandui, H., Fullagar, R., Hayes, E., Leavesley, M., Lovave, M., & Kealhofer, L. (2020). Functional studies of flaked and ground stone artefacts reveal starchy tree nut and root exploitation in mid-Holocene highland New Guinea. *The Holocene*, 30(9), 1360–1374. <https://doi.org/10.1177/0959683620919983>

- Frisk, C. A., Adams-Groom, B., & Smith, M. (2023). Isolating the species element in grass pollen allergy: A review. *Science of The Total Environment*, 883, 163661. <https://doi.org/10.1016/j.scitotenv.2023.163661>
- Frost, S. R., Saanane, C., Starkovich, B. M., Schwartz, H., Schrenk, F., & Harvati, K. (2017). New cranium of the large cercopithecoid primate *Theropithecus oswaldi leakeyi* (Hopwood, 1934) from the paleoanthropological site of Makuyuni, Tanzania. *Journal of Human Evolution*, 109, 46–56. <https://doi.org/10.1016/j.jhevol.2017.05.007>
- Frost, S. R., Schwartz, H. L., & Giemsch, L. (2012). Refined age estimates and paleoanthropological investigation of the Manyara Beds, Tanzania. *Journal of Anthropological Sciences*, 90, 1–12. <https://doi.org/10.4436/jass.90001>
- Fullagar, R., Field, J., Denham, T., & Lentfer, C. (2006). Early and mid Holocene tool-use and processing of taro (*Colocasia esculenta*), yam (*Dioscorea* sp.) and other plants at Kuk Swamp in the highlands of Papua New Guinea. *Journal of Archaeological Science*, 33(5), 595–614. <https://doi.org/10.1016/j.jas.2005.07.020>
- Galanidou, N. (1997). *“Home is where the hearth is”: The spatial organisation of the Upper Paleolithic rockshelter occupations at Klithi and Kastritsa in Northwest Greece*. BAR.
- Galanidou, N. (2000). Patterns in Caves: Foragers, Horticulturists, and the Use of Space. *Journal of Anthropological Archaeology*, 19(3), 243–275. <https://doi.org/10.1006/jaar.1999.0362>
- Gebashe, F., Aremu, A. O., Finnie, J. F., & Van Staden, J. (2019). Grasses in South African traditional medicine: A review of their biological activities and phytochemical content. *South African Journal of Botany*, 122, 301–329. <https://doi.org/10.1016/j.sajb.2018.10.012>
- Gebashe, F., Aremu, A. O., Gruz, J., Finnie, J. F., & Van Staden, J. (2020). Phytochemical Profiles and Antioxidant Activity of Grasses Used in South African Traditional Medicine. *Plants*, 9(3), 371. <https://doi.org/10.3390/plants9030371>
- Giemsch, L., Hertler, C., Märker, M., Quénéhervé, G., Saanane, C., & Schrenk, F. (2018). Acheulean Sites at Makuyuni (Lake Manyara, Tanzania): Results of Archaeological Fieldwork and Classification of the Lithic Assemblages. *African Archaeological Review*, 35(1), 87–106. <https://doi.org/10.1007/s10437-018-9284-4>
- Gudmundsson, G. (1996). Gathering and processing of lyme-grass (*Elymus arenarius*) in Iceland: An ethnohistorical account. *Vegetation History and Archaeobotany*, 5(1/2), 13–23.
- Guibert-Cardin, J., Turloukis, V., Thompson, N., Panagopoulou, E., Harvati, K., Nicoud, E., & Beyries, S. (2022). The function of small tools in Europe during the Middle Pleistocene: The case of Marathousa 1 (Megalopolis, Greece). *Journal of Lithic Studies*, 9(1). <https://doi.org/10.2218/jls.5553>

- Harlan, J. R. (1989a). Wild-grass seed harvesting in the Sahara and sub-Saharan of Africa. In D. R. Harris & G. C. Hillman (Eds.), *Foraging and farming: The evolution of plant exploitation*. (pp. 79–98). Routledge.
- Hart, T. C. (2011). Evaluating the usefulness of phytoliths and starch grains found on survey artifacts. *Journal of Archaeological Science*, 38(12), 3244–3253.  
<https://doi.org/10.1016/j.jas.2011.06.034>
- Hayes, E., Fullagar, R., Kamminga, J., Prinsloo, L. C., Bordes, L., Sutikna, T., Tocheri, M. W., Wahyu Saptomo, E., Jatmiko, & Roberts, R. G. (2021). Use-polished stone flakes from Liang Bua, Indonesia: Implications for plant processing and fibre-craft in the Late Pleistocene. *Journal of Archaeological Science: Reports*, 40, 103199. <https://doi.org/10.1016/j.jasrep.2021.103199>
- Hayes, E., Fullagar, R., Mulvaney, K., & Connell, K. (2018). Food or fibre-craft? Grinding stones and Aboriginal use of *Triodia* grass (*spinifex*). *Quaternary International*, 468, 271–283.  
<https://doi.org/10.1016/j.quaint.2016.08.010>
- Henry, A. G., Ungar, P. S., Passey, B. H., Sponheimer, M., Rossouw, L., Bamford, M., Sandberg, P., De Ruiter, D. J., & Berger, L. (2012). The diet of *Australopithecus sediba*. *Nature*, 487(7405), 90–93. <https://doi.org/10.1038/nature11185>
- International Committee for Phytolith Taxonomy (ICPT), Neumann, K., Strömberg, C. A. E., Ball, T., Albert, R. M., Vrydaghs, L., & Cummings, L. S. (2019). International Code for Phytolith Nomenclature (ICPN) 2.0. *Annals of Botany*, 124(2), 189–199.  
<https://doi.org/10.1093/aob/mcz064>
- Kaiser, T. M., Seiffert, C. C., Fiedler, L., Schwartz, H. L., Frost, S. R., & Nelson, S. V. (2010). Makuyuni, a new lower Palaeolithic hominid site in Tanzania. *Mitteilungen Hamburgisches Zoologischen Museum Institut*, 106, 69–110.
- Katewa, S. S., & Jain, A. (2003). Aromatic and medicinal grasses of Aravalli hills of Rajasthan. *Ethnomedicine and Pharmacognosy*, 11, 7–57.
- Kealhofer, L., Torrence, R., & Fullagar, R. (1999). Integrating Phytoliths within Use-Wear/Residue Studies of Stone Tools. *Journal of Archaeological Science*, 26(5), 527–546.  
<https://doi.org/10.1006/jasc.1998.0332>
- Klee, M., Zach, B., & Neumann, K. (2000). Four thousand years of plant exploitation in the Chad Basin of northeast Nigeria I: The archaeobotany of Kursakata. *Vegetation History and Archaeobotany*, 9(4), 223–237. <https://doi.org/10.1007/BF01294637>
- Kooyman, B., Newman, M. E., & Ceri, H. (1992). Verifying the Reliability of Blood Residue Analysis on Archaeological Tools. *Journal of Archaeological Science*, 19, 265–269.

- Le Moyne, C., Fuller, D. Q., & Crowther, A. (2023). Microbotanical signatures of kreb: Differentiating inflorescence phytoliths from northern African wild grasses. *Vegetation History and Archaeobotany*, 32(1), 49–63. <https://doi.org/10.1007/s00334-022-00880-3>
- Levin, N. E., Haile-Selassie, Y., Frost, S. R., & Saylor, B. Z. (2015). Dietary change among hominins and cercopithecids in Ethiopia during the early Pliocene. *Proceedings of the National Academy of Sciences*, 112(40), 12304–12309. <https://doi.org/10.1073/pnas.1424982112>
- Macho, G. A. (2014). Baboon Feeding Ecology Informs the Dietary Niche of Paranthropus boisei. *PLoS ONE*, 9(1), e84942. <https://doi.org/10.1371/journal.pone.0084942>
- Madella, M., Jones, M. K., Goldberg, P., Goren, Y., & Hovers, E. (2002). The Exploitation of Plant Resources by Neanderthals in Amud Cave (Israel): The Evidence from Phytolith Studies. *Journal of Archaeological Science*, 29(7), 703–719. <https://doi.org/10.1006/jasc.2001.0743>
- Mercader, J. (2009). Mozambican Grass Seed Consumption During the Middle Stone Age. *Science*, 326(5960), 1680–1683. <https://doi.org/10.1126/science.1173966>
- Mulholland, S. C. (1989). Phytolith shape frequencies in North Dakota grasses: A comparison to general patterns. *Journal of Archaeological Science*, 16(5), 489–511. [https://doi.org/10.1016/0305-4403\(89\)90070-8](https://doi.org/10.1016/0305-4403(89)90070-8)
- Murungi, M. L., & Bamford, M. K. (2020). Revised taxonomic interpretations of Cyperaceae phytoliths for (paleo)botanical studies with some notes on terminology. *Review of Palaeobotany and Palynology*, 275, 104189. <https://doi.org/10.1016/j.revpalbo.2020.104189>
- Nadel, D., Weiss, E., Simchoni, O., Tsatskin, A., Danin, A., & Kislev, M. (2004). Stone Age hut in Israel yields world's oldest evidence of bedding. *Proceedings of the National Academy of Sciences*, 101(17), 6821–6826. <https://doi.org/10.1073/pnas.0308557101>
- Newman, M. E., Yohe, R. M., Ceri, H., & Sutton, M. Q. (1993). Immunological protein residue analysis of non-lithic archaeological materials. *Journal of Archaeological Science*, 20, 93–100.
- Newman, M., & Julig, P. (1989). The identification of protein residues on lithic artifacts from a stratified boreal forest site. *Canadian Journal of Archaeology/Journal Canadien d'Archeologie*, 119–132.
- Paine, O. C. C., Koppa, A., Henry, A. G., Leichliter, J. N., Codron, D., Codron, J., Lambert, J. E., & Sponheimer, M. (2018). Grass leaves as potential hominin dietary resources. *Journal of Human Evolution*, 117, 44–52. <https://doi.org/10.1016/j.jhevol.2017.10.013>
- Patterson, D. B., Braun, D. R., Allen, K., Barr, W. A., Behrensmeyer, A. K., Biernat, M., Lehmann, S. B., Maddox, T., Manthi, F. K., Merritt, S. R., Morris, S. E., O'Brien, K., Reeves, J. S., Wood, B. A., & Bobe, R. (2019). Comparative isotopic evidence from East Turkana supports a dietary shift

- within the genus *Homo*. *Nature Ecology & Evolution*, 3(7), 1048–1056.  
<https://doi.org/10.1038/s41559-019-0916-0>
- Pearsall, D. M. (2016). *Paleoethnobotany*. Routledge. <https://doi.org/10.4324/9781315423098>
- Pearsall, D. M., Chandler-Ezell, K., & Zeidler, J. A. (2004). Maize in ancient Ecuador: Results of residue analysis of stone tools from the Real Alto site. *Journal of Archaeological Science*, 31(4), 423–442. <https://doi.org/10.1016/j.jas.2003.09.010>
- Peppe, D. J., Cote, S. M., Deino, A. L., Fox, D. L., Kingston, J. D., Kinyanjui, R. N., Lukens, W. E., MacLatchy, L. M., Novello, A., Strömberg, C. A. E., Driese, S. G., Garrett, N. D., Hillis, K. R., Jacobs, B. F., Jenkins, K. E. H., Kityo, R. M., Lehmann, T., Manthi, F. K., Mbua, E. N., ... McNulty, K. P. (2023). Oldest evidence of abundant C<sub>4</sub> grasses and habitat heterogeneity in eastern Africa. *Science*, 380(6641), 173–177. <https://doi.org/10.1126/science.abq2834>
- Peters, C. R., & Vogel, J. C. (2005). Africa's wild C<sub>4</sub> plant foods and possible early hominid diets. *Journal of Human Evolution*, 48(3), 219–236. <https://doi.org/10.1016/j.jhevol.2004.11.003>
- Piperno, D. R. (2006). *Phytoliths: A comprehensive guide for archaeologists and paleoecologists*. AltaMira Press.
- Renfrew, C., & Bahn, P. G. (2000). *Archaeology: Theories, methods and practice with over 600 illustrations* (3rd ed). Thames & Hudson.
- Rossouw, L., & Scott, L. (2011). Phytoliths and Pollen, the Microscopic Plant Remains in Pliocene Volcanic Sediments Around Laetoli, Tanzania. In T. Harrison (Ed.), *Paleontology and Geology of Laetoli: Human Evolution in Context* (pp. 201–215). Springer Netherlands.  
[https://doi.org/10.1007/978-90-481-9956-3\\_9](https://doi.org/10.1007/978-90-481-9956-3_9)
- Schoeninger, M. J. (2014). Stable Isotope Analyses and the Evolution of Human Diets. *Annual Review of Anthropology*, 43(1), 413–430. <https://doi.org/10.1146/annurev-anthro-102313-025935>
- Schwartz, H., Renne, P. R., Morgan, L. E., Wildgoose, M. M., Lippert, P. C., Frost, S. R., Harvati, K., Schrenk, F., & Saanane, C. (2012). Geochronology of the Manyara Beds, northern Tanzania: New tephrostratigraphy, magnetostratigraphy and <sup>40</sup>Ar/<sup>39</sup>Ar ages. *Quaternary Geochronology*, 7, 48–66. <https://doi.org/10.1016/j.quageo.2011.09.002>
- Semenov, S. A., & Semenov, S. A. (1970). *Prehistoric technology: An experimental study of the oldest tools and artefacts from traces of manufacture and wear*. Cory, Adams & Mackay.
- Shea, J. J. (2013). *Stone Tools in the Paleolithic and Neolithic Near East: A Guide* (1st ed.). Cambridge University Press. <https://doi.org/10.1017/CBO9781139026314>
- Stevanato, M., Rasbold, G. G., Parolin, M., Domingos Luz, L., Lo, E., Weber, P., Trevisan, R., & Galeazzi Caxambu, M. (2019). New characteristics of the papillae phytolith morphotype recovered

- from eleven genera of cyperaceae. *Flora*, 253, 49–55.  
<https://doi.org/10.1016/j.flora.2019.03.012>
- Strömberg, C. A. E. (2003). *The Origin and Spread of Grass-dominated Ecosystem during the Tertiary of North America and How it Relates to Evolution of Hypsodont in Equids*. [PhD thesis]. University of California.
- Strömberg, C. A. E. (2004). Using phytolith assemblages to reconstruct the origin and spread of grass-dominated habitats in the great plains of North America during the late Eocene to early Miocene. *Palaeogeography, Palaeoclimatology, Palaeoecology*, 207(3–4), 239–275.  
<https://doi.org/10.1016/j.palaeo.2003.09.028>
- Strömberg, C. A. E., Dunn, R. E., Crifò, C., & Harris, E. B. (2018). Phytoliths in Paleoecology: Analytical Considerations, Current Use, and Future Directions. In D. A. Croft, D. F. Su, & S. W. Simpson (Eds.), *Methods in Paleoecology* (pp. 235–287). Springer International Publishing.  
[https://doi.org/10.1007/978-3-319-94265-0\\_12](https://doi.org/10.1007/978-3-319-94265-0_12)
- Ungar, P. S., & Sponheimer, M. (2011). The Diets of Early Hominins. *Science*, 334(6053), 190–193.  
<https://doi.org/10.1126/science.1207701>
- van der Merwe, N., J., Masao, F. T., & Bamford, M. K. (2008). Isotopic evidence for contrasting diets of early hominins *Homo habilis* and *Australopithecus boisei* of Tanzania. *South African Journal of Science*, 108, 153–155.
- Wadley, L., Sievers, C., Bamford, M., Goldberg, P., Berna, F., & Miller, C. (2011). Middle Stone Age Bedding Construction and Settlement Patterns at Sibudu, South Africa. *Science*, 334(6061), 1388–1391. <https://doi.org/10.1126/science.1213317>
- Wolf, N. D., Nelson, S. V, Schwartz, H. L, Semprebon, G. M, Kaiser, T. M, & Bernor, R. L. (2010). Taxonomy and paleoecology of the Pleistocene Equidae from Makuyuni, northern Tanzania. *Palaeodiversity*, 3, 249–269.
- Yost, C. L., Jackson, L. J., Stone, J. R., & Cohen, A. S. (2018). Subdecadal phytolith and charcoal records from Lake Malawi, East Africa imply minimal effects on human evolution from the ~74 ka Toba supereruption. *Journal of Human Evolution*, 116, 75–94.  
<https://doi.org/10.1016/j.jhevol.2017.11.005>
- Zurro, D. (2018). One, two, three phytoliths: Assessing the minimum phytolith sum for archaeological studies. *Archaeological and Anthropological Sciences*, 10(7), 1673–1691.  
<https://doi.org/10.1007/s12520-017-0479-4>
- Zurro, D., & Gaddekar, C. (2023). Is It Worth It? A Review of Plant Residue Analysis on Knapped Lithic Artifacts. *Lithic Technology*, 1–18. <https://doi.org/10.1080/01977261.2023.2188343>

## Chapter 5: Conclusions and Future Research

The main objective of this study was to understand and interpret phytoliths recovered from the early Middle Pleistocene Manyara Beds and relate them to early hominin habitat preferences and the environment. To achieve the main objective, the research presented and discussed in this thesis focused on answering three broad questions, each corresponding to a chapter in the dissertation:

1. What phytoliths are preserved in the modern plants and soils near the Manyara Beds?
2. How did vegetation cover change through time and space in the lower Manyara Beds? What kind of microhabitats were hominins using in the Lake Manyara region during the Middle Pleistocene?
3. What phytoliths are preserved on stone tools?

### Conclusions

This study utilized a generalized morphotype scheme to establish past environmental records, which considers all phytolith morphotypes and size fractions (Strömberg, 2004). The first question was met by creating a reference collection of 21 plants and 25 composite surface soil samples collected from five sites. An investigation of modern phytoliths assemblages from plants and surface soils is among the preconditions for interpreting ancient phytoliths assemblages (Eichhorn et al., 2010; Piperno, 2006; Strömberg, 2004).

As a part of the larger study that aims at reconstructing past environment, Chapter 2 of this thesis details the phytolith assemblages from the *Acacia-Commiphora* ecosystem surrounding the Manyara Beds. This study is significant because it shows the pattern of phytolith production for common plants in this ecosystem and their signature in surface soils. A broadly similar environment is said to exist during the early Middle Pleistocene (see Kaiser et al., 2010). In addition, the *Acacia-Commiphora* vegetation is thought to occur even earlier in this region, related to the evolution of *Australopithecus* around 3.7-3.5 Mya and genus *Homo* around 1.7-1.5 Mya (Barboni et al., 2019; Bonnefille, 2010; Dominguez-Rodrigo et al., 2001). This study documents phytolith production from several new species from the *Acacia-Commiphora* ecosystem. Using Strömberg's (2003) standardized classification and interpretive scheme, this study has shown that the phytoliths for *Commiphora* are polyhedral epidermal cells and *Acacia* spp. in this study produce faceted blocky. However, the soil assemblage does not preserve the polyhedral epidermal cells; therefore, the soils does not reflect some of the important plants growing in this ecosystem. Moreover, morphotypes representing trees, shrubs, and herbs are poorly reflected in the surface soils of the Manyara Beds. It is GSSC phytoliths, especially bilobates representing other PACMADs, saddles, and rondels that



represent chloridoids that are the most common morphotypes found in the soils of the *Acacia-Commiphora* vegetation.

The second question was addressed by examining phytolith assemblages from the ancient sediments of the Manyara Beds. Chapter 3 provides the first detailed comparisons of the habitats present at archaeological and non-archaeological sites in this area. This is critical because it gives important insight into the use of plant resources, habitat preferences, and the environmental context the early hominins at the Manyara Beds were exploiting. At the archaeological site MK 4, phytoliths are linked to cultural layer 3 (see Chapter 4) showing evidence of hominin occupation (Kaiser et al., 2010; Ring et al., 2005; Schwartz et al., 2012). The detailed paleoenvironmental reconstruction of the site from faunal composition and stable isotopes suggests the occurrence of open habitat environments consisting of C<sub>4</sub> dominated grasslands. The phytolith assemblages from all archaeological and non-archaeological sites confirms the presence of C<sub>4</sub> grasses, but other vegetation types were also available, and their presence could have not been detected by previous methods.

Each site showed vegetation changes through time. The most interesting results come from archaeological site MK 4, where there is evidence of a change between closed and open woodlands, and palm is the most dominant type of vegetation that represents forests. Palm and other arboreal taxa would have played an important role in attracting hominins by offering shade during tool making, and nuts would have been a source of food. Palms, members of the Commelinaceae, aquatic monocots, and sedges indicate the presence of a wetland environment, which would have included a permanent water source at MK 4. The grass communities show evidence of shifting from warm-wet to warm-dry conditions. In addition, the forest area from MK 4 would likely offer a refuge (home base) for hominins to avoid predators and would have offered the early hominins plenty of food resources, shade where they would have stayed and socialized while engaging in tool making (see Blumenschine & Masao, 1991; Blumenschine & Peters, 1998). These varied ecological niches at MK 4 explains why hominins preferred the site and avoided the non-archaeological sites, which are dominated by grassland with very few scattered trees, where competition for scavenging resources, for instance, will be high in open areas with other scavengers like vultures and hyenas (Blumenschine & Peters, 1998).

The third objective was addressed by examining 106 phytolith residues extracted from sediments adhering to the stone tools and comparing them to those collected beneath them. This is the first attempt to try to recover phytoliths from stone tools at the Manyara Beds to understand early hominins' exploitation of plant resources. The sediments beneath stone tools did not yield any phytoliths, strongly indicating that the phytoliths adhering to the stone tools were deposited during

tool use, not post-depositionally. From the 106 residues examined, only 10 tools yielded phytoliths. The recovered phytoliths indicate the exploitation of grasses, sedges, palms, woody and herbaceous dicots, and herbaceous monocots.

### **Future Research**

In future, it would be desirable to include a larger modern plant sample and characterize phytoliths assemblages from different microhabitats (e.g., riverine, marshlands, etc.) of the *Acacia-Commiphora* ecosystem, with the assumption that they will have a high chance of appearing in the ancient assemblage. It is important to sample the whole middle Pleistocene section of the Manyara Beds to understand the end of the Acheulean Industry at the Manyara Beds. Unfortunately, Middle Stone Age tools occur at the Manyara Beds, but most are found on the surface; there is no available report of the discovery of MSA tools in stratigraphic context.

The exact timing of the onset of the Middle Stone Age (MSA) in Africa is hard to establish. For instance, at some sites such as Kapthurin Formation (Kenya) and Kathu Pan 1 (South Africa), early Middle Stone Age tools occur in association with Acheulean tools around 500 Kya (Wilkins, 2013; Johnson & McBrearty, 2012; McBrearty & Brooks, 2000; Tryon et al., 2006; Wilkins et al., 2014). Future research at the Manyara Beds should attempt to document MSA tools in a stratigraphic context by looking at sites beyond the vicinity of the Makuyuni village. Also, there is a need for detailed characterization of the Series 2 lithic industry at MK4. Finally, while this study focused on the earlier part of the Manyara Beds, there are younger deposits (early part 0.78-633Kya; middle part 633-400; Later 400-200 Kya). Study of the very youngest sequences at Manyara could help to better understand the ecological landscape associated with the emergence of our species, *Homo sapiens*.

## Literature Cited

- Barboni, D., Ashley, G. M., Bourel, B., Arráiz, H., & Mazur, J.-C. (2019). Springs, palm groves, and the record of early hominins in Africa. *Review of Palaeobotany and Palynology*, 266, 23–41. <https://doi.org/10.1016/j.revpalbo.2019.03.004>
- Blumenschine, R. J., & Masao, F. T. (1991). Living sites at Olduvai Gorge, Tanzania? Preliminary landscape archaeology results in the basal Bed II lake margin zone. *Journal of Human Evolution*, 21(6), 451–462. [https://doi.org/10.1016/0047-2484\(91\)90095-D](https://doi.org/10.1016/0047-2484(91)90095-D)
- Blumenschine, R. J., & Peters, C. R. (1998). Archaeological predictions for hominid land use in the paleo-Olduvai Basin, Tanzania, during lowermost Bed II times. *Journal of Human Evolution*, 34(6), 565–608. <https://doi.org/10.1006/jhev.1998.0216>
- Bonnefille, R. (2010). Cenozoic vegetation, climate changes and hominid evolution in tropical Africa. *Global and Planetary Change*, 72(4), 390–411. <https://doi.org/10.1016/j.gloplacha.2010.01.015>
- Dominguez- Rodrigo, M., Serrallonga, J., Juan-Tresserras, J., Alcalá, L., & Luque, L. (2001). Woodworking activities by early humans: A plant residue analysis on Acheulian stone tools from Peninj (Tanzania). *Journal of Human Evolution*, 40(4), 289–299. <https://doi.org/10.1006/jhev.2000.0466>
- Eichhorn, B., Neumann, K., & Garnier, A. (2010). Seed phytoliths in West African Commelinaceae and their potential for palaeoecological studies. *Palaeogeography, Palaeoclimatology, Palaeoecology*, 298(3–4), 300–310. <https://doi.org/10.1016/j.palaeo.2010.10.004>
- Jayne, W. (2013). *Technological Change in the Early Middle Pleistocene: The Onset of the Middle Stone Age at Kathu Pan 1, Northern Cape, South Africa* [Degree of Doctor of Philosophy]. University of Toronto.
- Johnson, C. R., & McBrearty, S. (2012). Archaeology of Middle Pleistocene lacustrine and spring paleoenvironments in the Kapthurin Formation, Kenya. *Journal of Anthropological Archaeology*, 31(4), 485–499. <https://doi.org/10.1016/j.jaa.2012.05.001>
- Kaiser, T.M., Seiffert, C. C., Fiedler, L., Schwartz, H. L., Frost, S. R., & Nelson, S. V. (2010). Makuyuni, a new lower Palaeolithic hominid site in Tanzania. *Mitteilungen Hamburgisches Zoolischen Museum Institut*, 106, 69–110.
- McBrearty, S., & Brooks, A. S. (2000). The revolution that wasn't: A new interpretation of the origin of modern human behavior. *Journal of Human Evolution*, 39(5), 453–563. <https://doi.org/10.1006/jhev.2000.0435>
- Piperno, D. R. (2006). *Phytoliths: A comprehensive guide for archaeologists and paleoecologists*. AltaMira Press.

- Ring, U., Schwartz, H. L., Bromage, T. G., & Sanaane, C. (2005). Kinematic and sedimentological evolution of the Manyara Rift in northern Tanzania, East Africa. *Geological Magazine*, 142(4), 355–368. <https://doi.org/10.1017/S0016756805000841>
- Schwartz, H., Renne, P. R., Morgan, L. E., Wildgoose, M. M., Lippert, P. C., Frost, S. R., Harvati, K., Schrenk, F., & Saanane, C. (2012). Geochronology of the Manyara Beds, northern Tanzania: New tepthrostratigraphy, magnetostratigraphy and  $^{40}\text{Ar}/^{39}\text{Ar}$  ages. *Quaternary Geochronology*, 7, 48–66. <https://doi.org/10.1016/j.quageo.2011.09.002>
- Strömberg, C. A. E. (2003). *The Origin and Spread of Grass-dominated Ecosystem during the Tertiary of North America and How it Relates to Evolution of Hypsodont in Equids*. [PhD thesis]. University of California.
- Strömberg, C. A. E. (2004). Using phytolith assemblages to reconstruct the origin and spread of grass-dominated habitats in the great plains of North America during the late Eocene to early Miocene. *Palaeogeography, Palaeoclimatology, Palaeoecology*, 207(3–4), 239–275. <https://doi.org/10.1016/j.palaeo.2003.09.028>
- Tryon, C. A., McBrearty, S., & Texier, P.-J. (2006). Levallois Lithic Technology from the Kapthurin Formation, Kenya: Acheulian Origin and Middle Stone Age Diversity. *African Archaeological Review*, 22(4), 199–229. <https://doi.org/10.1007/s10437-006-9002-5>
- Wilkins, J., Schoville, B. J., & Brown, K. S. (2014). An Experimental Investigation of the Functional Hypothesis and Evolutionary Advantage of Stone-Tipped Spears. *PLoS ONE*, 9(8), e104514. <https://doi.org/10.1371/journal.pone.0104514>

## **Appendices**

### **Appendix A: An Excel spreadsheet contains all the raw data for the thesis.**

The following data tables are included:

- a. A1: Phytolith count data from modern plant samples
- b. A2: Phytolith count data from modern soil samples
- c. A3: Phytolith count data from ancient sediments
- d. A4: Phytolith count data from stone tools
- e. A5: Phytolith count data from control sediment samples

## Appendix B: Phytolith morphotype descriptions

Table 1: Phytolith morphotypes used in this study followed Strömberg's (2003) scheme and full morphotype descriptions can be found therein. A small modification was made to the category “Anisopolar Prismatic Domed cylinder”, as indicated below.

Morphotype group	Morphotype description	Morphotype code	Indicative of/function group
Saddles and saddle-like morphotypes (SA)	True saddle (Squat & Tall)	SA-1	CHLORIDOID
Conical rondels (CO)	Crescentic conical rondel	CO-5	
Crosses (CR)	Matchbox body with ears	CR4-10	
Bilobates (BI)	Symmetry B bilobate (simple lobate)	BI-5	PACMADs
	Symmetry C bilobate (Inverted)	BI-6	
	Symmetry D bilobate (almost panicoid)	BI-7	
	Broken bilobate (BI-5) (This thesis)	BI-BR (BI-5)	
	Broken bilobate (BI-7) (This thesis)	BI-BR (BI-7)	
Polylobates/complex dumbbells (PO)	Polylobate with larger top	PO-3	PANICOID
Bilobates (BI)	Symmetry E bilobate (Panicoid type)	BI-8	
Crosses (CR)	Four lobed crosses with near cross shaped top	CR4-2	
	Three lobed crosses with near cross shaped top	CR3-2	
	Irregular cross with a near-cross shaped top	CRI-1	
	Perfect four-lobed cross	CR4-1	

Polylobates/complex dumbbells (PO)	Polylobate with the top and bottom the same size	PO-4	GRASS/MONO-ND
Blo-bodies: Plates (Blo)	Rectangular plate	Blo-1	
Epidermal ground mass cells (Epi)	Spiny elongate	Epi-9	
Stomatal complexes (St)	Monocotyledon stomata	St-4	
	Elongate with branched process	Epi-10	
Tracheary elements and related bodies (Tra)	Pitted rod tracheary	Tra-8	
Trichomes (Tri)	Spindle-shaped trichome	Tri-8	
Blo-bodies: Plates (Blo)	Large, faceted/scalloped sphere	Blo-11	DICOT-GEN
Epidermal ground mass cells (Epi)	Anticlinal epidermis	Epi-2	
	Polyhedral epidermis	Epi-1	
S-bodies (Scl)	Small, worm like body	Scl-5	
Parenchyma/mesophyll bodies (M)	Infilled parenchyma/honeycomb aggregate	M-2	
	Solid parenchyma/mesophyll cell	M-10	
Stomatal complexes (St)	Dicotyledon stomata	St-1	
Trichome (Tri)	Non-segmented, armed trichome	Tri-3	
Spherical and subspherical bodies (Cl, VI)	Vesicular Infillings- VI sphere	VI-1	
	Smooth VI spheres and subspheres	Cl-1	
	Large verrucate sphere	Cl-3	

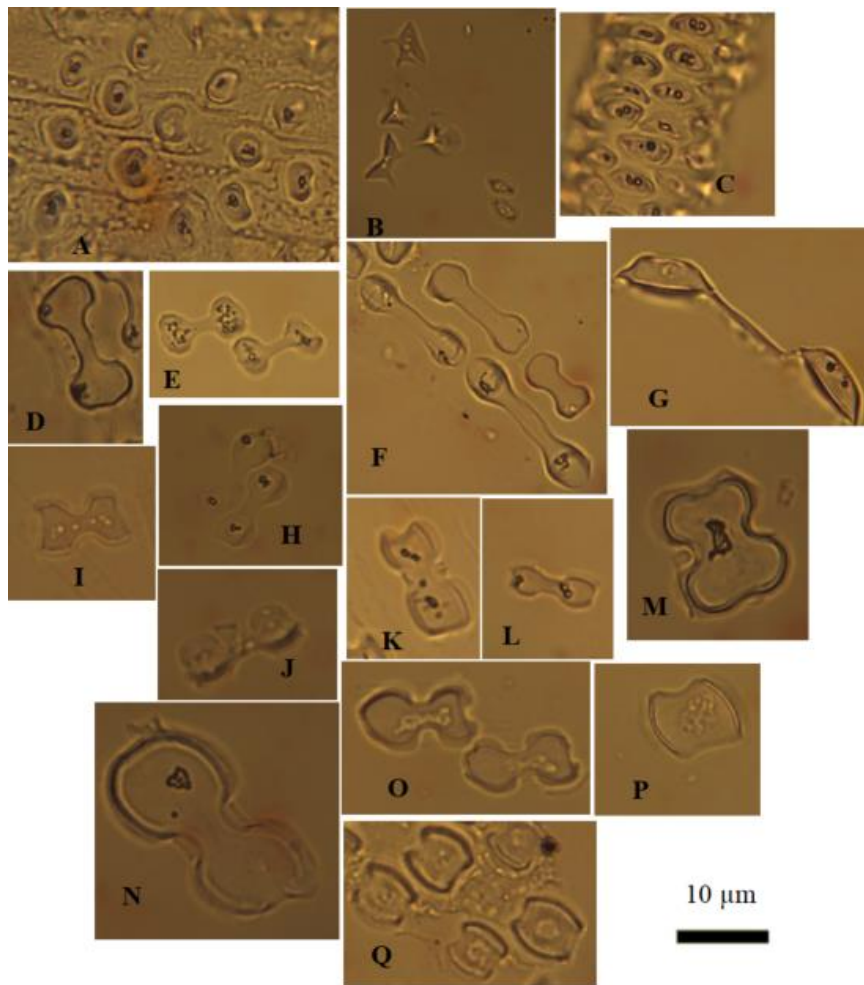
	Small smooth pink spheres	Cl-4	
Polygonal prism (Pris-Cl)	Anisopolar Prismatic Domed cylinder- Commelinaceae species phytoliths with conical, flat, or anisopolar tops, with cylindric/subcylindric body (Eichhorn et al., 2010; Yost et al., 2018)	Pris-Cl	COMMELINACEAE
Spherical and subspherical bodies (Clm)	Echinate sphere	Clm-2	PALM
Epidermal ground mass cells (Epi)	Epidermal plate of sedges	Epi-6	SEDGE
	Elongate with indented ends	Epi-11	GRASS-D
	Papillate epidermal cell	Epi 12	
Parenchyma/mesophyll bodies (M)	Vertebral column body (mesophyll cell)	M-7	
Trichomes (Tri)	Multilayered trichome	Tri-9	
Blo-bodies: Plates, blocky bodies, plates, and chunks (Blo)	Bulliform keystone-shaped	Blo-10	MONO/CONI
	Radiator shaped blocky	Blo-9	
	Faceted rectangular plate	Blo-3	
Epidermal ground mass cells (Epi)	Wavy elongate	Epi-8	
S-bodies (Scl)	Stellate parenchyma (rounded to slightly elongate)	SclF-7	AQ-MONO
	Stellate parenchyma	SclF-6	
Elongate bodies ("elongates") (Elo)	MD elongate	Elo-18	DICOT-WO



Spherical and subspherical bodies (CI, VI)	Large nodular sphere	CI-8	FI-GEN
S-bodies (Scl)	Compact, irregular S body	Scl-8	
	Multifaceted terminal tracheid	Scl-3	
Tracheary elements and related bodies (Tra)	Infilled helix tracheary	Tra-1	
	Worm like-Infilled helix tracheary	Tra-2	
Spherical and subspherical bodies (CI)	Compound sphere	CI-5	
	MD clump body (sphere with MD surface materials)	CI-10	
	Pillose-rugose body	CI-9	
	Small rugulose sphere	CI-7	
S-bodies (Scl)	Spongy mesophyll body	Scl-4	
	Elongate body with longitudinal facets	Scl-1	
	Short Scl-1	Scl-2	
Parenchyma/mesophyll bodies (M)	Parenchyma/honeycomb aggregate	M-1	
Conical rondels (CO)	Generic truncated rondel	CO-1	POOID-ND
Crenates (CE)	Crenate/trapeziform sinuate <i>Dactylis</i> spp. type	CE-3	
	Crenate/trapeziform sinuate with symmetry D	CE-4	
Saddles and saddle-like morphotypes (SA)	Collapsed saddle	SA-3	APPBO

Conical rondels (CO)	<i>Chusquea</i> rondel with spiked top	CO-3	
Elongate bodies ("elongates") (Elo)	Smooth elongate	Elo-1	OTH
	Thick trapezoidal 'smooth elongate'	Elo-2	
	Faceted elongate	Elo-3	
	Smooth, cylindrical rod	Elo-7	
Blo-bodies: Plates (Blo)	Thickened rectangular plate	Blo-2	
Conical rondels (CO)	Small spiked rondel	CO-4	OTHG

## Appendix C: Figures of representative modern phytoliths.



**C 1:** GSSC phytoliths from leaves, flower, and stem

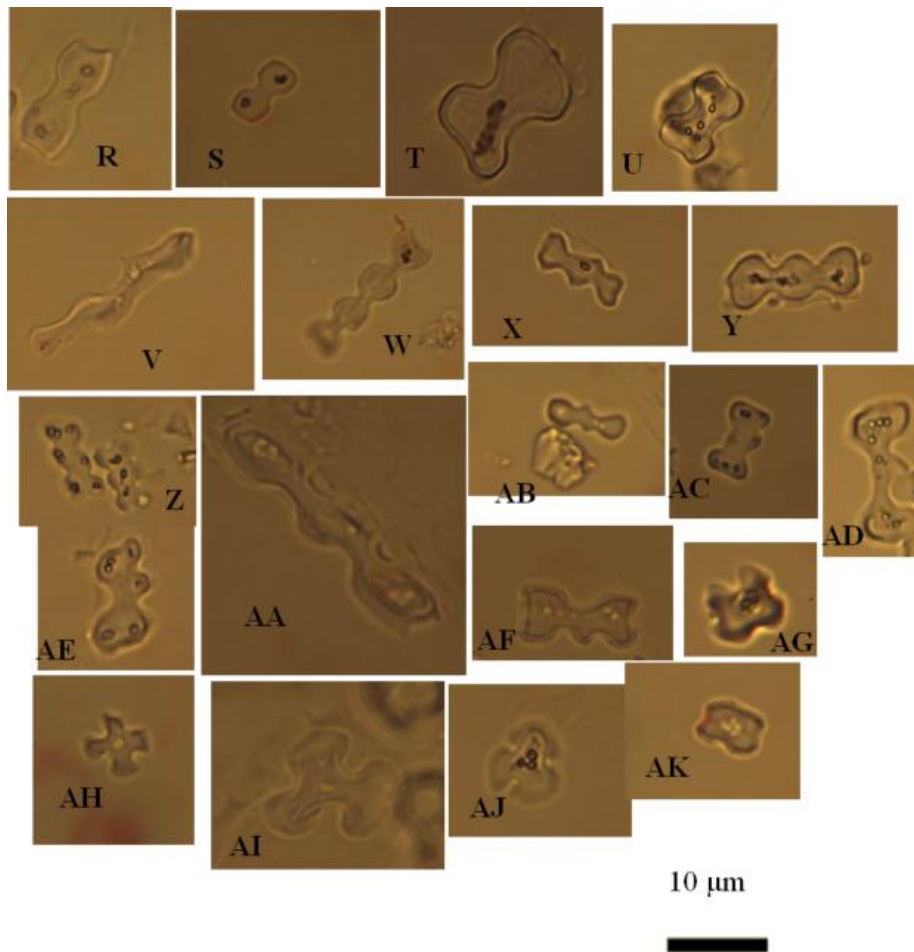
**A-C:** Crescentic conical rondel (CO-5). A. *Sporobolus consimilis*. B-C. *Sporobolus ioclados* B-side view showing the 'horns' and C-Top view.

**D-J:** Symmetry B bilobate (Simple lobate) (BI-5). D. *Diheteropogon* sp. E. *Pennisetum* spp. F-G. *Aristida adscensionis*. H: *Cenchrus ciliaris*.

**I-J:** Symmetry C bilobate (Inverted) (BI-6). I. *Brachiaria deflexa*., J. *Diheteropogon* spp.,

**K-O:** Symmetry D bilobate (almost panicoid) (BI-7). K. *Pennisetum* spp., L. *Cenchrus ciliaris*., M-N. *Diheteropogon* spp.,

**P-Q:** True saddle (SA-1). P. *Chloris pychnothrix*. Q. *Chloris gayana*.



**C 2: GSSC phytoliths from leaves, flowers, roots, and stem.**

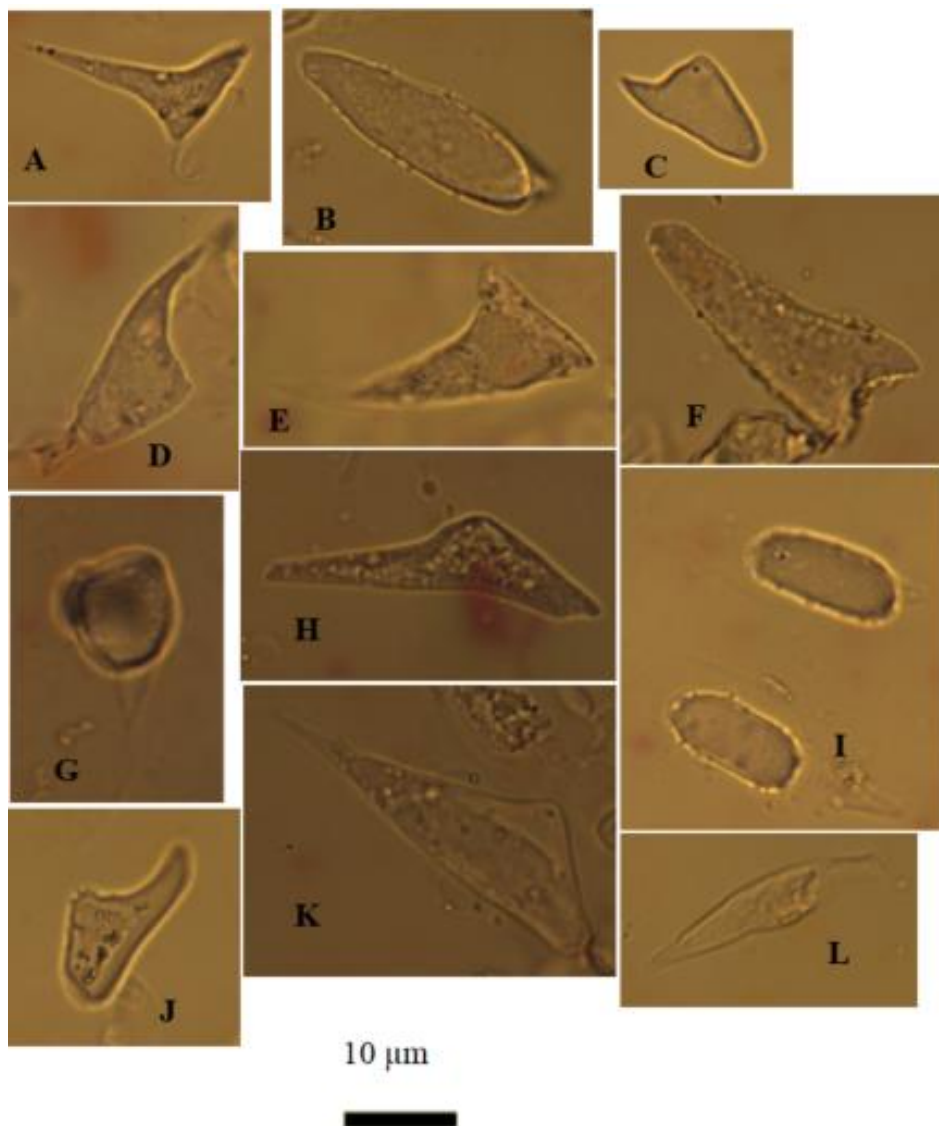
**R-U:** Symmetry E bilobate (Panicoid type) (BI-8). R. *Pennisetum* spp., S. *Centhrus ciliaris*., T. *Diheteropogon* spp., U. *Bothriochloa insculpta*

**V-AB.** Polylobate with larger top (symmetry C) (PO-3). V. *Aristida adscensionis*., W. *Bothriochloa insculpta*., X. *Brachiaria deflexa*., Y. *Panicum coloratum*, Z. *Bothriochloa insculpta*. AA. *Diheteropogon* spp. AB. *Centhrus ciliaris*.

**AC-AF.** Polylobate with the top and bottom the same size (PO-4). AC. *Diheteropogon* spp., AD. *Pennisetum* spp., AE. *Panicum coloratum*, AF. *Brachiaria deflexa*.

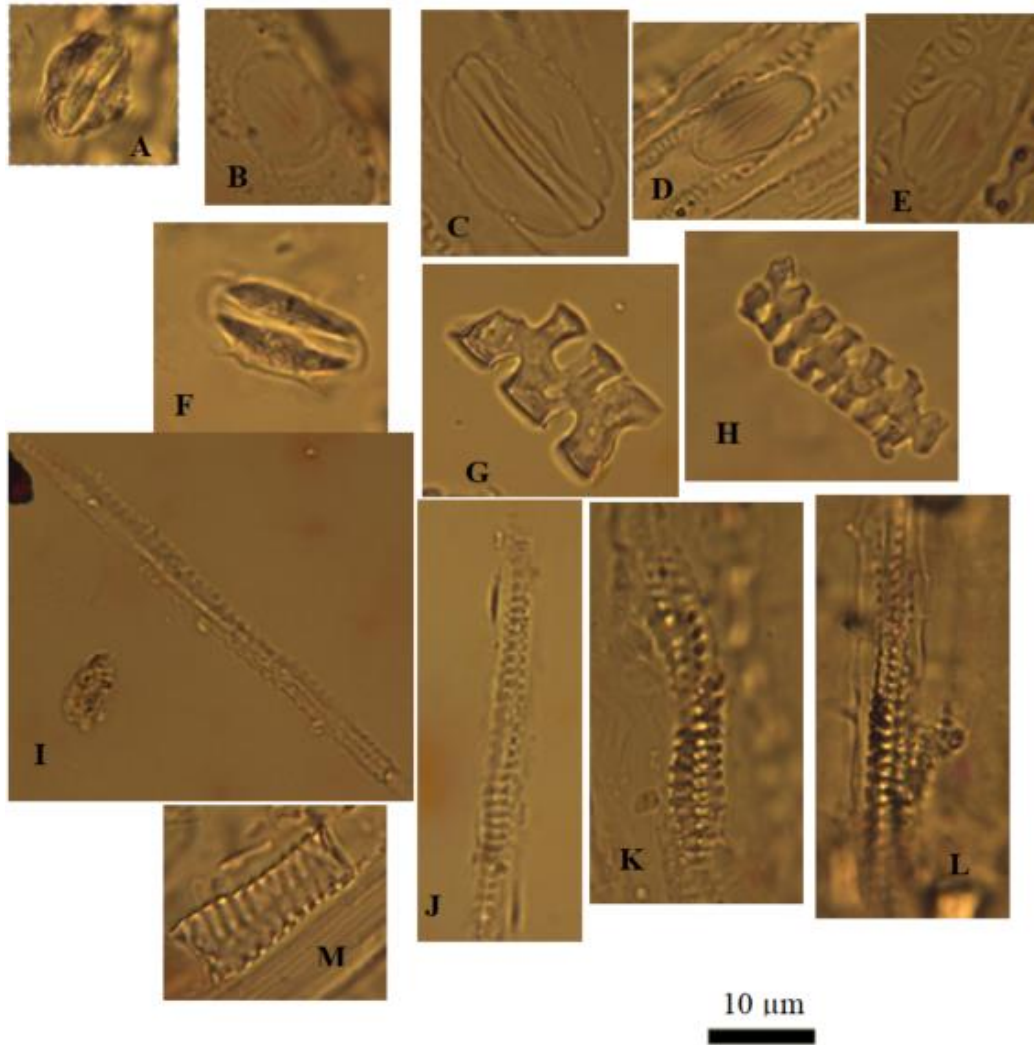
**AG-AH.** Four lobed crosses with near cross shaped to cross shaped top (CR4-2). AG. *Panicum coloratum*. AH. *Brachiaria deflexa*.

**AI-AK.** Cross. AI-AJ. Three-lobed cross with near cross shaped top (CR3-2). AI. *Diheteropogon* spp., AJ. *Bothriochloa insculpta*., AK. Matchbox body with ears: cross/bilobate (CR4-10) *Sporobolus ioclados*.



**C 3:** Grass phytoliths: spindle shaped trichomes (Tra-8).

A. *Aristida adscensionis*., B. *Chloris pycnothrix*., C. *Pennisetum* spp., D. *Cenchrus ciliaris*., E. *Chloris gayana*., F. *Bothriochloa insculpta*., G. *Diheteropogon* spp., H. *Panicum coloratum*., I. *Brachiaria deflexa*., J. *Sporobolus consimilis*., K. *Sporobolus ioclados*., and L. Multilayered trichome (Tra-9) from *Chloris pycnothrix*.

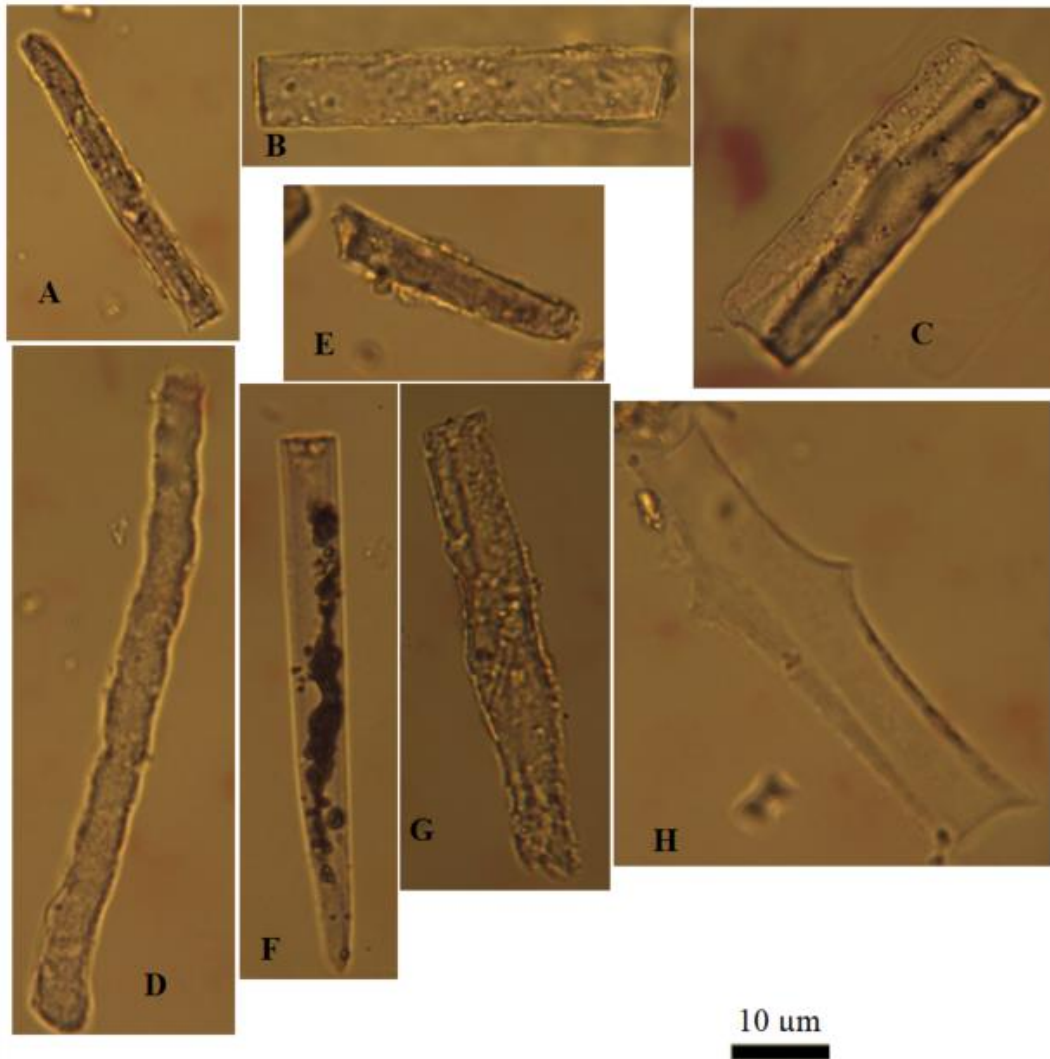


**C 4:**Grass phytoliths: stomata, mesophyll, and tracheid phytoliths.

**A-F** Monocotyledon stomata (ST-4) A. Infilled with grainy stomata *Aristida adscensionis*., B. thin transparent silica stomata *Chloris gayana*., C. *Panicum coloratum*., D. *Bothriochloa insculpta*., E. *Centhrus ciliaris*. F. *Brachiaria deflexa*.

**G-H.** Mesophyll cells- Vertebral column (M-7). G. *Aristida adscensionis*. H. *Bothriochloa insculpta*.

**I-M.** Pitted rod tracheary (Tra-8). I. *Chloris gayana*., J. *Aristida adscensionis*., K. *Bothriochloa insculpta*., L. *Brachiaria deflexa*., and M. *Panicum coloratum*.

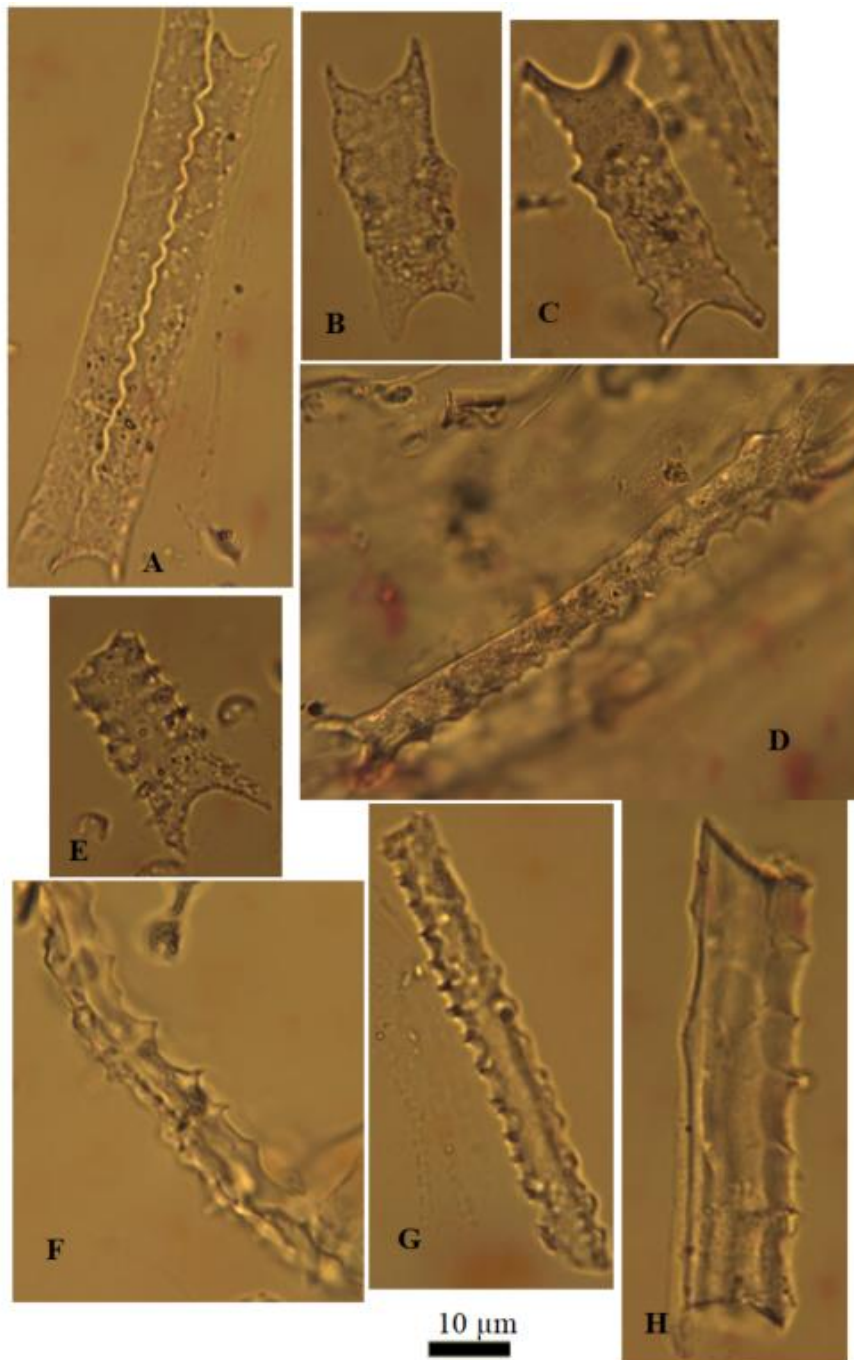


**C 5:** Grass phytoliths: smooth elongates and thick trapezoidal 'smooth elongate'.

**A-G** Smooth elongate (Elo-1). A. *Aristida adscensionis*., B. *Chloris Pycnothrix*., C. *Chloris gayana*., D. *Panicum coloratum*., E. *Bothriochloa insculpta*., F. *Centhrus ciliaris*., G. *Brachiaria deflexa*.

**H.** thick trapezoidal elongate (Elo-2) *Chloris gayana*.



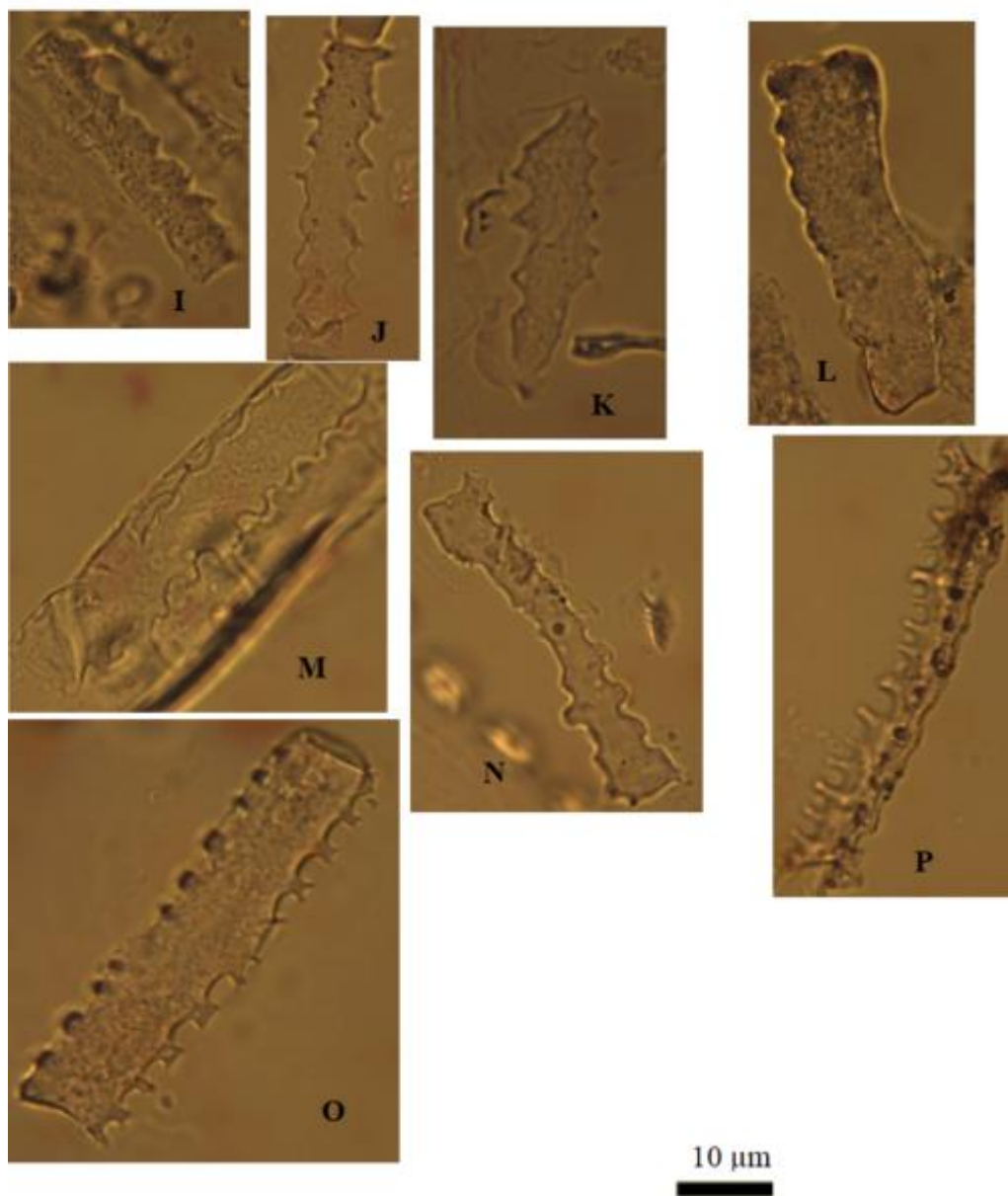


**C 6:** Grass phytoliths: epidermal cells phytoliths (1).

**A-E.** elongate with indented ends (Epi-11) A. *Aristida adscensionis*., B. *Chloris gayana*., C. *Bothriochloa insculpta*., D. *Panicum coloratum*., E. *Sporobolus ioclados*.

**F-H.** Spiny elongate (Epi-9). F. *Pennisetum* spp., G. *Chloris Pycnothrix*., and H. *Chloris gayana*.



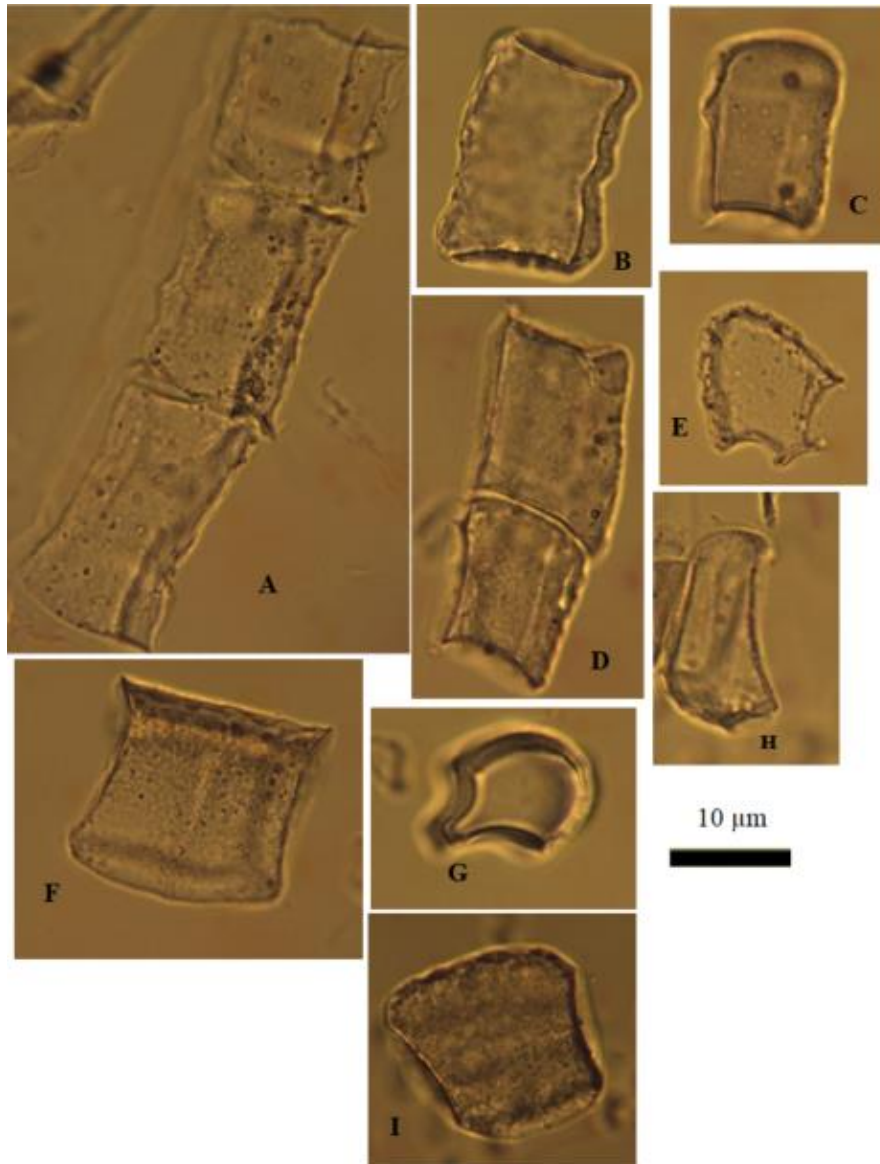


**C 7: Grass phytoliths: epidermal cells phytoliths (2).**

**I-K.** Spiny elongate (Epi-9). I. *Sporobolus ioclados.*, J. *Brachiaria deflexa.*, K. *Diheteropogon* spp.

**L-N.** Wavy elongate (Epi-8). L. *Aristida adscensionis.*, M. *Sporobolus ioclados.*, N. *Chloris gayana.*

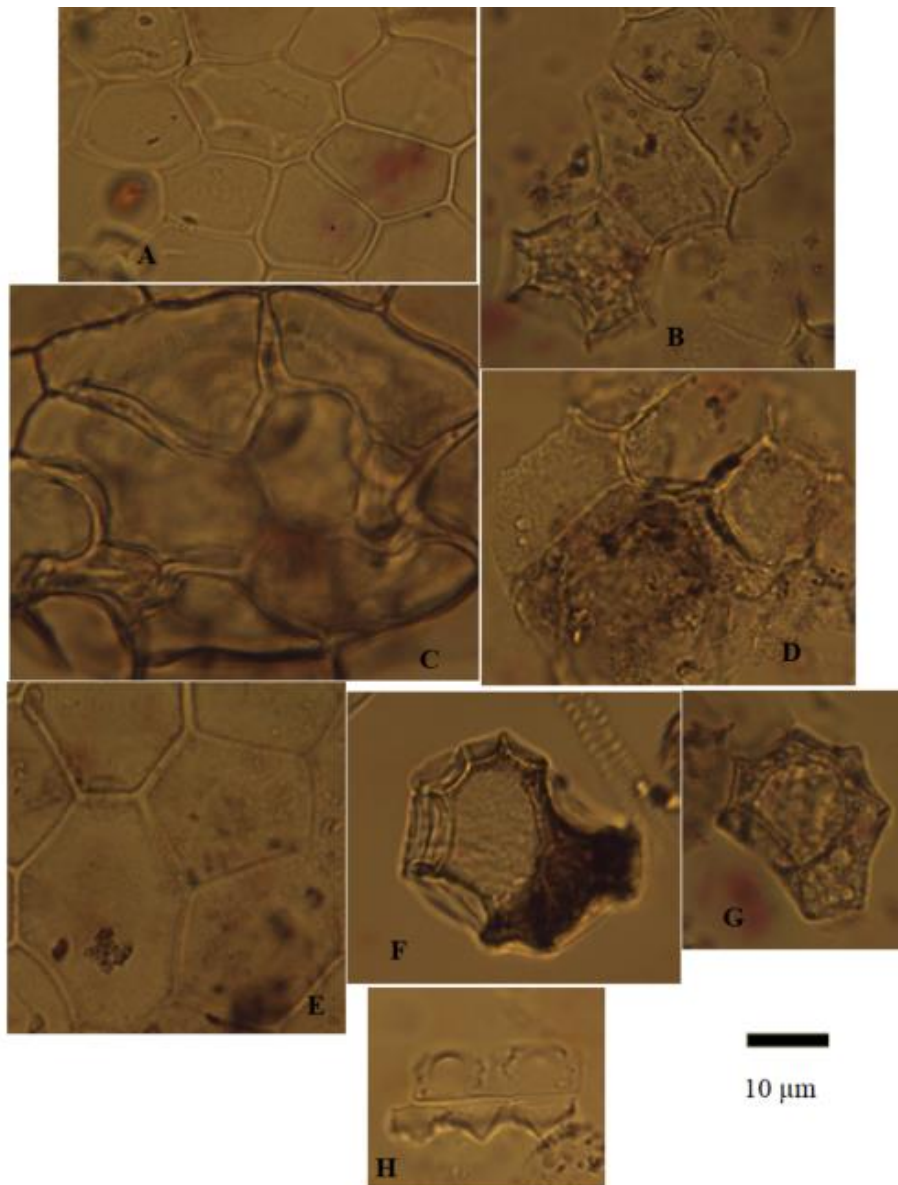
**O-P.** Elongate with branched process (Epi-10). O. *Panicum coloratum.*, and P. *Bothriochloa insculpta.*



**C 8:** Grass phytoliths: Blo-bodies, plates, and chunks.

**A-D.** thickened rectangular plate (Blo-2). A. *Aristida adscensionis*., B. *Chloris pycnothrix*., C. *Bothriochloa insculpta*., D. *Chloris gayana*.

**E-I.** Bulliform keystone-shaped plate (Blo-10). E. *Pennisetum* sp. F. *Bothriochloa insculpta*., G. *Chloris pycnothrix*., H. *Brachiaria deflexa*., and I. *Sporobolus ioclados*.

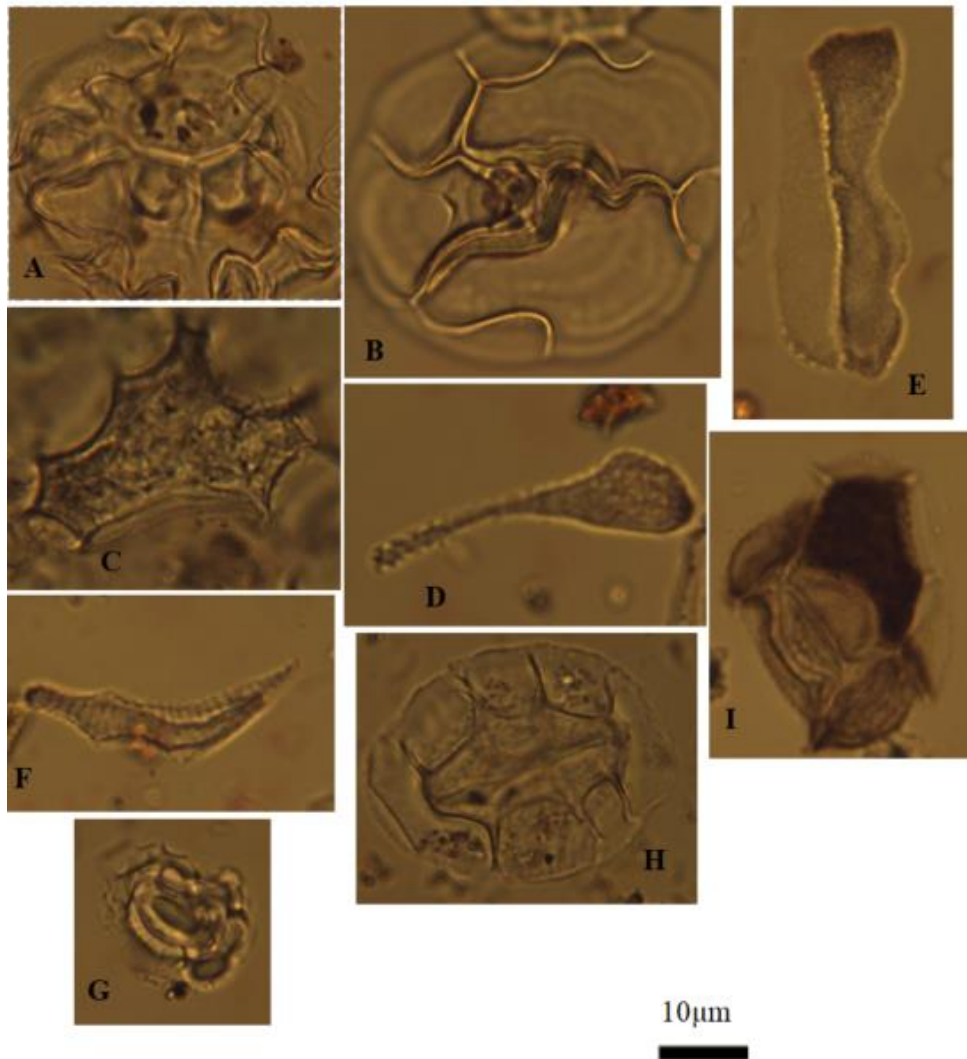


**C 9:** Non-grass phytoliths: epidermal ground mass cell phytoliths (Epi-1).

**A-E.** Polyhedral epidermis. A *Lochocarpus eriocalyx*. B. *Zanthoxylum chalybeum*. C. Epi-1 (with Intermediate cells close to Epi-2) *Launeae cornuta*. D. *Grewia villosa*., E. *Commiphora* spp.

**F-G.** Isolated infilled epidermal polyhedral (Epi-1) with facets. F. *Launeae cornuta* Leaves, flowers, stem G. *Zanthoxylum chalybeum* Leaves.

**H.** Epidermal plate of sedges with cone shaped bumps *Cyperus* (Epi-6) *rotundus*.



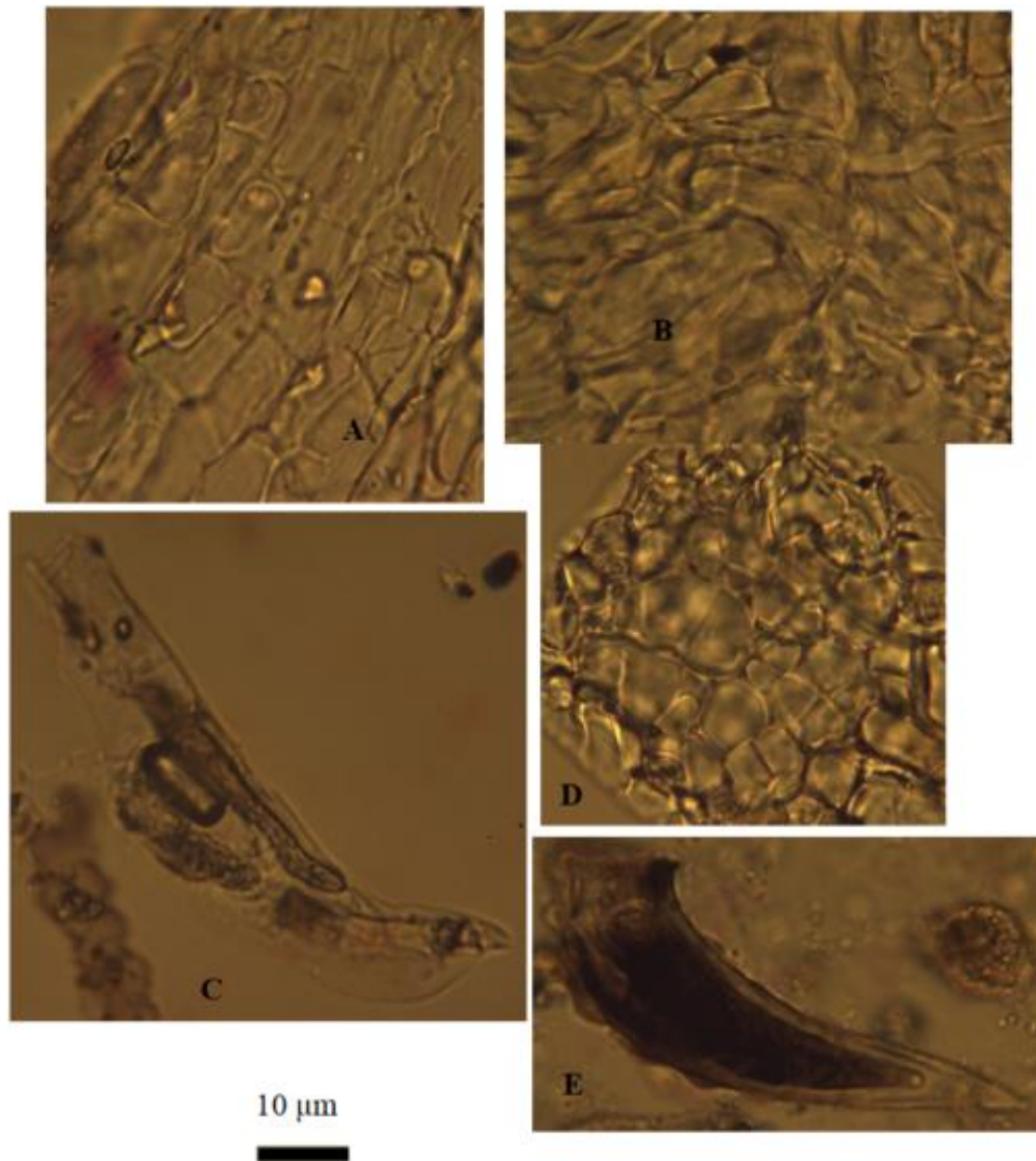
**C 10:** Non-grass phytoliths: epidermal ground mass cells, S-bodies, and stomatal complexes.

**A-C.** Anticlinal epidermis (Epi-2). A. *Solanum aculeatissimum*. B. *Launea cornuta*. C. *Zanthoxylum chalybeum*.

**D-F.** sclereids. **D-E.** Small, worm like (Scl-5) *Lochocarpus eriocalyx*. F. small, multifaceted with terminal tracheid (Scl-3) *Lochocarpus eriocalyx*.

**G-I.** Dicotyledon stomata (St-1). G. *Solanum aculeatissimum*., H. *Zanthoxylum chalybeum*., and I. *Launea cornuta*.

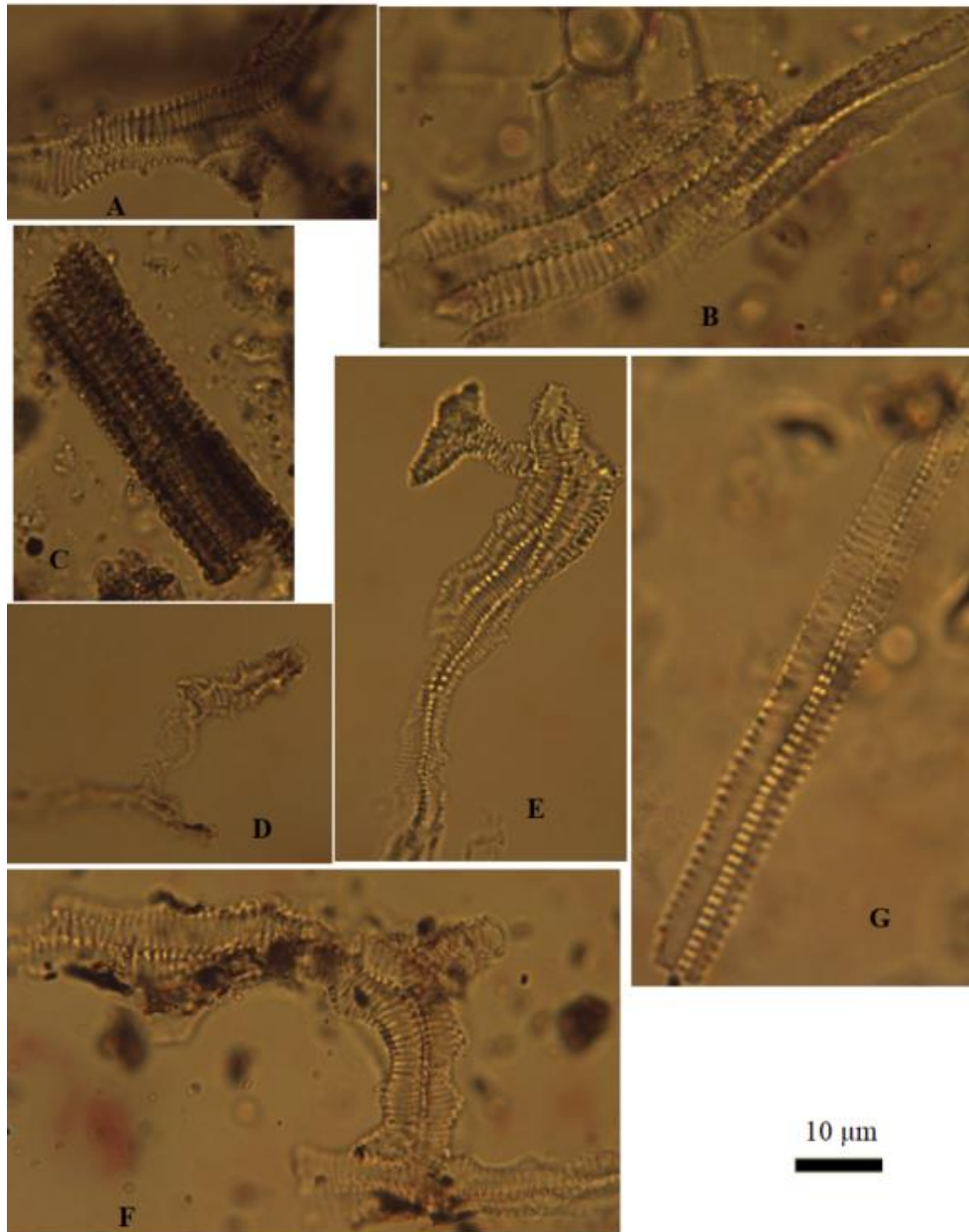




**C 11:** Non-grass phytoliths: parenchyma/mesophyll bodies and trichome.

**A-D.** Parenchyma/mesophyll bodies (M). A. Parenchyma/honeycomb aggregate (M-1) *Lochocarpus eriocalyx*., B. Parenchyma/honeycomb aggregate (M-1) *Solanum aculeatissimum*., C. Solid parenchyma/mesophyll cell *Launea cornuta*., D. Parenchyma/honeycomb aggregate (M-1) *Solanum aculeatissimum*.,

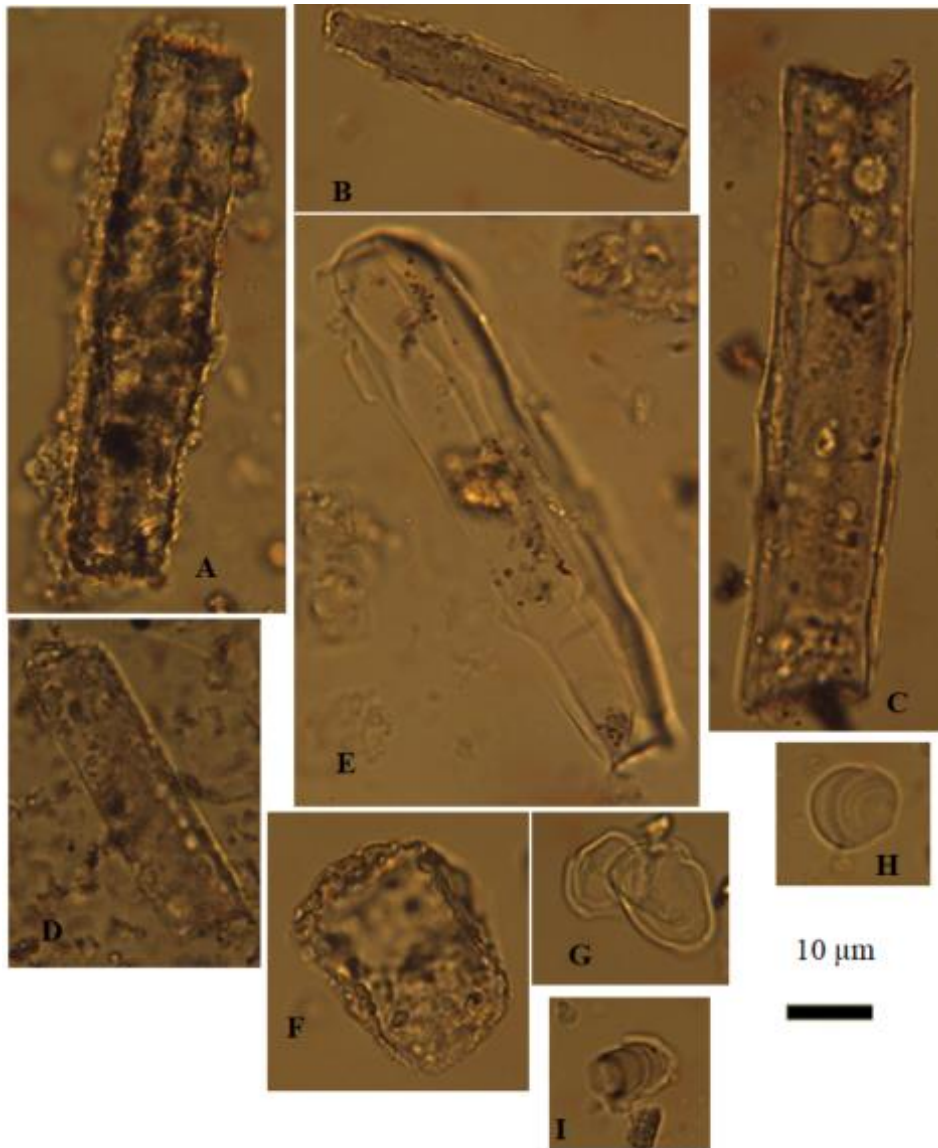
**E.** Non-segmented, armed trichome (Tri-3)-*Grewia villosa*.



**C 12:** Non-grass phytoliths: hollow and infilled helix (helical tracheary element) and pitted rod tracheary.

**A-F.** hollow and infilled helix (helical tracheary element) (Tra-1) from leaves. A. *Zanthoxylum chalybeum*., B. *Lochocarpus eriocalyx*., C. *Grewia villosa*., D. *Solanum aculeatissimum*., E. *Launeae cornuta*., F. *Cyperus rotundus* tuber, rhizomes.

**G.** pitted rod tracheary (Tra-8) *Cyperus rotundus* leaves, stem.



**C 13: Non-grass phytoliths**

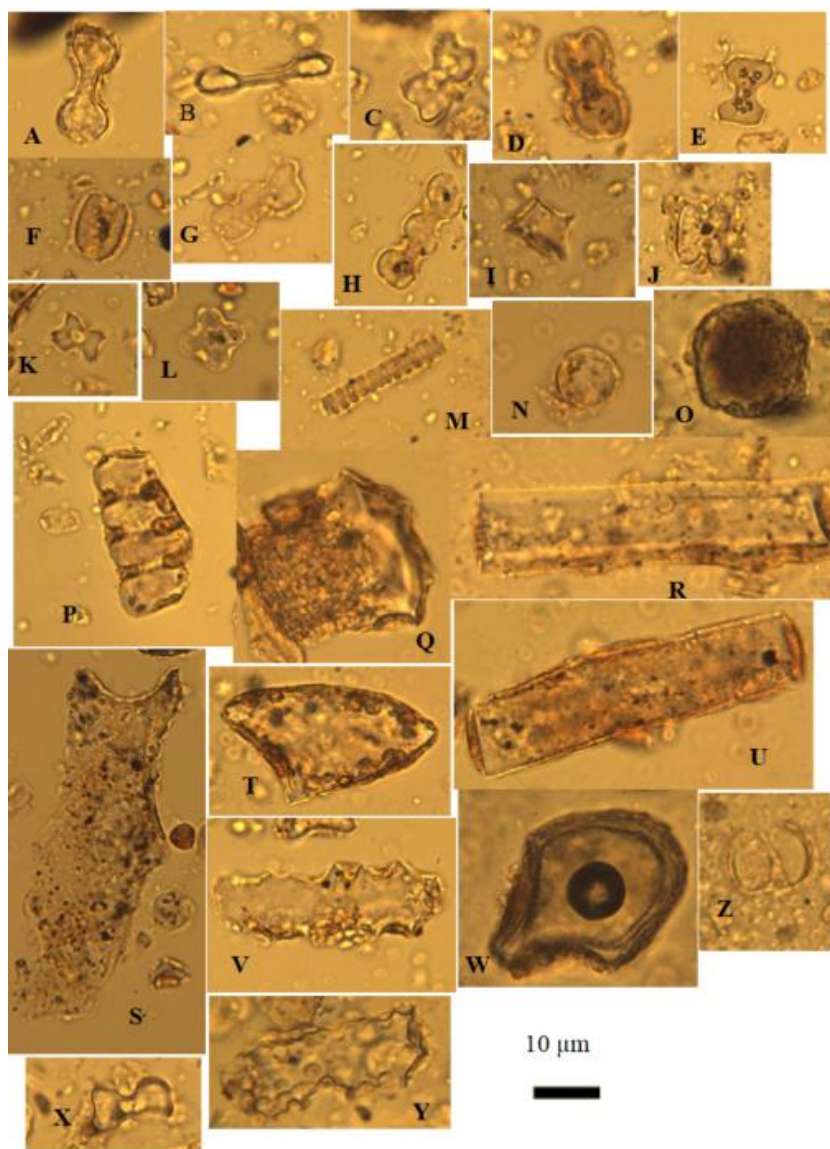
**A-D.** smooth elongate (Elo-1). A. *Commiphora* spp., B. *Ecbolium revolutum*., C. *Solanum aculeatissimum*., D. *Zanthoxylum chalybeum*.,

**E.** faceted elongate (Elo-3) *Cyperus rotundus*.

**F.** Blocky (BLO) *Acacia* spp.,

**G-I.** VI spheres (VI-1). G. *Launeae cornuta*., H. *Lochocarpus eriocalyx*., I. *Commiphora* spp.





**C 14:** Selected diagnostic phytoliths from modern surface soil samples.

**A-B.** Symmetry B bilobate (Simple lobate) (BI-5), B. probably *Aristida* spp. **C.** Symmetry C bilobate (Inverted) (BI-6). **D.** Symmetry D bilobate (almost panicoid) (BI-7). **E.** Symmetry E bilobate (Panicoid type) (BI-8). **F.** True saddle (SA-1). **G.** Polylobate with the top and bottom the same size (PO-4). **H.** Polylobate with larger top (symmetry C) (PO-3). **I.** Crescentic conical rondel (*Sporobolus* type) (CO-5). **J.** Three-lobed cross with near cross shaped top (CR3-2). **K.** Matchbox body with ears: cross/bilobate (CR4-10). **L.** Four lobed crosses with near cross shaped to cross shaped top (CR4-2). **M.** Infilled helix (helical tracheary element) (Tra-1). **N.** Smooth VI sphere (CI-1). **O.** Large verrucate sphere (CI-3). **P.** Mesophyll body-vertebral column. **Q.** Heteropolar (anisopolar) cylinders with a prismatic domed end and decorated end (Pris-CI). **R.** Smooth elongate (Elo-1). **S.** Elongate with indented ends (Epi-11). **T.** Spindle-shaped body (trichome infilling) (Tri-8). **U.** Smooth elongate (Elo-1). **V.** Spiny elongate (Epi-9). **W-Z.** Taphonomy post depositional impact on phytoliths. **W.** Eroded keystone shaped blocky (Blo-10). **X.** Broken bilobate (BI-7). **Y.** Heavily pitted smooth elongate (Elo-1). **Z.** Broken saddle (SA-1).